RENATA MICHELI MARTINEZ

TRANS-CHALCONA, HESPERIDINA METIL CHALCONA E NARINGENINA:

POTENCIAL TERAPÊUTICO E MECANISMOS DE AÇÃO NOS DANOS CUTÂNEOS INFLAMATÓRIOS E OXIDATIVOS INDUZIDOS PELA RADIAÇÃO ULTRAVIOLETA B EM CAMUNDONGOS SEM PÊLO

Londrina
2015

RENATA MICHELI MARTINEZ

TRANS-CHALCONA, HESPERIDINA METIL CHALCONA E NARINGENINA:

POTENCIAL TERAPÊUTICO E MECANISMOS DE AÇÃO NOS DANOS CUTÂNEOS INFLAMATÓRIOS E OXIDATIVOS INDUZIDOS PELA RADIAÇÃO ULTRAVIOLETA B EM CAMUNDONGOS SEM PÊLO

Tese apresentada ao Programa de Pós-Graduação em Ciências da Saúde do Centro de Ciências da Saúde da Universidade Estadual de Londrina

Orientadora: Profa. Dra. Rúbia Casagrande

Londrina
2015

Catalogação elaborada pela Divisão de Processos Técnicos da Biblioteca Central da Universidade Estadual de Londrina

DADOS INTERNACIONAIS DE CATALOGAÇÃO-NA-PUBLICAÇÃO (CIP)

M385t Martinez, Renata Micheli.
Trans-chalcona, hesperidina metil chalcona e naringerina : potencial terapêutico e mecanismos de ação nos danos cutâneos inflamatórios e oxidativos induzidos pela radiação ultravioleta B em camundongos sem pêlo / Renata Micheli Martinez. – Londrina, 2015.
205 f. il.

Orientador: Rúbia Casagrande.
Tese (Doutorado em Ciências da Saúde) – Universidade Estadual de Londrina, Centro de Ciências da Saúde, Programa de Pós-Graduação em Ciências da Saúde, 2015.
Inclui bibliografia.

1. Flavonóides – Teses. 2. Antioxidantes – Teses. 3. Estresse oxidativo – Teses. 4. Pele – Efeito da radiação – Teses. 5. Inflamação – Teses. I. Casagrande, Rúbia. II. Universidade Estadual de Londrina. Centro de Ciências da Saúde. Programa de Pós-Graduação em Ciências da Saúde. III. Título.

CDU 615:616.5

RENATA MICHELI MARTINEZ

TRANS-CHALCONA, HESPERIDINA METIL CHALCONA E NARINGENINA: POTENCIAL TERAPÊUTICO E MECANISMOS DE AÇÃO NOS DANOS CUTÂNEOS INFLAMATÓRIOS E OXIDATIVOS INDUZIDOS PELA RADIAÇÃO ULTRAVIOLETA B EM CAMUNDONGOS SEM PÊLO

Tese apresentada ao programa de pós-graduação em Ciências da Saúde da Universidade Estadual de Londrina - UEL.

BANCA EXAMINADORA

_____

Orientadora: Profa. Dra. Rúbia Casagrande
Universidade Estadual de Londrina – UEL

_____

Prof. Dr. Décio Sabbatini Barbosa
Universidade Estadual de Londrina – UEL

_____

Prof. Dr. Celso Vataru Nakamura
Universidade Estadual de Maringá – UEM

_____

Prof. Dra. Maria José Vieira Fonseca
Universidade de São Paulo – USP

_____

Prof. Dra. Sandra Regina Georgetti
Universidade Estadual de Londrina – UEL

Londrina, 30 de abril de 2015.

Dedico este trabalho:

A Deus por me conceder uma vida repleta de bençõe e oportunidades

Aos meus pais Josefa e Roberto pelo apoio, incentivo, educação, conduta pessoal e profissional. A eles o meu eterno agradecimento.

Ao meu esposo Márcio Giocondo, por estar ao meu lado nesta trajetória. Obrigada pela compreensão, incentivo e paciência. Seu amor foi um suporte importante para realização deste trabalho.

AGRADECIMENTOS

À Prof. Dra. Rúbia Casagrande, que há 9 anos me acompanha na jornada acadêmica. Obrigada pela oportunidade, orientação, confiança, incentivo e acima de tudo, pela amizade gerada nesses anos. Obrigada pelo exemplo constante de dedicação ao trabalho. Sem dúvida será uma referência para toda minha vida, não só profissional como pessoal também.

Ao Prof. Dr. Waldiceu A. Werri Júnior, obrigada pela ajuda constante, ensinamentos, pelo exemplo profissional e pela confiança depositada. Obrigada pelas orientações sempre motivadoras, suas contribuições foram essenciais.

Ao Prof. Dr. Décio Sabbatini Barbosa e a Profa Dra. María Emília Fávero por todo o auxílio e suporte oferecido.

Aos membros da banca Celso Vataru Nakamura, Maria José Vieira Fonseca, Sandra Regina Georgetti e Décio Sabbatini Barbosa, por terem aceitado o convite de participarem da banca examinadora da minha tese.

Ao Felipe A. Pinho-Ribeiro pela ajuda nos experimentos, e nas discussões e enriquecimento científico.

Aos amigos e colegas do Laboratório de Pós-graduação do Centro de Ciências da Saúde da UEL, Kamila, Carine, Alissana, Luciana, Francis, Chiara, Vitor Obara, Keiko que me auxiliaram quando necessário e me acolheram de braços abertos.

Aos amigos e colegas do laboratório de Dor, Inflamação, Neuropatia e câncer, do Departamento de Patologia da UEL, Daniela Balbinot, Talita, Ana Carla, Sandra, Miriam, Carla, Thacyana, Cássia, Larissa, Cátia, Vitor, Kenji, Camila, pela boa convivência. E, em especial, à Daniela Medeiros e Ana Carolina Rossaines pelos momentos de alegria compartilhados.

Aos amigos e colegas do grupo de pesquisa de estresse oxidativo e inflamação na radiação UVB, como iniciação científica e pós-graduandos, que seguiram seus caminhos ou continuam a participar dos experimentos, Carla, Carolina, Thaís, Ana Laura, Marcela, Andressa, Vitor Sottero, Danilo, Bárbara, pelos momentos compartilhados. Agradeço especialmente ao Vinícius pela constante disponibilidade e auxílio nos experimentos.

À nova geração de pós-graduandos e iniciação científica do grupo de pesquisa de estresse oxidativo e inflamação na radiação UVB, David, Camila, Talita Laiane, Cristina, Alessandro e Geórgia, que com entusiasmo dão continuidade aos trabalhos desenvolvidos, pela troca de experiências e momentos compartilhados.

À técnica do Laboratório de Pós-graduação (LPG) do Centro de Ciências da Saúde, Denise Duarte, pelo auxílio prestado.

Aos funcionários Izaltino e José pela ajuda com os animais do biotério.

Aos funcionários da Secretaria de Pós-graduação pelos auxílios prestados.

A todos os docentes do Programa de Pós-Graduação em Ciências da Saúde da UEL pelas aulas que enriqueceram nossos trabalhos e nossa formação profissional.

À Coordenação de Aperfeiçoamento de Pessoal de Nível Superior (CAPES) pelo auxílio financeiro concedido na forma de bolsa de estudo.

Ao Conselho Nacional de Desenvolvimento Científico e Tecnológico (CNPq) e a Fundação Araucária pelo apoio financeiro.

Aos meus familiares e amigos que durante este período estiveram presentes de alguma forma compartilhando comigo bons e maus momentos.

A todas as pessoas, que provavelmente, por um momento de descuido, acabei por não mencionar, mas que contribuíram direta ou indiretamente, para a realização deste trabalho, deixo o meu muito obrigada.

Descobrir consiste em olhar para o que todo mundo está vendo e pensar uma coisa diferente. (Roger Von Oech)

MARTINEZ, Renata Micheli. **Trans-chalcona, hesperidina metil chalcona e naringenina:** potencial terapêutico e mecanismos de ação nos danos cutâneos inflamatórios e oxidativos induzidos pela radiação ultravioleta B em camundongos sem pêlo. 2015. 205 f. (Doutorado em Ciências da Saúde) - Universidade Estadual de Londrina, Londrina, Paraná.

RESUMO

A pele é uma barreira física entre o organismo e o ambiente continuamente exposta a fatores que ameaçam a integridade de suas estruturas celulares. A radiação ultravioleta B (UVB) é um dos principais fatores de risco para doenças dermatológicas e a exposição crônica à radiação UVB tem sido relacionada ao câncer de pele e ao envelhecimento cutâneo prematuro. Estes eventos estão relacionados com a formação de espécies reativas de oxigênio (EROs), produção de moléculas pró-inflamatórias como as citocinas e recrutamento de leucócitos como os neutrófilos. Considerando a relação entre o aumento do estresse oxidativo e os efeitos danosos causados pela radiação UVB na pele, o uso de antioxidantes exógenos, como os flavonóides, torna-se uma alternativa importante para controlar os danos cutâneos induzidos pela radiação UVB. Desta forma, na presente pesquisa, foram avaliados os mecanismos de atividade antioxidante *in vitro* dos flavonóides trans-chalcona (TC), hesperidina metil chalcona (HMC) e naringenina (NGN) e os efeitos terapêuticos e mecanismos de ação destes três flavonóides quando administrados pela via intraperitoneal e da NGN quando veiculada em formulação tópica, nos danos cutâneos inflamatórios e oxidativos induzidos pela radiação UVB em camundongos sem pêlo. Os resultados *in vitro* demonstraram que a TC não atua como um antioxidante e que a HMC e a NGN possuem poder antioxidante em reduzir o ferro e o radical 2,2' azinobis (3-etilbenzotiazolina-6-ácido sulfônico) (ABTS), capacidade de neutralizar o radical hidroxil e de inibir a peroxidação lipídica. No entanto, *in vitro* a HMC e a NGN não apresentaram capacidade doadora de átomos de hidrogênio ao radical 2,2' azinobis (3-etilbenzotiazolina-6-ácido sulfônico) (DPPH•) e atividade queladora do íon ferro. Os tratamentos sistêmicos (intraperitoneal) com TC, HMC e NGN reduziram a inflamação cutânea induzida pela radiação UVB, reduzindo o edema de pele, o recrutamento de neutrófilos, a atividade da metaloproteinase-9 e a produção de diferentes citocinas. Os tratamentos com estes três flavonóides também protegeram a pele do estresse oxidativo induzido pela radiação UVB, por manter os níveis de glutationa reduzida (GSH) e a atividade da catalase, e por reduzir a produção de hidroperóxidos lipídicos e de ânion superóxido, e a expressão de RNAm para gp91phox (subunidade da NADPH oxidase). Foram preparadas três formulações tópicas contendo NGN, sendo que a composta pela base auto-emulsionante NET FS® demonstrou ser a mais estável no estudo de estabilidade físico-química e funcional e protegeu a pele dos danos induzidos pela radiação UVB por manter a expressão de RNAm de componentes antioxidantes celulares (glutationa peroxidase-1, glutationa redutase e fator de transcrição relacionado a expressão de enzimas antioxidantes [Nrf2]), por induzir a expressão de RNAm da hemeoxigenase-1 e por reduzir a expressão de RNAm para gp91phox. Estes efeitos da formulação contendo NGN resultaram em uma melhora da capacidade antioxidante da pele pela manutenção do poder redutor de ferro, da capacidade em reduzir o radical ABTS, dos níveis de GSH e atividade da catalase, e pela redução da produção de ânion superóxido. Além disso, a formulação tópica contendo NGN reduziu o edema cutâneo, a produção de hidroperóxidos lipídicos e de diferentes citocinas induzidas pela radiação UVB. Em suma, estes resultados sugerem o uso da TC, da HMC e da NGN como estratégias relevantes para controlar doenças cutâneas causadas pela exposição à radiação UVB, além de contribuir para a elucidação dos mecanismos de ação destes flavonóides.

Palavras-chaves: Trans-chalcona. Hesperidina metil chalcona. Naringenina. Estresse oxidativo. Inflamação. Radiação UVB.

MARTINEZ, Renata Micheli. **Trans-chalcone, hesperidin methyl chalcone and naringenin:** therapeutic potential and mechanism of action on ultraviolet B radiationinduced skin inflammation and oxidative stress in hairless mice. 2015. 205 p. (Health Science Thesis) - Londrina State University, Londrina, Parana.

ABSTRACT

Skin is a physical barrier between the organism and the environment exposed continuously to factors that threaten the integrity of its cellular structures. Ultraviolet B (UVB) radiation is one of the major risk factors for dermatologic diseases and chronic UVB radiation exposure has been related to skin cancer and premature skin aging. These events are related to the reactive oxigen species (ROS) generation, inflammatory molecules generation, including the cytokines, and to the leukocyte recruitment, including neutrophils. Taking into account the relation between the increases of oxidative stress and the deleterious effects induced by UVB radiation in the skin, the use of exogenous antioxidants becomes an important alternative to control the skin damages induced by UVB. Thus, the purpose of this study was to evaluate the antioxidant activity in cell free systems of trans-chalcone (TC), hesperidin methyl chalcone (HMC) and naringenin (NGN) and the effects of intraperitoneal treatment with these compounds and topical formulation containing NGN on UVB radiation-induced skin inflammation and oxidative damage in hairless mice. *In vitro* results show that transchalcone not presented antioxidant activity, and that HMC and NGN presented ferric reducing power, ability to reduce 2,2′-azino-bis (3-ethylbenzothiazoline-6-sulfonic acid) (ABTS) and to neutralize hydroxyl radical, and to inhibit lipid peroxidation. However, HMC and NGN not presented ability to donate hydrogen to 2,2-diphenyl-1-picryl-hydrazyl radical (DPPH•) and iron-chelating activity. Systemic treatments (intraperitoneal) with TC, HMC and NGN reduced UVB radiation-induced skin edema, neutrophil recruitment, matrix metalloproteinase-9 activity and a wide range of cytokines. The treatments with these flavonoids also protected the skin from UVB radiation-induced oxidative stress by maintaining levels of reduced glutathione (GSH) and catalase activity, and by reducing lipid hydroperoxides and superoxide anion production, and gp91phox (NADPH oxidase subunit) mRNA expression. Three topical formulations containing NGN were prepared. The formulation with the self-emulsifying agent Net FS® demonstrated to be the most stable formulation in physico-chemical and functional stability study and protected the skin from UVB radiation-induced skin damage by maintaining mRNA expression of cellular antioxidant components (glutathione peroxidase 1, glutathione reductase and transcription factor Nrf2 the regulator of the expression of antioxidant enzymes), by inducing mRNA expression of heme oxygenase-1, and by reducing mRNA expression of NADPH oxidase sub-unit gp91phox. These effects of formulation containing NGN resulted in an improvement in antioxidant capacity in the skin by maintaining ferric reducing ability, ABTS radical reducing capacity, the levels of GSH and catalase activity and in an reduction of superoxide anion production. In addition, NGN-containing formulation reduced UVB radiation-induced edema, lipid hydroperoxides and different cytokine production. In conclusion, the present study suggests the use of TC, HMC and NGN as a relevant strategy to control UVB-induced skin disorders, and contribute to the elucidation of TC, HMC and NGN mechanisms of action.

Keywords: Trans-chalcone. Hesperidin methyl chalcone. Naringenin. Oxidative stress. Inflammation. UVB radiation.

LISTA DE FIGURAS

LISTA DE TABELAS

LISTA DE ABREVIATURAS

ABTS	2,2’ azinobis (3-etilbenzotiazolina-6-ácido sulfônico)
ANOVA	Análise de variância
AP-1	Ativador de proteína-1
APS	Persulfato de amônio
ARE	Elemento responsivo a antioxidante
BPX	Batofenantrolina
$CaCl_2$	Cloreto de cálcio
CAT	Catalase
DNA	Ácido desoxirribonucleico
$DPPH^{\bullet}$	2,2-difenil-1-picrilhidrazil
DTNB	Ácido 5,5’-ditio-bis-(2-nitrobenzóico)
EDTA	Ácido etilenodiamino tetra-acético
ELISA	Ensaio imunoenzimático
EPM	Erro padrão da média
ERK	Quinase regulada por sinal extracelular
EROs	Espécies reativas de oxigênio
Fe^{2+}	Ferro
$FeCl_3.6H_2O$	Cloreto férrico hexahidratado
FRAP	Poder antioxidante de redução férrica
GPx	Glutationa peroxidase
GR	Glutationa redutase
GSH	Glutationa reduzida
GSSG	Glutationa oxidada

HCl	Ácido clorídrico
HMC	Hesperidina metil chalcona
HO-1	Hemeoxigenase-1
H_2O	Água
H_2O_2	Peróxido de hidrogênio
HOCl	Ácido hipocloroso
H_3PO_4	Ácido ortofosfórico
HTAB	Brometo de hexadecil trietil amônio
IFN-γ	Interferon-gama
IL	Interleucina
i.p.	Intraperitoneal
JAK	Tirosinas quinases
JNK	Quinase c-Jun N-terminal
KCl	Cloreto de potássio
K_2HPO_4	Fosfato de potássio dibásico
KH_2PO_4	Fosfato de potássio monobásico
KOH	Hidróxido de potássio
LOOH	Hidroperóxidos lipídicos
LPO	Peroxidação lipídica
MAP	Proteína ativada por mitógeno
MDA	Malondialdeído
MMPs	Metaloproteinases da matriz
MPO	Mieloperoxidase
NaCl	Cloreto de sódio

NADPH	Nicotinamida adenina dinucleotídeo fosfato
NaOH	Hidróxido de sódio
NBT	*Nitroblue tetrazolium*
NF-κB	Fator nuclear kappa B
NGN	Naringenina
$NO^{\bullet}$	Radical óxido nitrico
NOX 2	NADPH oxidase 2
Nrf2	Fator nuclear eritróide 2 relacionado ao fator 2
O_2	Oxigênio molecular
$O_2^{\bullet-}$	Radical superóxido
$^1O_2$	Oxigênio singlete
O_3	Ozônio
OH	Hidroxila
$^{\bullet}OH$	Radical hidroxil
OPD	Ortofenilenodiamina
PBS	Tampão fosfato salino
PCR	Reação em cadeia da polimerase
RNAm	Ácido ribonucleico mensageiro
$RO_2^{\bullet}$	Radical peroxil
SDS	Dodecil sulfato de sódio
SDS-PAGE	Eletroforese em gel de poliacrilamida com duodecil sulfato de sódio
SOD	Superóxido dismutase
STAT	Transdutores de sinal e ativadores de transcrição
TBA	Ácido tiobarbitúrico

TBARS	Substâncias reativas ao ácido tiobarbitúrico
TCA	Ácido tricloro acético
TGF- β	Fator de transformação do crescimento *beta*
Th	*T helper*
TNF-α	Fator de necrose tumoral alfa
TPTZ	2,4,6 tripiridil-S-triazina
Tris	Hidroximetil aminometano
UV	Ultravioleta

SUMÁRIO

1 INTRODUÇÃO

1.1 PELE

A pele é um órgão altamente metabólico, com vários tipos de células e estruturas, que desempenha importante função na proteção do corpo humano. Com organização estratificada, é dividida em três camadas principais: epiderme, derme e hipoderme. A camada superior da pele é a epiderme um epitélio queratinizado, estratificado e escamoso. Os queratinócitos são as principais células (> 80%), mas há também melanócitos e células de Langerhans. Submetida à renovação contínua, a epiderme é subdividida em diferentes camadas não uniformes: estrato basal, estrato espinhoso, camada granulosa e a camada córnea, a mais externa da pele (KHAVKIN; ELLIS, 2011).

A derme situa-se abaixo da epiderme, une esta à hipoderme, e é constituída por tecido conjuntivo que confere elasticidade, firmeza e resistência à pele. É composta principalmente por colágeno e fibras elásticas (proteínas da matriz extracelular produzidas por fibroblastos), vasos sanguíneos e linfáticos, nervos e terminações nervosas, folículos pilosos e glândulas sebáceas e sudoríparas. Além de fibroblastos, a derme possui células relevantes imunologicamente como células dendríticas, macrófagos, mastócitos e linfócitos (HEATH; CARBONE, 2013). A hipoderme é composta por células adiposas que reforçam a estrutura do tecido conjuntivo e funciona como barreira protetora isolante (RITTIE; FISHER, 2002).

A pele está continuamente exposta a uma variedade de ataques químicos, biológicos e físicos que ameaçam a integridade de suas estruturas celulares. A radiação ultravioleta (RUV) é o fator físico mais abundante e a principal causa de danos na pele, o que em longo prazo pode resultar em lesões pré-cancerosas e cancerosas e aceleração do envelhecimento cutâneo (CASAGRANDE *et al.*, 2006a; TOUITOU; GODIN, 2008; QUAN *et al.*, 2009; AFAQ; KATIYAR, 2011).

1.2 RADIAÇÃO ULTRAVIOLETA

A RUV pode ser dividida em três regiões UVC (200 - 280 nm), UVB (280 - 320 nm) e UVA (320 - 400 nm). A UVC é a mais energética e causa grande dano biológico, porém, é praticamente toda retida pela camada de ozônio (AFAQ *et al.*, 2005a). A UVA e UVB penetram a atmosfera e são fatores causadores de diversas desordens cutâneas, incluindo o câncer de pele, porém a UVB é mais energética e cerca de mil vezes mais eficiente em causar queimaduras na pele (PAZ *et al.*, 2008). Estima-se que a cada 1% de destruição da

camada de ozônio há um aumento de 1-2% dos níveis de radiação UVB que alcança a superfície da Terra (BALOGH *et al.*, 2011).

Para manifestar efeitos nas células da pele, a energia eletromagnética da RUV é absorvida pelos cromóforos celulares e convertida em energia química. Cromóforos celulares como ácido desoxirribonucléico (DNA), ácido ribonucléico (RNA), melanina, proteínas, e aminoácidos aromáticos são capazes de absorver energia da RUV. Estes cromóforos energizados podem reagir com oxigênio molecular (O_2), resultando na geração de espécies reativas de oxigênio (EROs), que levam a um desequilíbrio do estado oxidativo da pele (XU; FISHER, 2005). Ambas as radiações UVA e UVB induzem a formação de EROs e causam danos cutâneos, porém a UVB causa também danos diretos ao DNA, RNA, proteínas e outros componentes da célula, sendo absorvida principalmente pelo DNA dos queratinócitos, e desta forma é mais relevante para a fotocarcinogênese (EMRI *et al.*, 2006).

1.3 RADICAIS LIVRES E ESTRESSE OXIDATIVO

Em sistemas biológicos, radicais livres são derivados principalmente do O_2 e por isso são denominados EROs. Radicais livres são moléculas que contêm um ou mais elétrons não pareados, altamente instáveis, com meia-vida curtíssima e quimicamente muito reativas (HALLIWELL, 1999). Entre as EROs destacam-se o radical superóxido ($O_2^{\bullet-}$), o radical hidroxil ($^{\bullet}OH$), o radical óxido nítrico ($NO^{\bullet}$), o radical peroxil ($RO_2^{\bullet}$), e algumas espécies reativas não radicalares como o peróxido de hidrogênico (H_2O_2), ácido hipocloroso (HOCl), e oxigênio singlete ($^1O_2$), que apesar de não possuírem elétron livre, podem facilmente sofrer reações e formar radicais livres (HALLIWELL, 2009).

Os radicais livres são produzidos fisiologicamente como, por exemplo, na respiração, ou em algumas células mediadoras da função imune. Porém, o excesso destas moléculas pode causar danos celulares e outras alterações bioquímicas como inflamação, ativação e inativação de certas enzimas e indução de reações de oxidação em diferentes biomoléculas (SHINDO *et al.*, 1994; PIETTA, 2000).

Em condições basais o $O_2^{\bullet-}$ é produzido em baixas quantidades e convertido em O_2 e H_2O_2 pela atividade da superóxido dismutase (SOD). No entanto, após exposição excessiva à radiação UVB, mediadores inflamatórios são responsáveis por uma produção adicional de $O_2^{\bullet-}$ via ativação da enzima nicotinamida adenina dinucleotídeo fosfato (NADPH) oxidase 2 (NOX 2) (AFAQ *et al.*, 2005a; CIRCU; AW, 2010; CAMPANINI *et al.*, 2014). Uma das sub-unidades da NADPH oxidase é a gp91phox, que catalisa a transferência de elétron ao O_2 e está diretamente envolvida na produção de $O_2^{\bullet-}$ induzida pela radiação UVB (TAKEYA; SUMIMOTO, 2003; HIRAMOTO *et al.*, 2012). A produção de EROs pela gp91phox é uma

etapa crítica e inicial para o estabelecimento do estresse oxidativo (ANRATHER *et al.*, 2006).

As células da pele possuem vários mecanismos de defesa contra as EROs induzidas pela RUV (HALLIWELL, 2009). O sistema de defesa é composto por dois grupos principais, os antioxidantes enzimáticos como a SOD, a catalase (CAT), a glutationa peroxidase (GPx) e a glutationa redutase (GR) e os antioxidantes de baixo peso molecular, como glutationa reduzida (GSH), o ácido ascórbico e o tocoferol (KOHEN, 1999; VICENTINI *et al.*, 2008; ROBBINS; ZHAO, 2011). Estes mecanismos de defesa antioxidante são complementares uns aos outros, e na pele se concentram na epiderme, visto ser a camada mais exposta às agressões (FUCHS, 1998).

A capacidade destes mecanismos de defesa antioxidante é limitada e pode ser prejudicada pela exposição excessiva à radiação UVB. Antioxidantes endógenos podem ser diretamente consumidos ou inativados pela exposição à RUV. Dessa forma, quando a produção de EROs excede a capacidade das células de reduzi-las quimicamente, a concentração de radicais livres aumenta incontrolavelmente, rompendo o equilíbrio oxidante/antioxidante no organismo em favor do primeiro (estresse oxidativo), com consequente danos nos lipídios de membrana, proteínas e ácidos nucléicos das células epidérmicas e dérmicas, que interrompe as funções celulares e em última instância leva a morte das células (HALLIDAY, 2005; VICENTINI *et al.*, 2008; PETROVA *et al.*, 2011; CAMPANINI *et al.*, 2014; IVAN *et al.*, 2014).

Vários estudos mostram que o dano cutâneo induzido pela radiação UVB resulta na depleção do tripeptídeo GSH, o antioxidante não enzimático produzido em maior quantidade pelas células epidérmicas (CARINI *et al.*, 2000; CASAGRANDE *et al.*, 2006a; CAMPANINI *et al.*, 2013; IVAN *et al.*, 2014). O grupamento sulfidrila deste composto permite a neutralização de radicais livres diretamente pela transferência de hidrogênio (CARINI *et al.*, 2000).

A depleção do GSH ocorre diretamente pelo seu uso em neutralizar EROs, ou também indiretamente pelo seu uso como substrato da GPx durante a detoxificação celular. Usando GSH a GPx catalisa a redução de EROs e produz a glutationa oxidada (GSSG). A glutationa redutase (GR) é a enzima responsável pela regeneração da GSH, por meio da redução da GSSG a GSH (HALLIWELL, 2009). Contudo, a exposição à RUV reduz a atividade da GR, impedindo a manutenção dos níveis fisiológicos de GSH, e também reduz a atividade de outras enzimas antioxidantes importantes, como a GPx e a CAT (LOPEZ-TORRES *et al.*, 1998). A CAT é uma enzima que converte H_2O_2 em O_2 e H_2O (CHELIKANI *et al.*, 2004). Com a depleção dos antioxidantes enzimáticos induzida pela RUV, há aumento excessivo dos níveis de H_2O_2 e $O_2^{\bullet-}$ que se torna prejudicial, uma vez que estas EROs

podem gerar derivados mais citotóxicos, como o radical $^{\bullet}OH$ (CHELIKANI *et al.*, 2004; SULLIVAN *et al.*, 2012).

A regulação dos sistemas de defesa antioxidante ao estresse oxidativo envolve diferentes moléculas sinalizadoras, dentre as quais se destaca o fator de transcrição Nrf2 (fator nuclear [derivado eritróide-2] tipo 2). Este fator regula a transcrição de genes para moléculas antioxidantes e anti-inflamatórias como a hemeoxigenase-1 (HO-1), a qual quebra o grupamento heme em biliverdina que apresenta efeito antioxidante e em monóxido de carbono que apresenta efeito anti-inflamatório (CHOI *et al.*, 2013). Neste contexto, o aumento da expressão da HO-1 tem sido descrita como uma abordagem promissora contra os danos cutâneos induzidos pela radiação (ZHANG *et al.*, 2012).

Em resposta a diferentes estímulos como EROs, metais e RUV, o Nrf2 se liga ao elemento responsivo a antioxidante (ARE), sequência presente nas regiões promotoras de diversos genes (KOBAYASHI; YAMAMOTO, 2005). A interação do Nrf2 com o ARE é um mecanismo molecular que regula a transcrição de enzimas antioxidantes como SOD, CAT, GPx e HO-1 e de detoxificação de fase 2 como glutationa-S-transferase e quinona redutase, as quais tem como função proteger contra o estresse oxidativo, inflamação e carcinogênese (KOBAYASHI; YAMAMOTO, 2005).

A inibição da atividade do Nrf2 aumenta os danos cutâneos induzidos pela radiação UVB, por exemplo, devido ao aumento da produção de mediadores inflamatórios como interleucina (IL)-1β, IL-6 (SAW *et al.*, 2011) e metaloproteinase-9 (SAW *et al.*, 2014). Assim, compostos que ativam a via Nrf2 se tornam uma estratégia terapêutica para controlar doenças cutâneas, como o câncer (KUMAR *et al.*, 2011; CHUN *et al.*, 2014).

O excesso de EROs pode desencadear uma incontrolável reação em cadeia de peroxidação lipídica (LPO), um processo prejudicial, consequente da exposição à radiação UVB, e que induz a produção de produtos pró-inflamatórios (GIROTTI, 2001; HALLIDAY, 2005). A LPO leva a uma desorganização da membrana celular com liberação de ácido graxo como o ácido araquidônico a partir de fosfolipídios, o que desencadeia aumento da fosfolipase A2 e da cicloxigenase-2 (COX-2), resultando em níveis aumentados de prostaglandinas, incluindo a prostaglandina E_2 (PGE_2) e inflamação na pele (HALLIDAY, 2005).

1.4 RESPOSTA INFLAMATÓRIA

Após a exposição da pele à RUV os queratinócitos iniciam a inflamação cutânea por meio da imunidade inata, conduzida por citocinas e mediada inicialmente pela IL-1α. Paralelamente induz a amplificação da resposta inflamatória, por meio da imunidade

adaptativa, o qual promove interações entre os linfócitos, células de Langerhans, células dendríticas, macrófagos e demais células imunes residentes na pele (DEBENEDICTIS *et al.*, 2001). Os mediadores inflamatórios induzidos pela radiação UVB, promovem a atração de diferentes tipos celulares à epiderme (WITKO-SARSAT *et al.*, 2000; FILIP *et al.*, 2011). Em geral, os neutrófilos são as primeiras células recrutadas durante a inflamação aguda. Um dos produtos principais dos neutrófilos é a enzima mieloperoxidase (MPO), estocada em grande quantidade nestas células. Esta enzima produz ácido hipocloroso como um mecanismo de defesa celular contra agentes infecciosos (WITKO-SARSAT *et al.*, 2000). Adicionalmente, o sistema microbicida dos neutrófilos depende também de EROs geradas pela NADPH oxidase (HIRAMOTO *et al.*, 2012). Contudo, na ausência de um processo infeccioso, como ocorre durante a inflamação induzida pela radiação UVB, os neutrófilos representam uma fonte adicional de EROs e, dessa forma, intensificam o dano tecidual.

Neutrófilos também podem produzir metaloproteinases (MMPs), que são uma grande família de endopeptidases dependente de zinco, capazes de degradar as proteínas da matriz extracelular da derme e das membranas basais, e são altamente relacionadas com o potencial metastático e invasivo de células cancerígenas (JOHN; TUSZYNSKI, 2001). Outros tipos de células presentes na pele como queratinócitos, fibroblastos, monócitos, macrófagos e células endoteliais, durante a inflamação induzida por RUV, também produzem MMPs.

A RUV induz a expressão de genes da MMP-2 (gelatinase A) e da MMP-9 (gelatinase B), as quais têm sido associadas com o desenvolvimento de câncer de pele e fotoenvelhecimento (FISHER *et al.*, 1997; STANIFORTH *et al.*, 2012). A MMP-9 degrada o colágeno e os componentes das fibras elásticas (JENKINS, 2002). EROs e mediadores inflamatórios, como as citocinas, induzem a expressão das MMPs (CHOU *et al.*, 2010; J. ZHANG *et al.*, 2013). Ademais, os fatores de transcrição proteína ativadora-1 (AP-1) e fator de transcrição nuclear kappa B (NF-κB) ativados pela RUV, induzem a secreção de MMP-9/2 (VICENTINI *et al.*, 2011).

O NF-κB é um fator de transcrição sensível ao estresse oxidativo, com a função de regular a expressão de genes envolvidos na resposta inflamatória (FUCHS *et al.*, 2001; VICENTINI *et al.*, 2011). Sinais extracelulares como RUV, citocinas, alteração do estado redox, EROs ativam o NF-κB (IVAN *et al.*, 2014), o qual induz a transcrição de genes que codificam diferentes citocinas e moléculas de adesão celular, que promovem a ativação e recrutamento de células inflamatórias, além da liberação de proteases (CARINI *et al.*, 2000; VICENTINI *et al.*, 2011; HIRAMOTO *et al.*, 2012).

Neste contexto, o estresse oxidativo induzido pela radiação UVB provoca uma inflamação cutânea via amplificação inapropriada de vias de sinalização intracelular (HALLIDAY, 2005). A RUV induz a ativação das subfamílias de proteínas quinases ativadas

por mitógenos (MAP quinases), como a quinase regulada por sinal extracelular (ERK), quinase p38 e quinase c-Jun N-terminal (JNK), as quais são de grande importância no processo de ativação e controle da expressão gênica, por exemplo, ativam o NF-κB, AP-1, NADPH oxidase e induzem o recrutamento de leucócitos (HERLAAR; BROWN, 1999; HUSSEIN, 2005; VICENTINI *et al.*, 2011; CHOI *et al.*, 2014). A exposição à radiação UVB também ativa transdutores de sinal e ativadores de transcrição (STATs), os quais após fosforilação pelas tirosinas quinases (JAK), entram no núcleo para regular a transcrição de vários genes como de fatores de crescimento e de citocinas (AHSAN *et al.*, 2005).

1.4.1 Citocinas

A radiação UVB induz a produção de diversas citocinas pelos diferentes tipos de células da pele como queratinócitos, melanócitos e células de Langerhans da epiderme, fibroblastos, células endoteliais, células dendríticas, mastócitos, linfócitos e outras células inflamatórias da derme (KONDO, 2000). São exemplos de citocinas pró-inflamatórias induzidas pela radiação UVB: fator de necrose tumoral alfa (TNF-α) (MUTOU *et al.*, 2007; VICENTINI *et al.*, 2011; LOU *et al.*, 2013), IL-1β (CAMPANINI *et al.*, 2013; IVAN *et al.*, 2014), IL-6 (VICENTINI *et al.*, 2011; SUN *et al.*, 2014), interferon *gamma* (IFN-γ) (MUTOU *et al.*, 2007; YOKOGAWA *et al.*, 2013), IL-12 (YOKOGAWA *et al.*, 2013), IL-4 (MUTOU *et al.*, 2007), IL-5 (MUTOU *et al.*, 2007), IL-17 (YOKOGAWA *et al.*, 2013) e IL-23 (YOKOGAWA *et al.*, 2013) e anti-inflamatórias: IL-10 (MUTOU *et al.*, 2007; LOU *et al.*, 2013) e fator de transformação do crescimento beta (TGF-β) (SUN *et al.*, 2014).

A IL-1α liberada pelos queratinócitos após exposição à radiação UVB, sinaliza os queratinócitos vizinhos, os quais produzem mais IL-1α, assim como IL-1β, TNF-α e IL-6, que iniciam uma série de eventos como indução de quimiocinas e citocinas, aumento da expressão de moléculas de adesão e infiltração de células inflamatórias como os neutrófilos e linfócitos (DEBENEDICTIS *et al.*, 2001; JENKINS, 2002; STRIZ *et al.*, 2014).

Os linfócitos são subdivididos em células T auxiliadoras (Th do inglês *T helper*) baseados no painel de citocinas que secretam. Células Th1 (secretam, por exemplo, IFN-γ e IL-12) são importantes na defesa mediada por fagocitose e estão envolvidas em várias doenças auto-imunes específica de órgão e doenças inflamatórias crônicas (COSMI *et al.*, 2014). Células Th2 (secretam IL-4, IL-5 e IL-13) são responsáveis pela iniciação, manutenção e amplificação de doenças alérgicas e são importantes em pacientes com asma (COSMI *et al.*, 2014). Células Th17 ativadas pela IL-23 (secretam IL-17 e IL-22) estão envolvidas em doenças inflamatórias e auto-imune como artrite reumatóide, esclerose

múltipla, doença intestinal inflamatória, psoríase, dermatite de contato alérgica e outras doenças cutâneas inflamatórias (PEISER, 2013; COSMI *et al.*, 2014).

As citocinas anti-inflamatórias IL-10 e TGF-β são produzidas por células T regulatórias (Tregs), com a função de regular negativamente a resposta imune (HAN *et al.*, 2014). No entanto, a IL-10 pode estar envolvida em doenças mediada por anticorpos e está associada com danos ao DNA e imunossupressão induzida pela radiação UVB (PISKIN *et al.*, 2005; HASEGAWA *et al.*, 2013). E a produção de TGF-β está envolvida no melanoma (DURÁN-ANIOTZ *et al*., 2013), além de possuir função importante em lesões fibrosas e na pele promove a remodelagem tecidual e neovascularização via indução da MMP-9 (LAMAR *et al.*, 2008). Neste contexto, a inibição da produção de diferentes padrões de citocinas é considerada uma estratégia terapêutica promissora contra várias doenças (VICENTINI *et al.*, 2011; LOU *et al.*, 2013; COSMI *et al.*, 2014; STRIZ *et al.*, 2014; SUN *et al.*, 2014). Ainda, citocinas induzem a produção de outras citocinas, e a inibição dos efeitos das citocinas limita a amplificação deste sistema (PORATH *et al.*, 2005).

É importante destacar que, existe um ciclo de estimulação recíproca entre citocinas e EROs, por exemplo, citocinas como o TNF-α são um dos fatores responsáveis pela produção adicional de $O_2^{\bullet-}$ via ativação da NADPH oxidase (KILPATRICK *et al.*, 2010). Por outro lado, a produção de $O_2^{\bullet-}$ é essencial para induzir a produção de citocinas e manter o direcionamento de neutrófilos (BOWIE; O'NEILL, 2000; HATTORI *et al.*, 2010). Ademais, os neutrófilos são a principal fonte da produção adicional de $O_2^{\bullet-}$ via atividade da NADPH oxidase (NATHAN; SHILOH, 2000), o que explica em parte a excessiva geração de EROs e depleção antioxidante após exposição à radiação UVB (CAMPANINI *et al.*, 2014). Portanto, o estresse oxidativo e a inflamação induzidos pela RUV estão intimamente relacionados e levam a um círculo vicioso, que resulta em danos teciduais e em longo prazo, pode conduzir a carcinogênese (REUTER *et al.*, 2010).

Considerando o contexto exposto acima, a RUV exerce múltiplos efeitos nas células da pele, sendo a interação entre tais efeitos determinante na resposta gerada pela exposição à radiação (WANG; KOCHEVAR, 2005). Normalmente, a exposição aguda à RUV pode causar queimaduras, eritemas dolorosos, edema, danos no DNA, degradação do tecido conectivo e alteração da função imune; já a exposição crônica, resulta em foto-envelhecimento, queda imunológica, podendo finalmente levar ao câncer de pele (FUCHS, 1998; AFAQ *et al.*, 2005a; YAAR; GILCHREST, 2007; AFAQ; KATIYAR, 2011). A incidência dessas doenças de pele cresce continuamente, à medida que a estimativa de vida da população aumenta e maiores quantidades de RUV atingem a superfície da Terra em decorrência da destruição da camada de ozônio (MANTENA; KATIYAR, 2006).

1.5 ANTIOXIDANTES EXÓGENOS

Estudos epidemiológicos indicam que os protetores solares não são totalmente efetivos em prevenir os danos cutâneos induzidos pela RUV (COOPER *et al.*, 2005). Considerando que, à exposição à RUV é difícil de ser evitada, agentes quimiopreventivos para prevenção e/ou tratamento dos danos cutâneos induzidos pela radiação UVB precisam ser identificados, desde que o câncer de pele é um problema significativo associado com mortalidade e morbidade. Segundo o INCa (2014), Instituto Nacional do Câncer, o câncer de pele não melanoma é o tumor mais incidente no país em ambos os sexos.

Levando em consideração o efeito sinérgico da produção de EROs e de mediadores inflamatórios, a melhora do sistema antioxidante endógeno se torna uma abordagem promissora para prevenir e/ou tratar os danos cutâneos induzidos pela radiação UVB. Neste contexto, torna-se relevante a avaliação de antioxidantes exógenos para enriquecer o sistema de proteção endógeno e assim controlar os danos cutâneos induzidos pela radiação UVB (CASAGRANDE *et al.*, 2006a; FILIP *et al.*, 2011; PETROVA *et al.*, 2011; CAMPANINI *et al.*, 2013; CAMPANINI *et al.*, 2014; K. S. CHOI *et al.*, 2014; IVAN *et al.*, 2014; SUN *et al.*, 2014).

Substâncias podem atuar como antioxidantes por diferentes mecanismos, por exemplo, neutralização direta de EROs, quelação de metais, aumento de antioxidantes de baixo peso molecular, ativação de genes que codificam enzimas antioxidantes e consequentemente aumento de enzimas antioxidantes e também pela inibição de oxidases (KOHEN, 1999; PROCHAZKOVA *et al.*, 2011).

Atenção tem sido dada aos antioxidantes de fontes naturais, por exemplo, os polifenóis, os quais além de propriedades antioxidantes muitos possuem propriedades anti-inflamatórias, e consequentemente, reduzem os danos cutâneos oxidativos e inflamatórios induzidos pela radiação UVB (PIETTA, 2000; CASAGRANDE *et al.*, 2006a; NICHOLS; KATIYAR, 2010; AFAQ, 2011; VICENTINI *et al.*, 2011; STANIFORTH *et al.*, 2012; CAMPANINI *et al.*, 2013; CHOI *et al.*, 2014). Ainda, os compostos naturais de maneira geral são de baixo custo e, portanto, considerados abordagens terapêuticas promissoras em controlar diversas doenças humanas (DHANALAKSHMI *et al.*, 2004; ZHOU *et al.*, 2009).

1.5.1 Flavonóides

Os flavonóides representam o grupo mais comum e amplamente distribuído de compostos fenólicos sintetizados nas plantas (BOHM *et al.*, 1998). A estrutura básica dos flavonóides consiste em 15 átomos de carbono arranjados em três anéis (C6-C3-C6),

nomeados A, B e C (Figura 1). As várias classes de flavonóides diferem no grau de oxidação e padrão de substituição do anel central, e compostos da mesma classe diferem no padrão de substituição dos anéis A e B (BOHM *et al.*, 1998). As principais classes dos flavonóides são: chalconas, flavanonas, flavonas, isoflavonas, flavonóis, flavanonóis, flavan-3-óis, antocianidinas e auronas (VERRI *et al*., 2012).

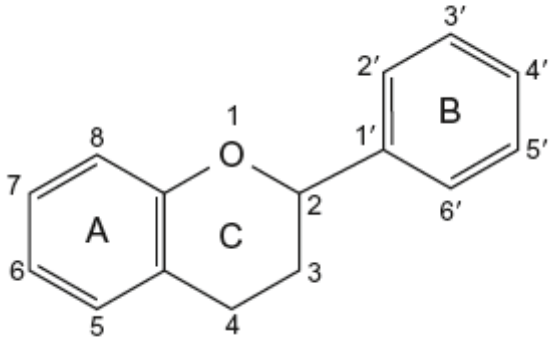

Figura 1. Estrutura básica dos flavonóides.

Os flavonóides estão presentes em frutas, vegetais, chás, café e vinho tinto, e por isso são ingeridos diariamente. Podem ser não glicosilados ou glicosilados, estes sofrem hidrólise para que sejam absorvidos e se tornem biologicamente ativos (VERRI *et al*., 2012). A estrutura química dos flavonóides confere um baixo potencial redox e uma alta probabilidade em transferir elétrons nas reações, o que tem sugerido o uso potencial destas substâncias como agentes terapêuticos (BOHM *et al.*, 1998).

As características estruturais, requisitos determinantes dos flavonóides em relação às atividades biológicas, incluem a ligação dupla 2,3 em conjugação com a função 4-oxo e a presença de substituintes hidroxilas (OH) nos carbonos 5, 7 e 3 e no anel B nos carbonos 3’ e 4’ (grupo catecol) (BORS *et al.*, 1990; SAIJA *et al.*, 1995; VAN ACKER *et al.*, 1996; SUGIHARA *et al.*, 1999; BURDA; OLESZEK, 2001; LEMANSKA *et al.*, 2001). Substituintes OH permitem que os flavonóides doem elétrons aos radicais livres, permitindo adquirir uma estrutura estável e, portanto, neutralizando radicais livres (HEIM *et al.*, 2002).

Diversos estudos demonstraram que os flavonóides possuem várias atividades biológicas importantes como: antioxidante, anti-inflamatória, analgésica, anti-cancerígena e antimicrobiana (IWATA *et al.*, 1995; BOHM *et al.*, 1998; DUTHIE; CROZIER, 2000; PIETTA, 2000; LEE *et al.*, 2001; CASAGRANDE *et al.*, 2006a; PARI; GNANASOUNDARI, 2006; SHEN *et al.*, 2007; JAYARAMAN *et al.*, 2009; VAFEIADOU *et al.*, 2009; KUMAR *et al.*, 2011; LIM *et al.*, 2011; SIKANDER *et al.*, 2011; VICENTINI *et al.*, 2011; YADAV *et al.*, 2011; YANG *et al.*, 2011; T. H. KIM *et al.*, 2013; LIN; SHIH, 2014; VERRI *et al*., 2012).

Os flavonóides além de apresentarem propriedades antioxidantes, por meio da neutralização direta de EROs (BORS *et al.*, 1990), quelação de metais (CASAGRANDE *et al.*, 2006b), aumento de antioxidantes endógenos (RENUGADEVI; PRABU, 2009; BARCELOS *et al.*, 2011), ativação de genes que codificam enzimas antioxidantes (KUMAR et al., 2011) e/ou inibição de oxidases (CAMPANINI *et al.*, 2013), também podem reduzir a resposta inflamatória, por exemplo, por reduzir a produção de diferentes citocinas e a atividade de enzimas como MPO e MMP-9 (CASAGRANDE *et al.*, 2006a; S. Y. PARK *et al.*, 2012; AL-REJAIE *et al.*, 2013; RAZA *et al.*, 2013; BAI *et al.*, 2014; LIN; SHIH, 2014). Os flavonóides podem reduzir a produção de citocinas por inibir a sinalização do NF-κB e/ou por inibir a atividade da NOX 2 (VICENTINI *et al.*, 2011; H. Y. PARK *et al.*, 2012; S. Y. PARK *et al.*, 2012; CAMPANINI *et al.*, 2013; DOU *et al.*, 2013). Ainda, flavonóides podem inibir MAP quinases como ERK, p38 e/ou JNK e consequentemente reduzir a produção de mediadores inflamatórios e EROs (NAM *et al.*, 2008; VAFEIADOU *et al.*, 2009; YANG *et al.*, 2011).

É importante que as terapias para o controle da inflamação e estresse oxidativo induzidos pela radiação UVB tenham como alvo os mecanismos fisiopatológicos da radiação UVB. Neste contexto, fica evidente que os mecanismos envolvidos nos danos cutâneos induzidos pela radiação UVB como o recrutamento de neutrófilos, produção de citocinas, estresse oxidativo, bem como mecanismos que reduzem os danos na radiação UVB como a indução do Nrf2 e da HO-1, são mecanismos passíveis de serem alvos ou induzidos, respectivamente, por flavonóides.

Dependendo da concentração utilizada e da estrututa química os flavonóides podem inibir diversas vias de sinalização intracelular e interferir na ação de diferentes biomoléculas que participam do estresse oxidativo e inflamação, o que sugere o potencial destes compostos em controlar os danos cutâneos induzidos pela radiação UVB. No entanto, nem todos os flavonóides apresentam os mesmos efeitos biológicos descritos na literatura, assim cada flavonóide deve ser avaliado individualmente com a utilização de diferentes ensaios *in vitro* e *in vivo*.

1.5.1.1 *Trans-chalcona*

As chalconas quimicamente conhecidas como 1,3-difenil-2-propen-1-ona são intermediários comuns considerados precursores na biossíntese dos flavonóides e encontrados frequentemente em quantidades significativas em plantas de uso terapêutico (DUTHIE; CROZIER, 2000; NOWAKOWSKA, 2007; YADAV *et al.*, 2011). O isômero trans

da chalcona (Figura 2) é considerado a forma mais estável termodinamicamente e, portanto, o produto majoritário nas plantas (HIJOVA, 2006).

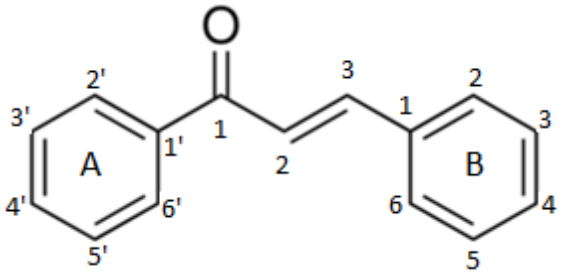

Figura 2. Estrutura química da trans-chalcona.

As chalconas são quimicamente conhecidas como cetonas α-β-insaturadas, e a presença da ligação dupla 2,3 em conjugação com a função 1-oxo é a característica química importante a qual se atribui uma série de atividades biológicas (HIJOVA, 2006; NI *et al.*, 2004). Evidências indicam que a estrutura cetona α,β-insaturada das chalconas é importante para atividade anti-cancerígena (ANTO *et al.*, 1995; IWATA *et al.*, 1995; YADAV *et al.*, 2011), anti-inflamatória (YADAV *et al.*, 2011;YAMAZAKI *et al.*, 2012) e antioxidante em cultura de células (FORESTI *et al.*, 2005; YADAV *et al.*, 2011). Ainda, a redução desta dupla ligação das chalconas leva a perda parcial ou total dos seus efeitos biológicos (FUNAKOSHI *et al*., 2010; SINGH *et al*., 2014; ZHAO *et al*., 2003).

A trans-chalcona (TC) inibiu a atividade da MPO, a expressão de TNF-α, a produção de IL-6 e a translocação do NF-κB para o núcleo celular na colite induzida com ácido trinitrobenzeno sulfônico em ratos (PARK *et al.*, 2012). Em outro estudo a TC reduziu o edema de pata induzido pela formalina (RAZMI *et al.*, 2013). Shen et al. (2007), constataram que a TC inibiu a proliferação de cultura de células cancerígenas humanas por inibir a ativação do NF-κB, via aumento da expressão do I-κB (proteína inibitória kappa B) no citoplasma. Lin et al. (2014) demonstraram que a TC inibiu a expressão de MMP-2/-9 em células do adenocarcinoma gástrico humano por inibir a via de sinalização JNK. A TC também foi capaz de inibir a neovascularização da retina por inibir a expressão do fator de crescimento do endotélio vascular (VEGF) e moléculas de adesão intercelular-1 (ICAM-1), e estes efeitos foram correlacionados com a inibição do NF-κB e STAT3 (LAMOKE *et al.*, 2011). Ainda, a TC aumentou os níveis de GSH em células de fígados de ratos (WHITE *et al.*, 1998), e inibiu a LPO e a depleção de GSH e outros antioxidantes celulares no estresse oxidativo induzido por H_2O_2 em células do carcinoma hepatocelular (SIKANDER *et al.*, 2011).

Ademais, a estrutura cetona α,β-insaturada da TC foi atribuída como responsável pela inibição da produção de TNF-α e NO em macrófagos estimulados com lipopolissacarídeo (YAMAZAKI *et al*., 2012) e pela ativação da via Nrf2/ARE e consequentemente indução de enzimas antioxidantes e de detoxificação em cultura de células (FORESTI *et al.*, 2005; KUMAR *et al.*, 2011).

Apesar da estrutura química da TC não possuir substituintes OH, conhecidos como os grupamentos importantes para atividade antioxidante, estudos demonstraram a eficácia antioxidante deste flavonóide em cultura de células (WHITE *et al.*, 1998; SIKANDER *et al.*, 2011). No entanto, os efeitos da TC nos danos cutâneos oxidativos e inflamatórios induzidos pela radiação UVB ainda não foram descritos na literatura.

1.5.1.2 *Hesperidina metil chalcona*

Flavanonas pertencem a uma classe de flavonóides encontradas em quantidades significativas em frutas cítricas, portanto, estas frutas e os seus respectivos sucos são a maior fonte de flavanonas ingeridos pelo homem. Muitos dos efeitos benéficos do consumo do suco de laranja têm sidos atribuídos a presença da quantidade elevada da flavanona hesperidina (MANACH *et al.*, 2003). A hesperidina possui efeitos antioxidantes e anti-inflamatórios (GALATI *et al.*, 1994; PARHIZ *et al.*, 2014), no entanto, assim como outros flavonóides sua absorção intestinal é baixa. A metilação de flavonóides aumenta a estabilidade metabólica, biodisponibilidade oral, distribuição tecidual, e ainda a inibição da proliferação de células cancerígenas (WALLE, 2007). A metilação da flavanona hesperidina em condições alcalinas produz a hesperidina metil chalcona (HMC) (GIL-IZQUIERDO *et al.*, 2001), uma chalcona com melhor distribuição e resistência metabólica em comparação a hesperidina.

A HMC é uma chalcona glicosídica (Figura 3), conhecida por apresentar efeitos vasoprotetores (CLUZAN *et al.*, 1996; BELTRAMINO *et al.*, 1999; BOUAZIZ *et al.*, 1999; BELTRAMINO *et al.*, 2000; BOYLE *et al.*, 2003; STOIANOVA, 2006; AGUILAR PERALTA *et al.*, 2007; GUEX *et al.*, 2009; PORTO *et al.*, 2009; GUEX *et al.*, 2010; ALLAERT *et al.*, 2011). A estrutura química da HMC apresenta: 2,3 ligação dupla conjugada com a função 1-oxo e a presença de OH nos carbonos 3 e 2’ que podem ser importantes para sua atividade farmacológica.

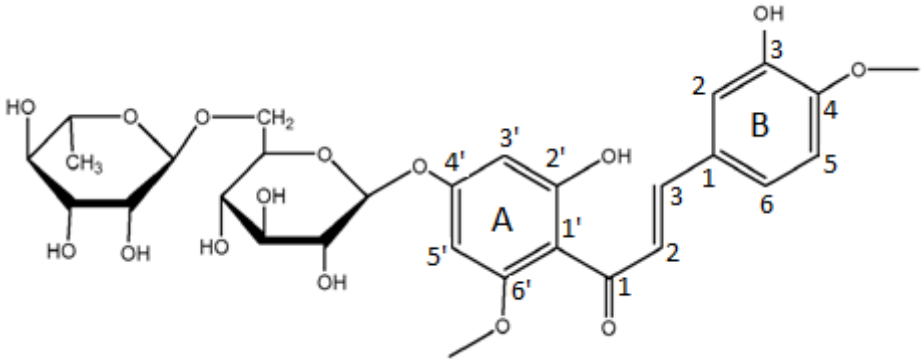

Figura 3. Estrutura química da hesperidina metil chalcona.

Devido a atividade vasoprotetora a HMC é encontrada em medicamentos usados para tratar clinicamente insuficiência venosa crônica como Cyclo 3 Fort® (150 mg do extrato das raízes de *Ruscus aculeatus*, 150 mg de HMC e 100 mg de ácido ascórbico, por cápsula) (CLUZAN *et al.*, 1996; BELTRAMINO *et al.*, 1999; BELTRAMINO *et al.*, 2000; BOYLE *et al.*, 2003; STOIANOVA, 2006; ALLAERT *et al.*, 2011) e Cirkan® (40 mg do extrato das raízes de *Ruscus aculeatus*, 100 mg de HMC e 200 mg e ácido ascórbico, por cápsula) (AGUILAR PERALTA *et al.*, 2007; LASCASAS-PORTO *et al.*, 2008; PORTO *et al.*, 2009). O tratamento com HMC em associação com ácido ascórbico e *Ruscus aculeatus* por 12 semanas melhorou a qualidade de vida e reduziu significativamente os sintomas clínicos de pacientes com insuficiência venosa crônica (GUEX *et al.*, 2009; GUEX *et al.*, 2010).

A HMC melhorou o tônus vascular em animais (TARAYRE; LAURESSERGUES, 1976; TARAYRE; LAURESSERGUES, 1977) e em pacientes com estresse cardíaco (RUDOFSKY, 1989), inibiu o edema de pata induzido pela carragenina em ratos (GABOR; RAZGA, 1991) e inibiu o aumento da permeabilidade vascular induzida por vários agentes em modelo animal (BOUSKELA *et al.*, 1993).

Sabe-se que distúrbios no fluxo sanguíneo resultam em inflamação e levam a um círculo vicioso de inflamação crônica observado na insuficiência venosa crônica (TAKASE *et al.*, 1999). Apesar dos efeitos antioxidantes e anti-inflamatórios dos flavonóides (CAZAROLLI *et al.*, 2008; VERRI *et al.*, 2012; J. PETERSON 1998), e do uso clínico da HMC em condições inflamatórias (CLUZAN *et al.*, 1996; BELTRAMINO *et al.*, 1999; BELTRAMINO *et al.*, 2000; BOYLE *et al.*, 2003; STOIANOVA, 2006; AGUILAR PERALTA *et al.*, 2007; GUEX *et al.*, 2009; PORTO *et al.*, 2009; GUEX *et al.*, 2010; ALLAERT *et al.*, 2011), os efeitos deste flavonóide no estresse oxidativo e inflamação cutânea ainda não foram descritos na literatura.

É importante mencionar que, o tratamento com a HMC mostrou-se seguro em pacientes que receberam 150 mg de HMC diariamente por 90 dias (BELTRAMINO *et al.*,

1999; BELTRAMINO *et al.*, 2000). A HMC também se mostrou segura quando administrada em doses elevadas, como 15 g por dia (KIRTLEY; PECK, 1948), e não demonstrou efeitos citotóxicos *in vitro* (KIM *et al.*, 2013), o que enfatiza a possibilidade de aplicação terapêutica da HMC.

1.5.1.3 *Naringenina*

A naringenina (5,7,4′,-trihidroxi flavanona) (NGN) é uma das mais abundantes flavanonas encontradas em frutas como limão, laranja e tangerina (LEE *et al.*, 2001). A NGN possui em sua estrutura química OH nos carbonos 5, 7 e 4' e o grupo 4 ceto que podem ser importantes para sua atividade farmacológica (Figura 4).

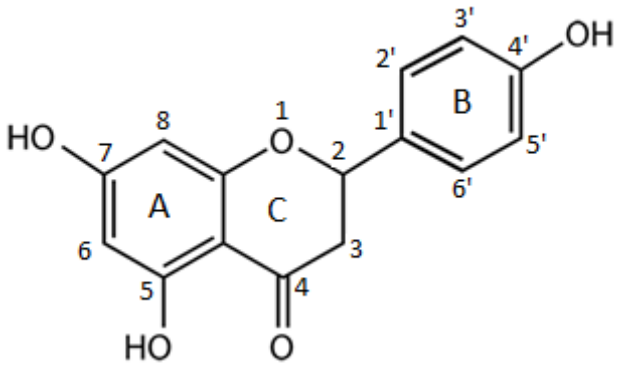

Figura 4. Estrutura química da naringenina

Vários estudos mostraram que a NGN possui diversas atividades farmacológicas importantes como antioxidante, anti-inflamatória, anti-cancerígena e anti-aterogênica (LEE *et al.*, 2001; PARI; GNANASOUNDARI, 2006; EL-MAHDY *et al.*, 2008; JAYARAMAN *et al.*, 2009; RENUGADEVI; PRABU, 2009; VAFEIADOU *et al.*, 2009; YEN *et al.*, 2009; IWAMURA *et al.*, 2010; ORSOLIC *et al.*, 2011; PARK *et al.*, 2012; AL-REJAIE *et al.*, 2013; AZUMA *et al.*, 2013; DOU *et al.*, 2013; HERMENEAN *et al.*, 2013; KIM *et al.*, 2013; MERSHIBA *et al.*, 2013; RAZA *et al.*, 2013; SUBRAMANIAN; ARUL, 2013; C. XU *et al.*, 2013; YILMA *et al.*, 2013; BAI *et al.*, 2014; XU *et al.*, 2014). *In vitro* a NGN reduz o radical ABTS, inibe a LPO, e inibe a formação do $O_2^{\bullet-}$, formado principalmente por sistema enzimático (xantina oxidase) (CAVIA-SAIZ *et al.*, 2010).

Estudos demonstraram que a NGN na nefrotoxicidade aguda em camundongos inibe a depleção de GSH, GPx, CAT e SOD (RENUGADEVI; PRABU, 2009; HERMENEAN *et al.*, 2013), nos danos hepáticos em ratos inibe a depleção de GSH e CAT e a LPO (PARI;

GNANASOUNDARI, 2006; JAYARAMAN *et al.*, 2009; MERSHIBA *et al.*, 2013), na cardiotoxicidade em ratos inibe a depleção de GPx, CAT, SOD e a LPO (SUBBURAMAN *et al*., 2014), e em doença neurodegenerativa em ratos inibe a depleção de GSH, GR, GPx, CAT e SOD (KHAN *et al.*, 2012). Xu *et al*. (2013) constataram que a NGN reduz a atividade da NOX 2 em células do músculo liso vascular tratadas com angiotensina II. Ademais, já foi demonstrado que a NGN ativa a via do Nrf2 e consequentemente aumenta a expressão da HO-1 na inflamação hepática em ratos (ESMAEILI *et al*., 2014) e na toxicidade de células epiteliais humanas (PODDER *et al*., 2014).

Diversos trabalhos demonstraram o potencial anti-inflamatório da NGN. Por exemplo, o tratamento com NGN inibiu o edema cerebral em ratos (BAI *et al.*, 2014), a atividade da MPO na injúria isquêmica cerebral em ratos (RAZA *et al.*, 2013) e a atividade da MMP-9 no carcinoma hepatocelular (SUBRAMANIAN; ARUL, 2013), na neovascularização coroideia (XU *et al.*, 2014) e na injúria isquêmica cerebral em ratos (BAI *et al.*, 2014). Ainda, o tratamento com NGN reduziu os níveis de TNF-α, IL-1β e IL-6 na colite ulcerativa em ratos (AL-REJAIE *et al.*, 2013), a produção de IFN-γ na dermatite atópica em camundongos (KIM *et al.*, 2013), a produção de citocinas Th2 (IL-4, IL-5, IL-13) na asma em camundongos (IWAMURA *et al.*, 2010), os níveis de IL-17 na colite em ratos (AZUMA *et al.*, 2013), os níveis de IL-23 na osteoclastogênese em humanos (LA *et al.*, 2009), os níveis de TNF-α, IL-1β, IL-6 e IL-10 na inflamação induzida por *Chlamydia trachomatis* (YILMA *et al.*, 2013) e a expressão de TGF-β na nefrotoxicidade em camundongos (HERMENEAN *et al.*, 2013). Estudos mostraram que a NGN reduz a produção de citocinas por inibir a sinalização do NF-kB (PARK *et al.*, 2012; DOU *et al.*, 2013; RAZA *et al.*, 2013). Além disso, a NGN foi capaz de inibir a ativação das vias de sinalização MAPK, p38, ERK, JAK, STAT e AP-1 (VAFEIADOU *et al.*, 2009; MUKAI *et al.*, 2010; LIM *et al.*, 2011; YANG *et al.*, 2011).

El-Mahdy et al. (2008) constataram que a NGN protegeu os queratinócitos humanos contra o envelhecimento e carcinogênese induzida pela radiação UVB. No entanto, apesar de vários estudos de atividade farmacológica da NGN, ainda não foi descrito na literatura os efeitos terapêuticos e mecanismos de ação da NGN nos danos cutâneos inflamatórios e oxidativos induzidos pela radiação UVB *in vivo*.

A efetividade de substâncias em prevenir e/ou tratar doenças é dependente da biodisponibilidade. Eventualmente, esta pode ser difícil porque somente uma pequena proporção de substâncias podem permanecer disponível após administração via oral, devido, por exemplo, a baixa solubilidade e/ou permeabilidade e instabilidade no trato gastrointestinal. De fato, muitos flavonóides administrados via oral podem sofrer degradação no ambiente ácido do estômago e apresentam baixa solubilidade (VERRI *et al*., 2012). Neste contexto, a via de administração intraperitoneal em estudos pré-clínicos torna-se uma

alternativa para substâncias que apresentam baixa biodisponibilidade quando administradas via oral.

Yen et al. (2009) demonstraram que a NGN apresenta baixa solubilidade aquosa e pode sofrer degradação no ambiente ácido do estômago, o que resulta em baixa biodisponibilidade quando administrada pela via oral. Uma estratégia terapêutica para administração destes compostos é a via de administração tópica, que previne a degradação gastrointestinal.

A pele tem se mostrado uma eficiente via de administração de formulações medicamentosas. A aplicação tópica possibilita a administração de medicamentos de forma segura e efetiva, além de evitar efeitos como irritação gastrointestinal, toxicidade sistêmica e metabolismo hepático. Diante disso, a administração de antioxidantes por via tópica tem se mostrado uma alternativa simples e efetiva para a proteção da pele contra os danos oxidativos e inflamatórios causados pela radiação UVB (CASAGRANDE *et al.*, 2007; CAMPANINI *et al.*, 2013).

Considerando as evidências discutidas anteriormente, torna-se interessante o estudo da TC, da HMC e da NGN, nos danos cutâneos inflamatórios e oxidativos induzidos pela radiação UVB.

2 OBJETIVOS

2.1 OBJETIVO GERAL

O presente estudo teve como objetivo investigar os mecanismos de atividade antioxidante *in vitro* da TC, da HMC e da NGN e os seus efeitos terapêuticos e mecanismos de ação em modelo de inflamação e estresse oxidativo induzidos por radiação UVB.

2.2 OBJETIVOS ESPECÍFICOS

- Investigar os mecanismos de atividade antioxidante da TC, da HMC e da NGN utilizando diferentes métodos *in vitro*;
- Avaliar os efeitos terapêuticos e mecanismos de ação da TC, da HMC e da NGN administrados pela via intraperitoneal em modelo de inflamação e estresse oxidativo induzidos por radiação UVB ;
- Preparar três formulações tópicas contendo NGN;
- Avaliar a estabilidade físico-química e funcional das formulações contendo NGN em diferentes condições de temperatura;
- Avaliar os efeitos terapêuticos e mecanismos de ação de formulação tópica contendo NGN em modelo de inflamação e estresse oxidativo induzidos por radiação UVB.

3 MATERIAL E MÉTODOS

3.1 MATERIAL

3.1.1 Materiais de Consumo

Corante azul brilhante, glutationa reduzida (GSH), brometo de hexadecil trietil amônio (HTAB), ácido linoléico, n-etilmaleimida, *o*-dianisidina, fluoreto de fenilmetilsulfonila, ácido tiobarbitúrico (TBA), fenantrolina, 2,2-difenil-1-picrilhidrazil (DPPH$^{\bullet}$), 2,2' azinobis (3-etilbenzotiazolina-6-ácido sulfônico) (ABTS), 2,4,6 tripiridil-S-triazina (TPTZ), Trolox e ácido 5,5'-ditio-bis-(2-nitrobenzóico) (DTNB), bisacrilamida, *nitroblue tetrazolium* (NBT) foram obtidos da Sigma-Aldrich (St. Louis, MO, USA). Naringenina (NGN), hesperidina metil chalcona (HMC) e trans-chalcona (TC) da Santa Cruz Biotechnology (Dallas, Texas, USA). 2-deoxi-D-ribose, batofenantrolina (BPS), tert-butil hidroperóxido da Acros (Pittsburgh, PA, USA). Xilene cianol e hidroximetil aminometano (Tris) da Amresco (Solon, OH, USA). Kits de Ensaio imunoenzimático (ELISA) para dosagem das citocinas da eBioscience (San Diego, CA, USA). Acrilamida, dodecil sulfato de sódio (SDS), enzima transcriptase reversa (Superscript® III), Oligo (dT)12-18 primers, Platinum SYBRGreen® e primers da Invitrogem (Carlsbad, CA, USA). Os excipientes usados para o preparo das formulações foram obtidos da Galena (Campinas, SP, Brasil). Todos os outros reagentes utilizados foram de grau analítico.

3.1.2 Materais Permanentes

Agitador mecânico, Fisatom®; ● Agitador Orbital, 255, Fanem®; ● Balança analítica, HR-120, A&d®, precisão de 4 casas; ● Banho-Maria, 314/2 DN, Nova Ética®; ● Banho-Maria, 100, Fanem; ● Centrífuga, Baby I 206-BL, Fanem®; ● Centrífuga refrigerada, Rotina 46 R, Hettich Zentrifugen®; ● Compartimento de madeira projetado para radiação; ● Contador β, LS 6000, Beckman® LS 6000; ● Deionizador de água, Purebal Option-Q, Elga®; ● Espectrofotômetro, Evolution 60, Thermo Scientific®; ● Espectrofotômetro, Helios alfa, Thermo Spectronic®; ● Estufa 0-120 °C, De LEO & Cia®; ● Fonte elétrica para eletroforese, MS 300V, Major Science®; ● Homogeneizador de tecidos Ultra Turrax®, T18 basic, IKA; ● Homogeneizador de tecido, Tissue-Tearor, Biospec®; ● Lâmpada ultravioleta fluorescente, PHILIPS TL/12 40W RS-UVB, MedicalHoland®; ● Leitor de microplaca, Asys Expert Plus, Biochrom®; ● Leitor de microplaca, EnSpire, Perkin Elmer®; ● Leitor de microplaca, Multiskan

GO, Thermo Scientific; ● pHmetro, Tec-3MP, TECNAL®; ● Radiômetro IL 1700 Research Radiometer. Detectores: SED240 – filtro UVB (290 nm), SED005 – filtro UV (350 nm); SED033 – filtro TRED (633 nm), International Light-USA; ● Sistema de eletroforese Mini Vertical, Mini-Protean® Tetra System, Bio-RAD®; ● Sistema de PCR em tempo real, StepOnePlusTM, Applied Biosystems; ● Termociclador, TX96, Amplitherm®; ● Ultra-som, TSO, Thornton®.

3.2 MÉTODOS

3.2.1 Avaliação *in Vitro* da Atividade Antioxidante dos Flavonóides

3.2.1.1 *Determinação da atividade doadora de átomos de hidrogênio ao radical DPPH•*

A atividade doadora de átomos de hidrogênio ao radical estável DPPH• foi determinada pelo decaimento da absorvância mensurado em 517 nm (IVAN *et al.*, 2014). Alíquotas de 50 µL das amostras dos flavonóides em diferentes concentrações, foram adicionadas ao meio reacional contendo 1 mL de tampão acetato 0,1 M (pH 5.5), 1 mL de etanol e 0,5 mL de solução etanólica de DPPH• 250 µM. A mudança na absorvância foi medida em espectrofotômetro após 30 minutos de incubação à temperatura ambiente.

O branco foi constituído de 1 mL de tampão acetato 0,1M (pH 5,5) e 1,5 mL de etanol. O controle positivo não continha amostra (foi preparado com 50 µL de etanol absoluto, o veículo utilizado para diluir os flavonóides), assim, indica o máximo de elétrons livres do DPPH•, o qual é considerado 100% de radical livre na solução para calcular-se a capacidade doadora de hidrogênio (%) dos flavonóides por meio da seguinte equação:
Equação I: % atividade = [1- (absorvância amostra / absorvância do controle)] x 100.

3.2.1.2 *Determinação da atividade doadora de elétrons ao radical ABTS*

A capacidade redutora do radical livre ABTS é medida pela supressão da cor do radical devido à diminuição do mesmo no meio e consequente queda de absorvância, quando substâncias antioxidantes com capacidade em doar elétrons são adicionadas (PRIOR *et al.*, 2005). O método foi realizado de acordo com Sánchez-Gonzalez et al. (2005), com algumas modificações.

A solução ABTS foi preparada em meio aquoso e o cátion ABTS foi obtido após a reação de 7 mM da solução de ABTS com 2,45 mM de persulfato de potássio. A mistura foi armazenada em frasco âmbar e em geladeira por no mínimo 16 horas antes do uso. A

solução ABTS foi diluída com tampão fosfato 20 mM (pH 7,4) até uma atingir absorvância de 0,7 a 0,8 em 730 nm. Alíquotas de 50 µL de diferentes concentrações dos flavonóides estudados foram adicionadas a 4 mL da solução de ABTS diluída. A mudança de absorvância foi mensurada após 6 minutos de incubação à temperatura ambiente em 730 nm.

O controle positivo foi preparado com 50 µL de etanol absoluto em 4 mL da solução de ABTS diluída e o branco foi preparado com uma solução de persulfato de potássio diluída em tampão fosfato 20 mM (pH 7,4). A avaliação da capacidade em remover o radical ABTS foi calculada pela equação I.

3.2.1.3 *Determinação do poder antioxidante redutor do ferro (FRAP)*

O potencial antioxidante de redução do ferro foi avaliado segundo Sanchez-Gonzalez et al. (2005). O reagente de FRAP foi preparado como segue: 2,5 mL de uma solução de TPTZ 10 mM em ácido clorídrico (HCl) 40 mM foram adicionados a 2,5 mL de cloreto férrico hexahidratado ($FeCl_3.6H_2O$) 20 mM e 25 mL de tampão acetato 0,3 mM (pH 3,6). Esta solução foi incubada a 37 °C por 30 minutos antes do uso.

Para a avaliação da capacidade antioxidante, 900 µL do reagente de FRAP preparado previamente foram adicionados a 90 µL de água deionizada e 10 µL de diferentes concentrações dos flavonóides estudados. Após, as amostras foram incubadas a 37°C por 30 minutos e o aumento da absorvância foi mensurado espectrofotometricamente a 595 nm.

O branco foi constituído de 900 µL do reagente FRAP e 90 µL de água deionizada e 10 µL do veículo utilizado para diluir os flavonóides (etanol absoluto). Para comparação do poder redutor dos flavonóides uma curva analítica com diferentes concentrações de trolox (4,0; 8,0; 10,0; 12,5 e 20,0 µmol/L) foi utilizada para posterior cálculo dos resultados em µmol/L equivalente de trolox/ µg/mL de amostra.

3.2.1.4 *Determinação da atividade sequestradora do radical hidroxil (˙OH)*

A atividade sequestradora do radical ˙OH foi determinada pela diminuição da formação de substâncias reativas ao ácido tiobarbitúrico (TBARS) provenientes da degradação da deoxirribose pelo radical ˙OH gerado na reação de Fenton (HALLIWELL *et al.*, 1987).

Ao meio reacional contendo 1 mL de tampão fosfato de potássio monobásico/hidróxido de potássio (KH_2PO_4/KOH) 20 mM (pH 7,4), 100 µM de ascorbato, 50 µM de $FeCl_3.6H_2O$, 52 µM de ácido etilenodiamino tetra-acético (EDTA), 2,8 mM de

deoxirribose e 1 mM de H_2O_2 foram adicionados 10 μL das amostras de flavonóides em diferentes concentrações. A reação foi incubada a 37°C por 30 minutos. Para determinar as TBARS que foram formadas, 1 mL de TBA 1% preparado em 50 mM de hidróxido de sódio (NaOH), 0,1 mL de NaOH 10 M e 0,5 mL de ácido ortofosfórico (H_3PO_4) 20% foram adicionados. Em seguida incubou-se a reação por 20 minutos a 85°C e posteriormente a absorvância foi determinada em 535 nm.

O controle positivo foi preparado com o veículo utilizado para diluir os flavonóides (tampão fosfato pH 7,4 com 2% de Tween 80), o controle negativo foi preparado com a mistura reacional sem o ferro e o branco sem flavonóides e deoxirribose. Ao teste foi incluído o controle das amostras preparado com a mistura reacional e as diferentes concentrações dos flavonóides utilizadas, porém sem a deoxirribose. A atividade sequestradora do radical $^{\bullet}OH$ foi calculada pela equação II:

Equação II: % atividade = [1- (absA – absCA / absC)] x 100.

Onde: absA é a absorvância da amostra, absCA é a absorvância do controle das amostras e absC é a absorvância do controle positivo.

3.2.1.5 *Determinação da atividade inibidora da peroxidação lipídica independente de* Fe^{2+}

A atividade inibidora da peroxidação lipídica (LPO) independente de Fe^{2+} pelos flavonóides foi determinada pela diminuição da formação de hidroperóxido lipídico (LOOH), um produto primário da LPO (LINGNERT *et al*., 1979).

Primeiramente, preparou-se a emulsão de ácido linoléico 10 mM, em tampão fosfato de potássio monobásico/dibásico (KH_2PO_4/K_2HPO_4) 0,1 M (pH 6.5), com auxílio de Tween 20. Em 2 mL da emulsão foram adicionados 10 μL das amostras em diferentes concentrações. A determinação de LOOH foi realizada antes e após a incubação da emulsão contendo as amostras, a 37°C por 8 h. Assim, em 0,1 mL da emulsão incubada ou não, foram adicionados a 1 mL de metanol e 3 mL de metanol 60% e a absorvância foi determinada em 234 nm (MARTINEZ *et al*., 2012).

No teste foi incluído o controle positivo com 10 μL do veículo (etanol). O branco foi constituído de tampão KH_2PO_4/K_2HPO_4 0,1 M (pH 6,5) com Tween 20. A atividade inibidora da LPO independente de Fe^{2+} foi calculada pela seguinte equação:

Equação III: % atividade = 1- (absA após incubação - absA sem incubação)
/ (absC após incubação - absC sem incubação) x 100.

Onde: absA é a absorvância da amostra e absC é a absorvância do controle positivo.

3.2.1.6 *Determinação da atividade inibidora da peroxidação lipídica induzida por* Fe^{2+}

As mitocôndrias utilizadas nos experimentos de LPO induzida por Fe^{2+} foram obtidas por meio do fígado de camundongos hairless provenientes do biotério do Hospital Universitário da UEL. Cerca de 10 camundongos pesando aproximadamente 30 g foram eutanasiados por deslocamento cervical, os fígados (10 a 15 g) foram removidos e a eles foram adicionados 50 mL de tampão fosfato salino (PBS) (pH 7,0). A mistura foi homogeneizada em turrax (T18 basic, IKA) até a obtenção de um homogenato. A suspensão obtida foi centrifugada a 1350 g por 5 minutos a 4°C. O sobrenadante resultante foi novamente centrifugado a 5000 g por 10 minutos a 4°C. O precipitado obtido foi ressuspendido em 10 mL de PBS e novamente centrifugado a 3000 g por 15 minutos a 4°C. O sedimento final contendo o concentrado de mitocôndrias, foi suspenso em 1 mL de tampão KCl/tris-HCl 130 mM e 10 mM respectivamente (pH 7,4) e submetido a dosagem de proteínas pelo método de Biureto (CAIN; SKILLETER, 1987). As mitocôndrias obtidas foram utilizadas como fonte de lipídios para a avaliação da LPO.

A medida da atividade inibidora de LPO induzida por Fe^{2+} foi determinada pela diminuição da formação de TBARS provenientes da LPO (BUEGE; AUST, 1978). Foram adicionados em 1 mL de meio de reação (130 mM de KCl e 10 mM de tris-HCl, pH 7,4), 2 mM de citrato de sódio, 10 μL das amostras do flavonóide em diferentes concentrações, suspensão de mitocôndria correspondente a 1 mg de proteína e 50 μM de sulfato ferroso amoniacal. A reação foi incubada a 37 °C por 30 minutos. As substâncias reativas ao TBA foram estimadas pelo método descrito no item 3.2.1.4. As TBARS foram extraídas com 2 mL de n-butanol e as amostras foram centrifugadas a 2000 g por 10 minutos. A absorvância do sobrenadante foi determinada por espectrofotometria em 535 nm.

Ao teste foi incluído o controle positivo com 10 µL do veículo utilizado para diluir os flavonóides (etanol absoluto) e o controle negativo preparado sem os flavonóides e sem o ferro. O branco foi preparado com a mistura da reação sem mitocôndria. A atividade inibidora da lipoperoxição lipídica induzida por Fe^{2+} foi calculada pela equação I.

3.2.1.7. Determinação da atividade queladora do Fe^{2+}

Uma vez que o íon Fe^{2+} é um pró-oxidante, catalizador de reações oxidativas, a atividade queladora deste íon foi determinada. A atividade queladora do Fe^{2+} foi determinada utilizando a batofenantrolina (BPS), um forte quelador de Fe^{2+} que forma um complexo colorido quando ligada a este íon. Esta metodologia se baseia na redução da formação do complexo $Fe_2(BPS)_3$ por amostras antioxidantes por meio do decaimento da absorvância mensurado em 530 nm e 700 nm (BOLANN; ULVIK, 1987).

No meio reacional contendo 2 mL KCl/Tris-HCl 130 mM e 10 mM respectivamente (pH 7,4), foram adicionados 50 μM de sulfato ferroso amoniacal e 50 μL das amostras de flavonóides em diferentes concentrações. Após 15 minutos de incubação à temperatura ambiente foram adicionados 0,2 mM de BPS. Em seguida a reação foi incubada novamente por 15 minutos à temperatura ambiente e posteriormente as absorvâncias foram determinadas em 530 e 700 nm (CASAGRANDE *et al.*, 2006b).

No teste foi incluído o controle positivo com 50 μL do veículo utilizado para diluir os flavonóides (etanol absoluto). O branco foi preparado sem os flavonóides e BPS. A atividade queladora de íons Fe^{2+} foi calculada pela equação I.

3.2.1.8 *Determinação da atividade sequestradora do radical ânion superóxido*

A atividade sequestradora do ânion superóxido ($O_2^{\bullet-}$) foi determinada usando o ensaio de redução de *nitroblue tetrazolium* (NBT). Alíquotas de 10 μL das amostras dos flavonóides em diferentes concentrações foram adicionadas a 100 μL de NBT (1 mg/mL). Em seguida, foi adicionado o doador do $O_2^{\bullet-}$, superóxido de potássio (KO_2, 25 μL, 30 μg). Após 15 minutos de incubação a temperatura ambiente o sobrenadante foi cuidadosamente removido. O precipitado formado, que consiste de partículas de formazan (NBT reduzido), foi solubilizado pela adição de 120 μL de KOH 2M e 120 μL de dimetilsulfóxido (DMSO). A redução do NBT foi determinada espectrofotometricamente em 620 nm (WANG et al., 1998). A avaliação da atividade sequestradora do $O_2^{\bullet-}$ foi calculada pela equação I.

3.2.2 Avaliação da Eficácia *In Vivo* dos Flavonóides em Controlar a Inflamação e o Estresse Oxidativo Induzidos pela Radiação UVB

3.2.2.1 *Animais experimentais*

Como modelo animal foi utilizado camundongos sem pêlo da linhagem HRS/J, de ambos os sexos, adultos e com peso de 20 a 30 g. Os animais foram mantidos no biotério do Hospital Universitário de Londrina-PR, em sala com temperatura controlada, ciclo claro/escuro de 12 horas e com suprimento de água e ração *ad libitum.* Os experimentos foram conduzidos conforme as normas da Comissão de Ética no uso de Animais (CEUA) da Universidade Estadual de Londrina (registrado no CEUA sob o n° 90/12, processo nº 3344.2012.08 e sob o nº 162/2013, processo nº 19972.2013.46).

3.2.2.2 *Sistema e fonte de radiação UVB*

A fonte de luz utilizada nos experimentos para indução da inflamação/estresse oxidativo foi uma lâmpada UVB fluorescente modelo PHILIPS TL/12 40W RS (Medical-Holand). A lâmpada emite radiação na faixa de λ de 270 a 400 nm com pico máximo de emissão em 313 nm. A fonte de radiação UVB foi instalada em um compartimento de madeira desenvolvido para os experimentos.

Os animais foram colocados em caixas de plástico e cobertos com uma tela plástica (1 mm de espessura, com rede de malha de 2 mm x 2 mm) para que os animais permanecessem dentro das caixas e para garantir que a exposição à luz UVB ocorresse diretamente na região dorsal dos mesmos. Os animais ficaram a 20 cm de distância da fonte de radiação e movimentavam-se livremente na caixa. Devido às variações de intensidade de radiação ao longo da lâmpada, as posições das caixas foram modificadas periodicamente durante a radiação (CASAGRANDE *et al.*, 2006a).

3.2.2.3 *Medida da radiância da lâmpada UVB*

A radiância é a taxa do fluxo de energia em watts (W) (ou J/seg) por unidade de área, ou seja, W/cm^2. A dose de exposição em J/cm^2 é obtida multiplicando-se a radiância (W/cm^2) pelo tempo de exposição em segundos. Para a medida da radiância, utilizou-se um radiômetro IL 1700 (Newburyport, MA, USA) equipado com detectores para radiação UV (SED005) e especialmente para UVB (SED240). A medida da radiância foi realizada em toda a extensão do compartimento, à distância de 20 cm e com a presença da tela plástica utilizada para conter os animais. A radiância da lâmpada utilizada foi de 0,384 mW/cm^2. Para indução da inflamação e estresse oxidativo foi utilizada a dose de radiação de 4,14 J/cm^2 (SHINDO *et al.*, 1994; CAMPANINI *et al.*, 2013; IVAN *et al.*, 2014). Shindo et al., 1994 demonstrou que a dose de 25 J/cm^2 equivale a 4-5 horas de exposição ao sol de outono na latitude da Califórnia (38°N).

3.2.2.4 *Protocolo experimental de avaliação da eficácia dos flavonóides administrados pela via intraperitoneal*

A RUV exerce múltiplos efeitos nas células da pele, os quais são tempo dependente da migração de células inflamatórias, da liberação de mediadores inflamatórios e da produção de EROs (AFAQ *et al.*, 2005a). Neste contexto, é importante determinar o melhor

tempo após a exposição à UVB para avaliação dos diferentes parâmetros de inflamação e estresse oxidativo.

Assim, depois de determinado os tempos após a radiação UVB para avaliação dos diferentes parâmetros do processo inflamatório e estresse oxidativo induzidos pela radiação UVB, foram realizados os tratamentos dos animais com os flavonóides. Os parâmetros avaliados com amostras de pele coletadas 12 horas após o fim da radiação foram padronizados anteriormente (IVAN *et* al., 2014; CAMPANINI *et* al., 2013), e os outros parâmetros avaliados com amostras de pele coletadas 2 horas e 4 horas após o fim da radiação foram padronizados no desenvolvimento deste trabalho. A Figura 5 resume os protocolos experimentais utilizados para avaliação da eficácia dos flavonóides administrados pela via intraperitoneal (i.p.).

Os animais foram tratados com diferentes doses de TC (10, 30, 100 e/ou 300 mg/kg), HMC (30, 100 e/ou 300 mg/kg), NGN (10, 30 e/ou 100 mg/kg), ou o veículo utilizado para diluir os flavonóides (solução salina a 0,9% para a HMC, ou solução de Tween 80 a 20% dissolvido em solução salina a 0,9 % para TC e NGN), via i.p., 1 hora antes do início da radiação e 8 horas após o primeiro tratamento, para os testes de edema, atividade da MPO, atividade de MMP-9, níveis de GSH, avaliação do FRAP e capacidade em reduzir o radical ABTS. Para os testes de atividade da CAT, produção de $O_2^{\bullet-}$ (NBT), LOOH e citocinas, e expressão de RNAm por reação em cadeia da polimerase (PCR) quantitativo os animais foram tratados apenas uma vez, 1 hora antes do início da radiação.

Os animais foram eutanasiados e amostras de pele foram coletadas 12 horas (para testes de edema, atividade da MPO, atividade da MMP-9, níveis de GSH, avaliação do FRAP, e capacidade em reduzir o radical ABTS), 2 horas (para os testes de produção de $O_2^{\bullet-}$ e atividade da CAT) e 4 horas (para os testes de produção de LOOH, citocinas e expressão de RNAm por PCR quantitativo) após o término da exposição à radiação UVB (4,14 J/cm^2). Em seguida, as amostras de pele do dorso dos animais foram divididas para os diferentes testes e armazenadas a -70°C para as análises. O teste de edema cutâneo foi realizado logo após a retirada das amostras de peles.

Os animais foram terminalmente anestesiados com 1,5 % de isoflurano para os testes de 12 horas, ou anestesiados seguido de decapitação para os testes de 2 horas e 4 horas após o término da exposição à radiação UVB.

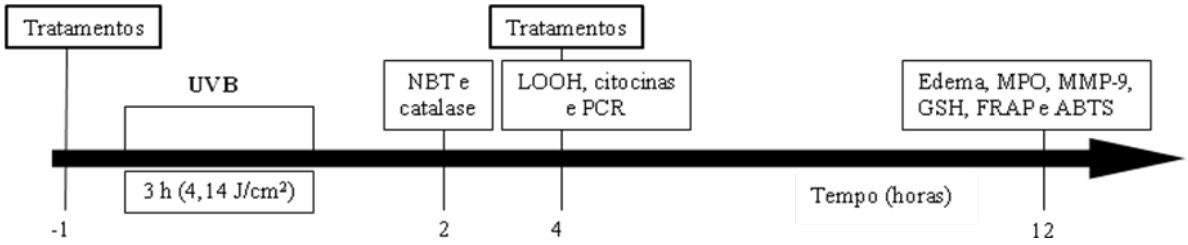

Figura 5. Esquema geral dos protocolos experimentais para avaliação da eficácia dos flavonóides administrados pela via intraperitoneal. Os animais foram radiados com radiação UVB durante 3 horas (4,14 J/cm^2). Uma hora antes do início da radiação os animais foram tratados com diferentes doses de trans-chalcona (TC, 10, 30, 100 e/ou 300 mg/kg), hesperidina metil chalcona (HMC, 30, 100 e/ou 300 mg/kg), naringenina (NGN, 10, 30 e/ou 100 mg/kg) ou o veículo utilizado para diluir os flavonóides (solução salina 0,9% para a HMC, ou solução de Tween 80 a 20% dissolvido em solução salina a 0,9% para TC e NGN) via intraperitoneal. Para os testes de edema, atividade da mieloperoxidase (MPO), atividade de metaloproteinase-9 (MMP-9), níveis de glutationa reduzida (GSH), avaliação do poder antioxidante redutor de ferro (FRAP) e capacidade em reduzir o radical ABTS os animais foram tratados duas vezes, 1 hora antes do início da radiação e 8 horas após o primeiro tratamento. Os animais foram eutanasiados e amostras de pele foram coletadas 2 horas (para os testes de produção de ânion superóxido [NBT] e atividade da catalase [CAT]), 4 horas (para os testes de produção hidroperóxidos lipídicos [LOOH], citocinas e expressão de RNAm por reação em cadeia da polimerase [PCR] quantitativo) e 12 horas (para os testes de edema, atividade de MPO, MMP-9, níveis de GSH, avaliação do FRAP e capacidade em reduzir o radical ABTS), após o fim da radiação UVB.

3.2.2.5 *Protocolo experimental de avaliação da eficácia de formulação tópica contendo NGN*

Figura 6 resume os protocolos experimentais utilizados para avaliação da eficácia de formulação tópica contendo NGN. Os animais foram tratados com formulação tópica contendo NGN ou tratados com a formulação controle (sem NGN). As formulações foram aplicadas em todo o dorso dos animais com o auxílio de um pincel, cerca de 0,5 g de formulação, 12 horas, 6 horas, 5 minutos antes da radiação e 6 horas após o início da radiação. Para os testes de atividade da CAT e produção de $O_2^{\bullet-}$ (NBT) os animais foram tratados com as formulações 12 horas, 6 horas e 5 minutos antes da radiação.

Os animais foram eutanasiados e amostras de pele foram coletadas 12 horas (para testes de edema, atividade da MPO, atividade da MMP-9, níveis de GSH, avaliação do FRAP, e capacidade em reduzir o radical ABTS), 2 horas (para os testes de produção de $O_2^{\bullet-}$ e atividade da CAT) e 4 horas (para os testes de produção de LOOH, citocinas e expressão de RNAm por PCR quantitativo) após o término da exposição à radiação UVB.

A dose de radiação utilizada foi de 4,14 J/cm^2 e os animais foram terminalmente anestesiados com 1,5 % de isofurano para os testes de 12 horas, ou anestesiados seguido de decapitação para os testes de 2 horas e 4 horas após o término da exposição à radiação UVB. Após anestesia terminal, as amostras de pele do dorso dos animais foram limpas com

auxílio de algodão e de água deionizada para total retirada das formulações presentes na superfície cutânea. Em seguida, a pele foi retirada, dividida para os diferentes testes e armazenada a -70°C para as análises. O teste de edema cutâneo foi realizado logo após a retirada da pele.

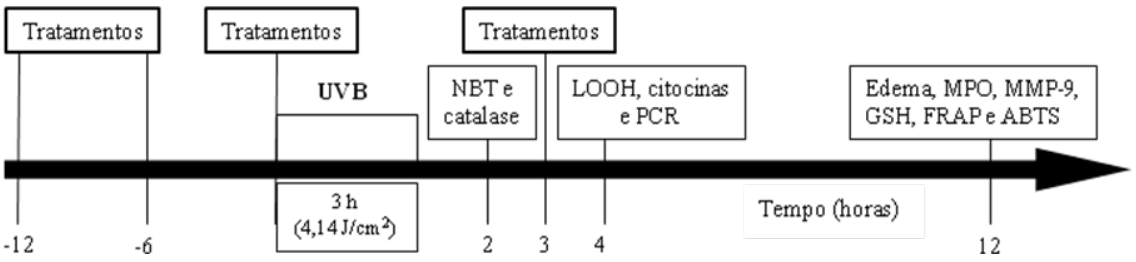

Figura 6. Esquema geral dos protocolos experimentais para avaliação da eficácia de formulação tópica contendo naringenina (NGN). Os animais foram radiados com radiação UVB durante 3 horas (4,14 J/cm^2). Doze horas, 6 horas, 5 minutos antes da radiação e 6 horas após o início da radiação os animais foram tratados com as formulações tópicas (com ou sem NGN). Para os testes de atividade da catalase (CAT) e produção de ânion superóxido (NBT) os animais foram tratados com as formulações 12 horas, 6 horas e 5 minutos antes da radiação. Os animais foram eutanasiados e amostras de pele foram coletadas 2 horas (para os testes de NBT e atividade da CAT), 4 horas (para os testes de produção hidroperóxidos lipídicos [LOOH], citocinas e expressão de RNAm por reação em cadeia da polimerase [PCR] quantitativo) e 12 horas (para os testes de edema, atividade de mieloperoxidase [MPO], atividade de metaloproteinase-9 [MMP-9], níveis de glutationa reduzida [GSH], avaliação do poder antioxidante redutor de ferro [FRAP] e capacidade em reduzir o radical ABTS), após o fim da radiação UVB.

3.2.2.6 *Preparo de soluções dos flavonóides*

Os flavonóides TC e NGN foram exatamente pesados e dissolvidos em Tween 80 20% a temperatura ambiente, posteriormente foram diluídos em solução salina estéril 0,9% até a obtenção das concentrações desejadas. O flavonóide HMC foi exatamente pesado e dissolvido a temperatura ambiente em solução salina estéril 0,9% no volume determinado. Foram preparadas soluções correspondentes as doses de 300 mg/kg de TC, 300 mg/kg de HMC e 100 mg/kg de NGN para a administração de 0,1 mL/10g peso animal via i.p.. Estas soluções foram diluídas em solução salina estéril 0,9% para obter as outras diferentes doses de cada um dos flavonóides estudados (10, 30 e 100 mg/kg para a TC; 30 e 100 mg/kg para a HMC e 10 e 30 mg/kg para a NGN).

Para tratamento dos animais dos grupos controles dos experimentos com TC e NGN foi preparado solução de Tween 80 a 20% dissolvido em solução salina estéril a 0,9 % (veículo correspondente). E, para tratamento dos animais dos grupos controles dos experimentos com HMC foi utilizada solução salina estéril a 0,9 % (veículo correspondente).

As doses utilizadas dos flavonóides foram baseadas nos seus efeitos terapêuticos em animais em outros modelos de doenças (GOLDSTEIN *et al.*, 1943; LAMOKE *et al.*, 2011; ORSOLIC *et al.*, 2011, PINHO-RIBEIRO et al., 2015) e nos resultados de experimentos realizados previamente.

3.2.2.7 *Preparo de formulações tópicas contendo NGN*

A comparação entre o tratamento por via i.p. e tópica é importante para determinar se o tratamento local (via tópica) é tão eficaz quanto o tratamento sistêmico (i.p.). Ademais, os princípios ativos possuem características químicas e físicas diferentes, e formulações como emulsões fluídas e semi-sólidas, possuem propriedades coloidais que podem influenciar a biodisponibilidade do fármaco, assim ressalta-se a importância da avaliação de diferentes formulações (BARRY, 1983).

Foram preparadas três formulações tópicas, as quais se distinguiam pelo uso das bases auto-emulsionantes (Polawax®, Hostacerin SAF® e Net FS®) e pela proporção de conteúdo aquoso e lipídico (Tabela 1). As formulações foram preparadas e divididas em 2 porções, sendo uma reservada para controle (sem a adição de NGN) e a outra acrescida de 0,5% de NGN.

As formulações de Polawax®, foram preparadas aquecendo-se as fases A (lipossolúvel) e B (hidrossolúvel) a 70°C e misturadas a esta temperatura sob constante agitação até resfriamento à temperatura ambiente, então, adicionou-se a fase C. As formulações que continham o Hostacerin SAF® em seu conteúdo foram preparadas adicionando-se à temperatura ambiente a base auto-emulsionante e água deionizada. Após agitação homogênea, adicionou-se o emoliente (triglicerídeos do ácido cáprico e caprílico) e a solução conservante (Phenonip®). Da mesma forma, as formulações com Net FS® foram preparadas por meio da mistura do gel de Carbopol 940® com a base auto-emulsionante, e a adição posterior do emoliente e da solução conservante.

Após 24 horas do preparo das formulações foi incorporada a temperatura ambiente 0,5% da NGN solubilizada em propilenoglicol com auxílio de um gral e pistilo, e nas formulações controle adicionou-se apenas o propilenoglicol.

Tabela 1. Componentes das formulações.

Matérias-primas	%		
	F1	F2	F3
A) Polawax®[1](emulsificante)	10	-	-
Hostacerin SAF®[2](emulsificante)	-	5	-
Net FS®[3](emulsificante)	-	-	2
Triglicerídeos do ácido cáprico e caprílico (emoliente)	5	5	5
B) Carbopol 940® (1%)[4] (espessante) qsp*	-	-	100
Trietanolamina (alcalinizante)	-	-	0,5
Água deionizada qsp*	100	100	-
C) Phenonip® (conservante)	0,4	0,4	0,4
D) Propilenoglicol (umectante e solubilizante)	6	6	6

*quantidade suficiente para;
[1]Polawax®: Base auto emulsionante não-iônica (álcool cetoestearílico + monoestearato de sorbitol polioxietileno 20 0E);
[2]Hostacerin SAF®: Base auto emulsionante aniônica (Aristoflex® AVC, Emulsogen®, Hostaphat®, óleo mineral e palmitato de isopropila);
[3]Net FS®: Microemulsão não-iônica (metilfenilpolisiloxano, glicerina e surfactantes);
[4]Carbopol 940®: Agente gelificante (polímero do ácido acrílico).

3.2.2.8 *Avaliação da estabilidade da NGN e das formulações acrescidas de NGN*

Na etapa de desenvolvimento de produtos são realizados os chamados estudos de estabilidade, testes de caráter preditivo, que permitem analisar a influência de condições como umidade e temperatura na estabilidade do produto ao longo do tempo. Desta forma, permitem a análise de fatores essenciais como prever as melhores condições de armazenamento, data de validade, segurança, influência dos componentes e também a escolha do material de embalagem (CASAGRANDE *et al.*, 2006b; KIM *et al.*, 2012).

Um dos testes de estabilidade realizado nas etapas de pré-formulação é o teste de estabilidade acelerada, que segundo a RE nº. 1, 29/07/2005 (ANVISA), tem como objetivo acelerar a degradação química e/ou física de um produto farmacêutico em condições extremas de armazenamento, desta forma, em um curto período de tempo, sob condições climáticas forçadas, é possível prever os perfis de estabilidade físico-químico e funcional dos produtos, de acordo com parâmetros específicos para cada forma farmacêutica.

Geralmente, formulações emulsionadas são armazenadas em temperaturas de -10°C ou 4°C, temperatura ambiente, e à 45°C ou 50°C pelo período de 180 dias (CASAGRANDE

et al., 2006b). Segundo a RE nº. 1, 29/07/2005 (ANVISA), produtos semissólidos acondicionados em embalagens primárias semi-permeáveis devem ser armazenados a 40±2°C/75±5% de umidade relativa (UR).

Neste contexto, as formulações de Polawax®, Hostacerin® e Net FS®, acrescidas ou não de NGN e a NGN pura foram armazenados a 4ºC (temperatura baixa, uma vez que a NGN pura deve ser estocada nestas condições) e a 40±2º C e 75% ±5% de UR por seis meses. Em intervalos de tempo determinados (0, 30, 60, 90 e 180 dias), alíquotas foram coletadas e analisadas quanto à estabilidade físico-química e funcional. As formulações foram armazenadas durante o período de estudo em frascos de polipropileno do tipo semipermeável (permeável a gases e à umidade).

3.2.2.8.1 *Avaliação da estabilidade físico-química*

3.2.2.8.1.1 *Avaliação visual*

As formulações foram analisadas quanto à consistência, homogeneidade, odor e alteração de cor (FONSECA *et al.*, 2011).

3.2.2.8.1.1 *Determinação do pH*

A determinação do pH é importante para assegurar que o valor de pH permanece compatível com os componentes da formulação e com o local de aplicação, evitando possíveis irritações da pele (CASAGRANDE *et al.*, 2006b; S. H. KIM *et al.*, 2012).

O pH das formulações foi determinado por meio de uma dispersão aquosa 1:10. Desta forma, pesou-se 2 g de cada formulação e adicionou-se 18 g de água deionizada. Após completa homogeneização o pH das amostras foi determinado em pHmetro (GEORGETTI *et al.*, 2006).

3.2.2.8.1.2 *Teste de centrifugação*

As emulsões são consideradas sistemas termodinamicamente instáveis, podendo se separar completamente após certo período de tempo. Desta forma, o teste de centrifugação, fornece informações preditivas sobre a instabilidade do sistema, uma vez que ao simular um aumento na força da gravidade, permite observar nas emulsões indícios de instabilidade como a separação da fase dispersa pela cremeação ou coalescência, que são responsáveis

por problemas como mudanças na aparência, consistência, redispersibilidade e desempenho das formulações (GEORGETTI *et al.*, 2006).

Em tubo de centrífuga, foi pesado 2 g de cada formulação e a mesmas foram submetidas a centrifugação a 1660× *g* por 30 minutos, à temperatura ambiente, observando-se a possível ocorrência de separação de fases (GEORGETTI *et al.*, 2006).

3.2.2.8.2 *Avaliação da estabilidade funcional*

A estabilidade funcional das formulações e da NGN pura foi avaliada utilizando-se o teste de determinação da capacidade em reduzir o radical ABTS conforme descrito previamente no item 3.2.1.2 (CAMPANINI *et al.*, 2014). As formulações contendo NGN foram diluídas em etanol para obter a concentração de 0,8 µg/mL. Esta foi à concentração de NGN pura utilizada no meio reacional da reação. Os seguintes controles foram incluídos no teste: 1) controle preparado com o veículo utilizado para diluir a NGN (etanol); 2) controle preparado com a adição de formulações sem NGN.

Após o estudo de estabilidade, a eficácia *in vivo* da formulação mais estável contendo NGN contra a inflamação e estresse oxidativo induzidos pela radiação UVB foi avaliada.

3.2.2.9 *Avaliação de parâmetros inflamatórios cutâneos*

3.2.2.9.1 *Avaliação do edema cutâneo*

Uma das consequências da exposição à RUV na pele é a inflamação, caracterizada por, entre outros fatores, aumento da permeabilidade vascular com extravasamento de líquido para o interstício, na epiderme, causando o edema (KVIETYS; GRANGER, 2012).

Com o auxílio de um molde de área fixa (5 mm diâmentro) foi coletada uma área constante de pele do dorso de cada animal, que posteriormente foi pesada (AFAQ *et al.*, 2005b; BHATIA *et al.*, 2011; CAMPANINI *et al.*, 2013; IVAN *et al.*, 2014). O efeito dos flavonóides no edema cutâneo induzido pela radiação UVB foi mensurado por meio da espessura da pele na região dorsal. A análise se deu pela diferença de peso de pele entre os diferentes grupos. Os resultados foram expressos em mg de pele.

3.2.2.9.2 *Avaliação da atividade da MPO*

A quantificação da migração de neutrófilos para a pele induzida por radiação UVB foi determinada indiretamente pela atividade da MPO, uma enzima oxidorredutora do peróxido de hidrogênio encontrada em grânulos de leucócitos, predominantemente em neutrófilos. Neste método, a MPO catalisa a oxidação do substrato o-dianisidina, resultando em um composto colorido que é detectado espectrofotometricamente em 540 nm (BRADLEY *et al.*, 1982; CASAGRANDE *et al.*, 2006a; CAMPANINI *et al.*, 2013; IVAN *et al.*, 2014).

As amostras de pele dos animais (aproximadamente 30 mg) foram coletadas em microtubos contendo 400 µL de tampão fostato de potássio 0,05 M (pH 6,0) com 0,5% de brometo de hexadecil trietil amônio (HTAB) e mantidas a - 80 °C até o uso. Para realização do ensaio, as amostras foram homogeneizadas com auxílio do homogeneizador Tissue-Tearor (Biospec®). O homogenato foi centrifugado a 16.100 g por 2 minutos a 4°C e o sobrenadante foi retirado para o ensaio.

Em microplaca de 96 poços, foi adicionado alíquota do sobrenadante das amostras (30 µL). A reação colorimétrica inicia-se pela adição de 200 µL de uma solução contendo 10% de tampão fosfato 0,05 M (pH 6,0), 0,0167 % de *o*-dianisidina e 0,05% de H_2O_2 em água deionizada. Após 20 minutos de reação a atividade da MPO das amostras foi determinada em 450 nm (Asys Expert Plus, Biochrom) e comparada com uma curva padrão de neutrófilos de concentração conhecida.

A curva padrão foi preparada na mesma placa com a adição de 100 µL de tampão fosfato 0,05 M e uma solução contendo 200.000 neutrófilos no primeiro poço (A1) com posterior diluição seriada até o décimo primeiro poço (A11). O décimo segundo poço (A12) foi utilizado como branco ao qual foi adicionado apenas 200 µL de água deionizada. Os resultados foram expressos como atividade da MPO (número de neutrófilos/mg de pele).

3.2.2.9.3 *Avaliação da atividade da MMP-9*

Para determinação da atividade da MMP-9 foi utilizado o ensaio de zimografia em gel de poliacrilamida com dodecil sulfato de sódio (SDS-PAGE) (FONSECA *et al.*, 2010; FONSECA *et al.*, 2011). A zimografia é um método amplamente utilizado para a detecção de proteases, consistindo em análise qualitativa da atividade por meio da degradação da gelatina adicionada ao gel de eletroforese (KIM *et al.*, 2007).

As amostras de pele dos animais foram coletadas em microtubos e para este teste foi feito um *pool* das amostras de cada grupo de animais. Primeiramente, as peles dos animais foram diluídas (1:4) e trituradas (T18 basic, IKA) em tampão Tris/HCl 50 mM (pH 7,4) contendo cloreto de cálcio ($CaCl_2$) 10 mM e 1% de inibidores de proteinases (fenantrolina, fluoreto de fenilmetilsulfonila e N-etilmaleimida). O homogenato foi duplamente

centrifugado a 12.000 g por 10 minutos a 4 °C e o sobrenadante utilizado no ensaio. Também foi realizada dosagem de proteínas das amostras pelo método de Lowry (LOWRY *et al.*, 1951). Alíquota de 50 µL do sobrenadante das amostras foi diluída em 10 µL de tampão Tris/HCl (pH 6,8) contendo 20% de glicerol, 4% de dodecil sulfato de sódio (SDS) e 0,001% de azul de bromofenol. Em seguida estas amostras foram colocadas em banho-maria a 37 ºC durante 8 minutos imediatamente antes de ser aplicada no gel de eletroforese.

A espessura do gel utilizado foi de 1 mm, composto por um gel de separação e um gel de concentração, preparado conforme tabela 2.

Tabela 2. Constituintes do gel de separação e do gel de concentração.

Substância	Quantidade (µL)	
	Gel de separação	Gel de concentração
Água miliQ	5870	4060
Tampão Tris/HCl 1 M (pH 8,8) com 0,4% SDS	3750	-
Tampão Tris/HCl 0,5 M (pH 6,8) com 0,4% SDS	-	1670
Acrilamida: bis-acrilamida (30:0,8)	5000	860
Gelatina 10%	375	-
Persulfato de amônio 10%	50	33
Temed 20%	10	6,6

O interior da cuba de eletroforese foi preenchido com tampão Tris/glicina 190 mM (pH 8,3) contendo 0,1% de SDS. Antes da aplicação das amostras, o gel foi submetido a uma pré-corrida de 10 mA por 15 minutos. Após, foram aplicados 25 µL de cada amostra. Durante a eletroforese a corrente aplicada foi de 10 mA para o gel de concentração e 13 mA para o gel de separação, sendo que a última corrente foi mantida constante por 15 minutos após a saída do corante do gel de separação.

Ao término da eletroforese o gel de poliacrilamida foi lavado por 1 hora com solução de Triton X-100 2% sob constante agitação, posteriormente o gel foi incubado por 16 horas a 37 °C em tampão Tris/HCl 50 mM (pH 7,4) contendo $CaCl_2$ 10 mM e 0,02% de azida sódica. Ao final da incubação o gel foi corado com uma solução contendo 0,25% de azul brilhante, 10% de ácido acético e 50% de metanol em água deionizada. Para visualização das bandas o gel foi descorado com ácido acético 20% (FONSECA *et al.*, 2011). A atividade

proteolítica foi analisada por meio da comparação das diferenças de densidades de cor entre as bandas de cada grupo pelo programa ImageJ® (NIH, Bethesda, MD, USA).

3.2.2.9.4 *Avaliação da produção de diferentes citocinas*

A quantificação das citocinas foi realizada utilizando-se a técnica de enzima imunoensaio (ELISA) com kits comerciais (eBioscience) de acordo com as instruções de uso do fabricante e conforme descrito previamente (VERRI *et al.*, 2008).
As amostras de pele dos animais (aproximadamente 30 mg) foram coletadas em microtubos contendo 500 µL de solução NaCl 0,9%. Para realização do ensaio as amostras foram trituradas com o triturador Tissue-Tearor (Biospec). Em seguida, foram centrifugadas a 2000 g por 15 minutos a 4 ^{o}C e o sobrenadante foi retirado para análise.

Para a realização do ensaio, microplacas com 96 poços foram incubadas por toda à noite a 4 ^{o}C com anticorpos de captura contra as proteínas de interesse. Após esse tempo de incubação, as placas foram lavadas com PBS com 0,05% de Tween 20 e incubadas por 1 hora à temperatura ambiente com uma solução a 1% de albumina bovina. Após esse bloqueio e lavagem das placas com tampão de lavagem, a curva padrão e as amostras foram adicionadas (50 µL) e incubadas a 4 ^{o}C por 16 horas. Posteriormente, as placas foram lavadas com tampão de lavagem e os anticorpos policlonais biotinilados (anticorpo de detecção) foram adicionados (100 µL). Após incubação em temperatura ambiente por 1 hora, as placas foram lavadas com tampão de lavagem e 100 µL de enzima avidina-peroxidase foram adicionados. As placas foram incubadas por 30 minutos à temperatura ambiente, lavadas, e adicionado 100 µL do substrato contendo 0,04% de ortofenilenodiamina (OPD) e 0,04% de H_2O_2 em tampão fosfato, a placa foi mantida no escuro em temperatura ambiente por 15 minutos. A reação enzimática foi interrompida com uma solução de H_3PO_4 1 M e as absorvâncias foram determinadas em 450 nm (Multiskan GO, Thermo Scientific).

Curvas padrões de cada uma das citocinas foram utilizadas para quantificar as citocinas presentes nas amostras e os resultados foram expressos em picogramas (pg) de citocina/mg de pele (VERRI *et al.*, 2008).

3.2.2.10 *Avaliação dos parâmetros de estresse oxidativo cutâneo*

3.2.2.10.1 *Avaliação do poder antioxidante redutor de ferro (FRAP)*

O método FRAP foi realizado para avaliar o poder antioxidante de redução férrica da pele. Amostras que apresentam poder redutor no teste do FRAP doam elétrons (PRIOR *et al.*, 2005) e correlacionam-se com os níveis plasmáticos dos antioxidantes ácido ascórbico, ácido úrico e α-tocoferol (BENZIE; STRAIN, 1996).

As amostras de pele dos animais (aproximadamente 30 mg) foram coletadas em microtubos contendo 500 µL de KCl 1,15%. Para a realização do ensaio, as amostras foram trituradas com auxílio de triturador (Tissue-Tearor, Biospec). Em seguida, foram centrifugadas a 1.000 g por 10 minutos a 4°C e o sobrenadante foi retirado para a análise. Para a reação foram utilizados 30 µL do sobrenadante e 1 mL de reagente FRAP preparado conforme item 3.2.1.3.

A reação foi incubada por 30 minutos a 37°C e posteriormente foi realizada a leitura em 595 nm (Helios Alfa, Thermo Spectronic). Uma curva analítica com diferentes concentrações de trolox (0,5 a 20 µM) foi preparada e utilizada para posterior cálculo dos resultados em µM equivalente de trolox/mg de pele (KATALINIC *et al.*, 2005).

3.2.2.10.2 *Avaliação da capacidade em reduzir o radical ABTS*

O ensaio é baseado na diminuição da absorvância devido à doação de elétrons ao radical ABTS (PRIOR *et al.*, 2005). Amostras que apresentam atividade neste teste correlacionam-se com os níveis de GSH (KATALINIC *et al.*, 2005).

As amostras de pele dos animais (aproximadamente 30 mg) foram coletadas em microtubos contendo 500 µL de KCl 1,15%. Para a realização do ensaio, as amostras foram trituradas com auxílio de triturador (Tissue-Tearor, Biospec). Em seguida, foram centrifugadas a 1.000 g por 10 minutos a 4°C, e o sobrenadante foi retirado para a análise. Para a reação foi adicionado 40 µL do sobrenadante a 1 mL de solução de ABTS, preparada conforme item 3.2.1.2.

A reação foi incubada por 6 minutos e posteriormente foi realizada a leitura em 730 nm (Helios Alfa, Thermo Spectronic). Uma curva analítica com diferentes concentrações de trolox (1 a 25 µM) foi preparada e utilizada para posterior cálculo dos resultados em µM equivalente de trolox/mg de pele (KATALINIC *et al.*, 2005).

3.2.2.10.3 *Avaliação dos níveis do antioxidante endógeno GSH*

O método baseia-se na detecção do ácido 5-mercapto-2-nitrobenzóico, um composto amarelo, liberado pela quebra da ligação dissulfeto do ácido 5',5'-ditio-bis-(2-nitrobenzóico) (DTNB) pelo grupo sulfidrila da glutationa.

As amostras de pele dos animais foram coletadas em microtubos e posteriormente diluídas (1:4) em EDTA 0,02 M e trituradas (Tissue-Tearor, Biospec). Ao homogenato foi adicionado ácido tricloroacético (TCA) 50% na proporção de 1: 0,2 de EDTA e TCA, respectivamente. A mistura foi centrifugada a 2.700 g por 10 minutos a 4°C. O sobrenadante foi recentrifugado a 2.700 g por 10 minutos a 4°C, e o sobrenadante final foi retirado para análise.

O ensaio para quantificação dos níveis de GSH na pele foi realizado em microplaca de 96 poços por meio da adição de 50 µL de amostra ao meio reacional contendo 100 µL de tampão Tris 0,4 M (pH 8,9) e 5 µL de uma solução de DTNB em metanol (1,9 mg/mL de metanol). O branco foi preparado com a adição de 50 µL de EDTA 0,02 M ao meio reacional. A absorvância foi determinada após 5 minutos de incubação das amostras no meio reacional a 405 nm (Asys Expert Plus, Biochrom). A curva analítica foi preparada com 5 a 150 µM de GSH. Os resultados foram expressos em µM de GSH/mg de pele (IVAN *et al.*, 2014).

3.2.2.10.4 *Determinação da atividade da CAT*

A análise da atividade da CAT foi determinada por meio do decaimento na concentração de H_2O_2 e geração de oxigênio, conforme previamente descrito (AEBI, 1984). As amostras de pele dos animais (aproximadamente 100 mg) foram coletadas em microtubos e diluídas em 500 µL de EDTA 0,02 M. Em seguida, foram trituradas (Tissue-Tearor, Biospec) e o homogenato foi centrifugado a 2.700 g por 10 minutos a 4°C. O sobrenadante foi recentrifugado a 2.700 g por 10 minutos a 4°C, e o sobrenadante final foi retirado para análise.

A determinação da atividade da CAT na pele foi realizada em microplaca de 96 poços por meio da adição de 10 µL de amostra, 160 µL de tampão Tris-HCl 1M com EDTA 5 mM pH 8,0, 20 µL de água deionizada e 20 µL de H_2O_2 200 mM. Ao teste foi incluído um branco para cada amostra preparado com 10 µL de amostra, 180 µL de tampão Tris-HCl 1M com EDTA 5 mM pH 8,0 e 20 µL de água deionizada. A velocidade com que o H_2O_2 é reduzido pela ação da CAT foi avaliada por meio da diminuição no valor da absorbância pela diferença entre a leitura inicial e a leitura 30 segundos após a adição do H_2O_2 200 mM. A leitura foi realizada em espectrofotômetro de microplaca (EnSpire, Perkin Elmer) em 240 nm com temperatura mantida em 25 ºC. Os valores de catalase foram expressos como unidade de catalase/mg de pele/minuto.

3.2.2.10.5 *Determinação de LOOH*

A avaliação da formação de LOOH por quimiluminescência (QL) foi realizada em uma adaptação da técnica descrita por Flecha et al. 1991. Este teste baseia-se no consumo das defesas antioxidantes e a formação de hidroperóxidos resultando em um aumento da emissão de fótons, ou seja, em um aumento de quimiluminescência que está relacionado com o estresse oxidativo.

As amostras de pele dos animais (aproximadamente 100 mg) foram coletadas em microtubos e homogeneizadas em 800 µL de tampão fosfato (pH 7,4) com triturador (Tissue-Tearor, Biospec). Em seguida, foram centrifugadas a 700 g por 2 minutos a 4 ºC e 250 µL do sobrenadante foram adicionados a 1730 µL de meio de reação (KCl 120mM, tampão fosfato pH 7,4 30 mM) e 20 µL de tert-butil hidroperóxido 3 mM. Este ensaio foi realizado em contador β marca Beckman® LS 6000 (Fullerton, CA, EUA) em uma faixa de contagem não coincidente com a resposta entre 300 e 620 nm. Todo o experimento foi realizado ao abrigo da luz para evitar a fosforescência dos frascos, a 30 ºC, durante 120 minutos. Os resultados foram medidos em contagem por minuto (cpm) por mg de pele.

3.2.2.10.6 *Determinação da produção de ânion superóxido*

A quantificação da produção do ânion superóxido foi realizada usando o ensaio de redução de *nitroblue tetrazolium* (NBT) (CAMPANINI *et al.*, 2013). As amostras de pele dos animais (aproximadamente 100mg) foram coletadas em microtubos, homogeneizadas em 500 µL de EDTA 0,02 M com triturador (Tissue-Tearor, Biospec), centrifugadas a 2000 g por 20 segundos e o sobrenadante foi retirado para a análise.

Para a reação 50 µL do sobrenadante foi incubado em placas de 96 poços por 1 hora. Em seguida o sobrenadante foi cuidadosamente removido e às células fixadas foi adicionado 100 µL de NBT (1 mg/mL). Após 15 minutos o sobrenadante foi cuidadosamente removido e ao precipitado foram adicionados 20 µL de metanol 100% para fixar, 120 µL de KOH 2M e 140 µL de dimetilsulfóxido (DMSO) para solubilizar as partículas de formazan (NBT reduzido) presentes dentro das células. A redução do NBT foi determinada espectrofotometricamente em 620 nm e os resultados foram apresentados como densidade óptica (OD)/10 mg de pele.

3.2.2.10.7 *Avaliação da expressão de RNAm pela reação em cadeia da polimerase (PCR) quantitativa*

As amostras de pele dos animais foram coletadas em microtubos e estocadas a temperatura de -70 ^{o}C. Materiais plásticos e soluções livres de DNase e RNase foram usados em todo procedimento. No momento do processamento, foram acrescentados 500 µL de reagente TRIzol® (Invitrogen) para a extração do RNA total conforme as instruções do fabricante.

A quantidade de RNA total foi mensurada em espectrofotômetro no comprimento de onda 260 nm, após constatada a pureza pela razão 260/280, a qual foi considerada aceitável entre 1,8 e 2,0. Dois microgramas do RNA total foram utilizados, e o RNAm total transcrito por ação da enzima transcriptase reversa (Superscript III, Invitrogen) em combinação com primers Oligo(dT)12-18 (Invitrogen). O DNAc proveniente do RNAm de interesse assim obtido foi quantificado utilizando primers específicos para os genes de interesse (VERRI *et al*., 2008). A quantificação de RNAm nas amostras foi realizada por meio de reações de PCR em Tempo Real, utilizando o kit Platinum SYBRGreen® (Invitrogen) conforme as especificações do fabricante. Para as reações de PCR em Tempo Real, foram utilizados 25 µL do reagente SYBR Green Master Mix (o qual contém fluoróforo SYBR Green 1; enzima polimerase AmpliTaq Gold; dNTPs; e os demais componentes de tampão, já devidamente otimizados), 8 µL da solução de DNAc (sintetizado como previamente descrito e diluído), 15 µL de água MiliQ tratada com dietilpirocarbonato, e 1 µL de cada primer. A reação de amplificação compreende basicamente 2 minutos a 50 ºC, 2 minutos a 95 ºC, e quarenta e cinco ciclos de 15 segundos a 95 ºC e 30 segundos a 55 ºC, além de um ciclo final de vinte minutos, com temperatura crescente de 60 a 95ºC empregada para a obtenção de uma curva de dissociação dos produtos da reação, utilizada para a análise da especificidade de amplificação. Previamente, as reações de PCR em Tempo Real foram otimizadas com relação às concentrações ideais de cada par de primers e temperatura de anelamento, de modo a maximizar eficiência e a especificidade de amplificação. O sistema utilizado realiza as reações de amplificação e detecção, e quantifica as amostras no termociclador (LightCycler® Nano, Roche) por meio da análise do nível de fluorescência gerado pela incorporação de fluoróforos (SYBRGreen) aos produtos de amplificação durante o curso da reação.

Os resultados foram analisados com base no valor de Cq (cycle quantification - ou ciclo de quantificação), sendo este o ponto correspondente ao número de ciclos onde a amplificação das amostras atinge um limiar (determinado entre o nível de fluorescência dos controles negativos e a fase de amplificação exponencial das amostras) que permite a análise quantitativa da expressão do gene avaliado. Todas as amostras também foram submetidas a reações para a detecção de RNAm para Gapdh, um gene de expressão constitutiva, utilizado como controle endógeno para a normalização dos níveis de expressão

do gene alvo (VERRI *et al.*, 2008). A sequência dos primers utilizados encontra-se na tabela 3.

Tabela 3. Sequência dos primers.

Gene	Primer sense	Primer antisense
gp91phox	AGCTATGAGGTGGTGATGTTAGTGG-	CACAATATTTGTACCAGACAGACTTGAG
GPx1	CCAACACCCAGTGACGACC	CTCAAAGTTCCAGGCAATGTC
GR	TGCGTGA	CCGGCATTCTCCAGTTCCT
	ATGTTGGATGTGTACCC	CG
Nrf2	TCACACGAGATGAGCTTAGGGCAA	TACAGTTCTGGGCGGCGACTTTAT
HO-1	CCCAAAACTGGCCTGTAAAA	CGTGGTCAGTCAACATGGAT
Gapdh	CATACCAGGAAATGAGCTTG	ATGACATCAAGAAGGTGGTG

3.3 ANÁLISE ESTATÍSTICA

Os resultados foram analisados pelo software GraphPad Prism®, versão 4.0 e expressos como média ± erro padrão da média (EPM). Os resultados *in vitro* foram apresentados de mensurações feitas em triplicata e foram representativos de dois experimentos separados. As concentrações dos flavonóides que inibem o processo oxidativo *in vitro* em 50% (IC_{50}) foram estimadas por meio de uma curva hiperbólica.

Os resultados dos testes *in vivo* foram analisados por análise de variância (ANOVA) com um fator seguido do teste de comparações múltiplas de Tukey e apresentados pela média ± EPM de mensurações feitas com 5 animais em cada grupo por experimento. Os resultados foram representativos de dois experimentos separados e foram considerados significativamente diferentes para $p<0,05$.

4 RESULTADOS E DISCUSSÃO – ARTIGOS CIENTÍFICOS

4.1 TRANS-CHALCONE, A FLAVONOID PRECURSOR, INHIBITS UVB-INDUCED SKIN INFLAMMATION AND OXIDATIVE STRESS IN MICE BY TARGETING NADPH OXIDASE AND CYTOKINE PRODUCTION

Renata M. Martinez,[†] Felipe A. Pinho-Ribeiro,[‡] Vinicius S. Steffen,[†] Carla V. Caviglione,[†] Nilton S. Arakawa,[†] Marcela M. Baracat,[†] Sandra R. Georgetti,[†] Waldiceu A. Verri, Jr.,[‡] and Rubia Casagrande*,[†]

[†]Departamento de Ciências Farmacêuticas, Universidade Estadual de Londrina-UEL, Avenida Robert Koch, 60, Hospital Universitário, 86039-440 Londrina, Paraná, Brazil

[‡]Departamento de Patologia, Universidade Estadual de Londrina-UEL, Rodovia Celso Garcia Cid, Km 380, PR445, Cx. Postal 10.011, 86057-970 Londrina, Paraná, Brazil

* Corresponding author. Address: Avenida Robert Koch, 60, Vila Operária, CEP 86039-440 Londrina, Paraná, Brazil. Tel.: +55 43 33712475. E-mail address: rubiacasa@yahoo.com.br (R. Casagrande).

Table of Contents Graphic

Trans-Chalcone, a Flavonoid Precursor, Inhibits UVB-Induced Skin Inflammation and Oxidative Stress in Mice by Targeting NADPH Oxidase and Cytokine Production

Renata M. Martinez, Felipe A. Pinho-Ribeiro, Vinicius S. Steffen, Carla V. Caviglione, Nilton S. Arakawa, Marcela M. Baracat, Sandra R. Georgetti, Waldiceu A. Verri, Jr., Rubia Casagrande

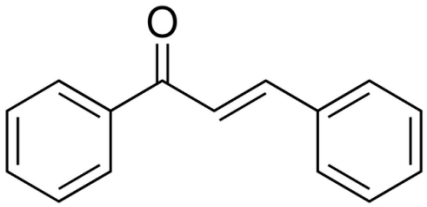

1

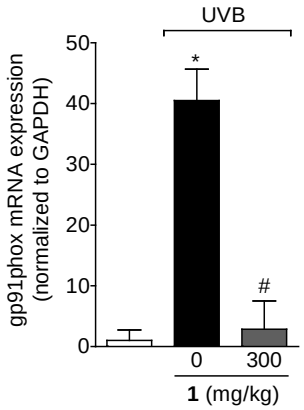

Cover letter

Dear Editor-in-Chief of the Journal of Natural Products
Professor A. Douglas Kinghorn,

We are submitting the manuscript entitled **"Trans-Chalcone, a Flavonoid Precursor, Inhibits UVB-Induced Skin Inflammation and Oxidative Stress in Mice by Targeting NADPH Oxidase and Cytokine Production"** of Martinez et al. Recent research supports the idea that exogenous supplementation with trans-chalcone (**1**) is an important approach to prevent skin damage induced by UVB irradiation. Flavonoids are important dietary antioxidants, and **1** is the precursor of all flavonoids' synthesis. Others reported that **1** exhibits anti-inflammatory activity, but the effects of **1** in UVB-induced inflammation and oxidative stress have not been addressed yet. Thus, to our knowledge, this is the first study demonstrating that **1** given systemically inhibits skin inflammation and oxidative induced by UVB exposure. Moreover, we also reported here the relation of this effect with inhibition of oxidative stress, gp91phox expression, and cytokine production. These results highlight the protective effects of **1** in UVB-induced skin damage, and reveal its anti-inflammatory activity, which might contribute to its inclusion as an exogenous supplement to prevent and treat inflammatory skin diseases. Therefore, we consider this research article suitable for the audience of Journal of Natural Products. This is the first submission of this manuscript to a journal, and we state that the content of the manuscript is original and is not submitted elsewhere.

Best regards,
Rubia

Prof. Rubia Casagrande, PhD
Universidade Estadual de Londrina
Centro de Ciências da Saúde
Departamento de Ciências Farmacêuticas
Avenida Robert Koch, 60, Hospital Universitário
CEP 86039-440 | Londrina - PR - Brasil
Tel: + 55 43 3323 4798 (home)
+ 55 43 3371 2475 (University)

ABSTRACT

The anti-inflammatory and antioxidant activities of a wide variety of plant polyphenols have been reported, and exogenous supplementation of flavonoids has been shown to prevent ultraviolet B (UVB) irradiation-induced skin damage. In the present study, the anti-inflammatory and antioxidant mechanisms of systemic administration with trans-chalcone (**1**), a flavonoid precursor, on UVB-induced skin inflammation and oxidative stress in hairless mice were investigated by the following parameters: skin edema, myeloperoxidase activity (neutrophil marker), matrix metalloproteinase-9 activity, reduced glutathione levels, catalase activity, lipid peroxidation products, superoxide anion production, gp91phox (NADPH oxidase sub-unity) mRNA expression by quantitative PCR and the cytokine production by ELISA. Systemic treatment with **1** prevented skin inflammation by reducing neutrophil recruitment and skin edema, and also inhibited matrix metalloproteinase-9 activity. Compound **1** also inhibited the mRNA expression of gp91phox, oxidative stress, and a wide range of cytokines production, while maintained regulatory T (Treg) cells associated cytokines induced by UVB irradiation. However, **1** not presented antioxidant activity *in vitro*. In conclusion, treatment with **1** inhibited UVB-induced skin inflammation that resulted in minor oxidative stress *in vivo*, which suggests that systemic supplementation with this compound may represent an important therapeutic approach in skin diseases induced by UVB irradiation.

Skin is the largest organ in mammals and is exposed daily to environmental sources of detrimental stresses. Among these sources, ultraviolet (UV) irradiation from the sun is one of the major risk factors for dermatologic diseases. Both UVA and UVB irradiation cause skin damage, but the ability of UVB to induce sunburn is much higher.[1] Excessive acute exposure to UVB radiation causes a variety of adverse skin reactions due to the resulting inflammatory response such as erythema and edema, while the chronic exposure contributes to hyperplasia, skin photoaging, and photocarcinogenesis.[1,2] Reactive oxygen species (ROS) are formed as a consequence of exposure to UVB irradiation *per se*, but its production is further increased by the pro-inflammatory cytokines interleukin-1β (IL-1β) and tumor necrosis factor-alpha (TNF-α).[3]

ROS are short-lived and highly-reactive oxygen derivatives that oxidize and damage cellular proteins, lipids, and deoxyribonucleic acid (DNA). Superoxide anion radical ($O_2^{\bullet-}$) enzymatic production represents the first step that leads to oxidative stress during inflammation. Pro-inflammatory cytokines (e.g. TNF-α and IL-1β) act on recruited neutrophils and increase $O_2^{\bullet-}$ production by these cells through activation of (phagocytic) NADPH oxidase 2 (NOX 2) complex.[4] This increased of $O_2^{\bullet-}$ production leads to changes and often to destruction of skin structures, which result in inhibition of its regular function.[5] Thus, the UVB-induced early decrease of endogenous antioxidants in skin and blood potentiates the deleterious effects of inflammation through inappropriate amplification of oxidative stress-responses, thereby increasing the risk of skin carcinogenesis.[6] Since skin cancer is a significant problem associated with mortality and morbidity, intensive efforts are required to develop broad strategies for the prevention of the deleterious effects of UVB exposition. In this sense, the protective effects of systemic treatments received considerable attention over the last years.

Exogenous supplementation of antioxidants has been shown to prevent UV irradiation-induced inflammation and oxidative damage.[7-9] A wide variety of plant polyphenols have been reported to possess antioxidant and anti-inflammatory properties, thereby protecting skin from photodamage.[10] Flavonoids represent the most common and widely distributed group of plant phenolics,[11] and trans-chalcone (**1**) (1,3-diphenyl-2-propen-1-one) is the biphenolic precursor for all flavonoids' synthesis in the phenylpropanoid pathway in plants.[12] Existing evidences of **1** protective effects in hydrogen peroxide-induced toxicity[13] and neovascularization[14] suggest its potential applicability to prevent both acute and chronic deleterious effects of UVB irradiation. Thus, the present study aimed to investigate the antioxidant activity *in vitro* of **1** and the *in vivo* efficacy of **1** in UVB-induced inflammatory and oxidative damage in the skin of hairless mice.

RESULTS AND DISCUSSION

Trans-Chalcone (1) not presented antioxidant activity *in vitro*. Primary antioxidants or free radical scavenging antioxidants can deactivate radicals and inhibit oxidation via chain terminating reactions. Inhibition occurs either by direct reduction via electron transfers or by radical quenching via H atom transfers.[15] Moreover, some compounds contribute to antioxidant defense by chelating transition metals and preventing them from catalyzing the production of free radicals in the cell.[16] Herein, we investigated whether compound **1** take action as primary antioxidant and as well as iron-chelating. Compound **1** not demonstrated antioxidant activity by ABTS (electron transfers), DPPH (H transfer), iron chelation and superoxide anion (free radical biological) assays. This result can be explained because **1** not posses "classical" groups antioxidants in your structure, for example hydroxyl group.

Trans-chalcone (1) Reduces UVB Irradiation-Induced Edema and Myeloperoxidase (MPO) Activity in the Skin. UVB irradiation stimulates the edema formation in the skin and the recruitment of inflammatory cells such as neutrophils as observed by MPO activity,[7,8] which can be considered markers of skin inflammation. Thus, standard size punches of skin were collected 12 h after UVB exposition and weighted in order to evaluate the capacity of **1** to reduce UVB irradiation-induced edema. As shown in Figure 1A, UVB irradiation induced significant skin edema compared to unexposed mice. The UVB irradiation-induced skin edema was significantly inhibited by treatment with **1** at the doses of 30, 100, and 300 mg/kg, and there was no statistical difference between these doses of **1** (Figure 1A). The dose of 10 mg/kg of **1** did not present significant activity (Figure 1A).

In general, neutrophils are the first cells recruited from peripheral blood to inflammatory sites where they produce large amounts of pro-inflammatory cytokines and ROS, enhancing the inflammatory response. In fact, it has been suggested that neutrophils are key players during skin damage after UV irradiation exposure.[17] Therefore, the neutrophil recruitment to the skin was evaluated by measuring the MPO activity in samples collected 12 h after UVB irradiation.[7] UVB irradiation resulted in elevated MPO activity in comparison with the non-irradiated control group, and treatment with **1** reduced UVB irradiation-induced MPO activity at the doses of 30, 100, and 300 mg/kg (Figure 1B). As observed with edema (Figure 1A), there was no significant difference between these 3 doses of **1** and 10 mg/kg did not present significant activity (Figure 1B). Supporting our results, the inhibitory effects of **1** in MPO activity were described in sulfonic acid-treated rat colon tissue.[18] Thus, as neutrophils are the major sources of enzymes that lead to the development of skin inflammation and oxidative stress, treatment with **1** may contribute to reduce skin diseases.

Trans-Chalcone (1) Reduces UVB Irradiation-Induced Matrix Metalloproteinase-9 (MMP-9) Activity in the Skin. MMPs are Zn-dependent endopeptidases which participate in tissue remodeling and inflammation. Dysregulation of MMPs activity, such as MMP-9 (gelatinase B), is associated with inflammatory skin diseases, angiogenesis, and with invasive and metastatic potentials of cancer cells.[19-22] Considering that neutrophil-derived mediators, such as inflammatory cytokines and $O_2^{\bullet-}$ radical, induce overexpression and activation of MMP-9,[23] and the role of MMP-9 in skin diseases, the effects of **1** treatment in MMP-9 activity in the skin submitted UVB exposition was investigated. The MMP-9 activity was measured in skin samples collected 12 h after UVB irradiation by SDS–PAGE (sodium dodecyl sulfate polyacrylamide gel electrophoresis) zymography. As observed in Figure 2, UVB irradiation induced significant increase of MMP-9 activity in the skin of hairless mice, and this increase was inhibited by treatment with **1** at the dose of 300 mg/kg. However, no inhibitory effect on MMP-9 activity was observed at the doses 30 and 100 mg/kg of **1**, suggesting that the dose of 300 mg/kg may protect mice skin by inhibiting others UVB irradiation-induced skin damage, such as the oxidative stress. Similarly, trans-chalcone inhibited MMP-2/-9 expression and activity in human gastric adenocarcinoma cell line,[24] suggesting that **1** may also prevent skin tumor progression by targeting MMPs.

Treatment With Trans-Chalcone (1) Prevents the UVB Irradiation-Induced Decrease of Antioxidant Capacity in the Skin of Hairless Mice. UVB irradiation produces ROS directly and indirectly via the inflammatory response, causing an impairment of cellular antioxidant defense system that leads to oxidative damage.[10,25] Fischer et al.[26] suggested that UV exposition induces skin damage that is not fully repaired, which highlights the importance of the antioxidant system. Reduced glutathione (GSH) is the most abundant cellular non-enzymatic antioxidant and its levels are indicators of redox state in cells and tissues.[27] Thus, skin samples were collected 12 h after UVB irradiation and used to evaluate GSH levels. The UVB irradiation was able to significantly reduce the endogenous antioxidant GSH compared with the non-irradiated control. Treatment with 300 mg/kg of **1** reduced UVB irradiation-induced GSH depletion, whereas no significant differences were observed with the other doses (Figure 3A). GSH depletion is a consequence of its use to neutralize ROS such as H_2O_2.[28] In agreement, it has been demonstrated that treatment with **1** exerts protective effect by delaying the consumption of GSH and/or other cellular antioxidants in oxidative stress caused by hydrogen peroxide (H_2O_2) in hepatocellular carcinoma (HepG2) cells.[13]

Catalase (CAT) is an important antioxidant enzyme that converts H_2O_2 into water and oxygen, and UVB irradiation decreases CAT activity in the skin, which contributes to increase H_2O_2 levels and to promote skin carcinogenesis.[29-31] In this line, UVB irradiation also reduced the CAT activity of skin compared with non-irradiated control group (Figure 3B). This early impairment of CAT activity represents an important step by which ROS production induce

skin damage that reflects in depletion of GSH levels. The treatment with 300 mg/kg of **1** significantly inhibited UVB irradiation induced loss of CAT activity (Figure 3B). Therefore, prevention of UVB-induced depletion of antioxidant defenses would provide a useful approach to protect UVB-irradiation induced photo-damage.

Trans-Chalcone (1) Reduces UVB Irradiation-Induced Lipid Peroxidation (LPO) and Superoxide Anion ($O_2^{\bullet-}$) Production in the Skin. The increased levels of H_2O_2 can be deleterious to the host as this molecule can generate cytotoxic derivatives such as hydroxyl radical ($HO^{\bullet}$), leading to lipid peroxidation (LPO) process, a well-established detrimental consequence of UVB exposure.[32] Using tert-butyl hydroperoxide-initiated chemiluminescence assay, it was observed that UVB irradiation induced significant increase of LPO in the skin of hairless mice, which was inhibited by **1** at the dose of 300 mg/kg (Figure 4A). Supporting this result, the protective effect of **1** on H_2O_2-induced lipid peroxidation has been reported in hepatocellular carcinoma (HepG2) cells.[13]

$O_2^{\bullet-}$ production occurs at low rates in basal conditions undergoing conversion to H_2O_2 by superoxide dismutase (SOD) activity. However, $O_2^{\bullet-}$ increases to large amounts under antioxidant depletion as occurs after UVB exposition,[7] which favors generation of $HO^{\bullet}$.[33] There was a significant increase of $O_2^{\bullet-}$ production in the skin of irradiated mice compared to non-irradiated control, and the treatment with 300 mg/kg of **1** significantly reduced UVB irradiation-induced $O_2^{\bullet-}$ production (Figure 4B). Thus, compound **1** reduced the excessive generation of $O_2^{\bullet-}$, which is crucial for preventing UVB-induced skin injury.[23,29,34]

Trans-Chalcone (1) Prevents UVB-Induced gp91phox mRNA Expression and Modulates the Production of Several Cytokines in the Skin. There is a tight relationship between acute inflammation and oxidative stress since neutrophils are the major sources of additional production of $O_2^{\bullet-}$ through NADPH oxidase 2 (NOX2) activity,[35] which accounts to the excessive generation of ROS following UVB exposure.[7] Furthermore, $O_2^{\bullet-}$ production is essential to maintain the directionality of neutrophils during chemotaxis.[36] In order to evaluate the effects of **1** over NOX2, skin samples were collected 4 h after UVB exposure, and the expression of NOX2 sub-unity gp91phox was measured by quantitative PCR. As shown in Figure 5, UVB irradiation increased gp91phox mRNA expression, and this increase was inhibited by **1** at the dose of 300 mg/kg.

It has been described that ROS derived from NOX2 sub-unity gp91phox play a crucial role in the UVB-induced inflammation by inducing IL-1β production.[37] ROS act as second messengers in pro-inflammatory signaling cascades that induce cytokine production.[37] It is known that, UVB irradiation induces the production of multiple cytokines, including TNF-α,[38-40] IL-1β,[7,41] interferon *gamma* (IFN-γ),[39,42] IL-12,[42] IL-4,[39] IL-23,[42] IL-10 [39,40] and transforming growth factor *beta* (TGF-β).[43] Thus, pathogenesis of skin inflammation is associated with reactive oxygen species-driven production of cytokines.[23,38] The release of these cytokines

plays a central role in the recruitment and activation of inflammatory cells, leading to skin damage after UVB exposure.[17,23,44-46]

Pro-inflammatory cytokines (e.g. TNF-α and IL-1β) up-regulation of adhesion molecules required for transendothelial trafficking of immune cells,[47] for example subpopulations of T helper (Th) cells, defined based on distinct cytokine secretion profiles. Th1 cells (secrete, for example, IFN-γ and IL-12) are implicated in various chronic inflammatory disorders and organ-specific autoimmune diseases.[48] Th2 cells (secrete IL-4 and IL-13) are responsible for initiation, maintenance, and amplification of human allergic inflammation and are important in patients with asthma.[48] Th17 cells activated by IL-23 (secrete IL-22) are implicated in inflammatory and autoimmune responses such as inflammatory bowel diseases, rheumatoid arthritis, multiple sclerosis, allergic contact dermatitis, psoriasis, among other inflammatory skin disorders.[48,49] In addition to the role in adaptive immune diseases, these cytokines also play roles in innate immune responses.[50] Therefore, the inhibition of these different cytokines profiles is considered a therapeutic approach to control skin cancer progression and metastasis, psoriasis, contact dermatitis and other several diseases.[38,40,42,43,47,48,51-52] Regulatory T (Tregs) cells (secrete IL-10 and TGF-β) regulate and counterbalance the immune response,[53] thus, the maintaining of Treg cells associated cytokines can effectively protects against inflammatory/immune skin disorders.

In this context, we investigated if treatment with **1** could modulate cytokines production UVB irradiation induced. As expected, UVB irradiation induced the production of several cytokines, including classic inflammatory (TNF-α and IL-1β), associated with Th1 (IFN-γ and IL-12), Th2 (IL-4 and IL-13) and Th17 (IL-22 and IL-23) cells. As shown in Figure 6A-D, treatment with **1** at the dose of 300 mg/kg inhibited the increases of all these pro-inflammatory cytokines (Figure 6A-D*).* We also observed that **1** maintained regulatory T (Treg) cells associated cytokines (TGF-β and IL-10) induced by UVB (Figure 6E). Corroborating our results, it was reported that compound **1** inhibited TNF-α expression in trinitrobenzene sulfonic acid (TNBS)-induced rat colitis model.[18] and the TNF-α production in lipopolysaccharide-stimulated macrophages.[54]

Taken together, our results suggest that flavonoids with anti-inflammatory activity *in vivo* not necessarily present antioxidant activity *in vitro.* So group's antioxidants do not prefigure anti-inflammatory activity *in vivo,* and probably the anti-inflammatory activity *in vivo* can be dissociated of the antioxidant activity *in vitro*. It is important to note, that the relation antioxidant structure-activity is more understand that the relation anti-inflammatory structure-activity. Evidences indicate that α, β-enone structure in chalcones is important to anti-inflammatory activity.[54,55] Finally, in this study we demonstrated, with trans-chalcone, that

anti-inflammatory effect result in lower oxidative stress *in vivo*, but not necessarily by an antioxidant effect direct.

In conclusion, the systemic administration of **1** may represent an important therapeutic approach in skin diseases, which needs to be further investigated. Moreover, as its mechanisms of action included targeting NOX2-related $O_2^{\bullet-}$ production and oxidative stress, and also the production of a wide range of cytokines, it is suggestive that the systemic treatment with **1** may exhibit benefits in inflammatory conditions other than UVB irradiation.

Experimental Section

General Experimental Procedures. 2,2'-azino-bis(3-ethylbenzothiazoline-6-sulfonic acid) (ABTS), 2,2-diphenyl-1-(picrylhydrazyl) (DPPH), brilliant blue R, reduced glutathione (GSH), hexadecyltrimethylammonium bromide (HTAB), N-ethylmaleimide, *o*-dianisidine dihydrochloride, phenylmethanesulfonyl fluoride, 5,5'-dithiobis(2-nitrobenzoic acid) (DTNB) and nitroblue tetrazolium (NBT), bisacrylamide were obtained from Sigma-Aldrich (St. Louis, MO, USA). Trans-chalcone (**1**) at 97% purity from Santa Cruz (Dallas, TX, USA). Tert-butyl hydroperoxide and bathophenanthroline (BPS) from Acros (Pittsburgh, PA, USA). Xylene cyanol and Tris were obtained from Amresco (Solon, OH, USA). ELISA kits for determination of cytokine were obtained from eBioscience (San Diego, CA, USA). Acrylamide, sodium dodecyl sulfate (SDS), glycerol, Superscript® III, Oligo(dT)12-18 primers, Platinum SYBRGreen® and primers from Invitrogen (Carlsbad, CA, USA). All other reagents used were of pharmaceutical grade.

***In vitro* ABTS assay.** The ability of compound **1** to transfer electron to reduce ABTS radical (10-250 µg/mL) was measured by the decrease of absorbance at 730 nm (Evolution 60, Thermo Scientific),[41] and calculated by the following equation: Equation I: % of activity = (1- sample absorbance/control absorbance) x 100.

***In vitro* DPPH assay.** The compound **1** (2.5-50 µg/mL) antioxidant ability to donate hydrogen and stabilize the free radical DPPH was evaluated by the reduction of DPPH radical by the change in absorbance measured at 517 nm (Evolution 60, Thermo Scientific).[41] The results were calculated by equation I.

***In vitro* bathophenanthroline (BPS) assay**. BPS is a strong chelator of ferrous ion that forms a colored complex when it reacts with this ion. The compound **1** (2.5-50 µg/mL) chelation of iron ions was determined by colorimetric change measured at 530 and 700 nm (Evolution 60, Thermo Scientific).[41] The iron chelating activity was calculated by equation I.

***In vitro* superoxide anion assay.** The ability of compound **1** to deactivate superoxide radical (0.1-240 µg/mL) was measured by nitroblue tetrazolium assay (NBT). Samples of **1** were added to 100 µL of NBT (1 mg/ml) followed by KO_2 (30 µg, 25 µL), one donor of $O_2^{\bullet-}$. After 15 min of incubation at room temperature, the supernatants were carefully removed. The formazan precipitates were solubilized by addition of 120 µL of KOH 2 M and 120 µL of dimethylsulfoxide, and the absorbances were read at 620 nm in a microplate reader (EnSpire, Perkin Elmer).[56]

Animals and experimental protocol. *In vivo* experiments were performed sex matched hairless mice (HRS/J), weighing 20-30 g. The animals were housed in a temperature-controlled room, with access to water and food *ad libitum*. They were housed within cages with a 12 h light and 12 h dark cycles. All experiments were conducted in accordance with National Institutes of Health guidelines for the welfare of experimental

animals and with the approval of the Ethics Committee of the Universidade Estadual de Londrina (registered under the number CEUA 90/12, process number 3344.2012.08). All efforts were made to minimize the number of animals used and their suffering. Hairless mice were randomly designed to different groups with 5 mice each: non-irradiated control group (20% of Tween 80 in saline), irradiated control group (20% of Tween 80 in saline), irradiated group and treated with solutions containing different doses of **1**. The doses of **1** used in these assays were selected based on therapeutic effects reported previously.[14] In the experiments presented in Figures 1 (10 – 300mg/kg), 2 (30 – 300mg/kg), and 3A (30 – 300mg/kg), mice were treated intraperitoneally 1 h before and 7 h after the beginning of UVB irradiation with **1**. In the experiments of Figures 3B (30 – 300mg/kg), 4 (30 – 300mg/kg), 5 (300mg/Kg) and 6 (300mg/Kg) mice were treated only once, 1 h before the irradiation beginning.[41]

Irradiation. The UVB source used in the experiments to induce oxidative stress was a Philips TL/12 RS 40W (Medical-Holand) emitting a continuous spectrum between 270 and 400 nm with a peak emission at 313 nm. The lamp was mounted 20 cm above the place where the mice were placed on, resulting in an irradiation of 0.384 mW/cm^2 as measured by an IL 1700 radiometer (Newburyport, MA, USA) equipped with sensor for UV (SED005) and UVB (SED240). The irradiation dose used for induction of oxidative stress was 4.14 J/cm^2 as employed previously.[7,41] The mice were terminally anesthetized 12 h (Figs. 1-2 and 3A), 2 h (Figs. 3B and 4B) or 4 h (Figs. 4A, 5 and 6) after the UVB exposure, and the full thickness of the dorsal skins was removed and stored at -70°C until analysis. The samples collected for verification of cutaneous edema were weighed when removed and were not frozen.[8]

Skin edema. The effect of **1** on UVB-induced skin edema of hairless mice was measured as an increase in the dorsal skin weight. After dorsal skin removal, a constant area (5 mm diameter) was delimited with the aid of a mold, followed by weighing of this constant area.[7,41] The analysis was obtained by comparing the weight of the skin between groups and the result was expressed in mg of skin.

Myeloperoxidase (MPO) activity. The UVB-induced leukocyte migration to the skin of hairless mice was evaluated using the MPO colorimetric assay.[7,8] The samples of skin were homogenized in K_2HPO_4 buffer 0.05 M (pH 6.0) containing 0.5% HTAB using a Tissue-Tearor (Biospec). The homogenates were centrifuged at 16100 *g* for 2 min at 4°C. The supernatant was removed to assay. Briefly, 30 µL of the resulting supernatant were mixed with 200 µL of 0.05 M K_2HPO_4 buffer (pH 6.0), containing 0.0167% *o*-dianisidine dihydrochloride and 0.05% hydrogen peroxide. The absorbance was determined at 450 nm (Asys Expert Plus, Biochrom). The MPO activity of samples was compared to a standard curve of neutrophils. The results are presented as MPO activity (number of neutrophils per mg of skin).

Analyses of skin proteinase by substrate-embedded enzymography. SDS-PAGE (sodium dodecyl sulphate polyacrylamide gel electrophoresis) substrate-embedded enzymography was used to detect enzymes with gelatinase activity. Assays were carried out as previously described.[7,41] The total skin of hairless mice (1:4, w/w dilution) were homogenized (T 18 basic, IKA) in 0.05 M Tris-HCl buffer (pH 7.4) containing 0.01 M $CaCl_2$ and 1% protease inhibitor cocktail. Whole homogenates were centrifuged at 12000 *g* for 10 min at 4°C twice. The Lowry method was used to measure protein levels in skin homogenates.[57] Aliquots of 50 µL of samples were mixed with 10 µL of 0.1 M Tris-HCl (pH 7.4) containing 20% glycerol, 4% SDS and 0.005% xylene cyanol, and 25 µL of the mixture (40 µg of protein) were taken for electrophoresis in a gel containing 10% acrylamide and 0.025% gelatin. After electrophoresis, the gels were incubated for 1 h with 2.5% Triton X-100 under constant shaking, incubated overnight in 0.05 M Tris-HCl (pH 7.4), 0.01 M $CaCl_2$ and 0.02% sodium azide at 37°C, and stained the following day with brilliant blue R. After destaining in 20% acetic acid, the zone of enzyme activity were analyzed by comparing the groups in the ImageJ Program (NIH, Bethesda, MD, USA).

Reduced glutathione (GSH) assay. GSH was determined as described previously.[41] Briefly, skin samples were homogenized in 0.02 M EDTA using a Tissue-Tearor (Biospec). Whole homogenates were treated with 50% trichloroacetic acid and were centrifuged twice at 2700 *g* for 10 min at 4°C. The reaction mixture contained 50 µL of sample, 100 µL of 0.4 M Tris and 5 µL DTNB (1.9 mg/mL in methanol). The color developed was read at 405 nm (Multiskan GO, Thermo Scientific). The standard curve was prepared with GSH 5-150 µM. The results are presented as µM of GSH per mg of skin.

Catalase (CAT) assay. The analysis of CAT activity was evaluated by measuring the decay in the concentration of hydrogen peroxide (H_2O_2) and the generation of oxygen as described previously.[58] Skin of hairless mice were homogenized in 500 µL of 0.02 M EDTA using a Tissue-Tearor (Biospec), and centrifuged twice at 2700 *g* for 10 min at 4°C. The reaction mixture contained 10 µL of sample, 160 µL of buffer Tris-HCl 1 M with EDTA 5 mM pH 8,0, 20 µL of deionized water and 20 µL of H_2O_2 200 mM. Measurement of CAT activity was estimated through the difference between the initial reading and the reading conducted 30 seconds after the addition of H_2O_2 at 240 nm in a microplate reader (EnSpire, Perkin Elmer) at 25ºC. The CAT values were expressed as unit of CAT/mg of skin/minute.

Lipid hydroperoxides (LOOH). LOOH-initiated chemiluminescence (QL) was determined according to an adaptation of the technique described previosly.[59] The test is based on the premise that there is an increase in chemiluminescence (CL) associated with oxidative stress leading to the consumption of the antioxidant defenses from the formation of hydroperoxides. Samples of skin were homogenized in 800 µL of phosphate buffer (pH 7.4) using a Tissue-Tearor (Biospec), centrifuged at 700 *g* for 2 min at 4°C. Then, 250 µL the

supernatant was diluted in 1730 µL reaction medium (120 mM KCl, 30 mM phosphate buffer, pH 7.4) and mixed with 20 µL of 3 mM tert-butyl hydroperoxide. The reading was conducted in a β-counter Beckman®LS 6000SC (Fullerton, CA, USA) in a non-coincident counting for 30 s with a response range between 300 and 620 nm. The vials were kept in the dark up to the moment of the assay, and determinations were obtained in dark in order to avoid vial phosphorescence activated by light. The experiment was conducted at 30°C for 120 min. The results were measured in counts per min (cpm) per mg of skin.

$O_2^{\bullet-}$ production. The measurement of $O_2^{\bullet-}$ production in the skin was performed using the nitroblue tetrazolium assay (NBT) as described previously.[7] Samples of skin were homogenized in 500 µL of 0.02 M EDTA using a Tissue-Tearor (Biospec) and centrifuged (2000 *g*, 20 seconds, 4°C). Then, 50 µL of the supernatant were incubated in 96-well plate for 1 h. The non-adherent/non-precipitated supernatant was carefully removed, 100 µL of NBT (1 mg/ml) was added to each well and incubated over 15 min. NBT reaction medium was then carefully removed followed by fixation in methanol 100%. Formazan particles were dissolved by adding 120 µL of KOH 2M and 140 µL of dimethylsulfoxide. Reduction of NBT to formazan was measured at 600 nm using a microplate spectrophotometer reader (Asys Expert Plus, Biochrom) and the results are presented as optical density (OD) per 10 mg of skin.

Quantitative polymerase chain reaction (qPCR). Quantitative polymerase chain reaction (qPCR) qPCR was performed as previously described.[7] Samples were homogenized in TRIzol reagent, and total RNA was extracted. The purity of total RNA was measured with a spectrophotometer and the wavelength absorption ratio (260/280 nm) was between 1.8 and 2.0 for all preparations. Reverse transcription of total RNA to cDNA was carried out using Superscript® III kit (Invitrogen) and Oligo(dT)12-18 primers. Real time PCR (qPCR) was performed with Platinum SYBRGreen® kits (Invitrogen) in a 50 µL reaction volume following the manufacturer's cycling conditions: 50 ºC for 2 min, 95 ºC for 2 min, followed by 45 cycles of 95 ºC for 15 s and 55 ºC for 30 s. Melting curve analysis was performed (65–95 °C) in order to verify that only one product was amplified. Samples with more than one peak were excluded. qPCR was performed in LightCycler® Nano Instrument (Roche).[7] The relative gene expression was measured using the comparative $2^{-(\Delta\Delta Cq)}$ method. The expression of GAPDH mRNA was used as a control for tissue integrity in all samples. The primers used were: *Gp91phox*, sense: 5'-AGCTATGAGGTGGTGATGTTAGTGG-3', antisense: 5'-CACAATATTTGTACCAGACAGACTTGAG-3'; and *Gapdh* sense: 5-ATGACATCAAGAAGGTGGTG-3, Antisense: 5'-CATACCAGGAAATGAGCTTG-3.

Cytokine measurement. The samples of hairless mouse skin (30 mg approximately) were homogenized in 500 µL of saline solution using Tissue-Tearor (Biospec). The homogenates were centrifuged at 2000 *g* for 15 min at 4 °C and stored at -70 ºC until further

use. Supernatants were used to measure the cytokine levels as described previously[7] by an enzyme- linked immunosorbent assay (ELISA) according to manufacturer's instructions (eBioscience). Absorbances were determined at 450 nm using a microplate spectrophotometer reader (Multiskan GO, Thermo Scientific) and the results are expressed as picograms (pg) of each cytokine/mg of skin.

Statistical analysis. Results were determined by GraphPad Prism® software, version 4.00 and expressed as means ± standard error of the mean (SEM). *In vitro* data were presented of triplicate analysis and results are representative of two separated experiments. *In vivo* results are presented of 5 mice per group per experiment and are representative of two separated experiments. The differences were evaluated by ANOVA followed by by Tukey's *t* test. Statistical differences were considered to be significant at $p < 0.05$.

Acknowledgment. This work was supported by Brazilian grants from Coordenadoria de Aperfeiçoamento de Pessoal de Nível Superior (CAPES), Conselho Nacional de Desenvolvimento Científico e Tecnológico (CNPq), Ministério da Ciência, Tecnologia e Inovação (MCTI), Secretaria da Ciência, Tecnologia e Ensino Superior (SETI)/Fundação Araucária and Governo do Estado do Paraná. Financiadora de Estudos e Projetos (FINEP) for LightCycler® Nano Instrument (Roche) acquisition (CT INFRA 2008, Conv. 01.09.0367.02). We thank the technical assistance of Denise Duarte.

REFERENCES

(1) Svobodova, A.; Psotova, J.; Walterova, D. *Biomed Pap Med Fac Univ Palacky Olomouc. Czech. Repub.* 2003, *147*, 137-145.

(2) Yaar, M.; Gilchrest, B. A. *Br. J. Dermatol.* 2007, *157*, 874-887.

(3) Liu, X.; Wang, J. *J. Ethnopharmacol.* 2011, *133*, 780-787.

(4) Anrather, J.; Racchumi, G.; Iadecola, C. *J. Biol. Chem.* 2006, *281*, 5657-5667.

(5) Valko, M.; Leibfritz, D.; Moncol, J.; Cronin, M. T.; Mazur, M.; Telser, J. *Int. J. Biochem. Cell Biol.* 2007, *39*, 44-84.

(6) Halliday, G. M.; Lyons, J. G. *Photochem. Photobiol.* 2008, *84*, 272-283.

(7) Campanini, M. Z.; Pinho-Ribeiro, F. A.; Ivan, A. L.; Ferreira, V. S.; Vilela, F. M.; Vicentini, F. T.; Martinez, R. M.; Zarpelon, A. C.; Fonseca, M. J.; Faria, T. J.; Baracat, M. M.; Verri, W. A., Jr.; Georgetti, S. R.; Casagrande, R. *J. Photochem. Photobiol. B.* 2013, *127*, 153-160.

(8) Casagrande, R.; Georgetti, S. R.; Verri, W. A., Jr.; Dorta, D. J.; dos Santos, A. C.; Fonseca, M. J. *J. Photochem. Photobiol. B.* 2006, *84*, 21-27.

(9) Filip, A.; Clichici, S.; Daicoviciu, D.; Adriana, M.; Postescu, I. D.; Perde-Schrepler, M.; Olteanu, D. *Exp. Oncol.* 2009, *31*, 9-15.

(10) Nichols, J. A.; Katiyar, S. K. *Arch. Dermatol. Res.* 2010, *302*, 71-83.

(11) Pietta, P. G. *J. Nat. Prod.* 2000, *63*, 1035-1042.

(12) Duthie, G.; Crozier, A. *Curr. Opin. Clin. Nutr. Metab. Care.* 2000, *3*, 447-451.

(13) Sikander, M.; Malik, S.; Yadav, D.; Biswas, S.; Katare, D. P.; Jain, S. K. *Asian Pac .J. Cancer Prev.* 2011, *12*, 2513-2516.

(14) Lamoke, F.; Labazi, M.; Montemari, A.; Parisi, G.; Varano, M.; Bartoli, M. *Exp. Eye Res.* 2011, *93*, 350-354.

(15) Prior, R. L.; Wu, X.; Schaich, K. *J. Agric. Food Chem.* 2005, *53*, 4290-4302.

(16) Oresajo, C.; Pillai, S.; Manco, M.; Yatskayer, M.; McDaniel, D. *Dermatol. Ther.* 2012, *25*, 252-259.

(17) Rijken, F.; Bruijnzeel-Koomen, C. A. *Clin. Pharmacol. Ther.* 2011, *89*, 120-124.

(18) Park, S. Y.; Ku, S. K.; Lee, E. S.; Kim, J. A. *Chem. Biol. Interact.* 2012, *196*, 39-49.

(19) Pilcher, B. K.; Wang, M.; Qin, X. J.; Parks, W. C.; Senior, R. M.; Welgus, H. G. *Ann. N. Y. Acad. Sci.* 1999, *878*, 12-24.

(20) Devillers, A. C.; van Toorenenbergen, A. W.; Klein Heerenbrink, G. J.; Muldert, P. G.; Oranje, A. P. *Clin. Exp. Dermatol.* 2007, *32*, 311-313.

(21) Harper, J. I.; Godwin, H.; Green, A.; Wilkes, L. E.; Holden, N. J.; Moffatt, M.; Cookson, W. O.; Layton, G.; Chandler, S. *Br. J. Dermatol.* 2010, *162*, 397-403.

(22) John, A.; Tuszynski, G. *Pathol Oncol Res.* 2001, *7*, 14-23.

(23) Song, H. Y.; Ju, S. M.; Goh, A. R.; Kwon, D. J.; Choi, S. Y.; Park, J. *BMB Rep.* 2011, *44*, 462-467.

(24) Lin, S. H.; Shih, Y. W. *Mol. Cell Biochem.* 2014, *391*, 47-58.

(25) Meloni, M.; Nicolay, J. F. *Toxicol. In Vitro.* 2003, *17*, 609-613.

(26) Fisher, G. J.; Wang, Z. Q.; Datta, S. C.; Varani, J.; Kang, S.; Voorhees, J. J. *N. Engl. J. Med.* 1997, *337*, 1419-1428.

(27) Bray, T. M.; Taylor, C. G. *Can J. Physiol. Pharmacol.* 1993, *71*, 746-751.

(28) Ng, C. F.; Schafer, F. Q.; Buettner, G. R.; Rodgers, V. G. *Free Radic. Res.* 2007, *41*, 1201-1211.

(29) Pence, B. C.; Naylor, M. F. *J. Invest. Dermatol.* 1990, *95*, 213-216.

(30) Sullivan, N. J.; Tober, K. L.; Burns, E. M.; Schick, J. S.; Riggenbach, J. A.; Mace, T. A.; Bill, M. A.; Young, G. S.; Oberyszyn, T. M.; Lesinski, G. B. *J. Invest. Dermatol.* 2012, *132*, 695-702.

(31) Gupta, A.; Butts, B.; Kwei, K. A.; Dvorakova, K.; Stratton, S. P.; Briehl, M. M.; Bowden, G. T. *Cancer Lett.* 2001, *173*, 115-125.

(32) Girotti, A. W. *J. Photochem. Photobiol B.* 2001, *63*, 103-113.

(33) Gutteridge, J. M. *FEBS Lett.* 1986, *201*, 291-295.

(34) Fang, Y.; Hu, X. H.; Jia, Z. G.; Xu, M. H.; Guo, Z. Y.; Gao, F. H. *Australas J Dermatol.* 2012, *53*, 172-180.

(35) Nathan, C.; Shiloh, M. U. *Proc Natl Acad Sci U S A.* 2000, *97*, 8841-8848.

(36) Hattori, H.; Subramanian, K. K.; Sakai, J.; Jia, Y.; Li, Y.; Porter, T. F.; Loison, F.; Sarraj, B.; Kasorn, A.; Jo, H.; Blanchard, C.; Zirkle, D.; McDonald, D.; Pai, S. Y.; Serhan, C. N.; Luo, H. R. *Proc. Natl. Acad. Sci. U S A.* 2010, *107*, 3546-3551.

(37) Schulze-Osthoff, K.; Bauer, M. K.; Vogt, M.; Wesselborg, S. *Int. J. Vitam. Nutr. Res.* 1997, *67*, 336-342.

(38) Vicentini, F. T.; He, T.; Shao, Y.; Fonseca, M. J.; Verri, W. A., Jr.; Fisher, G. J.; Xu, Y. *J. Dermatol. Sci.* 2011, *61*, 162-168.

(39) Mutou, Y.; Ibuki, Y.; Kojima, S. *Photodermatol. Photoimmunol. Photomed.* 2007, *23*, 135-144.

(40) Lou, J. S.; Chen, X. E.; Zhang, Y.; Gao, Z. W.; Chen, T. P.; Zhang, G. Q.; Ji, C. *Exp. Ther. Med.* 2013, *6*, 1022-1028.

(41) Ivan, A. L.; Campanini, M. Z.; Martinez, R. M.; Ferreira, V. S.; Steffen, V. S.; Vicentini, F. T.; Vilela, F. M.; Martins, F. S.; Zarpelon, A. C.; Cunha, T. M.; Fonseca, M. J.; Baracat, M. M.; Georgetti, S. R.; Verri, W. A., Jr.; Casagrande, R. *J. Photochem. Photobiol. B.* 2014, *138*, 124-133.

(42) Yokogawa, M.; Takaishi, M.; Nakajima, K.; Kamijima, R.; Digiovanni, J.; Sano, S. *Mol. Carcinog.* 2013, *52*, 760-769.

(43) Sun, Z. W.; Hwang, E.; Lee, H. J.; Lee, T. Y.; Song, H. G.; Park, S. Y.; Shin, H. S.; Lee, D. G.; Yi, T. H. *J. Nat. Med.* 2014.

(44) Hiramoto, K.; Kobayashi, H.; Yamate, Y.; Ishii, M.; Sato, E. F. *Exp. Dermatol.* 2012, *21*, 911-914.

(45) Strickland, I.; Rhodes, L. E.; Flanagan, B. F.; Friedmann, P. S. *J. Invest. Dermatol.* 1997, *108*, 763-768.

(46) Lin, W. W.; Karin, M. *J. Clin. Invest.* 2007, *117*, 1175-1183.

(47) Striz, I.; Brabcova, E.; Kolesar, L.; Sekerkova, A. *Clin Sci (Lond).* 2014, *126*, 593-612.

(48) Cosmi, L.; Maggi, L.; Santarlasci, V.; Liotta, F.; Annunziato, F. *Cytometry A.* 2014, *85*, 36-42.

(49) Peiser, M. *Clin. Dev. Immunol.* 2013, *2013*, 261037.

(50) McKenzie, A. N.; Spits, H.; Eberl, G. *Immunity*. **2014**, *41,* 366–374.

(51) Chiricozzi, A.; Guttman-Yassky, E.; Suarez-Farinas, M.; Nograles, K. E.; Tian, S.; Cardinale, I.; Chimenti, S.; Krueger, J. G. *J. Invest. Dermatol.* 2011, *131*, 677-687.

(52) Lewis, A. M.; Varghese, S.; Xu, H.; Alexander, H. R. *J. Transl. Med.* 2006, *4*, 48.

(53) Han, S.; Koo, D.; Kang, N.; Yoon, W.; Kang, G.; Kang, H.; Yoo, E. *J. Invest. Dermatol.* 2014.

(54) Yamazaki, Y.; Kawano, Y.; Nagashima, U. *J. Computer Chem.* 2012, *11*, 159-163.

(55) Yadav, V. R.; Prasad, S.; Sung, B.; Aggarwal, B. B. *Int. Immunopharmacol.* 2011, *11*, 295-309.

(56) Wang, H. D.; Pagano, P. J.; Du, Y.; Cayatte, A. J.; Quinn, M. T.; Brecher, P.; Cohen, R. A. *Circ. Res.* 1998, *82*, 810-818.

(57) Lowry, O. H.; Rosebrough, N. J.; Farr, A. L.; Randall, R. J. *J. Biol. Chem.* 1951, *193*, 265-275.

(58) Aebi, H. *Methods Enzymol.* 1984, *105*, 121-126.

(59) Gonzalez Flecha, B.; Llesuy, S.; Boveris, A. *Free Radic. Biol. Med.* 1991, *10*, 93-100.

Figures

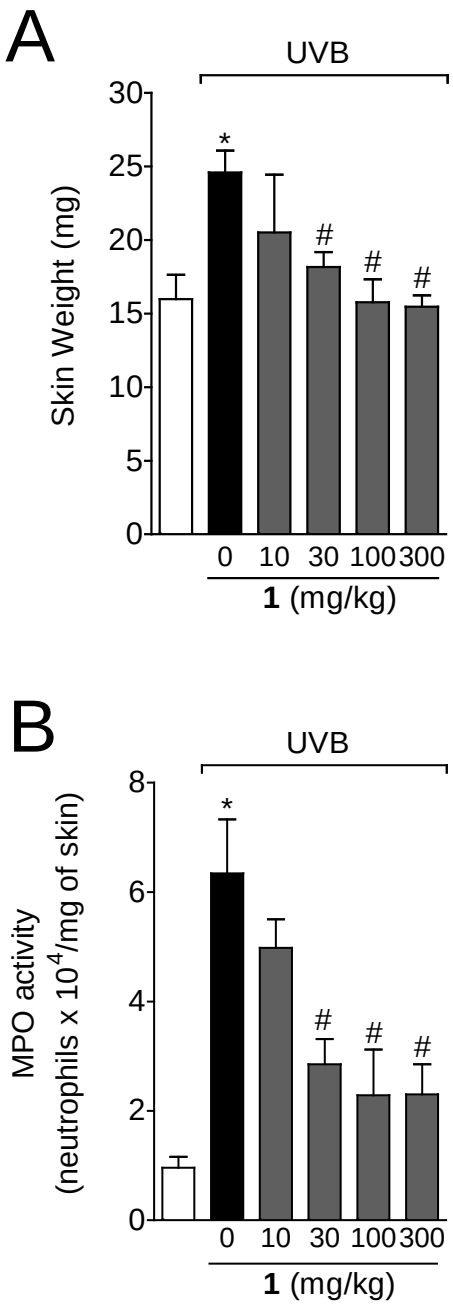

Figure 1. Trans-chalcone (**1**) inhibits UVB irradiation-induced skin edema and MPO activity in hairless mice. The skin edema (A) and MPO activity (B) were determined in samples collected 12 h after the end of irradiation. Bars represent means ± SEM of 5 mice per group per experiment and are representative of two separated experiments. [*p<0.01 compared to the non-irradiated control group; $^{\#}p$<0.05 compared to the irradiated control group (vehicle)].

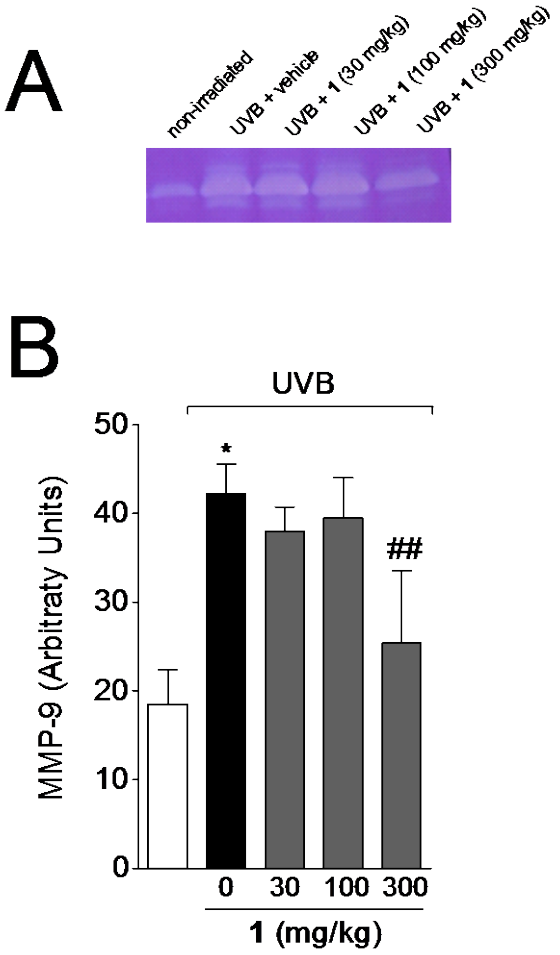

Figure 2. Effect of trans-chalcone (**1**) on UVB irradiation-induced increase of MMP-9 activity. The MMP-9 activity was determined in samples collected 12 h after the end of irradiation. (A) Image of gelatin zymography. (B) Bars represent means ± SEM of 5 mice per group per experiment and are representative of two separated experiments. [*p<0.001 compared to the non-irradiated control group; $^{\#\#}p$<0.05 compared to the irradiated control group (vehicle) and the doses of 30 and 100 mg/kg of **1**].

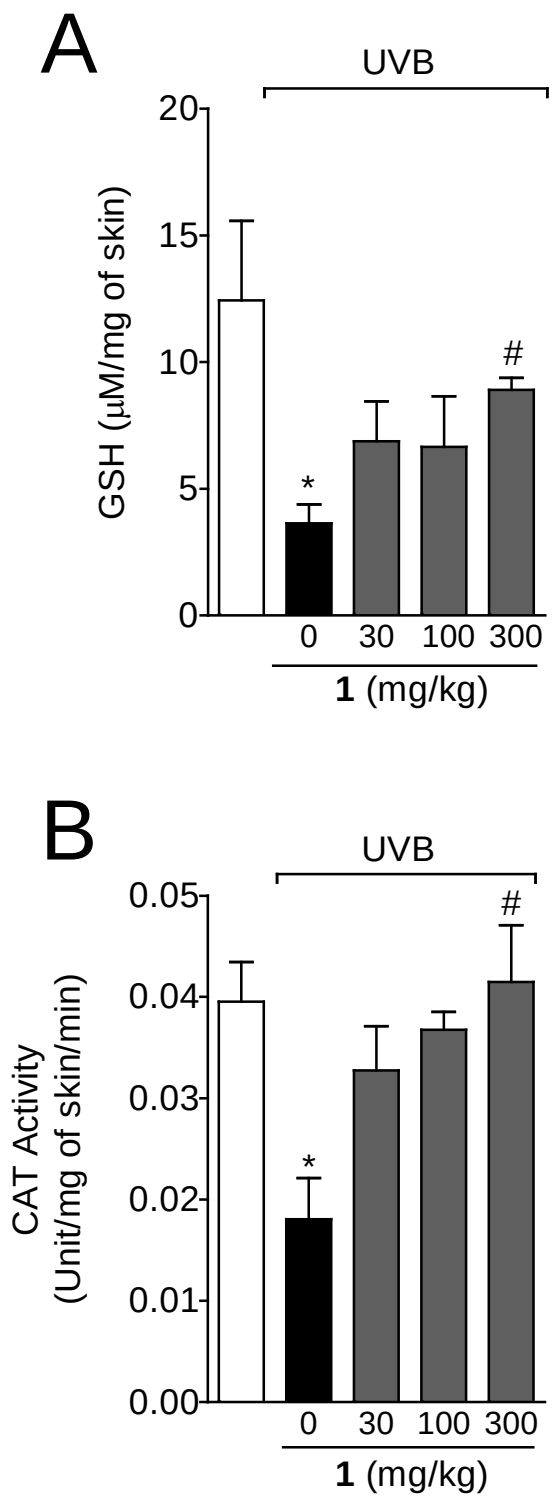

Figure 3. Trans-chalcone (**1**) inhibits UVB irradiation-induced GSH and CAT depletion. The GSH levels (A) and CAT activity (B) were determined in samples collected 12 h and 2 h after the end of irradiation, respectively. Bars represent means ± SEM of 5 mice per group per experiment and are representative of two separated experiments. [*p<0.05 compared to the non-irradiated control group and $^{\#}p$<0.05 compared to the irradiated control group (vehicle)].

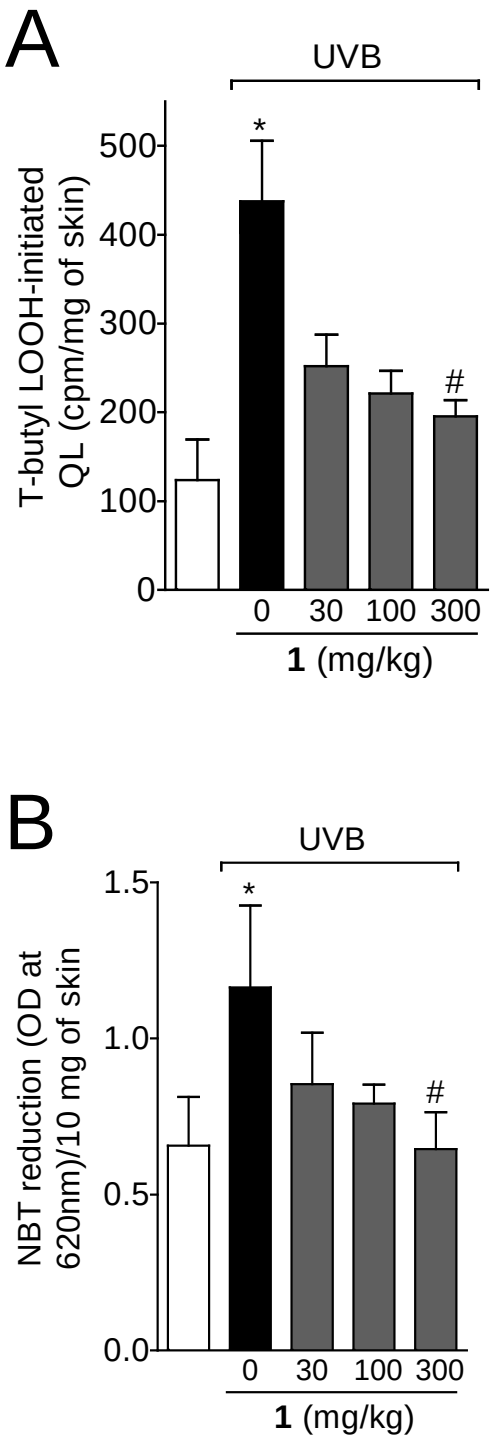

Figure 4. Trans-chalcone (**1**) inhibits UVB irradiation-induced LOOH and superoxide anion production. The t-butyl LOOH-initiated QL (A) and nitroblue tetrazolium reduction (B) tests were determined in samples collected 4 h and 2 h after the end of irradiation, respectively. Bars represent means ± SEM of 5 mice per group per experiment and are representative of two separated experiments. [*p<0.05 compared to the non-irradiated control group; $^{\#}p$<0.05 compared to the irradiated control group (vehicle)].

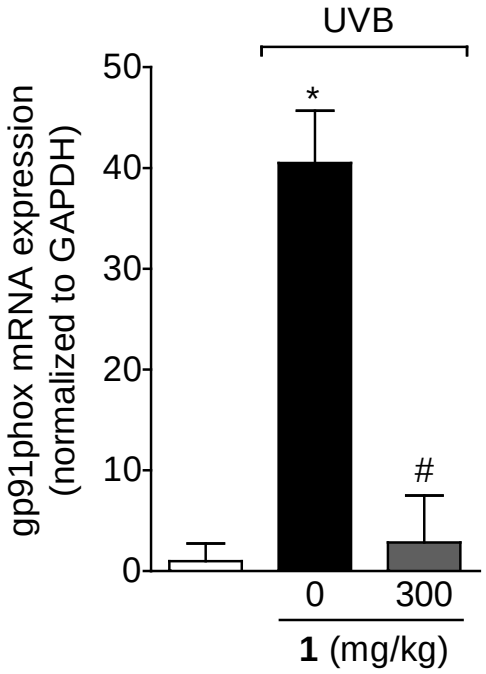

Figure 5. Trans-chalcone (**1**) inhibits UVB irradiation-induced gp91phox mRNA expression. The mRNA expression for gp91phox was determined 4 h after the end of irradiation. Bars represent means ± SEM of 5 mice per group per experiment and are representative of two separated experiments. [*p<0.001 compared to the non-irradiated control group; $^{\#}p$<0.01 compared to the irradiated control group (vehicle)].

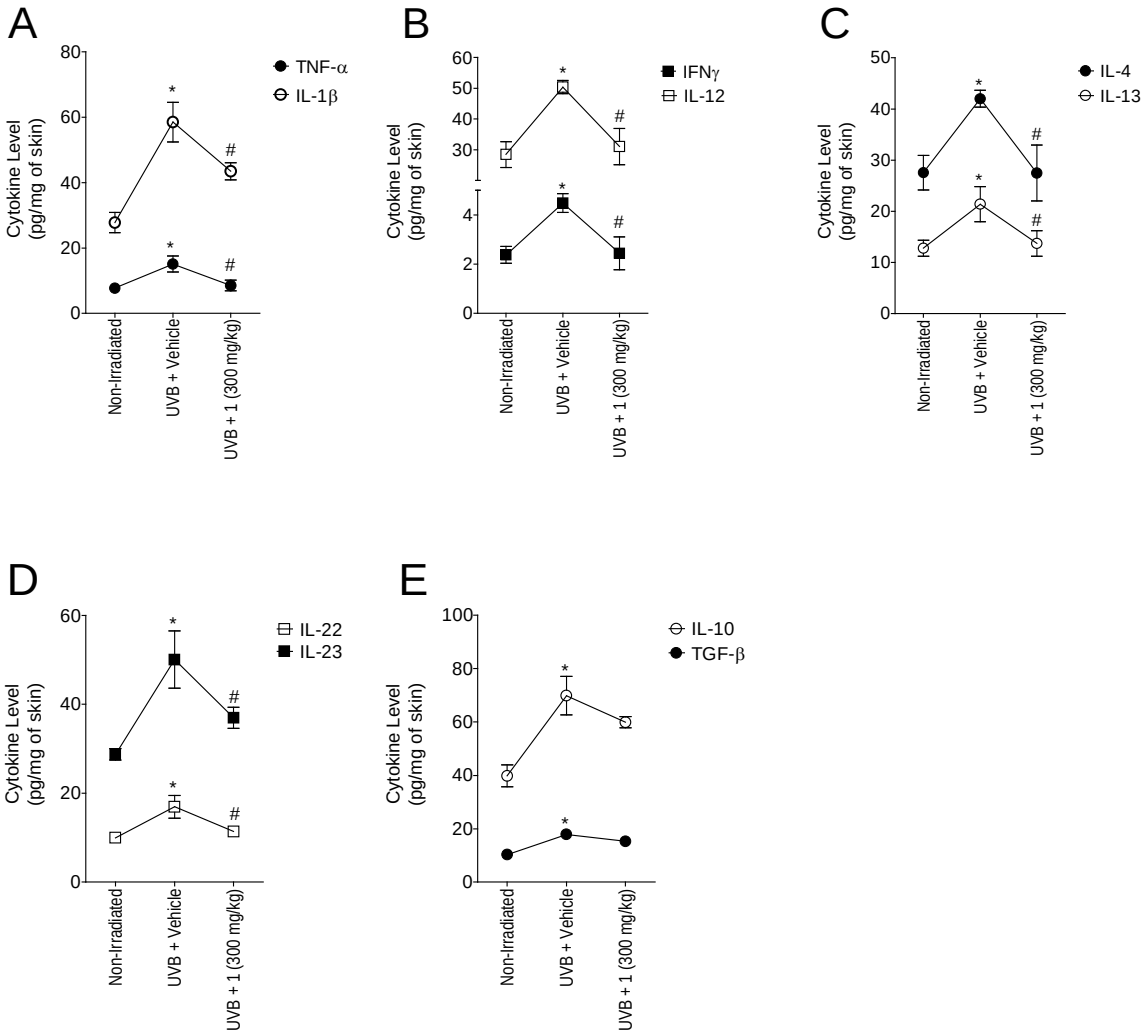

Figure 6. Trans-chalcone (**1**) inhibits UVB irradiation-induced pro-inflammatory and maintained regulatory T (Treg) cells associated cytokine production. The levels of classic inflammatory (TNF-α and IL-1β) (A), Th1 (IFN-γ and IL-12) (B), Th2 (IL-4 and IL-13) (C), IL-22 and IL-23 (D), and Treg cells associated (TGF-β and IL-10) (E) were determined in samples collected 4 h after the end of irradiation. Bars represent means ± SEM of 5 mice per group per experiment and are representative of two separated experiments. [**p*<0.05 compared to the non-irradiated control group; $^{\#}p$<0.05 compared to the irradiated control group (vehicle)].

4.2 HESPERIDIN METHYL CHALCONE INHIBITS OXIDATIVE STRESS AND INFLAMMATION IN A MOUSE MODEL OF ULTRAVIOLET B IRRADIATION-INDUCED SKIN DAMAGE

Journal of Photochemistry and Photobiology B: Biology

Renata M. Martinez[a], Felipe A. Pinho-Ribeiro[b], Vinicius S. Steffen[a], Carla V. Caviglione[a], Josiane A. Vignoli[c], Marcela M. Baracat[a], Sandra R. Georgetti[a], Waldiceu A. Verri, Jr.[b], Rubia Casagrande[a*]

[a] Departamento de Ciências Farmacêuticas, Universidade Estadual de Londrina-UEL, Avenida Robert Koch, 60, Hospital Universitário, 86039-440 Londrina, Paraná, Brazil

[b]Departamento de Ciências Patológicas, Universidade Estadual de Londrina-UEL, Rodovia Celso Garcia Cid, Km 380, PR445, Cx. Postal 10.011, 86057-970 Londrina, Paraná, Brazil

[c]Departamento de Bioquímica e Biotecnologia, Centro de Ciências Exatas, Universidade Estadual de Londrina, Rodovia Celso Garcia Cid, Km 380, PR445, Cx. Postal 10.011, 86057-970 Londrina, Paraná, Brazil

* Corresponding author. Address: Avenida Robert Koch, 60, Vila Operária, CEP 86039-440 Londrina, Paraná, Brazil. Tel.: +55 43 33712475. E-mail address: rubiacasa@yahoo.com.br (R. Casagrande).

Accepted paper

Journal of Photochemistry and Photobiology B: Biology 148 (2015) 145–153

Contents lists available at ScienceDirect

Journal of Photochemistry and Photobiology B: Biology

journal homepage: www.elsevier.com/locate/jphotobiol

Hesperidin methyl chalcone inhibits oxidative stress and inflammation in a mouse model of ultraviolet B irradiation-induced skin damage

Renata M. Martinez [a], Felipe A. Pinho-Ribeiro [b], Vinicius S. Steffen [a], Carla V. Caviglione [a], Josiane A. Vignoli [c], Marcela M. Baracat [a], Sandra R. Georgetti [a], Waldiceu A. Verri Jr. [b], Rubia Casagrande [a,*]

[a] Departamento de Ciências Farmacêuticas, Universidade Estadual de Londrina-UEL, Avenida Robert Koch, 60, Hospital Universitário, 86039-440 Londrina, Paraná, Brazil
[b] Departamento de Ciências Patológicas, Universidade Estadual de Londrina-UEL, Rodovia Celso Garcia Cid, Km 380, PR445, Cx. Postal 10.011, 86057-970 Londrina, Paraná, Brazil
[c] Departamento de Bioquímica e Biotecnologia, Centro de Ciências Exatas, Universidade Estadual de Londrina, Rodovia Celso Garcia Cid, Km 380, PR445, Cx. Postal 10.011, 86057-970 Londrina, Paraná, Brazil

ARTICLE INFO

Article history:
Received 24 December 2014
Received in revised form 24 March 2015
Accepted 26 March 2015
Available online 13 April 2015

ABSTRACT

Hesperidin methyl chalcone (HMC) is a safe flavonoid used to treat chronic venous diseases, but its effects and mechanisms on UVB irradiation-induced inflammation and oxidative stress have never been described *in vivo*. Thus, the purpose of this study was to evaluate the effects of systemic administration of HMC in skin oxidative stress and inflammation induced by UVB irradiation. To induce skin damage, hairless mice were exposed to an acute UVB irradiation dose of 4.14 J/cm^2, and the dorsal skin samples were collected to evaluate oxidative stress and inflammatory response. The intraperitoneal treatment with HMC at the dose of 300 mg/kg inhibited UVB irradiation-induced skin edema, neutrophil recruitment, and matrix metalloproteinase-9 activity. HMC also protected the skin from UVB irradiation-induced oxidative stress by maintaining ferric reducing antioxidant power (FRAP), 2,2′-azino-bis (3-ethylbenzothiazoline-6-sulfonic acid) radical (ABTS) scavenging ability and antioxidant levels (reduced glutathione and catalase). Corroborating, HMC inhibited UVB irradiation-induced superoxide anion generation and gp91phox (NADPH oxidase subunit) mRNA expression. Furthermore, the antioxidant effect of HMC resulted in lower production of inflammatory mediators, including lipid hydroperoxides and a wide range of cytokines. Taken together, these results unveil a novel applicability of HMC in the treatment of UVB irradiation-induced skin inflammation and oxidative stress.

1. Introduction

Skin is the largest human organ and is continuously exposed to environmental stress sources. Among them, ultraviolet B (UVB) irradiation from the sun is one of the major risk factors for dermatologic disorders [1]. It is well established that the inflammatory response induced by UVB irradiation in the skin is mediated by an overproduction of reactive oxygen species (ROS) and by impairment of antioxidant systems [1]. Furthermore, UVB modulates the production of several pro-inflammatory and anti-inflammatory cytokines [2,3], which increases the risk of developing auto-immune, inflammatory, allergic, and infectious skin diseases [4–6]. Due to the synergic effect of ROS and inflammatory response, the improvement of the endogenous antioxidant system is a promising approach to prevent and/or treat UVB irradiation-induced skin damage and the related diseases [7–9].

Flavonoids constitute a large group of polyphenolic compounds widely distributed in the plant kingdom. These compounds show biological properties interesting for medical applications such as antihepatotoxic, antitumoral, antimicrobial, anti-allergic, antioxidant and anti-inflammatory [10–12]. The flavonoid class of flavonones is found in high amounts in citrus fruits, and therefore, citrus fruits and juices are the major sources of flavonones intake by humans. Many of the beneficial effects obtained through the consumption of orange juice have been attributed to the high contents of flavonone hesperidin [13]. Hesperidin exhibits antioxidant and anti-inflammatory properties [14,15], but is poorly absorbed in the small intestine similarly to many other flavonoids. The methylation of flavonoids improves their bioavailability, metabolic stability, tissue distribution and, most important, some of their

* Corresponding author at: Avenida Robert Koch, 60, Vila Operária, CEP 86039-440 Londrina, Paraná, Brazil. Tel.: +55 43 33712475.
E-mail addresses: renatamimartinez@gmail.com (R.M. Martinez), pinho.fe@gmail.com (F.A. Pinho-Ribeiro), vsteffen@gmail.com (V.S. Steffen), carla_venturelli@hotmail.com (C.V. Caviglione), josivignoli@yahoo.com.br (J.A. Vignoli), baracat1903@yahoo.com.br (M.M. Baracat), sangeorgetti@gmail.com (S.R. Georgetti), waldiceujr@yahoo.com.br (W.A. Verri Jr.), rubiacasa@yahoo.com.br (R. Casagrande).

http://dx.doi.org/10.1016/j.jphotobiol.2015.03.030
1011-1344/

E-mail of each author:

Renata M. Martinez: renatamimartinez@gmail.com
Felipe A. Pinho-Ribeiro: pinho.fe@gmail.com
Vinicius S. Steffen: vsteffen@gmail.com
Carla V. Caviglione: carla_venturelli@hotmail.com
Josiane A. Vignoli: josivignoli@yahoo.com.br
Marcela M. Baracat: baracat1903@yahoo.com.br
Sandra R. Georgetti: sangeorgetti@gmail.com
Waldiceu A. Verri Jr: waldiceujr@yahoo.com.br
Rubia Casagrande: rubiacasa@yahoo.com.br

Highlights

- HMC protected the skin from the deleterious effects of UVB irradiation.

- HMC inhibited UVB-induced inflammatory edema and neutrophil recruitment.

- HMC inhibited UVB-induced skin oxidative stress and gp91phox mRNA expression.

- HMC reduced UVB-induced production of a wide range of cytokines.

Abbreviations

ABTS	2,2′ -azino-bis(3-ethylbenzothiazoline-6-sulfonic acid)
CAT	catalase
DTNB	5,5'-dithiobis(2-nitrobenzoic acid)
FRAP	ferric reducing antioxidant power
GSH	reduced glutathione
H_2O_2	hydrogen peroxide
HMC	hesperidin methyl chalcone
HTAB	hexadecyltrimethylammonium bromide
IL	Interleukin
IFN-γ	interferon *gamma*
LPO	lipid peroxidation
LOOH	lipid hydroperoxides
MMP	matrix metalloproteinase
MPO	Myeloperoxidase
NADPH	nicotinamide adenine dinucleotide phosphate
NBT	nitroblue tetrazolium
NOX 2	NADPH oxidase 2
$O_2^{\bullet-}$	superoxide anion
ROS	reactive oxygen species
SDS-PAGE	sodium dodecyl sulfate polyacrylamide gel electrophoresis
SEM	standard error mean
TGF-β	transforming growth factor *beta*
Th	T helper
TPTZ	2,4,6-Tris(2-pyridyl)-*s*-triazine
TNF-α	tumor necrosis factor-α
UV	Ultraviolet

ABSTRACT

Hesperidin methyl chalcone (HMC) is a safe flavonoid used to treat chronic venous diseases, but its effects and mechanisms on UVB irradiation-induced inflammation and oxidative stress have never been described *in vivo*. Thus, the purpose of this study was to evaluate the effects of systemic administration of HMC in skin oxidative stress and inflammation induced by UVB irradiation. To induce skin damage, hairless mice were exposed to an acute UVB irradiation dose of 4.14 J/cm^2, and the dorsal skin samples were collected to evaluate oxidative stress and inflammatory response. The intraperitoneal treatment with HMC at the dose of 300 mg/kg inhibited UVB irradiation-induced skin edema, neutrophil recruitment, and matrix metalloproteinase-9 activity. HMC also protected the skin from UVB irradiation-induced oxidative stress by maintaining ferric reducing antioxidant power (FRAP), 2,2′-azino-bis (3-ethylbenzothiazoline-6-sulfonic acid) radical (ABTS) scavenging ability and antioxidant levels (reduced glutathione and catalase). Corroborating, HMC inhibited UVB irradiation-induced superoxide anion generation and gp91phox (NADPH oxidase subunit) mRNA expression. Furthermore, the antioxidant effect of HMC resulted in lower production of inflammatory mediators, including lipid hydroperoxides and a wide range of cytokines. Taken together, these results unveil a novel applicability of HMC in the treatment of UVB irradiation-induced skin inflammation and oxidative stress.

Keywords: Hesperidin methyl chalcone; inflammation; oxidative stress; ultraviolet B

1. Introduction

Skin is the largest human organ and is continuously exposed to environmental stress sources. Among them, ultraviolet B (UVB) irradiation from the sun is one of the major risk factors for dermatologic disorders [1]. It is well established that the inflammatory response induced by UVB irradiation in the skin is mediated by an overproduction of reactive oxygen species (ROS) and by impairment of antioxidant systems [1]. Furthermore, UVB modulates the production of several pro-inflammatory and anti-inflammatory cytokines [2, 3], which increases the risk of developing auto-immune, inflammatory, allergic, and infectious skin diseases [4-6]. Due to the synergic effect of ROS and inflammatory response, the improvement of the endogenous antioxidant system is a promising approach to prevent and/or treat UVB irradiation-induced skin damage and the related diseases [7-9].

Flavonoids constitute a large group of polyphenolic compounds widely distributed in the plant kingdom. These compounds show biological properties interesting for medical applications such as antihepatotoxic, antitumoral, antimicrobial, anti-allergic, antioxidant and anti-inflammatory [10-12]. The flavonoid class of flavonones is found in high amounts in citrus fruits, and therefore, citrus fruits and juices are the major sources of flavonones intake by humans. Many of the beneficial effects obtained through the consumption of orange juice have been attributed to the high contents of flavonone hesperidin [13]. Hesperidin exhibits antioxidant and anti-inflammatory properties [14, 15], but is poorly absorbed in the small intestine similarly to many other flavonoids. The methylation of flavonoids improves their bioavailability, metabolic stability, tissue distribution and, most important, some of their major biological activities [16]. The methylation of hesperidin under alkaline conditions produces hesperidin methyl chalcone (HMC) [17], which presents higher metabolic resistance and transport.

HMC exhibits vasoprotective activity and thus is found in medication (Cyclo 3 Fort) used to treat chronic venous insufficiency [18-20], improving the life quality of patients [21, 22]. It is known that disturbances in the blood flow trigger inflammation and lead to the vicious circle of chronic inflammation observed in chronic venous insufficiency [23]. Despite the antioxidant and anti-inflammatory effect of flavonoids [10-12] and the clinical use of HMC in inflammatory conditions [18-20], it remains to be determined the underlying anti-inflammatory and antioxidant mechanisms of HMC. Furthermore, it has been reported that HMC is safe in patients receiving 150 mg daily for 90 days [18]. HMC seems to be safe even when administered in massive doses of as much as 15 g daily [24], which highlights its safety for medical use. Thus, the *in vivo* efficacy of HMC in preventing UVB irradiation-induced

inflammatory and oxidative damage in the skin of hairless mice was investigated in the present study.

2. Materials and methods

2.1. Chemicals

Brilliant blue R, reduced glutathione (GSH), hexadecyltrimethylammonium bromide (HTAB), N-ethylmaleimide, *o*-dianisidine dihydrochloride, phenylmethanesulfonyl fluoride, 2,2′-azino-bis (3-ethylbenzothiazoline- 6-sulfonic acid) (ABTS), (2,4,6-Tris(2-pyridyl)-*s*-triazine) (TPTZ), 5,5'-dithiobis(2-nitrobenzoic acid) (DTNB) and nitroblue tetrazolium (NBT), bisacrylamide were obtained from Sigma-Aldrich (St. Louis, MO, USA). Hesperidin methyl chalcone (HMC) from Santa Cruz Biotechnology (Dallas, Texas, USA). Tert-butyl hydroperoxide from Acros (Pittsburgh, PA, USA). Xylene cyanol and Tris were obtained from Amresco (Solon, OH, USA). Enzyme-linked immunosorbent assay (ELISA) kits for determination of cytokine levels were obtained from eBioscience (San Diego, CA, USA). Acrylamide, sodium dodecyl sulfate (SDS), glycerol, Superscript® III, Oligo(dT)12-18 primers, Platinum SYBRGreen® and primers from Invitrogem (Carlsbad, CA, USA).

2.2. Animals

Sex matched hairless mice (HRS/J) weighing 20-30 g were obtained from the University Hospital of Londrina State University. Mice were maintained with free access to water and food, and temperature of 23 ◦ C ± 2. A 12/12 h light/dark cycle was used with lights on at 6 and off at 18 h. Animal care and handling procedures were approved by Animal Ethics Committee (CEUA process number 3344.2012.08) of the Londrina State University.

2.3 Experimental protocols

Hairless mice were randomly assigned to the following groups: non-irradiated control group, irradiated control group (saline), and irradiated treated groups. In the experiments presented in Figs. 1, 2, 3 and 4A, mice were treated intraperitoneally with HMC (30 – 300 mg/kg, diluted in sterile saline) 1 h before and 7 h after the beginning of UVB irradiation. The doses of HMC used in these assays were selected based on therapeutic effects reported previously [25]. In the experiments of Figs. 4B, 5, 6 and 7, mice were treated only once, 1 h before the irradiation beginning. All experiments were performed twice with 5 mice per group per experiment.

2.4. Irradiation

The UVB source used was a Philips TL/12 RS 40W (Medical-Holand) emitting a continuous spectrum between 270 and 400 nm with a peak emission at 313 nm [19]. The

lamp was mounted 20 cm above the place where the mice were placed on, resulting in an irradiation of 0.384 mW/cm^2 as measured by an IL 1700 radiometer (Newburyport, MA, USA) equipped with sensor for UV (SED005) and UVB (SED240). The irradiation dose used to induce skin inflammation was 4.14 J/cm^2 as previously determined [8, 26, 27]. All groups were irradiated simultaneously. The mice were terminally anesthetized with 1.5% isoflurane (Abbott [Abbott Park, IL, USA]) at 12 h (Figs. 1-3 and 4A) or anesthetized following by decapitation at 2 h (Figs. 4B and 5B) or 4 h (Figs. 5A, 6 and 7) after the UVB exposure and dorsal skin samples were collected. Samples were stored at -70°C until analysis. The samples collected for verification of cutaneous edema were weighed immediately after collecting.

2.5. Skin edema

Samples of constant areas (5 mm diameter) of dorsal skin were removed from euthanized mice with the aid of a mold and weighed. The skin edema analysis was obtained by comparing the weight of irradiated groups with non-irradiated group, and the results were expressed in mg of skin [8].

2.6. Myeloperoxidase (MPO) activity

The UVB-induced leukocyte migration to the skin was evaluated using the MPO colorimetric assay as described previously [28, 29]. Samples of dorsal skin were homogenized in K_2HPO_4 buffer 0.05 M (pH 6.0) containing 0.5% HTAB using a Tissue-Tearor (Biospec). The homogenates were centrifuged at 16,100 *g* for 2 min at 4°C. The supernatant was removed to assay. Briefly, 30 µL of the resulting supernatant were mixed with 200 µL of 0.05 M K_2HPO_4 buffer (pH 6.0), containing 0.0167% *o*-dianisidine dihydrochloride and 0.05% hydrogen peroxide. The absorbance was determined at 450 nm (Asys Expert Plus, Biochrom). The MPO activity of samples was compared to a standard curve of neutrophils. The results are presented as MPO activity (number of neutrophils per mg of skin).

2.7. Matrix metalloproteinase-9 activity

SDS-PAGE (sodium dodecyl sulphate polyacrylamide gel electrophoresis) substrate-embedded enzymography was used to detect enzymes with gelatinase activity. Assays were carried out as described previously [28, 26]. The dorsal skin of hairless mice (1:4, w/w dilution) were homogenized (T 18 basic, IKA) in 0.05 M Tris-HCl buffer (pH 7.4) containing 0.01 M $CaCl_2$ and 1% protease inhibitor cocktail. Whole homogenates were centrifuged (12,000 *g*, 10 min, 4 °C) twice. The Lowry method was used to measure protein levels in skin homogenates. Aliquots of 50 µL were mixed with 10 µL of 0.1 M Tris-HCl (pH 7.4) containing

20% glycerol, 4% SDS and 0.005% xylene cyanol, and 25 µL of the mixture (40 µg of protein) were taken for electrophoresis in a gel containing 10% acrylamide and 0.025% gelatin. After electrophoresis, the gels were incubated for 1 h with 2.5% Triton X-100 under constant shaking, incubated overnight at 37°C in 0.05 M Tris-HCl (pH 7.4), 0.01 M $CaCl_2$ and 0.02% sodium azide, and stained on the following day with Brilliant blue R. After destaining in 20% acetic acid, the zone of enzyme activity was analyzed by comparing the groups in the ImageJ Program (NIH, Bethesda, MD, USA).

2.8. FRAP assay

The reducing ability of skin sample was determined by FRAP assay [8, 30]. The samples of skin were homogenized in 500 µL of KCl (1.15%) using a Tissue-Tearor (Biospec) and centrifuged (1,000 *g*, 10 min, 4°C), and the supernatant was employed to measure the antioxidant capacity of skin. The supernatant (30 µL) was mixed with the FRAP reagent (0.3 mM acetate buffer pH 3.6, 10 mM TPTZ in 40 mM hydrochloride acid, and 20 mM ferric chloride) and incubated at 37°C for 30 min. The absorbance was determined in 595 nm (Helios Alfa, Thermo Spectronic). Previously, a curve of trolox (0.5-20 µM) was prepared and the results are presented as µM trolox equivalent per mg of skin.

2.9. ABTS assay

The ABTS radical scavenging ability of skin sample was measured by the decrease of absorbance at 730 nm [8, 30]. The sample of skin were homogenized in 500 µL of KCl (1.15%) using a Tissue-Tearor (Biospec) and centrifuged (1,000 *g*, 10 min, 4°C), and the supernatant was employed to measure the antioxidant capacity of skin. The solution of ABTS was prepared with 7 mM of ABTS and 2.45 mM of potassium persulfate diluted with phosphate buffer pH 7.4 to an absorbance of 0.7-0.8 in 730 nm was prepared. The supernatant (40 µL) was mixed on ABTS solution and after 6 min the absorbance was determined in 730 nm (Helios Alfa, Thermo Spectronic). Previously, a curve of trolox (1-25 µM) was prepared and the results are presented as µM trolox equivalent per mg of skin.

2.10. Reduced glutathione (GSH) assay

GSH was determined as described previously [8]. The samples of skin were homogenized in 0.02 M EDTA using a Tissue-Tearor (Biospec). Whole homogenates were treated with 50% trichloroacetic acid and were centrifuged twice (2,700 *g*, 10 min, 4°C). The reaction mixture contained 50 µL of sample, 100 µL of 0.4 M Tris and 5 µL DTNB (1.9 mg/mL in methanol). The absorbance was read at 405 nm (Multiskan GO, Thermo Scientific). The standard curve was prepared with GSH (5-150 µM) and the results are presented as µM of GSH per mg of skin.

2.11. Catalase (CAT) assay

The analysis of CAT activity was evaluated by measuring the decay in the concentration of hydrogen peroxide (H_2O_2) and the generation of oxygen as described previously [31]. Skin of samples were homogenized in 500 µL of 0.02 M EDTA using a Tissue-Tearor (Biospec), and centrifuged twice (2,700 *g*, 10 min, 4°C). The reaction mixture contained 10 µL of sample, 160 µL of buffer Tris-HCl 1 M with EDTA 5 mM (pH 8.0), 20 µL of deionized water and 20 µL of H_2O_2 200 mM. Measurement of CAT activity was estimated through the difference between the initial reading and the reading conducted 30 seconds after the addition of H_2O_2 at 240 nm in a microplate reader (EnSpire, Perkin Elmer) at 25ºC. The CAT values were expressed as unit of CAT/mg of skin/minute.

2.12. Lipid peroxidation (LPO)

Lipid peroxidation were measured by t-butyl lipid hydroperoxides (LOOH)-initiated chemiluminescence according to an adaptation of the technique described previously [32]. This test is based on the premise that there is an increase in chemiluminescence associated with oxidative stress leading to the consumption of the antioxidant defenses from the formation of hydroperoxides. Samples of skin were homogenized in 800 µL of phosphate buffer (pH 7.4) using a Tissue-Tearor (Biospec)**,** centrifuged (700 *g*, 2 min, 4°C). Then, 250 µL the supernatant was diluted in 1730 µL reaction medium (120 mM KCl, 30 mM phosphate buffer, pH 7.4) and mixed with 20 µL of 3 mM tert-butyl hydroperoxide. The reading was conducted in a β-counter Beckman®LS 6000SC (Fullerton, CA, USA) in a non-coincident counting for 30 s with a response range between 300 and 620 nm. The vials were kept in the dark up to the moment of the assay, and determinations were obtained in dark in order to avoid vial phosphorescence activated by light. The experiment was conducted at 30°C for 120 min. The results were measured in counts per min (cpm) per mg of skin.

2.13. Superoxide anion production

The measurement of superoxide anion ($O_2^{\bullet-}$) production in skin was performed using the nitroblue tetrazolium assay (NBT) as described previously [26, 33]. Samples of skin were homogenized in 500 µL of 0.02 M EDTA using a Tissue-Tearor (Biospec) and centrifuged (2000 *g*, 20 seconds, 4°C). Then, 50 µL of the supernatant were incubated in 96-well plate for 1 h. The non-adherent/non-precipitated supernatant was carefully removed, 100 µL of NBT (1 mg/ml) was added to each well and incubated over 15 min. NBT reaction medium was then carefully removed followed by fixation in methanol 100%. Formazan particles were dissolved by adding 120 µL of KOH 2M and 140 µL of dimethylsulfoxide. Reduction of NBT to formazan was measured at 600 nm using a microplate spectrophotometer reader (Asys

Expert Plus, Biochrom) and the results are presented as optical density (OD) per 10 mg of skin.

2.14.Quantitative polymerase chain reaction (qPCR)

Skin samples were homogenized in TRIzol reagent (Invitrogen), and total RNA was extracted as recommended by manufacturer. RNA purity was confirmed by the 260/280 ratio. Complementary DNA was reverse transcribed from 2 µg of total RNA using kit (Invitrogen) and Oligo(dT)12-18 primers. qPCR was performed with Platinum SYBRGreen® kit (Invitrogen) following the manufacturer's directions [26]. Melting curve analysis was performed (65–95 °C) in order to verify that only one product was amplified. Samples with more than one peak were excluded. qPCR was performed in LightCycler® Nano Instrument (Roche). The relative gene expression was measured using the comparative $2^{-(\Delta\Delta Cq)}$ method. The expression of GAPDH mRNA expression was used as a control for tissue integrity in all samples. Primer sequences: *Gp91phox*, sense: 5'-AGCTATGAGGTGGTGATGTTAGTGG-3', antisense: 5'-CACAATATTTGTACCAGACAGACTTGAG-3'; and *Gapdh* sense: 5-ATGACATCAAGAAGGTGGTG-3, Antisense: 5'-CATACCAGGAAATGAGCTTG-3.

2.15. Cytokine measurement

Skin samples were homogenized in 500 µL of saline solution using Tissue-Tearor (Biospec). Homogenates were centrifuged (2,000 *g*, 15 min, 4 °C) and stored at -70 ºC. Supernatants were used to measure the cytokine levels by an enzyme-linked immunosorbent assay (ELISA) according to manufacturer's instructions (eBioscience) [8]. Absorbance was determined at 450 nm using a microplate spectrophotometer reader (Multiskan GO, Thermo Scientific) and the results are expressed as picograms (pg) of each cytokine/mg of skin.

2.16. Statistical analysis

The bars in the figures indicate the mean values ± standard error of the mean (SEM) of 5 mice per group per experiment and are representative of two separate experiments. Data were statistically analyzed by one-way ANOVA followed by Tukey's *t* test. Statistical analyses were performed using GraphPad Prism 4 software (GraphPad Software Inc., San Diego, CA, USA). Results were considered significantly different when $p < 0.05$.

3. Results

3.1. Treatment with HMC prevent UVB irradiation-induced skin edema and MPO activity

To evaluate the possible anti-inflammatory activity of HMC, skin inflammation was analyzed after UVB exposition by measuring edema and the MPO activity (neutrophil marker) (Fig. 1). Skin edema was inhibited by HMC treatment only at the dose of 300 mg/kg (Fig. 1A). On the other hand, all three doses of HMC (30, 100 and 300 mg/kg) showed a similar inhibition in MPO activity (Fig. 1B).

3.2. Treatment with HMC prevent UVB irradiation-induced skin MMP-9 activity

In the next set of experiment, the effect of HMC on UVB irradiation-induced MMP-9 activity was investigated. MMP-9 (also known as gelatinase B) degrades the components of extracellular matrix, therefore contributing to tissue damage [28]. As expected, MMP-9 activity in the skin was induced by UVB exposition, and this induction was inhibited by HMC at the dose of 300 mg/kg (Figs. 2A and B). No effect on MMP-9 activity was observed in mice treated with HMC at the doses of 30 and 100 mg/kg of HMC (Figs. 2A and B) similarly to edema test (Fig. 1A).

3.3. Treatment with HMC prevents the UVB irradiation-induced decrease of skin antioxidants

Antioxidant depletion occurs after excessive UVB exposition and plays a central role in skin photo-damage [1]. We first used the FRAP (Fig. 3A) and ABTS radical scavenging (Fig. 3B) assays to evaluate the effects of HMC in the antioxidant capacity of the skin. In both tests, HMC inhibited the antioxidant depletion only at the dose of 300 mg/kg, maintaining the antioxidant capacity similar to basal levels (Fig. 3). Next, we evaluated the effects of HMC on two crucial ROS elimination systems: reduced glutathione (GSH) (Fig. 4A) and catalase (CAT) (Fig. 4B). In line with the FRAP and ABTS results, HMC protected mice skin from UVB-induced GSH (Fig. 4A) and CAT depletion (Fig. 4B) at the dose of 300 mg/kg.

3.4. Treatment with HMC reduces UVB irradiation-induced lipid peroxidation (LPO) and superoxide anion ($O_2^{\bullet -}$) production

To further elucidate the antioxidant activity of HMC, we evaluated skin LPO, which is a hallmark of UVB-induced skin damage. HMC inhibited LPO at the dose of 300 mg/kg, while no inhibition was observed at the other tested doses (30 and 100 mg/kg) (Fig. 5A). ROS such as hydroxyl radicals ($HO^{\bullet}$), generated by $O_2^{\bullet -}$ reaction with H_2O_2, induce LPO. Lining up with the LPO data, HMC at the dose of 300 mg/kg inhibited UVB irradiation-induced $O_2^{\square}$ production (Fig. 5B). Thus, it is plausible that HMC inhibits $O_2^{\bullet -}$ production and all the deleterious effects that follow this early event.

3.5. Treatment with HMC prevents UVB irradiation-induced gp91phox mRNA expression

NADPH oxidase 2 (NOX 2) sub-unity gp91phox is the major enzymatic source of $O_2^{\bullet-}$ during acute inflammation and play an important role in the induction of UVB-induced skin inflammation [34-36]. The gp91phox mRNA expression in the skin was measured by qPCR to further investigate a possible relation between this enzyme and the levels of $O_2^{\bullet-}$. Confirming our hypothesis, HMC treatment was able to inhibit the gp91phox expression induced by UVB exposure at the same dose that inhibited $O_2^{\bullet-}$ production and oxidative stress (Fig. 6).

3.6. Treatment with HMC inhibits UVB irradiation-induced skin inflammation by reducing cytokine production

The development of skin diseases, including psoriasis and atopic dermatitis, is based on interactions between several cytokines in a not mutually exclusive way [37-39]. Based on this fact, we investigated whether the HMC treatment modulates cytokine production after UVB exposition. We found that UVB induced the production of all evaluated cytokines including the classic pro-inflammatory TNF-α, IL-1β, and IL-6 (Fig. 7A), T helper (Th) 1 (IFN-γ, IL-12) (Fig. 7B), Th2 (IL-4, IL-5, IL-13) (Fig. 7C), and Th17 (IL-17, IL-22, IL-23) (Fig. 7D) cytokines, and anti-inflammatory cytokines (IL-10 and TGF-β) (Fig. 7E). On the other hand, the treatment with 300 mg/kg of HMC inhibited the increases of all these cytokines (Fig. 7).

4. Discussion

ROS play an important role in the UVB-induced inflammatory response of the skin due to depletion of antioxidants and induction of cytokines [34, 40-42]. Our results support this concept and show that HMC prevents the depletion of GSH levels and CAT activity, and $O_2^{\bullet-}$ production induced by UVB irradiation. GSH removes radicals directly by hydrogen transfer, CAT maintains skin integrity by neutralizing H_2O_2 into water and O_2, thus, preventing the generation of hydroxyl radicals ($HO^{\bullet}$) which is induced by UVB directly and indirectly through $O_2^{\bullet-}$ production [43]. These ROS lead to lipid peroxidation (LPO), a very detrimental consequence of excessive UVB exposure that generates pro-inflammatory products [44]. In this sense, we demonstrated that HMC inhibited LPO and the production of a wide range of cytokines that have been related to skin diseases. In fact, the emerging literature suggests that ROS and cytokines act in synergy during allergic and inflammatory skin diseases [45, 46].

UVB irradiation stimulates the inflammatory response causing edema, vascular hyper-permeability, dilation of dermal blood vessels, recruitment of inflammatory cells, and production of inflammatory mediators such as cytokines contributing to skin diseases and premature skin ageing [5]. TNF-α is a pro-inflammatory cytokine that induces the production of other inflammatory mediators, including IL-1β, IL-6, chemokines, and adhesion molecules. These mediators recruit and activate neutrophils during acute inflammatory response, which increase tissue inflammation and contribute to skin damage [2, 47]. Considering HMC exhibits vasoprotective activity [21, 22], in the present study we investigated its potential as an anti-inflammatory agent and observed that HMC reduces neutrophil recruitment as a consequence of inhibiting TNF-α, IL-1β and IL-6 production. Corroborating, hesperidin inhibits the production of inflammatory molecules triggered by H_2O_2 in HaCaT cells, suggesting that hesperidin and related compounds such as HMC might contribute to the treatment of UV radiation-induced inflammatory diseases [48].

Moreover, these findings are in line with HMC reduction of $O_2^{\bullet-}$ production and gp91phox expression described in this study, once neutrophils are important sources of NADPH oxidase 2 (NOX 2)[49]. The gp91phox is the subunit of NOX 2 (also known as phagocyte NOX) that catalyzes electron transfer to O_2 and generates large amounts of $O_2^{\bullet-}$ during inflammatory response [35]. This oxidative burst phenomenon is key during infectious diseases, but is detrimental to host own tissues, especially at low antioxidant levels [47]. Targeting UVB irradiation activation of NADPH oxidase seems to be a consistent effect among flavonoids as also demonstrated for delphinidin [50]. Neutrophils also produce MMPs, which have a dual role by potentiating the destruction of skin structures accelerating aging and inappropriate amplification of inflammatory response [51] as well as tissue remodeling

and neovascularization [52] depending on its activity levels. HMC inhibited these parameters (neutrophil recruitment and MMP-9) and also reduced skin edema. Other flavonoids such as quercetin [28], myricetin [53], wogonin and baicalein [54] inhibit MMP-9 induced by UVB irradiation, providing skin photoprotection. Herein our results show consistently that HMC might be a conceivable photochemopreventive agent to limit the deleterious skin inflammatory and oxidative effects of UVB irradiation.

We also observed that HMC inhibited the production of several cytokines, which are involved in adaptive Th1 (IFN-γ and IL-12), Th2 (IL-4, IL-5 and IL-13), and Th17 (IL-17, IL-22 and IL-23) [55-57] as well as innate [58] inflammatory immune responses, and Th3 and regulatory T cells (TGF-β and IL-10) [59]. Importantly, these cytokines are related to skin diseases including: a) psoriasis in which an early phase involves innate immune cells such as neutrophils and mast cells as well as IFN-γ producing plasmacytoid dendritic cells, and a late phase with mononuclear cells and Th17 lymphocytes, and later on Th1 response; b) atopic dermatitis presenting Th2 response in acute phase and Th1 response in chronic disease; and c) melanoma with increased TGF-β producing Th3 cells [4, 37-39, 59-63]. Therefore, it remains to be determined if the inhibitory effect of HMC over cytokine production could be useful for the treatment of skin diseases other than that induced by UVB irradiation. Additionally, there is increased production of TNF-α and IFN-γ as detected in the plasma and in vein endothelial cells culture of chronic venous disease patients compared to healthy volunteers [64]. Thus, HMC inhibition of cytokine production and consequent recruitment of activated leukocytes may be a contributing mechanism to the therapeutic use of HMC in chronic venous disease.

Furthermore, despite of its anti-inflammatory effects, IL-10 is associated with UVB-induced immunosuppression and DNA damage [65-66], while TGF-β production in the skin promotes tissue remodeling and neovascularization through induction of MMP-9 [67]. Additionally, recruited neutrophils are also important sources of cytokines such as IL-10 and IL-4 in UVB-irradiated skin [65, 68] and thus represent a possible target of HMC to reduce the production of several inflammatory and immunosuppressive cytokines.

In conclusion, the systemic administration of HMC protected the skin from the deleterious effects of UVB irradiation. We demonstrated that its antioxidant effects are related to a reduction in $O_2^{\bullet-}$ radical production and gp91phox expression, which resulted in an improvement of antioxidant capacity in the skin by maintaining GSH and CAT levels near to the basal condition, and in the reduction of detrimental processes including LPO and inflammation. In agreement, HMC inhibited edema, neutrophil recruitment (MPO activity), and MMP-9 activity, and also reduced the production of a wide range of cytokines. Taken together, our results suggest that HMC may be a promising and safe approach to prevent and/or treat several skin diseases related to UVB exposition.

Acknowledgements

This study was supported by Brazilian grants from Coordenação de Aperfeiçoamento de Pessoal de Nível Superior (CAPES), Conselho Nacional de Desenvolvimento Científico e Tecnológico (CNPq), Ministério da Ciência, Tecnologia e Inovação (MCTI), Secretaria da Ciência, Tecnologia e Inovação (SETI), Fundação Araucária and Parana State Goverment. We thank the technical assistance of Denise Duarte from Post-graduation Laboratory of UEL. Authors declare no conflict of interest.

References

[1] M. Ichihashi, M. Ueda, A. Budiyanto, T. Bito, M. Oka, M. Fukunaga, K. Tsuru, T. Horikawa, UV-induced skin damage, Toxicology. 189 (2003) 21–39.

[2] M.M. Bashir, M.R. Sharma, V.P. Werth, UVB and proinflammatory cytokines synergistically activate TNF-alpha production in keratinocytes through enhanced gene transcription, J. Invest. Dermatol. 129 (2009) 994–1001.

[3] K. Kang, A.C. Gilliam, G. Chen, E. Tootell, K.D. Cooper, In human skin, UVB initiates early induction of IL-10 over IL-12 preferentially in the expanding dermal monocytic/macrophagic population, J. Invest. Dermatol. 111 (1998) 31–38.

[4] G.M. Halliday, Inflammation, gene mutation and photoimmunosuppression in response to UVR-induced oxidative damage contributes to photocarcinogenesis, Mutat. Res. 571 (2005) 107–120.

[5] F. Afaq, V.M. Adhami, H. Mukhtar, Photochemoprevention of ultraviolet B signaling and photocarcinogenesis, Mutat. Res. 571 (2005) 153–173.

[6] M. Yaar, B.A. Gilchrest, Photoageing: mechanism, prevention and therapy, Br. J. Dermatol. 157 (2007) 874–887.

[7] H. Hwang, T. Chen, R.G. Nines, H.C. Shin, G.D. Stoner, Photochemoprevention of UVB-induced skin carcinogenesis in SKH-1 mice by brown algae polyphenols, Int. J. Cancer. 119 (2006) 2742–2749.

[8] A.L. Ivan, M.Z. Campanini, R.M. Martinez, V.S. Ferreira, V.S. Steffen, F.T. Vicentini, F.M. Vilela, F.S. Martins, A.C. Zarpelon, T.M. Cunha, M.J. Fonseca, M.M. Baracat, S.R. Georgetti, W.A. Verri, Jr., R. Casagrande, Pyrrolidine dithiocarbamate inhibits UVB-induced skin inflammation and oxidative stress in hairless mice and exhibits antioxidant activity in vitro, J. Photochem. Photobiol. B 138 (2014) 124–133.

[9] V.E. Reeve, M. Allanson, S.J. Arun, D. Domanski, N. Painter, Mice drinking goji berry juice (Lycium barbarum) are protected from UV radiation-induced skin damage via antioxidant pathways, Photochem. Photobiol. Sci. 9 (2010) 601–607.

[10] L.H. Cazarolli, L. Zanatta, E.H. Alberton, M.S. Figueiredo, P. Folador, R.G. Damazio, M.G. Pizzolatti, F.R. Silva, Flavonoids: prospective drug candidates, Mini Rev. Med. Chem. 8 (2008) 1429–1440.

[11] J. Peterson, J. Dwyer, Flavonoids: Dietary occurrence and biochemical activity, Nutr. Res. 18 (1998) 1995–2018.

[12] W.A. Verri, F.T.M.C. Vicentini, M.M. Baracat, S.R. Georgetti, R.D.R. Cardoso, T.M. Cunha, et al., Flavonoids as anti-inflammatory and analgesic drugs: Mechanisms of action and perspectives in the development of pharmaceutical forms, Stud. Nat. Prod. Chem. 36 (2012) 297–330.

[13] C. Manach, C. Morand, A. Gil-Izquierdo, C. Bouteloup-Demange, C. Remesy, Bioavailability in humans of the flavanones hesperidin and narirutin after the ingestion of two doses of orange juice, Eur. J. Clin. Nutr. 57 (2003) 235–242.

[14] E.M. Galati, A. Trovato, S. Kirjavainen, A.M. Forestieri, A. Rossitto, M.T. Monforte, Biological effects of hesperidin, a Citrus flavonoid. (Note III): antihypertensive and diuretic activity in rat, Farmaco, 51 (1996) 219–221.

[15] H. Parhiz, A. Roohbakhsh, F. Soltani, R. Rezaee, M. Iranshahi, Antioxidant and Anti-Inflammatory Properties of the Citrus Flavonoids Hesperidin and Hesperetin: An Updated Review of their Molecular Mechanisms and Experimental Models, Phytother. Res. (2014).

[16] T. Walle, Methylation of dietary flavones greatly improves their hepatic metabolic stability and intestinal absorption, Mol. Pharm. 4 (2007) 826–832.

[17] A. Gil-Izquierdo, M.I. Gil, F. Ferreres, F.A. Tomas-Barberan, In vitro availability of flavonoids and other phenolics in orange juice, J. Agric. Food Chem. 49 (2001) 1035–1041.

[18] R. Beltramino, A. Penenory, A.M. Buceta, An open-label, randomized multicenter study comparing the efficacy and safety of Cyclo 3 Fort versus hydroxyethyl rutoside in chronic venous lymphatic insufficiency, Angiology 51 (2000) 535–544.

[19] V. Stoianova, [Cyclo 3 fort--alternative in chronic venous insufficiency], Akush Ginekol (Sofiia), 45 Suppl 3 (2006) 78–80.

[20] F.A. Allaert, C. Hugue, M. Cazaubon, J.M. Renaudin, T. Clavel, P. Escourrou, Correlation between improvement in functional signs and plethysmographic parameters during venoactive treatment (Cyclo 3 Fort), Int. Angiol. 30 (2011) 272–277.

[21] J.J. Guex, L. Avril, E. Enrici, E. Enriquez, C. Lis, C. Taieb, Quality of life improvement in Latin American patients suffering from chronic venous disorder using a combination of Ruscus aculeatus and hesperidin methyl-chalcone and ascorbic acid (quality study), Int. Angiol. 29 (2010) 525–532.

[22] J.J. Guex, D.M. Enriquez Vega, L. Avril, S. Boussetta, C. Taieb, Assessment of quality of life in Mexican patients suffering from chronic venous disorder - impact of oral Ruscus aculeatus-hesperidin-methyl-chalcone-ascorbic acid treatment - 'QUALITY Study', Phlebology 24 (2009) 157–165.

[23] S. Takase, F.A. Delano, L. Lerond, J.J. Bergan, G.W. Schmid-Schonbein, Inflammation in chronic venous insufficiency. Is the problem insurmountable?, J. Vasc. Res. 36 Suppl 1 (1999) 3–10.

[24] W.R. Kirtley, F.B. Peck, Administration of massive doses of vitamin P hesperidin methyl chalcone, Am. J. Med. Sci. 216 (1948) 64–70.

[25] F.A. Pinho-Ribeiro, M.S.N. Hohmann, S.M. Borghi, A.C. Zarpelon, C.F.S. Guazelli, M.F. Manchope, R. Casagrande, W.A.Jr Verri, Protective effects of the flavonoid hesperidin methyl chalcone in inflammation and pain in mice: role of TRPV1, oxidative stress, cytokines and NF-κB, Chem. Biol. Interact. 228 (2015) 88–99.

[26] M.Z. Campanini, F.A. Pinho-Ribeiro, A.L. Ivan, V.S. Ferreira, F.M. Vilela, F.T. Vicentini, R.M. Martinez, A.C. Zarpelon, M.J. Fonseca, T.J. Faria, M.M. Baracat, W.A. Verri, Jr., S.R. Georgetti, R. Casagrande, Efficacy of topical formulations containing Pimenta pseudocaryophyllus extract against UVB-induced oxidative stress and inflammation in hairless mice, J. Photochem. Photobiol. B 127 (2013) 153–160.

[27] Y. Shindo, E. Witt, D. Han, L. Packer, Dose-response effects of acute ultraviolet irradiation on antioxidants and molecular markers of oxidation in murine epidermis and dermis, J Invest Dermatol. 102 (1994) 470–475.

[28] R. Casagrande, S.R. Georgetti, W.A. Verri, Jr., D.J. Dorta, A.C. dos Santos, M.J. Fonseca, Protective effect of topical formulations containing quercetin against UVB-induced oxidative stress in hairless mice, J. Photochem. Photobiol. B, 84 (2006) 21–27.

[29] P.P. Bradley, D.A. Priebat, R.D. Christensen, G. Rothstein, Measurement of cutaneous inflammation: estimation of neutrophil content with an enzyme marker, J. Invest. Dermatol. 78 (1982) 206–209.

[30] V. Katalinic, D. Modun, I. Music, M. Boban, Gender differences in antioxidant capacity of rat tissues determined by 2,2'-azinobis (3-ethylbenzothiazoline 6-sulfonate; ABTS) and ferric reducing antioxidant power (FRAP) assays, Comp. Biochem. Physiol. C Toxicol. Pharmacol. 140 (2005) 47–52.

[31] H. Aebi, Catalase in vitro, Methods Enzymol. 105 (1984) 121–126.

[32] B. Gonzalez Flecha, S. Llesuy, A. Boveris, Hydroperoxide-initiated chemiluminescence: an assay for oxidative stress in biopsies of heart, liver, and muscle, Free Radic. Biol. Med. 10 (1991) 93–100.

[33] M.S. Hohmann, R.D. Cardoso, F.A. Pinho-Ribeiro, J. Crespigio, T.M. Cunha, J.C. Alves-Filho, R.V. da Silva, P. Pinge-Filho, S.H. Ferreira, F.Q. Cunha, R. Casagrande, W.A. Verri, Jr., 5-lipoxygenase deficiency reduces acetaminophen-induced hepatotoxicity and lethality, Biomed. Res. Int. 2013 (2013) 627046.

[34] K. Hiramoto, H. Kobayashi, Y. Yamate, M. Ishii, E.F. Sato, Intercellular pathway through hyaluronic acid in UVB-induced inflammation, Exp. Dermatol. 21 (2012) 911–914.

[35] R. Takeya, H. Sumimoto, Molecular mechanism for activation of superoxide-producing NADPH oxidases, Mol. Cells 16 (2003) 271–277.

[36] H. Wang, I.E. Kochevar, Involvement of UVB-induced reactive oxygen species in TGF-beta biosynthesis and activation in keratinocytes, Free Radic. Biol. Med. 38 (2005) 890–897.

[37] M. Grewe, C.A. Bruijnzeel-Koomen, E. Schopf, T. Thepen, A.G. Langeveld-Wildschut, T. Ruzicka, J. Krutmann, A role for Th1 and Th2 cells in the immunopathogenesis of atopic dermatitis, Immunol. Today 19 (1998) 359–361.

[38] J. Li, X. Chen, Z. Liu, Q. Yue, H. Liu, Expression of Th17 cytokines in skin lesions of patients with psoriasis, J. Huazhong Univ. Sci. Technolog. Med. Sci. 27 (2007) 330–332.

[39] S. Kagami, H.L. Rizzo, J.J. Lee, Y. Koguchi, A. Blauvelt, Circulating Th17, Th22, and Th1 cells are increased in psoriasis, J Invest Dermatol, 130 (2010) 1373–1383.

[40] T. Schwarz, T.A. Luger, Effect of UV irradiation on epidermal cell cytokine production, J. Photochem. Photobiol. B 4 (1989) 1–13.

[41] R. Kirnbauer, A. Kock, P. Neuner, E. Forster, J. Krutmann, A. Urbanski, E. Schauer, J.C. Ansel, T. Schwarz, T.A. Luger, Regulation of epidermal cell interleukin-6 production by UV light and corticosteroids, J. Invest. Dermatol. 96 (1991) 484–489.

[42] A. Kock, T. Schwarz, R. Kirnbauer, A. Urbanski, P. Perry, J.C. Ansel, T.A. Luger, Human keratinocytes are a source for tumor necrosis factor alpha: evidence for synthesis and release upon stimulation with endotoxin or ultraviolet light, J. Exp. Med. 172 (1990) 1609–1614.

[43] N.J. Sullivan, K.L. Tober, E.M. Burns, J.S. Schick, J.A. Riggenbach, T.A. Mace, M.A. Bill, G.S. Young, T.M. Oberyszyn, G.B. Lesinski, UV light B-mediated inhibition of skin catalase activity promotes Gr-1+ CD11b+ myeloid cell expansion, J. Invest. Dermatol. 132 (2012) 695–702.

[44] B. Halliwell, J.M. Gutteridge, Lipid peroxidation, oxygen radicals, cell damage, and antioxidant therapy, Lancet, 1 (1984) 1396–1397.

[45] Y. Okayama, Oxidative stress in allergic and inflammatory skin diseases, Curr. Drug Targets Inflamm. Allergy, 4 (2005) 517–519.

[46] D. Byamba, T.G. Kim, D.H. Kim, J.H. Je, M.G. Lee, The Roles of Reactive Oxygen Species Produced by Contact Allergens and Irritants in Monocyte-derived Dendritic Cells, Ann. Dermatol. 22 (2010) 269–278.

[47] C.D. Sadik, N.D. Kim, A.D. Luster, Neutrophils cascading their way to inflammation, Trends Immunol. 32 (2011) 452–460.

[48] P.D. Moon, H.M. Kim, Antiinflammatory effects of traditional Korean medicine, JinPi-tang and its active ingredient, hesperidin in HaCaT cells., Phytother. Res. 26 (2012) 657–662.

[49] M.T. Silva, Neutrophils and macrophages work in concert as inducers and effectors of adaptive immunity against extracellular and intracellular microbial pathogens, J. Leukoc. Biol. 87 (2010) 805–813.

[50] T.G. Lim, S.K. Jung, J. Kim, Y. Kim, H.J. Lee, T.S. Jang, K.W. Lee, NADPH oxidase is a novel target of delphinidin for the inhibition of UVB-induced MMP-1 expression in human dermal fibroblasts., Exp. Dermatol. 22 (2013) 428–430.

[51] J.I. Harper, H. Godwin, A. Green, L.E. Wilkes, N.J. Holden, M. Moffatt, W.O. Cookson, G. Layton, S. Chandler, A study of matrix metalloproteinase expression and activity in atopic dermatitis using a novel skin wash sampling assay for functional biomarker analysis, Br. J. Dermatol. 162 (2010) 397–403.

[52] A. Page-McCaw, A.J. Ewald, Z. Werb, Matrix metalloproteinases and the regulation of tissue remodelling, Nat. Rev. Mol. Cell Biol. 8 (2007) 221–233.

[53] S.K. Jung, K.W. Lee, H.Y. Kim, M.H. Oh, S. Byun, S.H. Lim, Y.S. Heo, N.J. Kang, A.M. Bode, Z. Dong, H.J. Lee, Myricetin suppresses UVB-induced wrinkle formation and MMP-9 expression by inhibiting Raf., Biochem. Pharmacol. 79 (2010) 1455–1461.

[54] Y. Kimura, M. Sumiyoshi, Effects of baicalein and wogonin isolated from Scutellaria baicalensis roots on skin damage in acute UVB-irradiated hairless mice., Eur. J. Pharmacol. 661 (2011) 124–132.

[55] M.K. Oyoshi, R. He, L. Kumar, J. Yoon, R.S. Geha, Cellular and molecular mechanisms in atopic dermatitis, Adv. Immunol. 102 (2009) 135–226.

[56] A. Iwasaki, R. Medzhitov, Toll-like receptor control of the adaptive immune responses, Nat. Immunol. 5 (2004) 987–995.

[57] S. Taleb, A. Tedgui, Z. Mallat, Adaptive T cell immune responses and atherogenesis, Curr. Opin. Pharmacol. 10 (2010) 197–202.

[58] A.N. McKenzie, H. Spits, G. Eberl, Innate lymphoid cells in inflammation and immunity, Immunity, 41 (2014) 366–374.

[59] C. Durán-Aniotz, G. Segal, L. Salazar, C. Pereda, C. Falcón, F. Tempio, R. Aguilera, R. González, C. Pérez, A. Tittarelli, D. Catalán, B. Nervi, M. Larrondo, F. Salazar-Onfray, M.N. López, The immunological response and post-treatment survival of DC-vaccinated melanoma patients are associated with increased Th1/Th17 and reduced Th3 cytokine responses., Cancer Immunol. Immunother. 62 (2013) 761–772.

[60] W.W. Lin, M. Karin, A cytokine-mediated link between innate immunity, inflammation, and cancer, J. Clin. Invest. 117 (2007) 1175–1183.

[61] S. Nakajima, A. Kitoh, G. Egawa, Y. Natsuaki, S. Nakamizo, C.S. Moniaga, A. Otsuka, T. Honda, S. Hanakawa, W. Amano, Y. Iwakura, S. Nakae, M. Kubo, Y. Miyachi, K. Kabashima, IL-17A as an inducer for Th2 immune responses in murine atopic dermatitis models, J. Invest. Dermatol. 134 (2014) 2122–2130.

[62] A. Chiricozzi, E. Guttman-Yassky, M. Suarez-Farinas, K.E. Nograles, S. Tian, I. Cardinale, S. Chimenti, J.G. Krueger, Integrative responses to IL-17 and TNF-alpha in human keratinocytes account for key inflammatory pathogenic circuits in psoriasis, J. Invest. Dermatol. 131 (2011) 677–687.

[63] R.J. Moore, D.M. Owens, G. Stamp, C. Arnott, F. Burke, N. East, H. Holdsworth, L. Turner, B. Rollins, M. Pasparakis, G. Kollias, F. Balkwill, Mice deficient in tumor necrosis factor-alpha are resistant to skin carcinogenesis, Nat. Med. 5 (1999) 828–831.

[64] V. Tisato, G. Zauli, E. Rimondi, S. Gianesini, L. Brunelli, E. Menegatti, P. Zamboni, P. Secchiero, Inhibitory effect of natural anti-inflammatory compounds on cytokines released by chronic venous disease patient-derived endothelial cells., Mediators Inflamm. 2013 (2013) 423407.

[65] G. Piskin, J.D. Bos, M.B. Teunissen, Neutrophils infiltrating ultraviolet B-irradiated normal human skin display high IL-10 expression, Arch. Dermatol. Res. 296 (2005) 339–342.

[66] T. Hasegawa, S. Shimada, H. Ishida, M. Nakashima, Chafuroside B, an Oolong tea polyphenol, ameliorates UVB-induced DNA damage and generation of photo-immunosuppression related mediators in human keratinocytes, PLoS One 8 (2013) e77308.

[67] J.M. Lamar, V. Iyer, C.M. DiPersio, Integrin alpha3beta1 potentiates TGFbeta-mediated induction of MMP-9 in immortalized keratinocytes, J. Invest. Dermatol. 128 (2008) 575–586.

[68] M.B. Teunissen, G. Piskin, S. di Nuzzo, R.M. Sylva-Steenland, M.A. de Rie, J.D. Bos, Ultraviolet B radiation induces a transient appearance of IL-4+ neutrophils, which support the development of Th2 responses, J. Immunol. 168 (2002) 3732–3739.

Figures

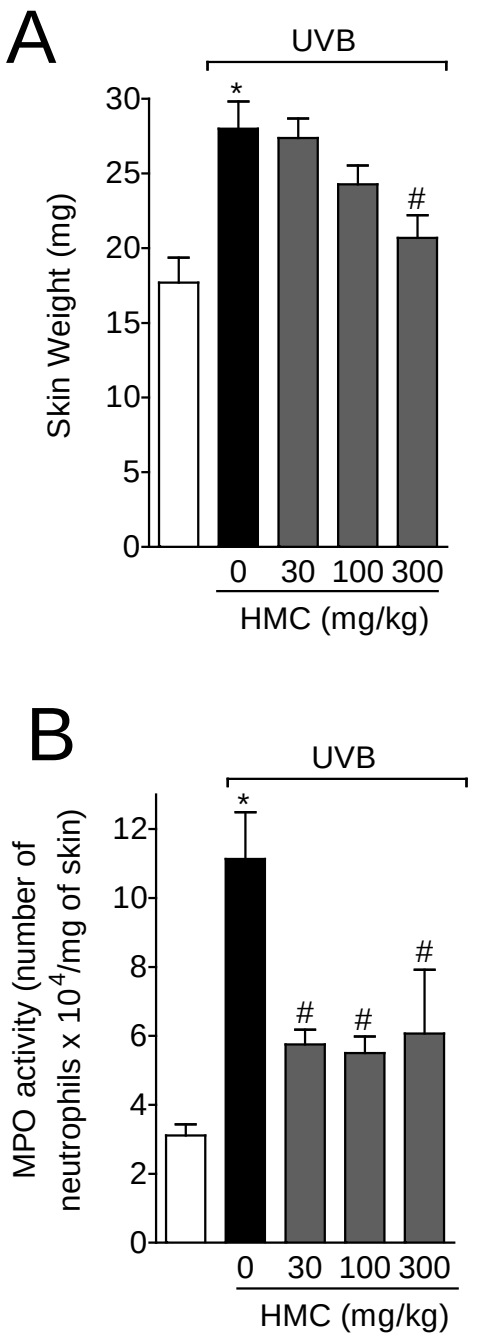

Fig. 1. HMC reduces UVB irradiation-induced skin edema and MPO activity. The skin edema (A) and MPO activity (B) were determined in samples collected 12 h after the end of irradiation. Bars represent means ± SEM of 5 mice per group per experiment and are representative of two separate experiments. [*p<0.05 compared to the non-irradiated control group; $^{\#}p$<0.05 compared to the irradiated control group (vehicle)].

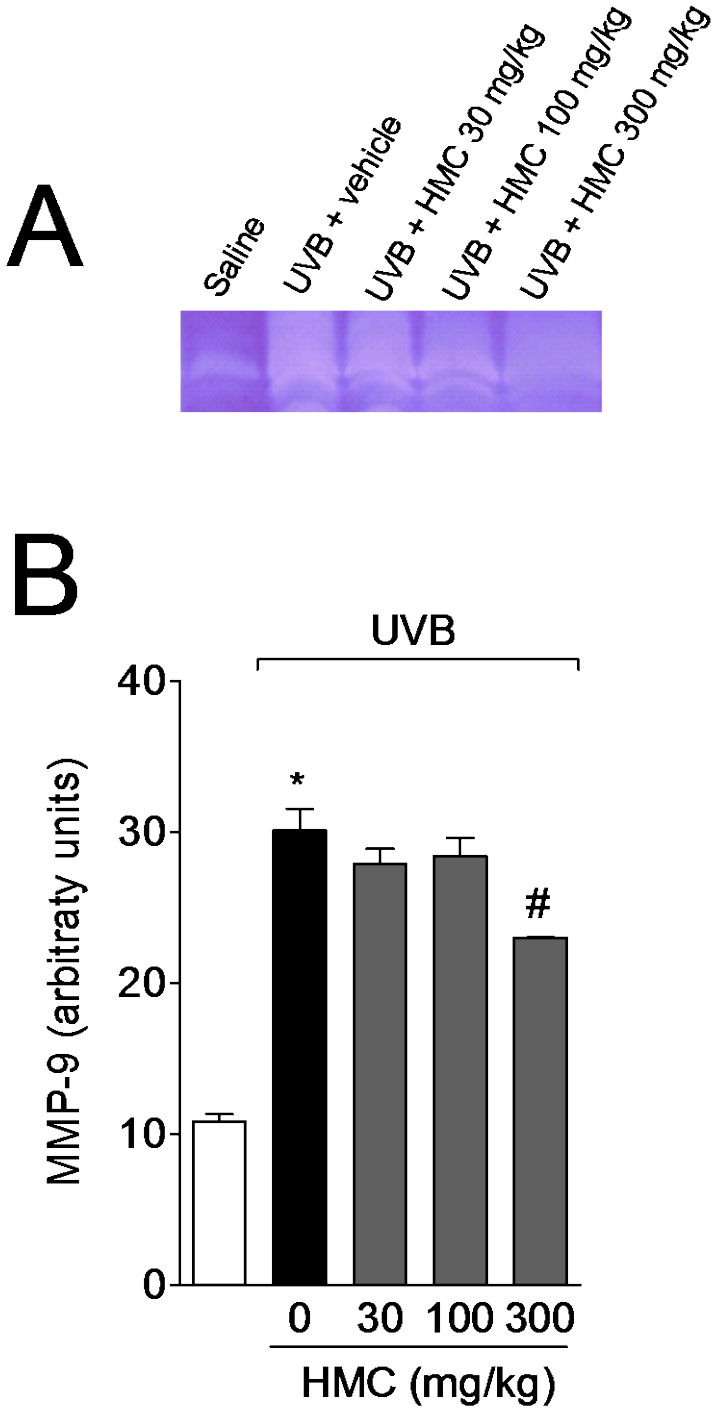

Fig. 2. HMC inhibits UVB irradiation-induced increase of MMP-9 activity. The MMP-9 activity was determined in samples collected 12 h after the end of irradiation. (A) Representative image of gelatin zymography. (B) Bars represent means ± SEM of 5 mice per group per experiment and are representative of two separate experiments. [*p<0.01 compared to the non-irradiated control group; $^{\#}p$<0.05 compared to the irradiated control group (vehicle)].

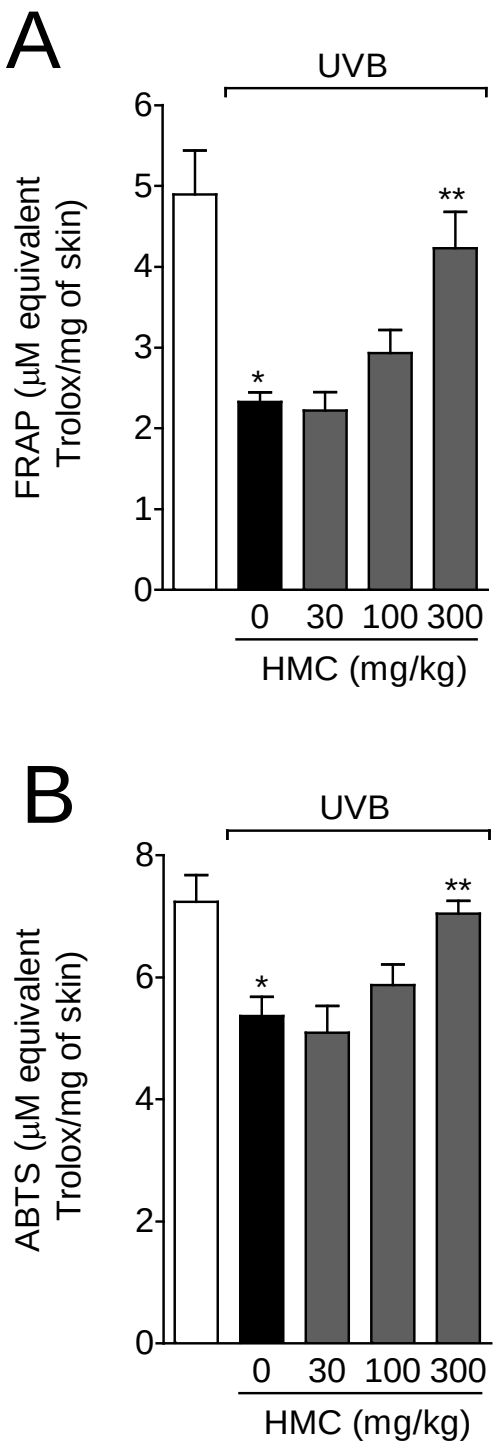

Fig. 3. HMC inhibits UVB irradiation-induced decrease of skin antioxidant capacity. The antioxidant capacity was determined by FRAP (A) and ABTS (B) assays in samples collected 12 h after the end of irradiation. Bars represent means ± SEM of 5 mice per group per experiment and are representative of two separate experiments. [*p<0.05 compared to the non-irradiated control group; **p<0.05 compared to the irradiated control group and HMC 30 mg/kg group].

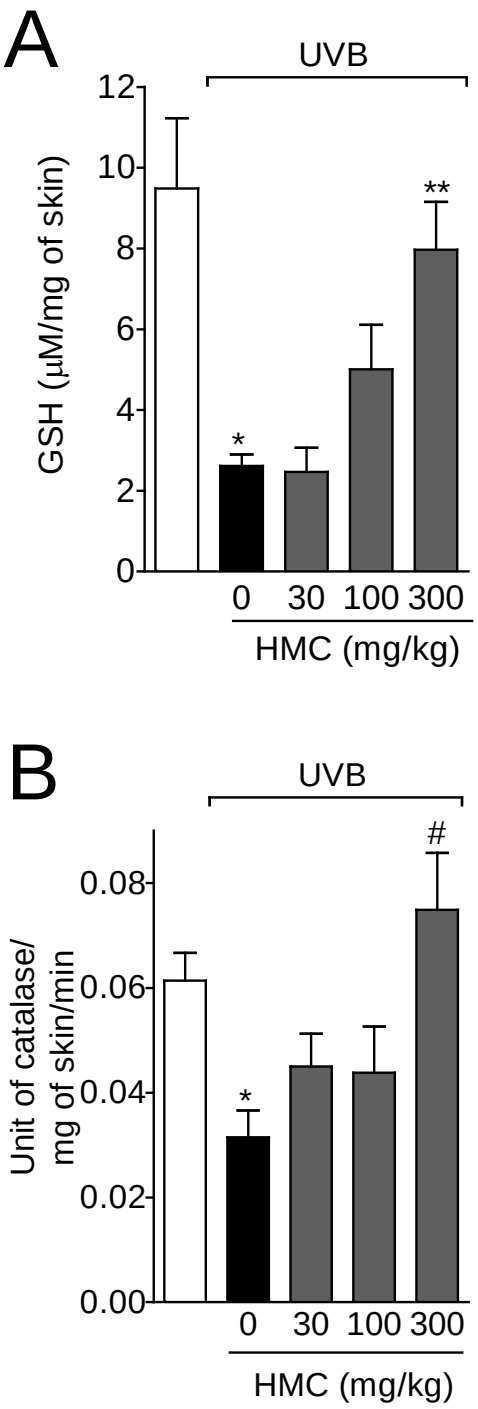

Fig. 4. HMC inhibits UVB irradiation-induced reduction of glutathione (GSH) levels and catalase (CAT) activity. The GSH levels (A) and CAT (B) activity were evaluated in skin samples collected 12 h and 2 h after the end of irradiation, respectively. Bars represent means ± SEM of 5 mice per group per experiment and are representative of two separate experiments. [**p*<0.05 compared to the non-irradiated control group; #*p*<0.05 compared to the irradiated control group (vehicle); ***p*<0.05 compared to the irradiated control group and HMC 30 mg/kg group].

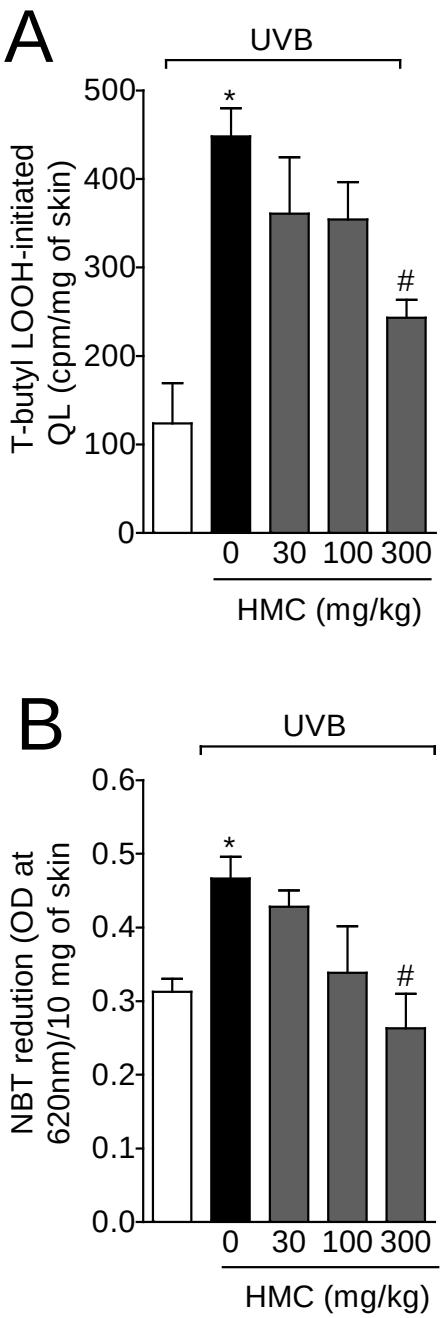

Fig. 5. HMC inhibits UVB irradiation-induced lipid peroxidation and superoxide anion generation. Lipid peroxidation (A) and superoxide anion production (B) were measured by t-butyl lipid hydroperoxides (LOOH)-initiated chemiluminescence and nitroblue tetrazolium (NBT) reduction assay in samples collected 4 and 2 h after the end of irradiation, respectively. Bars represent means ± SEM of 5 mice per group per experiment and are representative of two separate experiments. [*p<0.05 compared to the non-irradiated control group and $^{\#}p$<0.05 compared to the irradiated control group (vehicle)].

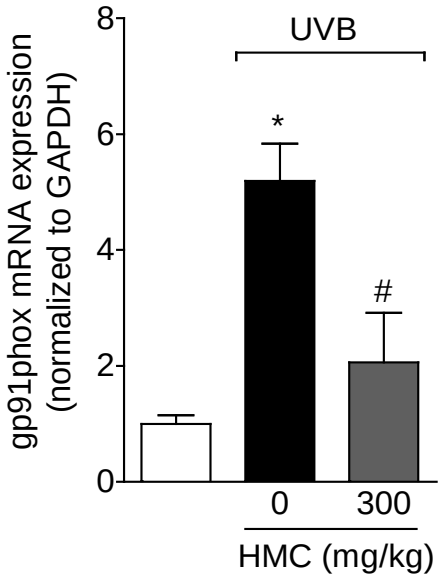

Fig. 6. HMC inhibits UVB irradiation-induced gp91phox mRNA expression. The gp91phox mRNA expression was determined in samples collected 4 h after the end of irradiation by qPCR. Bars represent means ± SEM of 5 mice per group per experiment and are representative of two separate experiments. [*p<0.001 compared to the non-irradiated control group; #p<0.001 compared to the irradiated control group (vehicle)].

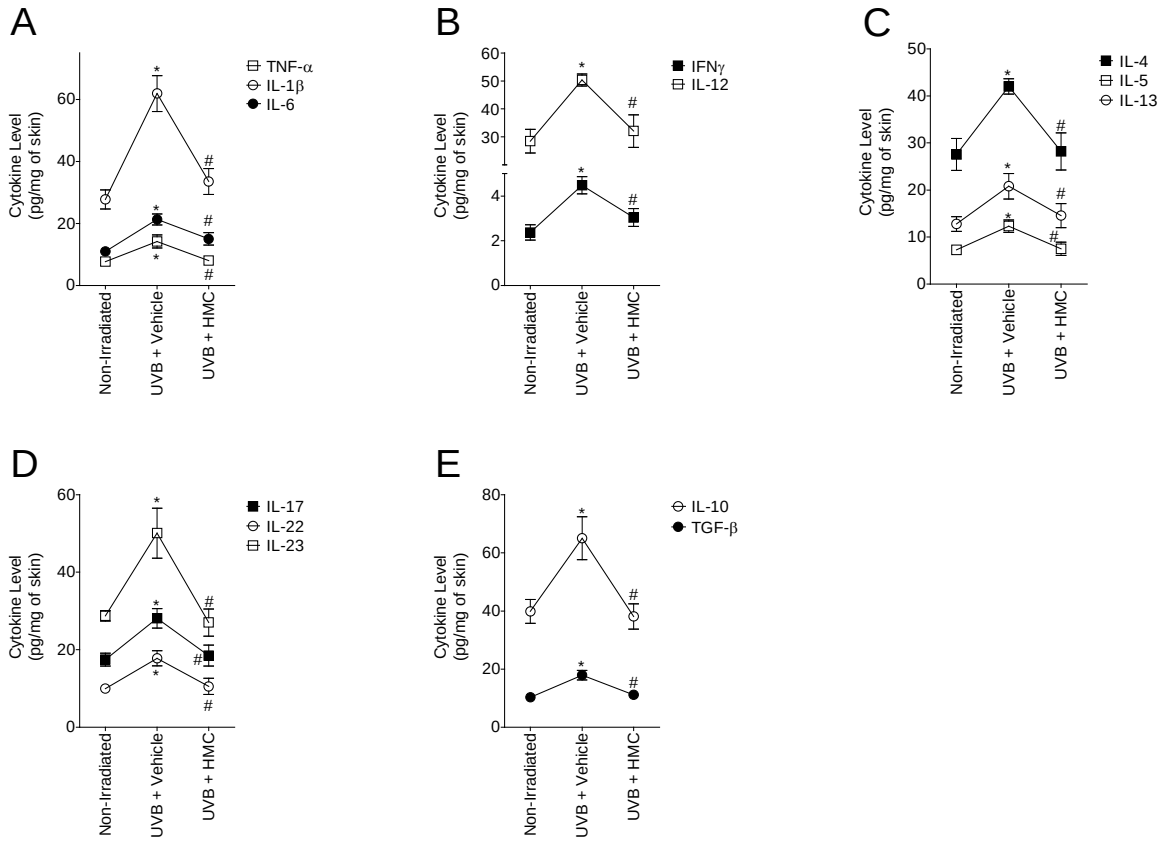

Fig. 7. HMC inhibits UVB irradiation-induced cytokine production. The levels of classic pro-inflammatory (TNF-α, IL-1β and IL-6) (A), Th1 (IFN-γ and IL-12) (B), Th2 (IL-4, IL-5 and IL-13) (C), Th17 (IL-17, IL-22 and IL-23) (D), and anti-inflammatory (IL-10 and TGF-β) (E) cytokines were determined in skin samples collected 4 h after the end of irradiation. HMC dose was 300 mg/kg, i.p. Bars represent means ± SEM of 5 mice per group per experiment and are representative of two separate experiments. [**p*<0.05 compared to the non-irradiated control group; #*p*<0.05 compared to the irradiated control group (vehicle)].

4.3 NARINGENIN INHIBITS UVB IRRADIATION-INDUCED INFLAMMATION AND OXIDATIVE STRESS IN THE SKIN OF HAIRLESS MICE

Renata M. Martinez,[†] Felipe A. Pinho-Ribeiro,[‡] Vinicius S. Steffen,[†] Carla V. Caviglione,[†] Josiane A. Vignoli,[§] Décio S. Barbosa,[T] Marcela M. Baracat,[†] Sandra R. Georgetti,[†] Waldiceu A. Verri, Jr.,[‡] and Rubia Casagrande*[,†]

[†]Departamento de Ciências Farmacêuticas, Universidade Estadual de Londrina-UEL, Avenida Robert Koch, 60, Hospital Universitário, 86039-440 Londrina, Paraná, Brasil

[‡]Departamento de Ciências Patológicas, Universidade Estadual de Londrina-UEL, Rodovia Celso Garcia Cid, Km 380, PR445, Cx. Postal 10.011, 86057-970 Londrina, Paraná, Brasil

[§]Departamento de Bioquímica e Biotecnologia, Universidade Estadual de Londrina-UEL, Rodovia Celso Garcia Cid, Km 380, PR445, Cx. Postal 10.011, 86057-970 Londrina, Paraná, Brasil

[T]Departamento de Patologia, Análises Clínicas e Toxicológicas, Universidade Estadual de Londrina-UEL, Avenida Robert Koch, 60, Hospital Universitário, 86039-440 Londrina, Paraná, Brasil

*Corresponding author. Address: Avenida Robert Koch, 60, Vila Operária, CEP 86039-440 Londrina, Paraná, Brazil. Tel.: +55 43 33712475. E-mail address: rubiacasa@yahoo.com.br (R. Casagrande).

Table of Contents Graphic

Naringenin Inhibits UVB-Irradiation-Induced Skin Inflammation and Oxidative Stress in Hairless Mice

Renata M. Martinez, Felipe A. Pinho-Ribeiro, Vinicius S. Steffen, Carla V. Caviglione, Josiane A. Vignoli, Décio S. Barbosa, Marcela M. Baracat, Sandra R. Georgetti, Waldiceu A. Verri, Jr., Rubia Casagrande

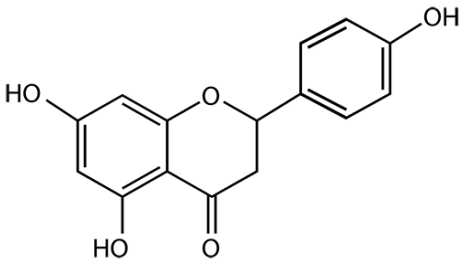

1

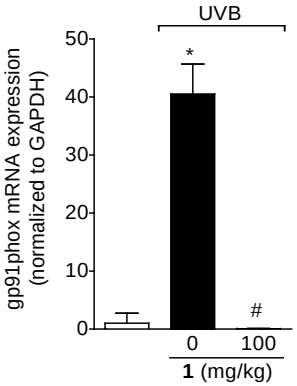

Cover letter

Dear Editor-in-Chief of the Journal of Natural Products
Professor A. Douglas Kinghorn,

We are submitting the manuscript entitled "**Naringenin Inhibits UVB-Irradiation-Induced Skin Inflammation and Oxidative Stress in Hairless Mice**" of Martinez et al. Recent research supports the idea that exogenous supplementation with antioxidants is an important approach to prevent skin from photodamage. Naringenin (**1**) is a flavonoid found in citrus fruits that exhibits anti-inflammatory and antioxidant activities, but its protective effect against UVB-induced skin inflammation and oxidative stress have not been addressed yet. Thus, to our knowledge, this is the first study demonstrating that **1** given systemically inhibits skin inflammation and oxidative stress induced by UVB exposure. Moreover, we also reported here the relation of this effect with inhibition of varied cytokine profiles, NADPH oxidase sub-unit gp91phox-related $O_2^{\bullet-}$ production and oxidative stress. These results highlight the protective effects of **1** in UVB-induced skin damage, and reveal its anti-inflammatory and antioxidant mechanisms, which might contribute to its inclusion as an exogenous supplement to prevent and/or treat skin disease. Therefore, we consider this research article suitable for the audience of Journal of Natural Products. This is the first submission of this manuscript to a journal, and we state that the content of the manuscript is original and is not submitted elsewhere.

Best regards,
Rubia

Prof. Rubia Casagrande, PhD
Universidade Estadual de Londrina
Centro de Ciências da Saúde
Departamento de Ciências Farmacêuticas
Avenida Robert Koch, 60, Hospital Universitário
CEP 86039-440 | Londrina - PR - Brasil
Tel: + 55 43 3323 4798 (home)
+ 55 43 3371 2475 (University)

ABSTRACT

Ultraviolet B (UVB) irradiation may cause inflammation- and oxidative stress- dependent skin cancer and premature aging. Naringenin (**1**) has been reported to have anti-inflammatory and antioxidant properties, but its effects and mechanisms on UVB irradiation-induced inflammation and oxidative stress are still not known. Thus, the present study aimed to investigate the potential of **1** on UVB irradiation-induced inflammation and oxidative damage in the skin of hairless mice. Skin edema, myeloperoxidase (neutrophil marker) and matrix metalloproteinase-9 (MMP-9) activity, and cytokine production were measured after UVB irradiation. The oxidative stress was evaluated by 2,2′-azino-bis (3-ethylbenzothiazoline-6-sulfonic acid) radical (ABTS) scavenging ability, ferric reducing antioxidant power (FRAP), reduced glutathione levels, catalase activity, lipid peroxidation products, superoxide anion production, and gp91phox (NADPH oxidase sub-unity) mRNA expression by quantitative PCR. The intraperitoneal treatment with **1** reduced skin inflammation by inhibiting skin edema, neutrophil recruitment, MMP-9 activity, and pro-inflammatory (TNF-α, IFN-γ, IL-1β, IL-4, IL-5, IL-6, IL-12, IL-13, IL-17, IL-22, and IL-23) and anti-inflammatory (TGF-β and IL-10) cytokines. Compound **1** also inhibited the oxidative stress by reducing superoxide anion production and the mRNA expression of gp91phox. Therefore, **1** inhibits UVB irradiation-induced skin damage and may be a promising therapeutic approach to control skin disease.

Ultraviolet (UV) irradiation from the sun is one of the major risk factors for dermatologic disorders.[1] Excessive exposure to UVB irradiation causes a variety of skin damages such as erythema, edema, sunburn, hyperplasia, inflammation, immunosuppression, skin photoaging, and photocarcinogenesis.[2] It is well established that the inflammatory response following acute exposure to UVB irradiation of the skin and the degenerative processes related to chronic exposure to UVB irradiation are largely mediated by the overproduction of reactive oxygen species (ROS) and by the impairment of antioxidant defense.[3]

ROS are reactive oxygen derivatives that oxidize and damage cellular proteins, lipids, and deoxyribonucleic acid (DNA). The human body has several endogenous ROS-eliminating systems such as glutathione and catalase. UVB exposure increases ROS production and decreases antioxidant levels in the skin, and this disruption of intracellular redox homeostasis (oxidative stress) can promote cell death.[4] ROS act as second messengers in pro-inflammatory signaling cascades that induce cytokine production.[5,6] Pro-inflammatory cytokines, including tumor necrosis factor-alpha (TNF-α), interleukin-1 beta (IL-1β) and IL-6, act on recruited neutrophils and increase the superoxide anion ($O_2^{\bullet-}$) production by these cells through activation of nicotinamide adenine dinucleotide phosphate (NADPH) oxidase 2 (NOX 2) complex.[7] The production of ROS by the NOX 2 system is an initial and critical event for the onset of oxidative stress conditions.[4,7] UVB irradiation also induces the activity of matrix metalloproteinase-9 (MMP-9), which is closely correlated with inflammatory skin diseases, increases the metastatic potential of cancer cells, and accelerates photoaging.[8,9] Thus, UVB irradiation-induced oxidative stress triggers skin inflammation through inappropriate amplification of intracellular signaling pathways, thereby increasing the risk of skin carcinogenesis.[10]

Many studies have focused on the establishment and evaluation of exogenous antioxidants to enrich the endogenous protection system and thus to prevent and/or treat UVB irradiation-induced oxidative damage.[11-15] In this context, much attention has been paid to natural products possessing antioxidant and anti-inflammatory properties, thereby protecting the skin from photodamage.[11,14,15] Flavonoids represent the most common and widely distributed group of plant phenolics.[16] Flavonoids are free radical scavengers because they are highly reactive as hydrogen or electron donors, which have led to their potential use as therapeutic drugs.[16,17]

The subgroup of flavanones is found almost exclusively in citrus fruits. Naringenin (**1**) (5,7,4'-trihydroxyflavanone) is one of the most abundant flavanones found in fruits such as lemon, orange, tangerine and grapefruit.[18] It has many pharmacological activities such as anti-inflammatory, antioxidant, anti-cancer, DNA protective, and anti-atherogenic.[18-36] It has been described that **1** protects HaCaT human keratinocytes against UVB-induced aging and

carcinogenesis.[37] However, the effect of **1** on UVB irradiation-induced skin inflammation and oxidative stress has not been investigated yet. Thus, the present study aimed to investigate the *in vivo* efficacy of systemic administration of **1** in UVB irradiation-induced inflammation and oxidative damage in the skin of hairless mice and the underlying mechanisms.

RESULTS AND DISCUSSION

Treatment with Naringenin (1) Reduces UVB Irradiation-Induced Edema and Myeloperoxidase (MPO) Activity in the Skin of Hairless Mice. UVB irradiation stimulates the inflammatory response, causing edema and inducing the recruitment of neutrophils.[12] As shown in Figure 1A, UVB irradiation induced significant skin edema, which was significantly inhibited by treatment with **1** at the doses of 30 and 100 mg/kg. No effect was observed in mice treated with **1** at the dose of 10 mg/kg. Supporting our results, it was described that **1** treatment decreased ischemic cerebral edema in rats.[21]

Infiltrating neutrophils are important players during skin damage after irradiation exposure.[38] These cells produce large amounts of pro-inflammatory cytokines and reactive oxygen species (ROS), enhancing the inflammatory response. Therefore, the neutrophil recruitment to the skin was evaluated by colorimetric assay of MPO activity, an indirect manner to assess the neutrophil counts.[39] UVB irradiation elevated MPO activity in comparison with the non-irradiated group. As observed with edema (Figure 1A), the treatment with **1** at the doses of 30 and 100 mg/kg inhibited MPO activity in the skin (Figure 1B). Again, no effect was observed in mice treated with **1** at the dose of 10 mg/kg. Similarly, **1** lowers the levels of MPO in the rat model of focal cerebral ischemia/reperfusion injury.[22] Thus, the treatment with **1** may contribute to reduce skin inflammation since neutrophils are important sources of inflammatory mediators such as cytokines and $O_2^{\bullet-}$.

Treatment with Naringenin (1) Reduces UVB Irradiation-Induced MMP-9 Activity in the Skin of Hairless Mice. MMP are primary mediators of connective-tissue damage in skin exposed to UV irradiation and of the premature skin aging.[40] MMP-9 (gelatinase B) is one of the primary enzymes related to degradation of skin collagen and components of the elastic fibers network. It displays the greatest elastolytic and fibrillin-degrading activity. Dysregulation of MMP-9 is associated with inflammatory skin diseases and also with the invasive and metastatic potential of cancer cells.[8] MMP-9 is overexpressed in UVB irradiated skin and contributes to the development of skin cancer and acceleration of photoaging.[9] Considering that MMP-9 may be produced by neutrophils and neutrophil-derived mediators may induce activation and overexpression of MMP-9, we investigated the effects of **1** treatment in MMP-9 activity in the skin after UVB irradiation exposition by SDS–PAGE (sodium dodecyl sulfate polyacrylamide gel electrophoresis) zymography. It was observed that UVB irradiation induced a significant increase of MMP-9 activity in the skin of hairless mice, which was inhibited by the dose of 100 mg/kg and unaffected by the doses 10 and 30 mg/kg of **1** (Figure 2). Supporting our results, the inhibitory effects of **1** over MMP-9 activity were also described in models of cerebral ischemic injury,[21] choroidal neovascularization,[24] and hepatocellular carcinoma.[25]

Naringenin (1) Inhibits UVB Irradiation-Induced Cytokine Production. It has been described that ROS play a crucial role in UVB-induced skin inflammation.[6,15] ROS activate oxidative stress-sensitive transcription factors, such as nuclear factor *kappa* B (NF-κB), a pro-inflammatory transcription factor that induces the production of several cytokines.[6] Activation of NF-κB pathway by UVB irradiation contributes to skin damage, photoaging and skin tumor formation.[6] Furthermore, UVB irradiation induces the production of multiple cytokines, including TNF-α,[6,41,42] IL-1β,[15,43] IL-6,[6,13] interferon *gamma* (IFN-γ),[41,44] IL-12,[44] IL-4,[41] IL-5,[41] IL-17,[44] IL-23,[44] IL-10[41,42] and transforming growth factor *beta* (TGF-β).[13]

Pro-inflammatory cytokines (e.g. TNF-α, IL-1β, and IL-6) initiate the cascade of inflammatory events by inducing chemokine release from bystander cells and by the up-regulation of adhesion molecules required for transendothelial trafficking of immune cells[45], for example subpopulations of T helper (Th) cells, defined based on distinct cytokine secretion profiles. Th1 cells (secrete, for example, IFN-γ and IL-12) are implicated in various organ-specific autoimmune diseases and chronic inflammatory disorders.[46] Th2 cells (secrete IL-4, IL-5 and IL-13) are responsible for initiation, maintenance, and amplification of human allergic inflammation and are important in patients with asthma.[46] Th17 cells activated by IL-23 (secrete IL-17 and IL-22) are implicated in inflammatory and autoimmune responses such as rheumatoid arthritis, multiple sclerosis, inflammatory bowel diseases, psoriasis, allergic contact dermatitis among other inflammatory skin disorders.[46,47] IL-10 and TGF-β down-regulate immune responses.[45] On the other hand, IL-10 may also play a pro-inflammatory role in antibody-mediated immunopathologies and TGF-β plays an important role in the immunopathogenesis of fibrose disorders.[45] In addition to the role in adaptive immune diseases, these cytokines also play roles in innate immune responses.[48] In this context, the possibility to inhibit the secretion of varied cytokine profiles can be considered a possible target for developing novel therapeutic strategies in several diseases.

As shown in Figures 3, UVB irradiation increased the production of several pro-inflammatory cytokines, including TNF-α, IL-1β, and IL-6, Th1 (IFN-γ, IL-12), Th2 (IL-4, IL-5, IL-13), and Th17 (IL-17, IL-23, IL-22) cytokines, and also increased anti-inflammatory cytokines (IL-10 and TGF-β). Additionally, treatment with **1** at the dose of 100 mg/kg inhibited UVB-induced production of all these cytokines involved in adaptive as well as innate inflammatory immune responses (Figures 3).

Supporting our results, **1** treatment reduces the TNF-α, IL-1β, IL-6 levels on ulcerative colitis in rats,[27] IFN-γ production on atopic dermatitis mouse model,[30] Th2 cytokine production (IL-4, IL-5, IL-13) on allergic asthma in mouse,[29] IL-17 levels in murine colitis,[35] IL-23 levels in human osteoclastogenesis model,[49] TNF-α, IL-1β, IL-6 and IL-10 levels in *Chlamydia trachomatis*-induced inflammation,[36] and TGF-β expression in nephrotoxicity in mice.[26] The release of these cytokines plays a central role in the recruitment and activation of

inflammatory cells, leading to skin damage after UVB exposure.[6,13,15,42,43] Moreover, the inhibition of these cytokines is considered a therapeutic approach to control skin cancer progression and metastasis, psoriasis, contact dermatitis and other diseases.[6,13,42,44-46] It is likely that the inhibition of cytokines production by **1** might be related to the inhibition of early inflammatory events such as inhibition of production or effects of ROS and NF-κB activation.

Treatment with Naringenin (1) Reduces the UVB Irradiation-Induced Depletion of Antioxidant Capacity in the Skin of Hairless Mice. UVB irradiation produces reactive oxygen species (ROS) directly and indirectly via the inflammatory response.[50] Several antioxidant systems are present in mammalian tissues to eliminate ROS and protect cells. The balance between antioxidant defenses and ROS production is essential to maintain cell function, whereas a disturbance in favor of the oxidants leads to oxidative stress.[4]

Results of ferric reducing antioxidant power (FRAP) assay correlate well with the levels of antioxidants ascorbic acid, uric acid, and α-tocopherol,[51] while 2,2′ -azino-bis (3-ethylbenzothiazoline-6-sulfonic acid) (ABTS) radical scavenging capacity reflects the levels of endogenous antioxidant reduced glutathione (GSH).[51] In this study, UVB irradiation induced a decrease of FRAP and of ABTS scavenging capacity in the skin, reflecting the pro-oxidant effects of this stimulus as described previously.[14,15,43,52] Treatment with **1** at the dose of 100 mg/kg significantly inhibited this antioxidant depletion, maintaining the antioxidant capacity similar to control group (non-irradiated) in both tests (Figures 4A and B). Corroborating the present data, it was demonstrated that **1** scavenges the ABTS radical cation *in vitro*.[53]

Several reports indicate that tissue injury induced by UV irradiation results in GSH depletion, which represents the most abundant cellular non-enzymatic antioxidant.[54] Its sulfhydryl group (SH) is highly polarizable and allows the removal of radicals directly by hydrogen transfer.[54] Then, GSH depletion is a consequence of its use to neutralize excessive ROS production, such as $O_2^{\bullet-}$ and its derivatives. The dose of UVB irradiation used here was able to reduce significantly the GSH levels in the skin, which is in line with the results in ABTS assay described above. Treatment with 100 mg/kg of **1**, but not 10 or 30 mg/kg, reduced significantly UVB irradiation induced GSH depletion (Figure 4C). Supporting this result, it has been reported that the treatment with **1** restored the levels of GSH to control values in acute nephrotoxicity in mouse kidney,[26] hepatic and renal dysfunction in rats[33] and on oxidative damage in rat liver[34]. Therefore, **1** treatment prevents antioxidant depletion and protects the skin from UVB irradiation-induced damage.

Treatment with Naringenin (1) Prevents UVB Irradiation-Induced Catalase (CAT) Depletion, Lipid Peroxidation (LPO), and $O_2^{\bullet-}$ Production in the Skin of Hairless Mice. Catalase (CAT) is an important antioxidant enzyme that breaks down H_2O_2 into O_2 and H_2O.[55] UVB irradiation and photoaging reduce CAT activity contributing to increase H_2O_2

levels and to promote skin carcinogenesis.[55] In the present study, UVB irradiation also reduced CAT activity (Figure 5A). The treatment with **1** reversed this loss of CAT activity only at the dose of 100 mg/kg (Figure 5A). Supporting our results, the activity of CAT was found increased by **1** treatment in ulcerative colitis in rats,[27] acute nephrotoxicity in mouse kidney,[26] hepatic and renal dysfunction in rats,[28,33] and rat liver oxidative damage.[33,34]

In the presence of UV irradiation, H_2O_2 generates the highly cytotoxic derivative hydroxyl radical ($HO^{\bullet}$) that, in turn, causes cellular damage and other biochemical alterations such lipid peroxidation (LPO) process, a well-established detrimental consequence of UV exposure.[10] In this line, it was observed by tert-butyl hydroperoxide-initiated chemiluminescence (QL) assay that UVB irradiation induced a significant increase of LPO in the skin of hairless mice, which was inhibited by **1** at the dose of 100 mg/kg, but not by the doses of 10 or 30 mg/kg (Figure 5B). In agreement, the protective effect of **1** in LPO has also been reported in others models.[28,33,34]

$O_2^{\bullet-}$ production occurs at low rates under basal conditions and superoxide dismutase (SOD) converts $O_2^{\bullet-}$ into H_2O_2. Nevertheless, inflammatory cytokines are produced after UVB exposition and lead to additional production of $O_2^{\bullet-}$ by NOX2 activation, which explains in part the excessive generation of ROS and antioxidant depletion following UVB exposure.[2,4] Furthermore, the production of $O_2^{\bullet-}$ is essential to induce cytokine production and to guide neutrophils during chemotaxis.[5,56]. There was a significant increase in $O_2^{\bullet-}$ production in the skin of irradiated mice, which was inhibited by the doses of 10, 30 and 100 mg/kg of **1** (Figure 5C). Corroborating our results, it was reported *in vitro* that **1** is an $O_2^{\bullet-}$ scavenger.[57] Thus, we suggest that this could be a contributing mechanism by which **1** reduces cytokine production and neutrophil recruitment.[15,56]

Treatment with Naringenin (1) Prevents UVB-Induced gp91phox mRNA Expression in the Skin of Hairless Mice. gp91phox is the NOX 2 sub-unity responsible for generating $O_2^{\bullet-}$.[7] ROS produced by gp91phox has emerged as an important messenger of several cellular signaling pathways, including the activation of nuclear transcription factors such as NF-κB and AP-1 that are associated with inflammatory cytokine and MMPs production, respectively.[5,6] Therefore, gp91phox-derived ROS play an important role in UVB-induced inflammation. As shown in Figure 6, UVB irradiation increased gp91phox mRNA expression, and this increase was inhibited by the dose of 100 mg/kg of **1**. Corroborating the present data, **1** decreased the NOX2 activity in angiotensin II-treated vascular smooth muscle cells.[23]

As described here, **1** acts as an anti-inflammatory agent that prevents skin photodamage, and its mechanisms of action include targeting the production of cytokines. Moreover, it is possible that **1** act as antioxidant on UVB-irradiation induced skin damage by

scavenging free radicals and consequentely decreasing depletion of endogenous antioxidants and by inhibiting gp91phox-dependent production of $O_2^{\bullet-}$ and its derivatives.

In summary, the beneficial effectiveness of **1** included targeting varied cytokine profiles and also the NOX2-related $O_2^{\bullet-}$ production and oxidative stress. These data suggest the systemic administration of **1** as a promising therapeutic approach in skin photodamage and other inflammatory diseases in which excessive ROS production is involved.

Experimental Section

General Experimental Procedures. Brilliant blue R, reduced glutathione (GSH), hexadecyltrimethylammonium bromide (HTAB), N-ethylmaleimide, *o*-dianisidine dihydrochloride, phenylmethanesulfonyl fluoride, 2,2′-azino-bis(3-ethylbenzothiazoline-6-sulfonic acid) (ABTS), 5,5'-dithiobis(2-nitrobenzoic acid) (DTNB), (2,4,6-Tris(2-pyridyl)-*s*-triazine) (TPTZ), nitroblue tetrazolium (NBT) and bisacrylamide were obtained from Sigma-Aldrich (St. Louis, MO, USA). Naringenin (**1**) at 95% purity from Santa Cruz Biotechnology (Dallas, TX, USA). Tert-butyl hydroperoxide from Acros (Pittsburgh, PA, USA). Xylene cyanol and Tris were obtained from Amresco (Solon, OH, USA). ELISA kits for determination of cytokine were obtained from eBioscience (San Diego, CA, USA). Acrylamide, sodium dodecyl sulfate (SDS), glycerol, Superscript® III, Oligo(dT)12-18 primers, Platinum SYBRGreen® and primers from Invitrogen (Carlsbad, CA, USA). All other reagents used were of pharmaceutical grade.

Animals and experimental protocol. *In vivo* experiments were performed in sex matched hairless mice (HRS/J), weighing 20-30 g. Mice were housed in temperature-controlled room, 12 h light and 12 h dark cycles and access to water and food *ad libitum*. All experiments were conducted in accordance with National Institutes of Health guidelines for the welfare of experimental animals and with the approval of the Ethics Committee of the Universidade Estadual de Londrina (registered under the number CEUA 90/12, process number 3344.2012.08). All efforts were made to minimize the number of animals used and their suffering. Hairless mice were randomly designed to different groups with 5 mice each: non-irradiated control group (20% of Tween 80 in saline), irradiated control group (20% of Tween 80 in saline), irradiated group and treated with solutions containing different doses of **1**. The doses of **1** used in these assays were selected based on therapeutic effects reported previously.[19] In the experiments presented in Figures 1-2, and 4, mice were treated intraperitoneally 1 h before and 7 h after the beginning of UVB irradiation with **1**. In the experiments of Figures 3, 5 and 6 mice were treated only once, 1 h before the irradiation beginning.[43]

Irradiation. The UVB source used in the experiments to induce oxidative stress was a Philips TL/12 RS 40W (Medical-Holand) emitting a continuous spectrum between 270 and 400 nm with a peak emission at 313 nm. The lamp was mounted 20 cm above mice position, resulting in an irradiation of 0.384 mW/cm^2 as measured by an IL 1700 radiometer (Newburyport, MA, USA) equipped with sensor for UV (SED005) and UVB (SED240). The irradiation dose used for induction of oxidative stress was 4.14 J/cm^2 as employed previously.[43,52] Mice were terminally anesthetized with 1.5% isoflurane (Abbott [Abbott Park, IL, USA])12 h (Figure 1-2 and 4), 2 h (Figure 5A and 5C) or 4 h (Figure 3, 5B and 6) after the UVB exposure, and the full thickness of the dorsal skins was removed. In the tests of 2 h and

4h after the UVB exposure, mice were decapitated immediately after anesthetization and dorsal skin samples were collected. Samples were stored at -70°C until analysis. Samples collected for cutaneous edema determination were weighed immediately after removal and were not frozen.[15]

Skin edema. The effect of **1** on UVB-induced skin edema of hairless mice was measured as an increase in the dorsal skin weight. After dorsal skin removal, a constant area (5 mm diameter) was delimited with the aid of a mold, followed by weighing of this constant area.[15,43] The analysis was obtained by comparing the weight of the skin between groups and the result was expressed in mg of skin.

Myeloperoxidase (MPO) activity. The UVB-induced leukocyte migration to the skin of hairless mice was evaluated using the MPO colorimetric assay.[14,15] The samples of skin were homogenized in K_2HPO_4 buffer 0.05 M (pH 6.0) containing 0.5% HTAB using a Tissue-Tearor (Biospec). The homogenates were centrifuged at 16100 *g* for 2 min at 4°C. The supernatant was removed to assay. Briefly, 30 µL of the resulting supernatant were mixed with 200 µL of 0.05 M K_2HPO_4 buffer (pH 6.0), containing 0.0167% *o*-dianisidine dihydrochloride and 0.05% hydrogen peroxide. The absorbance was determined at 450 nm (Asys Expert Plus, Biochrom). The MPO activity of samples was compared to a standard curve of neutrophils. The results are presented as MPO activity (number of neutrophils per mg of skin).

Analyses of skin proteinase by substrate-embedded enzymography. SDS-PAGE (sodium dodecyl sulphate polyacrylamide gel electrophoresis) substrate-embedded enzymography was used to detect enzymes with gelatinase activity. Assays were carried out as previously described.[15,43] The total skin of hairless mice (1:4, w/w dilution) were homogenized (T 18 basic, IKA) in 0.05 M Tris-HCl buffer (pH 7.4) containing 0.01 M $CaCl_2$ and 1% protease inhibitor cocktail. Whole homogenates were centrifuged at 12000 *g* for 10 min at 4°C twice. The Lowry method was used to measure protein levels in skin homogenates.[58] Aliquots of 50 µL of samples were mixed with 10 µL of 0.1 M Tris-HCl (pH 7.4) containing 20% glycerol, 4% SDS and 0.005% xylene cyanol, and 25 µL of the mixture (40 µg of protein) were taken for electrophoresis in a gel containing 10% acrylamide and 0.025% gelatin. After electrophoresis, the gels were incubated for 1 h with 2.5% Triton X-100 under constant shaking, incubated overnight in 0.05 M Tris-HCl (pH 7.4), 0.01 M $CaCl_2$ and 0.02% sodium azide at 37°C, and stained the following day with brilliant blue R. After destaining in 20% acetic acid, the zone of enzyme activity were analyzed by comparing the groups in the ImageJ Program (NIH, Bethesda, MD, USA).

Cytokine measurement. The samples of hairless mice skin were homogenized in 500 µL of saline solution using Tissue-Tearor (Biospec). The homogenates were centrifuged at 2000 *g* for 15 min at 4 °C and stored at -70 ºC until further use. Supernatants were used to

measure the cytokine levels as described previously[15,43] by enzyme- linked immunosorbent assay (ELISA) according to manufacturer's instructions (eBioscience). Absorbances were determined at 450 nm using a microplate spectrophotometer reader (Multiskan GO, Thermo Scientific) and the results are expressed as picograms (pg) of each cytokine/mg of skin.

FRAP assay. The reducing ability of skin sample was determined by FRAP assay.[43,51] The samples of skin were homogenized in 500 µL of KCl (1.15%) using a Tissue-Tearor (Biospec) and centrifuged at 1000 g for 10 min at 4°C, the supernatant was employed for measurement the antioxidant capacity of skin. The reaction consisted of adding the supernatant (30 µL) to the FRAP reagent prepared with 0.3 mM acetate buffer pH 3.6, 10 mM TPTZ in 40 mM hydrochloride acid and 20 mM ferric chloride. The FRAP reagent was warmed to 37°C during 30 min. The absorvance was determined in 595 nm (Helios Alfa, Thermo Spectronic). Previously, a curve of trolox (0.5-20 µM) was prepared and the results are presented as µM trolox equivalent per mg of skin.

ABTS assay. This assay is based on the inhibition of the absorbance of the radical ABTS. Skin samples were homogenized in 500 µL of KCl (1.15%) using a Tissue-Tearor (Biospec) and centrifuged at 1000 *g* for 10 min at 4°C, the supernatant was employed for measurement the antioxidant capacity of skin. The solution of ABTS was prepared with 7 mM of ABTS and 2.45 mM of potassium persulfate diluted with phosphate buffer pH 7.4 to an absorbance of 0.7-0.8 in 730 nm was prepared. The supernatant was mixed on ABTS solution and after 6 min the absorvance was determined in 730 nm (Helios Alfa, Thermo Spectronic).[43,51] Previously, a curve of trolox (1-25 µM) was prepared and the results are presented as µM trolox equivalent per mg of skin.

GSH assay. GSH was determined as described previously.[43] Briefly, skin samples were homogenized in 0.02 M EDTA using a Tissue-Tearor (Biospec). Whole homogenates were treated with 50% trichloroacetic acid and were centrifuged twice at 2700 *g* for 10 min at 4°C. The reaction mixture contained 50 µL of sample, 100 µL of 0.4 M Tris and 5 µL DTNB (1.9 mg/mL in methanol). The color developed was read at 405 nm (Multiskan GO, Thermo Scientific). The standard curve was prepared with GSH 5-150 µM. The results are presented as µM of GSH per mg of skin.

CAT assay. The analysis of CAT activity was evaluated by measuring the decay in the concentration of hydrogen peroxide (H_2O_2) and the generation of oxygen as described previously.[59] Skin samples of hairless mice were homogenized in 500 µL of 0.02 M EDTA using a Tissue-Tearor (Biospec), and centrifuged twice at 2700 *g* for 10 min at 4°C. The reaction mixture contained 10 µL of sample, 160 µL of buffer Tris-HCl 1 M with EDTA 5 mM pH 8,0, 20 µL of deionized water and 20 µL of H_2O_2 200 mM. Measurement of CAT activity was estimated through the difference between the initial reading and the reading conducted

30 seconds after the addition of H_2O_2 at 240 nm in a microplate reader (EnSpire, Perkin Elmer) at 25ºC. The CAT values were expressed as unit of CAT/mg of skin/minute.

Lipid hydroperoxides (LOOH). LOOH-initiated chemiluminescence (QL) was determined according to an adaptation of the technique described previously.[60] The test is based on the premise that there is an increase in QL associated with oxidative stress leading to the consumption of the antioxidant defenses from the formation of hydroperoxides. Samples of skin were homogenized in 800 µL of phosphate buffer (pH 7.4) using a Tissue-Tearor (Biospec)**,** centrifuged at 700 *g* for 2 min at 4°C. Then, 250 µL the supernatant was diluted in 1730 µL reaction medium (120 mM KCl, 30 mM phosphate buffer, pH 7.4) and mixed with 20 µL of 3 mM tert-butyl hydroperoxide. The reading was conducted in a β-counter Beckman®LS 6000SC (Fullerton, CA, USA) in a non-coincident counting for 30 s with a response range between 300 and 620 nm. The vials were kept in the dark up to the moment of the assay, and determinations were obtained in dark in order to avoid vial phosphorescence activated by light. The experiment was conducted at 30°C for 120 min. The results were measured in counts per min (cpm) per mg of skin.

$O_2^{\bullet-}$ production. The measurement of $O_2^{\bullet-}$ production in the skin was performed using the nitroblue tetrazolium assay (NBT) as described previously.[15] Samples of skin were homogenized in 500 µL of 0.02 M EDTA using a Tissue-Tearor (Biospec) and centrifuged (2000 *g*, 20 seconds, 4°C). Then, 50 µL of the supernatant were incubated in 96-well plate for 1 h. The non-adherent/non-precipitated supernatant was carefully removed, 100 µL of NBT (1 mg/ml) was added to each well and incubated over 15 min. NBT reaction medium was then carefully removed followed by fixation in methanol 100%. Formazan particles were dissolved by adding 120 µL of KOH 2M and 140 µL of dimethylsulfoxide. Reduction of NBT to formazan was measured at 600 nm using a microplate spectrophotometer reader (Asys Expert Plus, Biochrom) and the results are presented as optical density (OD) per 10 mg of skin.

Quantitative polymerase chain reaction (qPCR). Samples of skin were homogenized in TRIzol reagent, and total RNA was extracted. The purity of total RNA was measured with a spectrophotometer and the wavelength absorption ratio (260/280 nm) was between 1.8 and 2.0 for all preparations. Reverse transcription of total RNA to cDNA was carried out using Superscript® III kit (Invitrogen) and Oligo(dT)12-18 primers. Real time PCR (qPCR) was performed with Platinum SYBRGreen® kits (Invitrogen) in a 50 µl reaction volume following the manufacturer's cycling conditions: 50 ºC for 2 min, 95 ºC for 2 min, followed by 45 cycles of 95 ºC for 15 s and 55 ºC for 30 s. Melting curve analysis was performed (65–95 °C) in order to verify that only one product was amplified. Samples with more than one peak were excluded. qPCR was performed in LightCycler® Nano Instrument (Roche).[15] The relative gene expression was measured using the comparative $2^{-(\Delta\Delta Cq)}$

method. The expression of GAPDH mRNA was used as a control for tissue integrity in all samples. The primers used were: *Gp91phox*, sense: 5'-AGCTATGAGGTGGTGATGTTAGTGG-3', antisense: 5'-CACAATATTTGTACCAGACAGACTTGAG-3'; and *Gapdh* sense: 5-ATGACATCAAGAAGGTGGTG-3, Antisense: 5'-CATACCAGGAAATGAGCTTG-3.

Statistical analysis. The bars in the figures indicate the mean values ± standard error of the mean (SEM) of 5 mice per group per experiment and are representative of two separate experiments. Data were statistically analyzed by one-way ANOVA followed by Tukey's *t* test. Statistical analyses were performed using GraphPad Prism 4 software (GraphPad Software Inc., San Diego, CA, USA). Results were considered significantly different when $p < 0.05$.

Acknowledgment. This work was supported by Brazilian grants from Coordenadoria de Aperfeiçoamento de Pessoal de Nível Superior (CAPES), Conselho Nacional de Desenvolvimento Científico e Tecnológico (CNPq), Ministério da Ciência, Tecnologia e Inovação (MCTI), Secretaria da Ciência, Tecnologia e Ensino Superior (SETI)/Fundação Araucária and Governo do Estado do Paraná. Financiadora de Estudos e Projetos (FINEP) for LightCycler® Nano Instrument (Roche) acquisition (CT INFRA 2008, Conv. 01.09.0367.02). We thank the technical assistance of Denise Duarte, Marcelo Tempesta Oliveira and Cristina Aparecida Lopes.

REFERENCES

(1) Meloni, M.; Nicolay, J. F. *Toxicol. In Vitro.* **2003**, *17*, 609–613.

(2) Afaq, F.; Adhami, V. M.; Mukhtar, H. *Mutat. Res.* **2005**, *571*, 153–173.

(3) Aquino, R.; Morelli, S.; Tomaino, A.; Pellegrino, M.; Saija, A.; Grumetto, L.; Puglia, C.; Ventura, D.; Bonina, F. *J. Ethnopharmacol.* **2002**, *79*, 183–191.

(4) Circu, M. L.; Aw, T. Y. *Free Radic. Biol. Med.* **2010**, *48*, 749–762.

(5) Bowie, A.; O'Neill, L. A. *Biochem. Pharmacol.* **2000**, *59*, 13–23.

(6) Vicentini, F. T.; He, T.; Shao, Y.; Fonseca, M. J.; Verri, W. A., Jr.; Fisher, G. J.; Xu, Y. *J. Dermatol. Sci.* **2011**, *61*, 162–168.

(7) Anrather, J.; Racchumi, G.; Iadecola, C. *J. Biol. Chem.* **2006**, *281*, 5657–5667.

(8) John, A.; Tuszynski, G. *Pathol. Oncol. Res.* **2001**, *7*, 14–23.

(9) Staniforth, V.; Huang, W. C.; Aravindaram, K.; Yang, N. S. *J. Nutr. Biochem.* **2012**, *23*, 443–451.

(10) Halliday, G. M. *Mutat. Res.* **2005**, *571*, 107–120.

(11) Nichols, J. A.; Katiyar, S. K. *Arch. Dermatol. Res.* **2010**, *302*, 71–83.

(12) Filip, A.; Clichici, S.; Daicoviciu, D.; Catoi, C.; Bolfa, P.; Postescu, I. D.; Gal, A.; Baldea, I.; Gherman, C.; Muresan, A. *J. Physiol. Pharmacol.* **2011**, *62*, 385–392.

(13) Sun, Z. W.; Hwang, E.; Lee, H. J.; Lee, T. Y.; Song, H. G.; Park, S. Y.; Shin, H. S.; Lee, D. G.; Yi, T. H. *J. Nat. Med.* **2014**, *69,* 22–34.

(14) Casagrande, R.; Georgetti, S. R.; Verri, W. A., Jr.; Dorta, D. J.; dos Santos, A. C.; Fonseca, M. J. *J. Photochem. Photobiol B.* **2006**, *84*, 21–27.

(15) Campanini, M. Z.; Pinho-Ribeiro, F. A.; Ivan, A. L.; Ferreira, V. S.; Vilela, F. M.; Vicentini, F. T.; Martinez, R. M.; Zarpelon, A. C.; Fonseca, M. J.; Faria, T. J.; Baracat, M. M.; Verri, W. A., Jr.; Georgetti, S. R.; Casagrande, R. *J. Photochem. Photobiol. B.* **2013**, *127*, 153–160.

(16) Verri, W. V.; Vicentini, F. T. M. C.; Baracat, M. M.; Georgetti, S. R.; Cardoso, R. D. R.; Cunha, T. M.; Ferreira, S. H.; Cunha, F. Q.; Fonseca, M. J. V.; Casagrande, R. In Studies in Natural Products Chemistry; Atta-ur-Rahman, F. R. S., Ed.; Elsevier: Oxford, UK, 2012; Vol. 36, Chapter 9, pp 297−330.

(17) Yang, B.; Kotani, A.; Arai, K.; Kusu, F. *Anal. Sci.* **2001**, *17*, 599–604.

(18) Lee, C. H.; Jeong, T. S.; Choi, Y. K.; Hyun, B. H.; Oh, G. T.; Kim, E. H.; Kim, J. R.; Han, J. I.; Bok, S. H. *Biochem. Biophys. Res. Commun.* **2001**, *284*, 681–688.

(19) Orsolic, N.; Gajski, G.; Garaj-Vrhovac, V.; Dikic, D.; Prskalo, Z. S.; Sirovina, D. *Eur. J. Pharmacol.* **2011**, *656*, 110–118.

(20) Vafeiadou, K.; Vauzour, D.; Lee, H. Y.; Rodriguez-Mateos, A.; Williams, R. J.; Spencer, J. P. *Arch. Biochem. Biophys.* **2009**, *484*, 100–109.

(21) Bai, X.; Zhang, X.; Chen, L.; Zhang, J.; Zhang, L.; Zhao, X.; Zhao, T.; Zhao, Y. *Neurochem. Res.* **2014**, *39*, 1405–1415.

(22) Raza, S. S.; Khan, M. M.; Ahmad, A.; Ashafaq, M.; Islam, F.; Wagner, A. P.; Safhi, M. M.; Islam, F. *Neuroscience.* **2013**, *230*, 157–171.

(23) Xu, C.; Chen, J.; Zhang, J.; Hu, X.; Zhou, X.; Lu, Z.; Jiang, H. *Biol. Pharm. Bull.* **2013**, *36*, 1549–1555.

(24) Xu, X. R.; Yu, H. T.; Hang, L.; Shao, Y.; Ding, S. H.; Yang, X. W. *Biomed. Res. Int.* **2014**, *2014*, 623509.

(25) Subramanian, P.; Arul, D. *Cell Biochem. Funct.* **2013**, *31*, 511–517.

(26) Hermenean, A.; Ardelean, A.; Stan, M.; Herman, H.; Mihali, C. V.; Costache, M.; Dinischiotu, A. *Chem. Biol. Interact.* **2013**, *205*, 138–147.

(27) Al-Rejaie, S. S.; Abuohashish, H. M.; Al-Enazi, M. M.; Al-Assaf, A. H.; Parmar, M. Y.; Ahmed, M. M. *World J. Gastroenterol.* **2013**, *19*, 5633–5644.

(28) Renugadevi, J.; Prabu, S. M. *Toxicology.* **2009**, *256*, 128–134.

(29) Iwamura, C.; Shinoda, K.; Yoshimura, M.; Watanabe, Y.; Obata, A.; Nakayama, T. *Allergol. Int.* **2010**, *59*, 67–73.

(30) Kim, T. H.; Kim, G. D.; Ahn, H. J.; Cho, J. J.; Park, Y. S.; Park, C. S. *Life Sci.* **2013**, *93*, 516–524.

(31) Park, H. Y.; Kim, G. Y.; Choi, Y. H. *Int. J. Mol. Med.* **2012**, *30*, 204–210.

(32) Dou, W.; Zhang, J.; Sun, A.; Zhang, E.; Ding, L.; Mukherjee, S.; Wei, X.; Chou, G.; Wang, Z. T.; Mani, S. *Br J. Nutr.* **2013**, *110*, 599–608.

(33) Mershiba, S. D.; Dassprakash, M. V.; Saraswathy, S. D. *Mol. Biol. Rep.* **2013**, *40*, 3681–3691.

(34) Pari, L.; Gnanasoundari, M. *Basic Clin. Pharmacol. Toxicol.* **2006**, *98*, 456–461.

(35) Azuma, T.; Shigeshiro, M.; Kodama, M.; Tanabe, S.; Suzuki, T. *J. Nutr.* **2013**, *143*, 827–834.

(36) Yilma, A. N.; Singh, S. R.; Morici, L.; Dennis, V. A. *Mediators Inflamm.* **2013**, *2013*, 102457.

(37) El-Mahdy, M. A.; Zhu, Q.; Wang, Q. E.; Wani, G.; Patnaik, S.; Zhao, Q.; Arafa el, S.; Barakat, B.; Mir, S. N.; Wani, A. A. *Photochem. Photobiol.* **2008**, *84*, 307–316.

(38) Rijken, F.; Bruijnzeel-Koomen, C. A. *Clin. Pharmacol. Ther.* **2011**, *89*, 120–124.

(39) Bradley, P. P.; Priebat, D. A.; Christensen, R. D.; Rothstein, G. *J. Invest. Dermatol.* **1982**, *78*, 206–209.

(40) Fisher, G.J.; Wang, Z.Q.; Datta, S.C.; Varani, J.; Kang, S.; Voorhees, J.J. *N. Engl. J. Med.* **1997**, *337*, 1419–1429.

(41) Mutou, Y.; Ibuki, Y.; Kojima, S. *Photodermatol. Photoimmunol. Photomed.* **2007**, *23*, 135–144.

(42) Lou, J. S.; Chen, X. E.; Zhang, Y.; Gao, Z. W.; Chen, T. P.; Zhang, G. Q.; Ji, C. *Exp. Ther. Med.* **2013**, *6*, 1022–1028.

(43) Ivan, A. L.; Campanini, M. Z.; Martinez, R. M.; Ferreira, V. S.; Steffen, V. S.; Vicentini, F. T.; Vilela, F. M.; Martins, F. S.; Zarpelon, A. C.; Cunha, T. M.; Fonseca, M. J.; Baracat, M. M.; Georgetti, S. R.; Verri, W. A., Jr.; Casagrande, R. *J. Photochem. Photobiol. B.* **2014**, *138*, 124–133.

(44) Yokogawa, M.; Takaishi, M.; Nakajima, K.; Kamijima, R.; Digiovanni, J.; Sano, S. *Mol. Carcinog.* **2013**, *52*, 760–769.

(45) Striz, I.; Brabcova, E.; Kolesar, L.; Sekerkova, A. *Clin. Sci. (Lond).* **2014**, *126*, 593–612.

(46) Cosmi, L.; Maggi, L.; Santarlasci, V.; Liotta, F.; Annunziato, F. *Cytometry A.* **2014**, *85*, 36–42.

(47) Peiser, M. *Clin. Dev. Immunol.* **2013**, *2013*, 261037.

(48) McKenzie, A. N.; Spits, H.; Eberl, G. *Immunity*. **2014**, *41,* 366–374.

(49) La, V. D.; Tanabe, S.; Grenier, D. *J. Periodontal Res.* **2009**, *44*, 193–198.

(50) Wei, H.; Zhang, X.; Wang, Y.; Lebwohl, M. *Cancer Lett.* **2002**, *185*, 21–29.

(51) Katalinic, V.; Modun, D.; Music, I.; Boban, M. *Comp. Biochem. Physiol. C Toxicol. Pharmacol.* **2005**, *140*, 47–52.

(52) Campanini, M. Z.; Custodio, D. L.; Ivan, A. L.; Martins, S. M.; Paranzini, M. J.; Martinez, R. M.; Verri, W. A., Jr.; Vicentini, F. T.; Arakawa, N. S.; de, J. F. T.; Baracat, M. M.; Casagrande, R.; Georgetti, S. R. *AAPS PharmSciTech.* **2014**, *15*, 86–95.

(53) Mira, L.; Silva, M.; Rocha, R.; Manso, C. F. *Redox Rep.* **1999**, *4*, 69–74.

(54) Carini, M.; Aldini, G.; Piccone, M.; Facino, R. M. *Farmaco.* **2000**, *55*, 526–534.

(55) Chelikani, P.; Fita, I.; Loewen, P. C. *Cell Mol. Life Sci.* **2004**, *61*, 192–208.

(56) Hattori, H.; Subramanian, K. K.; Sakai, J.; Jia, Y.; Li, Y.; Porter, T. F.; Loison, F.; Sarraj, B.; Kasorn, A.; Jo, H.; Blanchard, C.; Zirkle, D.; McDonald, D.; Pai, S. Y.; Serhan, C. N.; Luo, H. R. *Proc. Natl. Acad. Sci. U. S. A.* **2010**, *107*, 3546–3551.

(57) Cavia-Saiz, M.; Busto, M. D.; Pilar-Izquierdo, M. C.; Ortega, N.; Perez-Mateos, M.; Muniz, P. *J. Sci. Food Agric.* **2010**, *90*, 1238–1244.

(58) Lowry, O. H.; Rosebrough, N. J.; Farr, A. L.; Randall, R. J. *J. Biol. Chem.* **1951**, *193*, 265–275.

(59) Aebi, H. *Methods Enzymol.* **1984**, *105*, 121–126.

(60) Gonzalez Flecha, B.; Llesuy, S.; Boveris, A. *Free Radic. Biol. Med.* **1991**, *10*, 93–100.

Figures

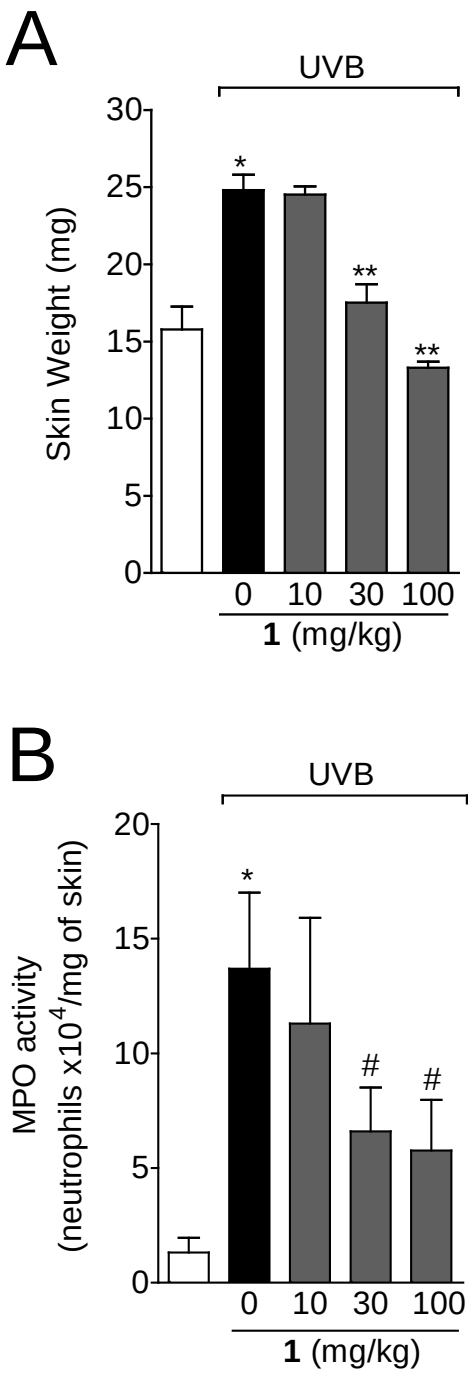

Figure 1. Naringenin (**1**) reduces UVB irradiation-induced skin edema and myeloperoxidase (MPO) activity in hairless mice. Skin edema (A) and MPO activity (B) were determined in samples collected 12 h after the end of irradiation. Bars represent means ± SEM of 5 mice per group and are representative of two separate experiments. [*p<0.001 compared to the non-irradiated control group; $^{\#}p$<0.01 compared to the irradiated control group (vehicle) and **p<0.01 compared to the irradiated control group and the dose of 10 mg/kg of **1**].

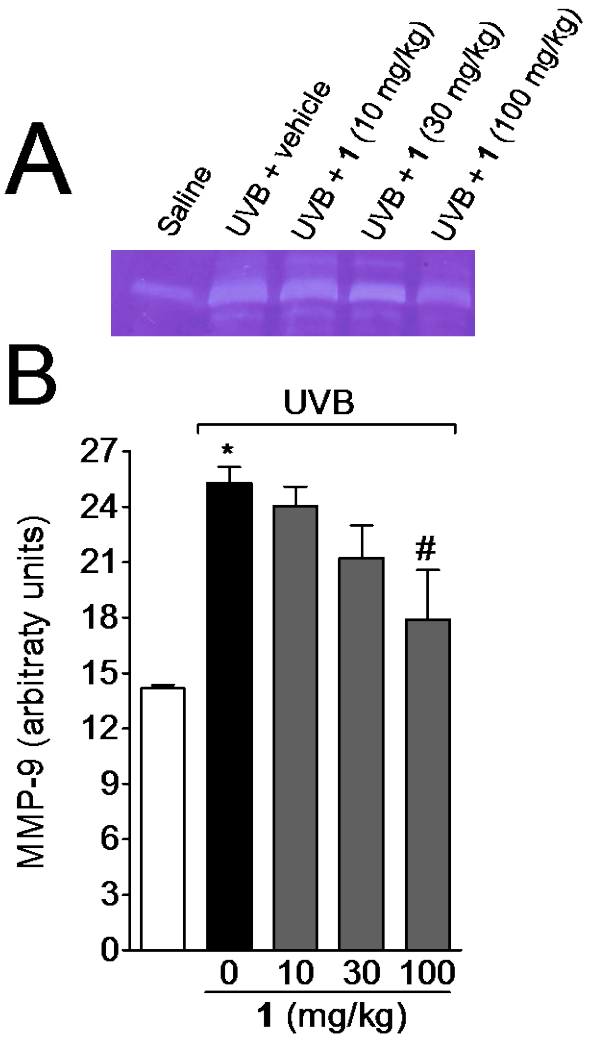

Figure 2. Effect of Naringenin (**1**) on UVB irradiation-induced increase of matrix metalloproteinase-9 (MMP-9) activity. The MMP-9 activity was determined in samples collected 12 h after the end of irradiation. (A) Image of gelatin zymography. (B) Bars represent means ± SEM of 5 mice per group and are representative of two separate experiments. [*p<0.01 compared to the non-irradiated control group; $^{\#}p$<0.05 compared to the irradiated control group (vehicle)].

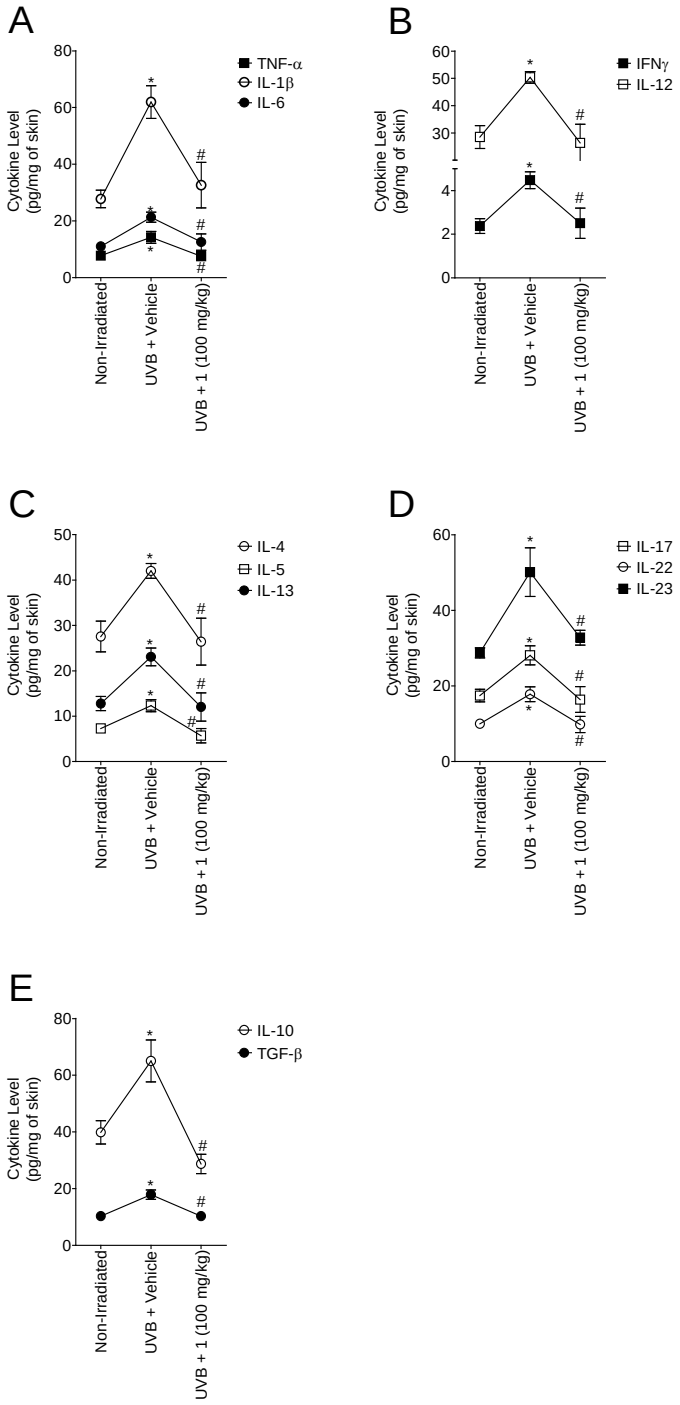

Figure 3. Naringenin (**1**) inhibits UVB irradiation-induced pro-inflammatory and anti-inflammatory cytokine production. The levels of TNF-α, IL-1β and IL-6 (Panel A), Th1 (IFN-γ and IL-12, Panel B), Th2 (IL-4, IL-5 and IL-13, Panel C), Th17 (IL-17, IL-23 and IL-22, Panel D) and anti-inflammatory (IL-10 and TGF-β, Panel E) cytokines were determined in samples collected 4 h after the end of irradiation. Bars represent means ± SEM of 5 mice per group and are representative of two separate experiments. [**p*<0.05 compared to the non-irradiated control group; #*p*<0.05 compared to the irradiated control group (vehicle)].

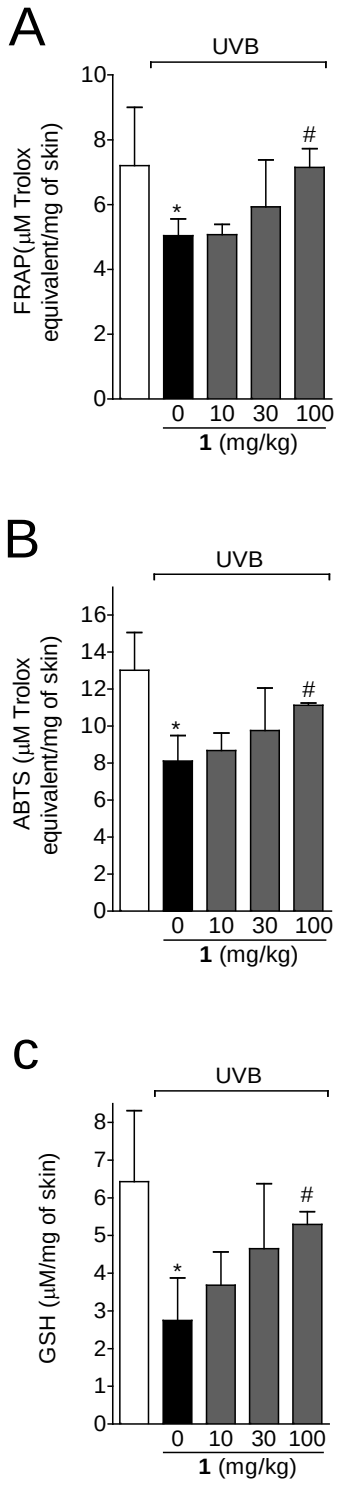

Figure 4. Effect of naringenin (**1**) on antioxidant capacity of skin after UVB irradiation. The antioxidant capacity was determined by FRAP (A), ABTS (B) and GSH (C) assays in samples collected 12 h after the end of irradiation. Bars represent means ± SEM of 5 mice per group and are representative of two separate experiments. [*p<0.05 compared to the non-irradiated control group; #p<0.05 compared to the irradiated control group (vehicle)].

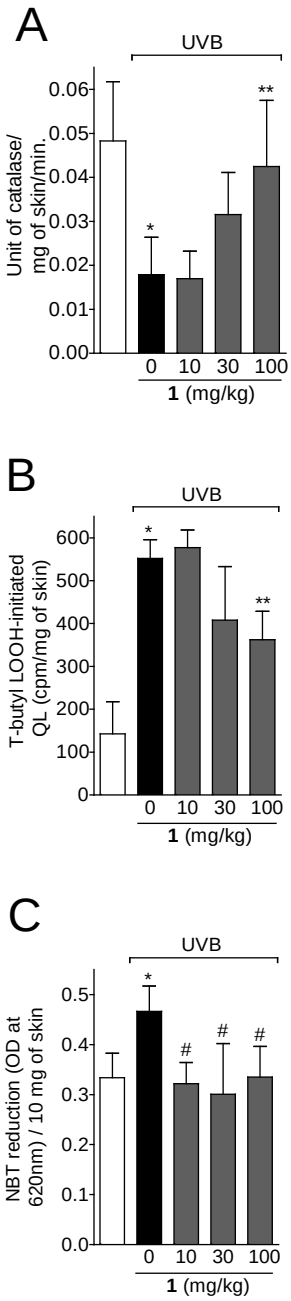

Figure 5. Naringenin (**1**) prevents UVB irradiation-induced catalase (CAT) depletion and lipid hydroperoxides (LOOH) and superoxide anion production. The CAT activity (A), t-butyl LOOH-initiated chemiluminescence (QL) (B), and nitroblue tetrazolium (NBT) reduction (C) were determined in samples collected 2, 4, and 2 h after the end of irradiation, respectively. Bars represent means ± SEM of 5 mice per group and are representative of two separate experiments. [*p<0.05 compared to the non-irradiated control group; $^{\#}p$<0.05 compared to the irradiated control group (vehicle) and ** p<0.05 compared to the irradiated control group and the dose of 10 mg/kg of **1**].

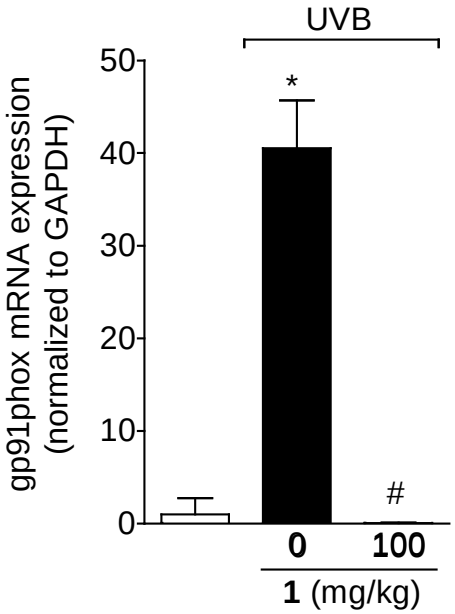

Figure 6. Naringenin (**1**) inhibits UVB irradiation-induced gp91phox mRNA expression. The gp91phox mRNA expression was determined 4 h after the end of irradiation by qPCR. Bars represent means ± SEM of 5 mice per group and are representative of two separate experiments. [*p<0.001 compared to the non-irradiated control group; #p<0.001 compared to the irradiated control group (vehicle)].

4.4 TOPICAL FORMULATION CONTAINING NARINGENIN: EFFICACY AGAINST ULTRAVIOLET B IRRADIATION-INDUCED SKIN INFLAMMATION AND OXIDATIVE STRESS IN MICE

Renata M. Martinez[a], Felipe A. Pinho-Ribeiro[b], Vinicius S. Steffen[a], Thais C. C. Silva[a], Carla V. Caviglione[a], Carolina Bottura[a], Maria J. V. Fonseca[c], Fabiana T. M. C. Vicentini[d], Marcela M. Baracat[a], Sandra R. Georgetti[a], Waldiceu A. Verri, Jr.[b], and Rubia Casagrande[a*]

[a]Departamento de Ciências Farmacêuticas, Universidade Estadual de Londrina-UEL, Avenida Robert Koch, 60, Hospital Universitário, 86039-440 Londrina, Paraná, Brasil

[b]Departamento de Ciências Patológicas, Universidade Estadual de Londrina-UEL, Rodovia Celso Garcia Cid, Km 380, PR445, Cx. Postal 10.011, 86057-970 Londrina, Paraná, Brasil

[c]Departamento de Ciências Farmacêuticas, Faculdade de Ciências Farmacêuticas de Ribeirão Preto-USP, Av. do Café s/n, 14049-903 Ribeirão Preto, São Paulo, Brasil

[d]Farmacore Biotecnologia LTDA, Rua Edson Souto, 738 - Anexo I, Lagoinha, 14095-250 Ribeirão Preto, São Paulo, Brasil

*Corresponding author. Address: Avenida Robert Koch, 60, Vila Operária, CEP 86039-440 Londrina, Paraná, Brasil. Tel/Fax: +55 43 33712475. E-mail address: rubiacasa@yahoo.com.br (R. Casagrande).

Universidade Estadual de Londrina
Departamento de Ciências Farmacêuticas
Centro de Ciências da Saúde
Av Robert Koch, 60 CEP: 86038-350

Dear Editor D.J. Burgess

Please find enclosed the manuscript entitled “Topical formulation containing naringenin: efficacy against ultraviolet B irradiation-induced skin inflammation and oxidative stress in mice” that we would like to submit for publication by International Journal of Pharmaceutics as an original research paper.

The experiments were carried out according to the National Institutes of Health guidelines for the welfare of experimental animals and with the approval of the Ethics Commitee of State University of Londrina (registered under the CEUA process n° 19972.2013.46).

All the authors have read, approved and made substantial contributions for the manuscript. None of the original material contained in this manuscript has been previously published nor is currently under review for publication elsewhere.

Importantly, this is the first in vivo demonstration of the efficacy of topical formulation containing naringenin against UVB irradiation-induced inflammation and oxidative stress. The stability of topical formulations containing naringenin was investigated to select one formulation to be tested in vivo. Furthermore, biochemical, immunological and molecular biology approaches were used to determine the mechanisms of action of formulation. These results evidence the promising therapeutic applicability of topical formulations containing naringenin to reduce skin inflammation.

We are looking forward to hearing from you soon.

Yours sincerely,

Prof Rubia Casagrande
Universidade Estadual de Londrina – UEL
Departamento de Ciências Farmacêuticas – DCF
Centro de Ciências da Saúde – CCS
Avenida Robert Koch, nº 60- Vila Operária
CEP: 86039-440 - Londrina-PR/Brasil

Abbreviations

ABTS	2,2′ -azino-bis (3-ethylbenzothiazoline-6-sulfonic acid)
CAT	catalase
DTNB	5,5'-dithio-bis-(2-nitrobenzoic acid)
FRAP	ferric reducing antioxidant Power
Gpx	glutathione peroxidase
Gr	glutathione reductase
GSH	reduced glutathione
$HO^{\bullet}$	hydroxyl radical
HO-1	heme oxygenase-1
H_2O_2	hydrogen peroxide
IL	Interleukin
LPO	lipid peroxidation
LOOH	lipid hydroperoxides
NADPH	nicotinamide adenine dinucleotide phosphate
NBT	nitroblue tetrazolium
NGN	Naringenin
NOX 2	NADPH oxidase 2
Nrf2	nuclear factor erythroid 2-related factor 2
$O_2^{\bullet-}$	superoxide anion
PCR	polymerase chain reaction
ROS	reactive oxygen species
SEM	standard error mean
SOD	dismutase depletion
TPTZ	2,4,6-Tris(2-pyridyl)-*s*-triazine
TNF-α	tumor necrosis factor-α
UV	Ultraviolet

Abstract

Naringenin (NGN) exhibits anti-inflammatory and antioxidant activities, but it remains undetermined its topical actions against ultraviolet B (UVB)-induced inflammation *in vivo*. The purpose of this study was to evaluate the NGN antioxidant activity in cell free systems and in topical formulations, and the effects of selected formulation containing NGN on UVB irradiation-induced skin inflammation and oxidative damage in hairless mice. NGN presented ferric reducing power, ability to scavenge ABTS and hydroxyl radical, and inhibited iron-independent and dependent lipid peroxidation. Among the three formulations containing NGN, only the F3 kept its physico-chemical and functional stability over 180 days. Topical application of F3 in mice protected from UVB-induced skin damage by inhibiting edema, cytokine production (TNF-α, IL-1β, IL-6, and IL-10) and lipid hydroperoxides. Furthermore, F3 inhibited gp91phox (NADPH oxidase sub-unity) mRNA expression, which resulted in inhibition of superoxide anion production and in maintenance of ferric reducing and ABTS scavenging abilities, catalase activity and reduced glutathione levels. In addition, F3 maintained mRNA expression of cellular antioxidants glutathione peroxidase 1, glutathione reductase and transcription factor Nrf2, and induced mRNA expression of heme oxygenase-1. In conclusion, formulation containing NGN may be a promising approach to control skin diseases related to UVB inflammation.

Keywords: Antioxidant activity, inflammation, naringenin, oxidative stress, topical formulation, ultraviolet B.

1. Introduction

The skin is a physical barrier between the organism and the environment being constantly challenged by deleterious effects of UV solar radiation, mainly ultraviolet B (UVB) irradiation (Ichihashi et al., 2003). The skin function is markedly modified after UVB irradiation exposure, which leads to the development of inflammatory processes mediated by an overproduction of reactive oxygen species (ROS) and depletion of endogenous antioxidants such as reduced glutathione (GSH), glutathione peroxidase (Gpx), and catalase (Afaq et al., 2005; Fischer et al., 2013). Moreover, accumulated damage resulting from chronic UVB irradiation exposure has been shown to cause skin cancer and premature skin aging (Afaq et al., 2005; Halliday, 2005).

UVB induces overproduction of ROS such as superoxide anion ($O_2^{\bullet-}$) through activation of (phagocytic) NADPH oxidase 2 (NOX 2) complex, which is an initial and critical event for the onset of oxidative stress conditions (Anrather et al., 2006; Circu and Aw, 2010). $O_2^{\bullet-}$ reacts with hydrogen peroxide (H_2O_2) generating the cytotoxic hydroxyl radical ($HO^{\bullet}$) (Sullivan et al., 2012) leading to lipid peroxidation (LPO) process, a well-established detrimental consequence of UVB exposure that induces pro-inflammatory products (Girotti, 2001). Thus, ROS contribute to pro-inflammatory signaling cascades and consequent production of cytokines such as interleukin-1β (IL-1β), and tumor necrosis factor-alpha (TNF-α) (Bowie and O'Neill, 2000). Importantly, there is reciprocal activation by oxidative stress and inflammatory mediators because cytokines such as TNF-α also induce $O_2^{\bullet-}$ production (Kilpatrick et al., 2010). Therefore, ROS and cytokines act in synergism during inflammatory skin diseases (Okayama, 2005) .

Epidemiological studies has indicated that sunscreens do not fully prevent UVB irradiation-induced skin injuries. Thus, novel chemopreventive treatments need to be identified (Azizi et al., 2000). Considering the synergic effect of ROS and inflammatory mediators, the use of molecules with antioxidants and anti-inflammatory effects is a promising approach to inhibit UVB irradiation-induced skin damage (Campanini et al., 2013; Casagrande et al., 2006a; Reeve et al., 2010). In this context, much attention has been paid to antioxidants from natural sources (Campanini et al., 2013; Casagrande et al., 2006a; Nichols and Katiyar, 2010). Moreover, naturally occurring agents are considered to be less toxic, of low cost, and more effective in controlling various human malignancies (Afaq and Katiyar, 2011; Dhanalakshmi et al., 2004).

Flavonoids represent the most common and widely distributed group of plant phenolics (Verri et al., 2012). In addition, most of the flavonoids have a structural innate antioxidant activity and are also known as natural anti-inflammatory agents (Verri et al., 2012), which strongly suggest the potential of these compounds to inhibit UVB irradiation-

induced skin damaging events (Afaq and Katiyar, 2011). Therefore, their topical use may provide the necessary photochemico protection in addition to human sunscreens. Moreover, the topical use of bioactive substances is a powerful strategy to avoid possible systemic toxicity.

Molecules of the flavonoid subgroup flavanones are found almost exclusively in citrus fruits and comprise the most common plant polyphenolic compounds in the human diet (Manach et al., 2004). Naringenin (NGN) (5,7,4'-trihydroxyflavanone) is one of the most abundant flavanones found in fruits such as grapefruit, lemon, tangerine and orange (Lee et al., 2001). It has many pharmacological activities such as anti-atherogenic, anti-cancer, antioxidant, and anti-inflammatory (El-Mahdy et al., 2008; Hermenean et al., 2013; Lee et al., 2001; Mershiba et al., 2013; Pari and Gnanasoundari, 2006; Renugadevi and Prabu, 2009; Subburaman et al., 2014; Yilma et al., 2013). It has been demonstrated that NGN protects HaCaT human keratinocytes against UVB-induced carcinogenesis and aging (El-Mahdy et al., 2008). However, there is no evidence of topical formulation containing NGN to prevent photodamage. The present study aimed to investigate the *in vitro* antioxidant activity of NGN alone, prepare and evaluate its physico-chemical and functional stabilities of topical formulations containing NGN as well as evaluate the *in vivo* protection of the most stable formulation containing NGN against skin inflammation and oxidative stress caused by UVB irradiation in hairless mice.

2. Material and Methods

2.1 Chemicals

2,2′ -azinobis (3-ethylbenzothiazoline- 6-sulfonic acid) (ABTS), reduced glutathione (GSH), 5,5'dithio-bis-(2-nitrobenzoic acid) (DTNB) and nitroblue tetrazolium (NBT) were obtained from Sigma Chemical Co. (St. Louis, MO, USA). Naringenin at 95% from Santa Cruz Biotechnology (Dallas, TX, USA). Tert-butyl hydroperoxide and 2-deoxy-D-ribose from Acros (Pittsburgh, PA, USA). Enzyme linked immunosorbent assay (ELISA) kits from eBioscience (San Diego, CA, USA). Superscript® III, Oligo(dT)12-18 primers, Platinum SYBRGreen® and primers from Invitrogen (Carlsbad, CA, USA). Materials for formulations were obtained from Galena (Campinas, SP, Brazil). All other reagents used were of pharmaceutical grade.

2.2. In vitro antioxidant activity of NGN

2.2.1. FRAP assay

The ferric reducing antioxidant power of NGN (60 µg/mL) was determined by FRAP assay at 595 nm (Ivan et al., 2014). A standard curve with trolox (4.0-20.0 µmol/L) was used for subsequent calculation of results in µmol/L of trolox equivalent per µg/mL of sample.

2.2.2. ABTS assay

The ABTS scavenging ability of NGN (0.125-2 µg/mL) was measured by the decrease of absorbance at 730 nm (Martinez et al., 2012) and calculated by the following equation: Equation I: % of activity = (1- sample absorbance/control absorbance) x 100.

2.2.3. Hydroxyl assay

The hydroxyl radical ($HO^{\bullet}$) scavenging ability of NGN (25-500 µg/mL) was measured by the reduction of thiobarbituric acid reactive substances (TBARS) from degradation of deoxyribose by $HO^{\bullet}$ generated in Fenton reaction (Halliwell et al., 1987; Martinez et al., 2012; Ivan et al., 2014). The scavenging of hydroxyl free radical was calculated by equation I.

2.2.4. Iron-independent lipid peroxidation

The inhibitory activity of lipid peroxidation of NGN (10-500 µg/mL) was determined by decreasing the production of lipid hydroperoxides, a primary product of lipid peroxidation (Martinez et al., 2012). The following equation was used:

% Activity = 1- (absA after incubation - absA without incubation) / (absC after incubation - absC without incubation) x 100. AbsA is the absorbance of sample, and absC is the absorbance of the control.

2.2.5. Iron-dependent lipid peroxidation

Mitochondria of hairless mice were used as a source of lipid membranes to evaluate lipid peroxidation and were prepared by standard differential centrifugation techniques. The ability of graded concentrations of NGN (2.5-500 µg/mL) to inhibit iron-induced lipid peroxidation was evaluated by reduction of TBARS formation (Buege and Aust, 1978; Martinez et al., 2012). The inhibition of iron-dependent lipoperoxidation was calculated by equation I.

2.3. Formulations

Formulations F1, F2, and F3 were developed varying the content of excipients (Table I). Self-emulsifying agents were Polawax®, Hostacerin SAF® or Net FS®. Carbopol® 940 was used as stabilizing agent. Caprylic/capric triglyceride was used as emollient, and propylene glycol as solubilizing agent and moisturizer. Phenonip was used as preservative and deionized water was used for the preparation of all formulation. NGN (0.5%) was solubilized in propylene glycol and then added to the formulations at room temperature. Control formulations did not contain NGN.

2.4. Physico-chemical and functional stability of formulations

Regarding stability studies, formulations were packaged in semipermeable polypropylene containers and stored at 4°C and 40±2°C/ 75±5% of relative humidity (RH) for 6 months. Samples were evaluated 0, 30, 60, 90, and 180 days after preparation (Campanini et al., 2014). NGN raw material was also stored in the same storage conditions to evaluate its functional stability. The physico-chemical and functional stability were determined at room temperature by the following methods.

2.4.1. Organoleptic test

The organoleptic features of the samples were examined at the same temperature, lighting and packaging conditions to assess variations in appearance, phase separation, color and smell (Fonseca et al., 2011).

2.4.2. pH measurements

One gram of each formulation was weighted and diluted with deionized water to a volume of 10mL. After homogenization, the pH of the samples was measured using a digital pH meter (Georgetti et al., 2006)

2.4.3. Centrifugation assay

Samples weighing 2 g were taken and centrifuged at 1660× *g* for 30 min. After centrifugation of samples, the separation of the dispersed phase due to either creaming or coalescence was observed (Georgetti et al., 2006).

2.4.4. Functional stability

The functional stability (Campanini et al., 2014) was measured by ABTS method as described in section “2.2.2. ABTS assay”. Formulations containing NGN were diluted in ethanol to obtain the concentration of 0.8 µg/mL. It was the sample concentration used for the analysis of NGN raw material in the reaction medium. The following controls were included in the test: (i) positive control in the absence of sample, and (ii) positive control added with formulations without NGN.

After the stability studies, the *in vivo* efficacy of the most stable formulation containing NGN against skin inflammation and oxidative stress caused by UVB irradiation was evaluated.

2.5. In vivo efficacy of topical formulation containing NGN

2.5.1. Animals

In vivo experiments were performed in sex matched hairless mice (HRS/J), weighing 20-30 g, obtained from the University Hospital of Londrina State University. Mice were maintained with free access to water and food, and temperature of 23 ºC ± 2. They were housed within cages with a 12 h light and 12 h dark cycles. Animal care and handling procedures were approved by Animal Ethics Committee (CEUA process number 19972.2013.46) of the Londrina State University.

2.5.2. Experimental protocol

Hairless mice were randomly designed to groups with 5 mice each as follows: non-irradiated control, irradiated control, irradiated and treated with formulation without NGN, irradiated and treated with the formulation containing NGN (F3). Mice received topical treatment on the dorsal surface with 0.5 g of the formulation, 12 h, 6 h and 5 min before, and 6 h after the beginning of irradiation session.

2.5.3. Irradiation

The UVB source used was a Philips TL/12 RS 40W (Medical-Holand) emitting a continuous spectrum between 270 and 400 nm with a peak emission at 313 nm (Campanini et al., 2014; Ivan et al., 2014). The lamp was mounted 20 cm above mice position resulting in an irradiation of 0.384 mW/cm^2 as measured by an IL 1700 radiometer (Newburyport, MA, USA) equipped with sensor for UV (SED005) and UVB (SED240). The irradiation dose used to induce skin inflammation was 4.14 J/cm^2 (Campanini et al., 2014; Ivan et al., 2014). All groups were irradiated simultaneously. Mice were terminally anaesthetized with 1.5% isoflurane (Abbott [Abbott Park, IL, USA]) 12 h (Figs. 3, 5A, 5B, and 7A), 2 h (Figs. 5C and 6A) or 4 h (Figs. 4A-D, 5D, 6B, 7B, 7C and 8A-B) after the UVB exposure and the full thickness of the dorsal skins was removed. In the tests of 2 h and 4h after the UVB exposure, mice were decapitated immediately after anesthetization and dorsal skin samples were collected. Samples were stored at -70°C until analysis. Samples collected for cutaneous edema determination were weighed immediately after removal and were not frozen.

2.5.4. Skin edema

The skin edema was measured as an increase in the dorsal skin weight. After dorsal skin removal, a constant area was delimitated with the aid of a mold, followed by weighing (Campanini et al., 2013; Ivan et al., 2014). The result is expressed in mg of skin.

2.5.5. Cytokine measurement

Skin samples were homogenized in 500 ìL of saline solution using Tissue-Tearor (Biospec). The homogenates were centrifuged (2,000 *g*, 15 min, 4°C) and supernatants were stored at -70 ºC. Supernatants were used to measure the cytokine levels by an enzyme-linked immunosorbent assay (ELISA) according to manufacturer's instructions (eBioscience) (Ivan et al., 2014). Absorbance was determined at 450 nm using a microplate spectrophotometer reader (Multiskan GO, Thermo Scientific) and the results are expressed as picograms (pg) of each cytokine/mg of skin.

2.5.6. FRAP assay

The reducing ability of skin sample was determined by FRAP assay (Campanini et al., 2014). The samples of skin were homogenized in 400 µL of KCl (1.15%) using a Tissue-Tearor (Biospec) and centrifuged (1,000 *g*, 10 min, 4°C), and the supernatant was employed to measure the antioxidant capacity of skin. Supernatant (30 µL) was mixed with the FRAP reagent (0.3 mM acetate buffer pH 3.6, 10 mM TPTZ in 40 mM hydrochloride acid, and 20

mM ferric chloride). The absorbance was determined at 595 nm in a microplate reader (EnSpire, Perkin Elmer). A trolox curve (0.01-20 nmol) was prepared and the results are presented as nmol trolox equivalent per mg of skin.

2.5.7. ABTS assay

The ABTS radical scavenging ability of skin was measured by the decrease of absorbance at 730 nm (Campanini et al., 2014). Skin of hairless mice was homogenized in 400 µL of KCl (1.15%) using a Tissue-Tearor (Biospec) and centrifuged (1,000 *g*, 10 min, 4°C), and the supernatant was employed to measure the antioxidant capacity of skin. The solution of ABTS was prepared with 7 mM of ABTS and 2.45 mM of potassium persulfate diluted with phosphate buffer pH 7.4 to an absorbance of 0.7-0.8 in 730 nm was prepared. The supernatant (7 µL) was mixed on ABTS solution and after 6 min the absorbance was determined at 730 nm in a microplate reader (EnSpire, Perkin Elmer). A trolox curve (0.01-20 nmol) was prepared and the results are presented as nmol trolox equivalent per mg of skin.

2.5.8. Catalase assay

The analysis of catalase activity was evaluated by measuring the decay in the concentration of hydrogen peroxide (H_2O_2) and the generation of oxygen as described previously (Aebi, 1984). Skin of samples were homogenized in 500 ìL of 0.02 M EDTA using a Tissue-Tearor (Biospec), and centrifuged twice (2,700 *g*, 10 min, 4°C). The reaction mixture contained 10 ìL of sample, 160 µL of buffer Tris-HCl 1 M with EDTA 5 mM (pH 8.0), 20 µL of deionized water and 20 µL of H_2O_2 200 mM. Measurement of catalase activity was estimated through the difference between the initial reading and the reading conducted 30 seconds after the addition of H_2O_2 at 240 nm in a microplate reader (EnSpire, Perkin Elmer) at 25ºC. The catalase values were expressed as unit of catalase/mg of skin/minute.

2.5.9. Lipid peroxidation (LPO)

LPO was measured by tert-butyl lipid hydroperoxides (LOOH)-initiated chemiluminescence according to an adaptation of the technique described previously (Gonzalez Flecha et al., 1991). This test is based on the premise that there is an increase in chemiluminescence associated with oxidative stress leading to the consumption of the antioxidant defenses from the formation of hydroperoxides. Samples of skin were homogenized in 800 ìL of phosphate buffer (pH 7.4) using a Tissue-Tearor (Biospec)**,** centrifuged (700 *g*, 2 min, 4°C). Then, 250 ìL of the supernatant were diluted in 1730 ìL reaction medium (120 mM KCl, 30 mM phosphate buffer, pH 7.4) and mixed with 20 ìL of 3 mM tert-butyl hydroperoxide. The reading was conducted in a â-counter Beckman®LS 6000SC (Fullerton, CA, USA) in a non-coincident counting for 30 s with a response range

between 300 and 620 nm. The vials were kept in the dark up to the moment of the assay, and determinations were obtained in dark in order to avoid vial phosphorescence activated by light. The experiment was conducted at 30°C for 120 min. The results were measured in counts per min (cpm) per mg of skin.

2.5.10. Superoxide anion ($O_2^{\bullet-}$) production

The measurement of $O_2^{\bullet-}$ production in the skin was performed using the nitroblue tetrazolium assay (NBT) as described previously (Campanini et al., 2013). Samples of skin were homogenized in 500 ìL of 0.02 M EDTA using a Tissue-Tearor (Biospec) and centrifuged (2000 *g*, 20 seconds, 4°C). Then, 50 ìL of the supernatant were incubated in 96-well plate for 1 h. The non-adherent/non-precipitated supernatant was carefully removed, 100 ìL of NBT (1 mg/ml) was added to each well and incubated over 15 min. NBT reaction medium was then carefully removed followed by fixation in methanol 100%. Formazan particles were dissolved by adding 120 ìL of KOH 2M and 140 ìL of dimethylsulfoxide. Reduction of NBT to formazan was measured at 600 nm using a microplate spectrophotometer reader (Asys Expert Plus, Biochrom) and the results are presented as optical density (OD) per 10 mg of skin.

2.5.11. Reduced glutathione (GSH) assay

GSH was determined as described previously (Ivan et al., 2014). Samples of skin were homogenized in 0.02 M EDTA using a Tissue-Tearor (Biospec). Whole homogenates were treated with 50% trichloroacetic acid and were centrifuged twice (2,700 *g*, 10 min, 4°C). The reaction mixture contained 50 ìL of sample, 100 ìL of 0.4 M Tris and 5 ìL DTNB (1.9 mg/mL in methanol). The absorbance was read at 405 nm (Multiskan GO, Thermo Scientific). The standard curve was prepared with GSH (5-150 ìM) and the results are presented as ìM of GSH per mg of skin.

2.5.12. Reverse transcriptase (RT) and quantitative polymerase chain reaction (qPCR)

Skin samples were homogenized in TRIzol® reagent (Life Technologies), and total RNA was isolated according to manufacturer's directions. RNA purity was confirmed by the 260/280 ratio. RT-PCR and quantitative PCR were performed using GoTaq® 2-Step RT-qPCR System (Promega) on a StepOnePlusTM Real-Time PCR System (Applied Biosystems®). The relative mRNA expression was measured using the comparative $2^{-(\Delta\Delta Cq)}$ method. The expression of GAPDH mRNA expression was used as a control for tissue integrity in all samples. Primer sequences are presented in Table 2 (Campanini et al., 2013).

2.6. Statistical analysis

Results were analyzed by GraphPad Prism® 4 software and expressed as mean ± standard error mean (SEM). *In vitro* data represent triplicate analysis per experiment and are representative of two separate experiments. The concentration of NGN necessary to inhibit the oxidative process by 50% (IC_{50}) was determined using hyperbolic curve. *In vivo* results are mean ± SEM of 5 mice per group per experiment and are representative of two separated experiments. The differences were evaluated by ANOVA followed by by Tukey's *t* test. Statistical differences were considered to be significant at $p < 0.05$.

3. Results

3.1. In vitro antioxidant activity of NGN

The antioxidant activity of NGN was evaluated by FRAP, ABTS, $HO^{\bullet}$, iron independent and iron dependent LPO assays. In the FRAP assay, NGN reducing power was 0.157 µmol/L trolox equivalent/µg/mL. NGN concentration-dependently scavenged the ABTS synthetic and $HO^{\bullet}$ radicals with IC_{50} of 0.71 µg/mL and 183 µg/mL, respectively (Fig. 1A and 1B). NGN also concentration-dependently inhibited *in vitro* iron independent and iron dependent LPO with IC_{50} of 101 µg/mL and 159 µg/mL, respectively (Fig. 1C and 1D).

3.2. Preparation and stability of formulations containing NGN

Three topical formulations containing NGN were prepared, and their physico-chemical and functional stability under 4°C and 40±2°C / 75±5% RH were evaluated. After six months at 4°C, F1, F2 and F3 (control and added with NGN) maintained their color and consistency characteristics. In addition, at 40±2°C/75±5% RH there was no color change in all formulations while there was consistency decrease of F1 and F2 (control and added with NGN). The pH values of F1, F2 and F3 remained compatible with the pH values of skin range from 5.0 to 6.0 (Kim et al., 2012), and all formulations also remained physically stable upon centrifugation assay, showing no phase separation in the two storage conditions evaluated.

Regarding functional stability study using ABTS scavenging activity, it was observed that temperature, storage time, and compound of formulation influenced the antioxidant activity of NGN. After six months stored at 4°C the ABTS radical scavenging ability of F1 and F2 decreased by 8.94% and 14.88%, respectively, while the antioxidant activity of F3 increased 4.98%. Moreover, at 40±2°C/75±5% RH, F1 and F2 lost 33.55% and 6.65% of their antioxidant activity, respectively. On the other hand, the antioxidant activity of F3 increased by 15.77% possibly due to water loss when stored at high temperatures since it is constitute by approximately 86% of water. It is important to mention that starting in the beginning of the study, ABTS radical scavenging ability of F2 was lower than NGN raw material. Taking into account all stability results, F3 demonstrated to be the most stable formulation, and was selected for evaluation of *in vivo* efficacy of NGN against skin inflammation and oxidative stress caused by UVB irradiation.

3.3. Formulation containing NGN reduces UVB irradiation-induced skin edema

Possible anti-inflammatory activity of formulation containing NGN was evaluated in UVB-induced skin inflammation in hairless mice. Firstly, it was observed that UVB irradiation induced significant increase of skin edema in untreated irradiated animals and irradiated animals treated with control formulation (Fig. 3). On the other hand, formulation containing NGN inhibited skin edema (Fig. 3).

3.4. Formulation containing NGN inhibits UVB irradiation-induced cytokine production

UVB irradiation induced significant increase of pro-inflammatory cytokines TNF-α (Fig. 4A), IL-1β (Fig. 4B) and IL-6 (Fig. 4C), and anti-inflammatory cytokine IL-10 (Fig. 4D) production compared to non-irradiated mice. Formulation containing NGN inhibited the production of all cytokines evaluated (Fig. 4). No effect was observed with formulation without NGN.

3.5. Formulation containing NGN prevents decrease of antioxidant capacity and inhibits lipid peroxidation (LPO) of skin induced by UVB irradiation

UVB irradiation induced a decrease of skin ferric reducing ability (FRAP) (Fig. 5A) and ABTS radical scavenging (Fig. 5B) activities compared to non-irradiated mice. In turn, the treatment with formulation containing NGN inhibited UVB irradiation-induced depletion of FRAP and ABTS activities, which were maintained at similar levels of non-irradiated control group (Fig. 5A and 5B). UVB irradiation also reduced the skin catalase activity, which was unaffected by control formulation without NGN. In line with the FRAP and ABTS results, formulation containing NGN was able to inhibit catalase activity depletion (Fig. 5C). UVB irradiation also increased skin LPO while treatment with formulation containing NGN inhibited this parameter reaching similar levels as for non-irradiated control group (Fig. 5D). No effect was observed with formulation without NGN.

3.6. Formulation containing NGN inhibits UVB irradiation-induced superoxide anion ($O_2^{\bullet-}$) production and gp91phox mRNA expression

UVB irradiation induced $O_2^{\bullet-}$ production in the skin while treatment with formulation containing NGN inhibited this production reaching non-irradiated control group levels (Fig. 6A). In agreement with this result, formulation containing NGN also inhibited UVB irradiation-induced gp91phox mRNA expression (Fig. 6B), a NADPH oxidase 2 (NOX 2) sub-unity

responsible for $O_2^{\bullet-}$ production during acute inflammation (Hiramoto et al., 2012; Takeya and Sumimoto, 2003). No effect was observed with formulation without NGN.

3.7. Formulation containing NGN inhibits UVB irradiation-induced down-regulation of glutathione system components

UVB irradiation induced significant decrease of reduced glutathione (GSH) levels (Fig. 7A), and glutathione peroxidase 1 (Gpx1) (Fig. 7B) and glutathione reductase (Gr) (Fig. 7C) mRNA compared to non-irradiated control group. The topical treatment with formulation containing NGN maintained GSH levels, and Gpx1 and Gr mRNA expression at basal levels (Fig. 7A, 7B and 7C). No effect was observed with formulation without NGN.

3.8. Formulation containing NGN inhibits UVB irradiation-induced Nrf2 down-regulation and improves HO-1 expression in the skin

UVB irradiation reduced Nrf2 mRNA expression in the skin compared to non-irradiated control group, an effect that was amenable by formulation containing NGN reaching levels similar to non-irradiated control (Fig. 8A). Nrf2 induced heme oxygenase-1 (HO-1) expression, and the enhanced HO-1 activity is involved in the protective response to cellular stress such as inflammation (Listopad et al., 2007). Formulation containing NGN enhanced UVB irradiation-induced HO-1 mRNA expression (Fig. 8B). No effect was observed with formulation without NGN.

4. Discussion

Naringenin (NGN) is a flavonoid with great perspectives to be used as anti-inflammatory and antioxidant (Hermenean et al., 2013; Mershiba et al., 2013; Pari and Gnanasoundari, 2006; Subburaman et al., 2014; Yilma et al., 2013). In the present study, we firstly determined the *in vitro* antioxidant properties of NGN, followed by functional stability studies of three topical formulations containing NGN resulting in the selection of F3 for *in vivo* testing. F3 containing NGN inhibited UVB-induced skin inflammation and oxidative stress in mice.

Our *in vitro* results on antioxidant properties of NGN show that it inhibits lipid peroxidation (LPO) in non-enzymatic systems in part by scavenging cationic (ABTS) and anionic ($HO^{\bullet}$) radicals. Of note, the antioxidant activity of NGN was more prominent in ABTS radical (IC_{50} = 0.71 µg/mL or 2.60 µM) than in $HO^{\bullet}$ radical (IC_{50} = 183 µg/mL or 672 µM) scavenging assays, suggesting that electron donation accounts for a direct antioxidant mechanism of NGN rather than hydrogen donation. Accordingly, we observed that NGN inhibits iron-independent LPO, which involves initial products of LPO such as hydroperoxide lipids formation (Martinez et al., 2012), and iron-dependent LPO as well, which is mediated by peroxyl and alkoxyl radicals during propagation and termination of LPO, with an IC_{50} of 101 µg/mL (370 µM) and 159 µg/mL (584 µM), respectively. Therefore, NGN can inhibit these three levels of lipid peroxidation in concentrations that are much higher than that necessary to scavenge ABTS radical. In line with these results, the ABTS scavenging activity of NGN was reported at an IC_{50} of 7.9 µM (Cavia-Saiz et al., 2010), while the IC_{50} in peroxyl- and hydroxyl-induced LPO was of 1210 µM and 230 µM, respectively (Cavia-Saiz et al., 2010). This relatively low capacity of NGN in scavenging anionic radicals has been related to a lack of a *orto*-hydroxyl structure in the B ring and to the lack of conjugation provided by the 2,3-double bond with the 4-oxo group (Johnson and Loo, 2000; Yu et al., 2005), suggesting that the powerful anti-inflammatory activity of NGN reported elsewhere (Al-Rejaie et al., 2013; Subburaman et al., 2014; Yilma et al., 2013) occurs by mechanisms other than solely scavenging free radicals.

The effectiveness of flavonoids, including NGN, in inhibiting disease depends on the pharmacokinetics of each compound preserving the bioavailability. NGN have weak water solubility and could undergo degradation in the acidic stomach environment (Yen et al., 2009). These properties cause low dissolution rates from oral dosage forms, resulting in a low absorption and bioavailability. On the other hand, topical formulations prevent gastrointestinal degradation and represent a promising route of administration for these compounds. An important step for the development of novel products is the stability

evaluation of active principles of formulations stored at varied climatic conditions for given times. It provides information about the shelf-life of pharmaceutical products as well as the conditions for their storage. Therefore, stability testing represents a crucial part of the testing program since the instability of the product modifies essential requisites, i.e., quality, efficacy, and safety (Casagrande et al., 2006b; Kim et al., 2012).

A stable emulsion maintains adequate proportions between its components and the interphase surface even after being exposed to tension resulting from factors such as temperature, agitation, and acceleration of gravity (Kim et al., 2012). The formulations developed in this study remained physically stable (no phase separation) and the pH values remained satisfactory in two storage conditions evaluated. Measuring the pH is necessary to detect pH alterations during a storage period, ensuring that the pH value is compatible with the components of the formulation and with the place of application, avoiding irritation (Casagrande et al., 2006b; Kim et al., 2012). F1 and F2 formulations stored at 40±2°C/75±5% RH presented decrease of consistency, while F3 remained unaltered. Moreover, F1 lost its antioxidant activity after six months in both storage conditions, and the antioxidant activity of F2 was lower than NGN raw material since the beginning of the study, indicating possible incompatibilities between F2 and NGN. Of note, F2 contains Hostacerin®, which is a complex mixture of excipients increasing the range of possible incompatibilities. F3 was the most stable formulation, thus we used F3 for evaluation of *in vivo* efficacy of NGN-containing formulation and demonstrated that this product was effective against skin inflammation and oxidative stress caused by UVB irradiation.

The pathogenesis of skin inflammation is associated with ROS-driven production of cytokines such as TNF-α, IL-1β and IL-6 (Vicentini et al., 2011). The release of these cytokines plays a central role in inflammation and skin damage after UVB exposure (Hiramoto et al., 2012; Strickland et al., 1997) and their inhibition is considered a therapeutic approach to control skin cancer progression and metastasis, and other skin diseases such as psoriasis (Chiricozzi et al., 2011; Lin and Karin, 2007; Moore et al., 1999; Vicentini et al., 2011). Herein, we demonstrated that a formulation containing NGN inhibited skin edema after UVB irradiation as well as the production of inflammatory cytokines (TNF-α, IL-1β, and IL-6). NGN-containing formulation also inhibited UVB-induced increases of IL-10 production in the skin. IL-10 is an anti-inflammatory cytokine in models of acute inflammation (Verri et al., 2006). On the other hand, IL-10 has been associated with UVB-induced immunosuppression and DNA damage and diminishing its production prevents these events (Hasegawa et al., 2013; Piskin et al., 2005). IL-10 is co-produced with pro-inflammatory cytokines to limit the inflammatory response (Verri et al., 2006). In this sense, the inhibition of TNF-α, IL-1β and IL-6 production might have as a consequence the reduction of IL-10 levels.

Taking into account that formulation containing NGN also inhibited the oxidative stress in the skin, including the UVB-induced catalase activity impairment and production of lipid peroxidation products, we aimed to describe the effects of this formulation containing NGN in the endogenous inflammatory sources of ROS. Superoxide anion ($O_2^{\bullet-}$) production represents an important step for the beginning of oxidative stress during inflammation (Circu and Aw, 2010). $O_2^{\bullet-}$ is essential to induce cytokine production (Bowie and O'Neill, 2000). The formulation containing NGN inhibited UVB irradiation-induced production of $O_2^{\bullet-}$ and inflammatory cytokines. *In vitro*, NGN exhibits low $O_2^{\bullet-}$ radical scavenging ability, reaching 12% inhibition at 1 mM (Turkkan et al., 2012). In this study, the authors used a non-enzymatic source of $O_2^{\bullet-}$ (phenazine methosulfate/NADH) and nitroblue tetrazolium (NBT) reduction test to evaluate $O_2^{\bullet-}$ scavenging ability (Turkkan et al., 2012), which suggests that our observations regarding the inhibition of NBT reduction *in vivo* are related to the anti-inflammatory activity of NGN rather than to an $O_2^{\bullet-}$ scavenging activity. Furthermore, the formulation containing NGN inhibited UVB-induced gp91phox mRNA expression, which is the sub-unit of NADPH oxidase that catalyzes O_2 reduction and represents the major source of $O_2^{\bullet-}$ during inflammatory response. In fact, it was demonstrated that UVB-induced skin inflammation is abolished in mice lacking gp91phox expression (Hiramoto et al., 2012).

Inhibition of $O_2^{\bullet-}$ generation by NGN was 18-fold greater in an enzymatic xanthine oxidase system (IC_{50} = 4.4 μM) compared to the non-enzymatic phenazine methosulfate/NADH reaction system (IC_{50} = 94.7 μM) (Cavia-Saiz et al., 2010), suggesting that NGN is able to modulate the production and activity of enzymes related to oxidative stress and that inhibition of $O_2^{\bullet-}$ radical production and gp91phox expression could be a contributing mechanism by which formulation containing NGN reduces cytokine production (Campanini et al., 2013). It has been reported that NGN inhibits superoxide dismutase depletion (SOD) induced by a wide range of pro-oxidant stimuli and in several organs, including kidney (Hermenean et al., 2013), liver (Renugadevi and Prabu, 2010), and brain (Khan et al., 2012). Therefore, SOD production may represent an additional mechanism that contributes to reduce $O_2^{\bullet-}$ production in mice treated with NGN-containing formulation.

Several ROS-eliminating systems are present in mammalian tissues to protect cells from ROS over-production as occurs after UVB irradiation exposition. However, excessive UVB irradiation exposure depletes endogenous antioxidants in the skin, including catalase and glutathione peroxidase (Gpx), which are the most important antioxidant enzymes during cell detoxification (Fischer et al., 2013; Halliday, 2005; Sullivan et al., 2012). Excessive ROS production after UVB irradiation induces the consumption of reduced glutathione (GSH), which is the most abundant non-enzymatic antioxidant in the cells (Fonseca et al., 2011). GSH depletion occurs directly by ROS production, but it can also be depleted indirectly because of it is a substrate for Gpx during detoxification (Meister, 1988). NGN-containing

formulation inhibited UVB-induced GSH consumption, but also inhibited the depletion of Gpx1 mRNA expression in the skin, which could be seam as unexpected and controversial results. Nevertheless, NGN-containing formulation also maintained glutathione reductase (Gr) mRNA expression at basal levels. These results suggest that formulation containing NGN (F3) keeps the basal levels of GSH by maintaining a balanced production of Gpx1 (oxidizes GSH to remove ROS-related products) and Gr (recycles GSH) and thus is a successful strategy to protect the skin from oxidative damage induced by UVB irradiation. In line with our results, the antioxidant activity of NGN was related to the inhibition of GSH, Gpx1 and Gr depletion in other studies (Hermenean et al., 2013; Khan et al., 2012; Renugadevi and Prabu, 2009; Subburaman et al., 2014).

The transcription factor Nrf2 (Nuclear factor erythroid 2-related factor 2) is the major redox-dependent regulator of the expression of detoxifying and antioxidant enzymes. Inhibition of Nrf2 activity potentiates UVB irradiation-induced skin damage due to enhanced production of inflammatory mediators, including IL-1β, IL-6 (Saw et al., 2011) and metalloproteinase-9 (Saw et al., 2014). We observed that UVB induced a reduction in Nrf2 mRNA expression, which was inhibited in mice treated with formulation containing NGN, suggesting that NGN enables the skin to respond more efficiently to oxidative stress induced by UVB in a Nrf2-dependent manner. Corroborating this, treatment with NGN-containing formulation enhanced UVB-induced heme oxygenase-1 (HO-1) mRNA expression. HO-1 expression in the skin is induced by Nrf2 in response to oxidative stress and thus is considered a stress-responsive antioxidant enzyme essential to maintain cellular resistance during stress conditions, which may explain why its production is induced while other antioxidant enzymes are inhibited (Listopad et al., 2007). Moreover, enhancing HO-1 expression has been described as a promising approach to inhibit skin damage after irradiation exposure (Zhang et al., 2012).

5. Conclusions

Topical formulations containing NGN were prepared and analyzed regarding their physico-chemical characteristics and antioxidant activity in varied storage conditions during six months. F3 was selected due to its stability compared to the other formulations. Topical application of F3 in the dorsal skin of hairless mice protected from UVB irradiation-induced skin damage by maintaining the mRNA expression of cellular antioxidant components (Gpx1, Gr, Nrf2), by inducing mRNA expression of HO-1, and by inhibiting mRNA expression of NADPH oxidase sub-unit gp91phox, which resulted in an improvement of antioxidant capacity in the skin by maintaining ferric reducing ability, ABTS radical scavenging capacity, the levels of reduced glutathione and catalase activity and inhibition of $O_2^{\bullet-}$ radical

production. F3 containing NGN also inhibited lipid hydroperoxides, edema and cytokine production (TNF-α, IL-1β, IL-6, and IL-10). Taken together, our results suggest that topical treatment with NGN-containing formulation may be explored as potential product to prevent and/or treat skin diseases related to UVB exposition.

Acknowledgement

This work was supported by Brazilian grants from Coordenadoria de Aperfeiçoamento de Pessoal de Nível Superior (CAPES), Conselho Nacional de Desenvolvimento Científico e Tecnológico (CNPq), Ministério da Ciência, Tecnologia e Inovação (MCTI), Secretaria da Ciência, Tecnologia e Ensino Superior (SETI), Fundação Araucária and Governo do Estado do Paraná. We thank Marcelo Tempesta Oliveira, Denise Duarte and Cristina Aparecida Lopes for their technical support to this research. StepOnePlusTM Real-Time PCR System (Applied Biosystems®) was purchased by FINEP funding (CT-INFRA 01/2013).

References

Aebi H., 1984. Catalase in vitro. Methods Enzymol. 105, 121-126.

Afaq F., Adhami, V.M., Mukhtar, H., 2005. Photochemoprevention of ultraviolet B signaling and photocarcinogenesis. Mutat. Res. 571, 153-173.

Afaq F., Katiyar, S.K., 2011. Polyphenols: skin photoprotection and inhibition of photocarcinogenesis. Mini Rev. Med. Chem. 11, 1200-1215.

Al-Rejaie S.S., Abuohashish, H.M., Al-Enazi, M.M., Al-Assaf, A.H., Parmar, M.Y., Ahmed, M.M., 2013. Protective effect of naringenin on acetic acid-induced ulcerative colitis in rats. World J. Gastroenterol. 19, 5633-5644.

Anrather J., Racchumi, G., Iadecola, C., 2006. NF-kappaB regulates phagocytic NADPH oxidase by inducing the expression of gp91phox. J. Biol. Chem. 281, 5657-5667.

Azizi E., Flint, P., Sadetzki, S., Solomon, A., Lerman, Y., Harari, G., Pavlotsky, F., Kushelevsky, A., Glesinger, R., Shani, E., Rosenberg, L., 2000. A graded work site intervention program to improve sun protection and skin cancer awareness in outdoor workers in Israel. Cancer Causes Control. 11, 513-521.

Bowie A., O'Neill, L.A., 2000. Oxidative stress and nuclear factor-kappaB activation: a reassessment of the evidence in the light of recent discoveries. Biochem Pharmacol. 59, 13-23.

Buege J.A., Aust, S.D., 1978. Microsomal lipid peroxidation. Methods Enzymol. 52, 302-310.

Campanini M.Z., Custodio, D.L., Ivan, A.L., Martins, S.M., Paranzini, M.J., Martinez, R.M., Verri, W.A., Jr., Vicentini, F.T., Arakawa, N.S., de, J.F.T., Baracat, M.M., Casagrande, R., Georgetti, S.R., 2014. Topical formulations containing Pimenta pseudocaryophyllus extract: In vitro antioxidant activity and in vivo efficacy against UV-B-induced oxidative stress. AAPS PharmSciTech. 15, 86-95.

Campanini M.Z., Pinho-Ribeiro, F.A., Ivan, A.L., Ferreira, V.S., Vilela, F.M., Vicentini, F.T., Martinez, R.M., Zarpelon, A.C., Fonseca, M.J., Faria, T.J., Baracat, M.M., Verri, W.A., Jr., Georgetti, S.R., Casagrande, R., 2013. Efficacy of topical formulations containing Pimenta pseudocaryophyllus extract against UVB-induced oxidative stress and inflammation in hairless mice. J. Photochem. Photobiol. B. 127, 153-160.

Casagrande R., Georgetti, S.R., Verri, W.A., Jr., Dorta, D.J., dos Santos, A.C., Fonseca, M.J., 2006a. Protective effect of topical formulations containing quercetin against UVB-induced oxidative stress in hairless mice. J. Photochem. Photobiol. B. 84, 21-27.

Casagrande R., Georgetti, S.R., Verri, W.A., Jr., Jabor, J.R., Santos, A.C., Fonseca, M.J., 2006b. Evaluation of functional stability of quercetin as a raw material and in different topical formulations by its antilipoperoxidative activity. AAPS PharmSciTech. 7, E10.

Cavia-Saiz M., Busto, M.D., Pilar-Izquierdo, M.C., Ortega, N., Perez-Mateos, M., Muniz, P., 2010. Antioxidant properties, radical scavenging activity and biomolecule protection capacity of flavonoid naringenin and its glycoside naringin: a comparative study. J. Sci. Food Agric. 90, 1238-1244.

Chiricozzi A., Guttman-Yassky, E., Suarez-Farinas, M., Nograles, K.E., Tian, S., Cardinale, I., Chimenti, S., Krueger, J.G., 2011. Integrative responses to IL-17 and TNF-alpha in human

keratinocytes account for key inflammatory pathogenic circuits in psoriasis. J. Invest. Dermatol. 131, 677-687.

Circu M.L., Aw, T.Y., 2010. Reactive oxygen species, cellular redox systems, and apoptosis. Free Radic. Biol. Med. 48, 749-762.

Dhanalakshmi S., Mallikarjuna, G.U., Singh, R.P., Agarwal, R., 2004. Silibinin prevents ultraviolet radiation-caused skin damages in SKH-1 hairless mice via a decrease in thymine dimer positive cells and an up-regulation of p53-p21/Cip1 in epidermis. Carcinogenesis. 25, 1459-1465.

El-Mahdy M.A., Zhu, Q., Wang, Q.E., Wani, G., Patnaik, S., Zhao, Q., Arafa el, S., Barakat, B., Mir, S.N., Wani, A.A., 2008. Naringenin protects HaCaT human keratinocytes against UVB-induced apoptosis and enhances the removal of cyclobutane pyrimidine dimers from the genome. Photochem. Photobiol. 84, 307-316.

Fischer T.W., Kleszczynski, K., Hardkop, L.H., Kruse, N., Zillikens, D., 2013. Melatonin enhances antioxidative enzyme gene expression (CAT, GPx, SOD), prevents their UVR-induced depletion, and protects against the formation of DNA damage (8-hydroxy-2'-deoxyguanosine) in ex vivo human skin. J. Pineal Res. 54, 303-312.

Fonseca Y.M., Catini, C.D., Vicentini, F.T., Cardoso, J.C., Cavalcanti De Albuquerque Junior, R.L., Vieira Fonseca, M.J., 2011. Efficacy of marigold extract-loaded formulations against UV-induced oxidative stress. J. Pharm. Sci. 100, 2182-2193.

Georgetti S.R., Casagrande, R., Moura-de-Carvalho Vicentini, F.T., Verri, W.A., Jr., Fonseca, M.J., 2006. Evaluation of the antioxidant activity of soybean extract by different in vitro methods and investigation of this activity after its incorporation in topical formulations. Eur. J. Pharm Biopharm. 64, 99-106.

Girotti A.W., 2001. Photosensitized oxidation of membrane lipids: reaction pathways, cytotoxic effects, and cytoprotective mechanisms. J. Photochem. Photobiol B. 63, 103-113.

Gonzalez Flecha B., Llesuy, S., Boveris, A., 1991. Hydroperoxide-initiated chemiluminescence: an assay for oxidative stress in biopsies of heart, liver, and muscle. Free Radic. Biol. Med. 10, 93-100.

Halliday G.M., 2005. Inflammation, gene mutation and photoimmunosuppression in response to UVR-induced oxidative damage contributes to photocarcinogenesis. Mutat. Res. 571, 107-120.

Halliwell B., Gutteridge, J.M., Aruoma, O.I., 1987. The deoxyribose method: a simple "test-tube" assay for determination of rate constants for reactions of hydroxyl radicals. Anal. Biochem. 165, 215-219.

Hasegawa T., Shimada, S., Ishida, H., Nakashima, M., 2013. Chafuroside B, an Oolong tea polyphenol, ameliorates UVB-induced DNA damage and generation of photo-immunosuppression related mediators in human keratinocytes. PLoS One. 8, e77308.

Hermenean A., Ardelean, A., Stan, M., Herman, H., Mihali, C.V., Costache, M., Dinischiotu, A., 2013. Protective effects of naringenin on carbon tetrachloride-induced acute nephrotoxicity in mouse kidney. Chem. Biol. Interact. 205, 138-147.

Hiramoto K., Kobayashi, H., Yamate, Y., Ishii, M., Sato, E.F., 2012. Intercellular pathway through hyaluronic acid in UVB-induced inflammation. Exp. Dermatol. 21, 911-914.

Ichihashi M., Ueda, M., Budiyanto, A., Bito, T., Oka, M., Fukunaga, M., Tsuru, K., Horikawa, T., 2003. UV-induced skin damage. Toxicology. 189, 21-39.

Ivan A.L., Campanini, M.Z., Martinez, R.M., Ferreira, V.S., Steffen, V.S., Vicentini, F.T., Vilela, F.M., Martins, F.S., Zarpelon, A.C., Cunha, T.M., Fonseca, M.J., Baracat, M.M., Georgetti, S.R., Verri, W.A., Jr., Casagrande, R., 2014. Pyrrolidine dithiocarbamate inhibits UVB-induced skin inflammation and oxidative stress in hairless mice and exhibits antioxidant activity in vitro. J. Photochem. Photobiol B. 138, 124-133.

Johnson M.K., Loo, G., 2000. Effects of epigallocatechin gallate and quercetin on oxidative damage to cellular DNA. Mutat. Res. 459, 211-218.

Khan M.B., Khan, M.M., Khan, A., Ahmed, M.E., Ishrat, T., Tabassum, R., Vaibhav, K., Ahmad, A., Islam, F., 2012. Naringenin ameliorates Alzheimer's disease (AD)-type neurodegeneration with cognitive impairment (AD-TNDCI) caused by the intracerebroventricular-streptozotocin in rat model. Neurochem. Int. 61, 1081-1093.

Kilpatrick L.E., Sun, S., Li, H., Vary, T.C., Korchak, H.M., 2010. Regulation of TNF-induced oxygen radical production in human neutrophils: role of delta-PKC. J. Leukoc. Biol. 87, 153-164.

Kim S.H., Jung, E.Y., Kang, D.H., Chang, U.J., Hong, Y.H., Suh, H.J., 2012. Physical stability, antioxidative properties, and photoprotective effects of a functionalized formulation containing black garlic extract. J. Photochem. Photobiol B. 117, 104-110.

Lee C.H., Jeong, T.S., Choi, Y.K., Hyun, B.H., Oh, G.T., Kim, E.H., Kim, J.R., Han, J.I., Bok, S.H., 2001. Anti-atherogenic effect of citrus flavonoids, naringin and naringenin, associated with hepatic ACAT and aortic VCAM-1 and MCP-1 in high cholesterol-fed rabbits. Biochem. Biophys. Res. Commun. 284, 681-688.

Lin W.W., Karin, M., 2007. A cytokine-mediated link between innate immunity, inflammation, and cancer. J. Clin. Invest. 117, 1175-1183.

Listopad J., Asadullah, K., Sievers, C., Ritter, T., Meisel, C., Sabat, R., Docke, W.D., 2007. Heme oxygenase-1 inhibits T cell-dependent skin inflammation and differentiation and function of antigen-presenting cells. Exp. Dermatol. 16, 661-670.

Manach C., Scalbert, A., Morand, C., Remesy, C., Jimenez, L., 2004. Polyphenols: food sources and bioavailability. Am. J. Clin. Nutr. 79, 727-747.

Martinez, R.M., Zarpelon, A.C., Zimermann, V.V.M., Georgetti, S.R., Baracat, M.M. , Fonseca, M.J.V., Vicentini, F.T.M.C., Moreira, I.C., Andrei, C.C., Verri Jr, W.A., Casagrande, R., 2012. *Tephrosia sinapou* extract reduces inflammatory leukocyte recruitment in mice: effect on oxidative stress, nitric oxide and cytokine production, Braz. J. Pharmacog. 22, 587-597.

Meister A., 1988. Glutathione metabolism and its selective modification. J. Biol. Chem. 263, 17205-17208.

Mershiba S.D., Dassprakash, M.V., Saraswathy, S.D., 2013. Protective effect of naringenin on hepatic and renal dysfunction and oxidative stress in arsenic intoxicated rats. Mol. Biol. Rep. 40, 3681-3691.

Moore R.J., Owens, D.M., Stamp, G., Arnott, C., Burke, F., East, N., Holdsworth, H., Turner, L., Rollins, B., Pasparakis, M., Kollias, G., Balkwill, F., 1999. Mice deficient in tumor necrosis factor-alpha are resistant to skin carcinogenesis. Nat. Med. 5, 828-831.

Nichols J.A., Katiyar, S.K., 2010. Skin photoprotection by natural polyphenols: anti-inflammatory, antioxidant and DNA repair mechanisms. Arch. Dermatol. Res. 302, 71-83.

Okayama Y., 2005. Oxidative stress in allergic and inflammatory skin diseases. Curr. Drug Targets Inflamm. Allergy. 4, 517-519.

Pari L., Gnanasoundari, M., 2006. Influence of naringenin on oxytetracycline mediated oxidative damage in rat liver. Basic Clin. Pharmacol. Toxicol. 98, 456-461.

Piskin G., Bos, J.D., Teunissen, M.B., 2005. Neutrophils infiltrating ultraviolet B-irradiated normal human skin display high IL-10 expression. Arch. Dermatol. Res. 296, 339-342.

Reeve V.E., Allanson, M., Arun, S.J., Domanski, D., Painter, N., 2010. Mice drinking goji berry juice (Lycium barbarum) are protected from UV radiation-induced skin damage via antioxidant pathways. Photochem. Photobiol. Sci. 9, 601-607.

Renugadevi J., Prabu, S.M., 2009. Naringenin protects against cadmium-induced oxidative renal dysfunction in rats. Toxicology. 256, 128-134.

Renugadevi J., Prabu, S.M., 2010. Cadmium-induced hepatotoxicity in rats and the protective effect of naringenin. Exp. Toxicol. Pathol. 62, 171-181.

Saw C.L., Huang, M.T., Liu, Y., Khor, T.O., Conney, A.H., Kong, A.N., 2011. Impact of Nrf2 on UVB-induced skin inflammation/photoprotection and photoprotective effect of sulforaphane. Mol. Carcinog. 50, 479-486.

Saw C.L., Yang, A.Y., Huang, M.T., Liu, Y., Lee, J.H., Khor, T.O., Su, Z.Y., Shu, L., Lu, Y., Conney, A.H., Kong, A.N., 2014. Nrf2 null enhances UVB-induced skin inflammation and extracellular matrix damages. Cell Biosci. 4, 39.

Strickland I., Rhodes, L.E., Flanagan, B.F., Friedmann, P.S., 1997. TNF-alpha and IL-8 are upregulated in the epidermis of normal human skin after UVB exposure: correlation with neutrophil accumulation and E-selectin expression. J. Invest. Dermatol. 108, 763-768.

Subburaman S., Ganesan, K., Ramachandran, M., 2014. Protective role of naringenin against Doxorubicin-induced cardiotoxicity in a rat model: histopathology and mRNA expression profile studies. J. Environ. Pathol. Toxicol. Oncol. 33, 363-376.

Sullivan N.J., Tober, K.L., Burns, E.M., Schick, J.S., Riggenbach, J.A., Mace, T.A., Bill, M.A., Young, G.S., Oberyszyn, T.M., Lesinski, G.B., 2012. UV light B-mediated inhibition of skin catalase activity promotes Gr-1+ CD11b+ myeloid cell expansion. J. Invest. Dermatol. 132, 695-702.

Takeya R., Sumimoto, H., 2003. Molecular mechanism for activation of superoxide-producing NADPH oxidases. Mol. Cells. 16, 271-277.

Turkkan B., Ozyurek, M., Bener, M., Guclu, K., Apak, R., 2012. Synthesis, characterization and antioxidant capacity of naringenin-oxime. Spectrochim. Acta A. Mol. Biomol. Spectrosc. 85, 235-240.

Verri, W.A., Cunha, T.M., Parada, C.A., Poole, S., Cunha, F.Q., Ferreira, SH, 2006. Hypernociceptive role of cytokines and chemokines: targets for analgesic drug development? Pharmacol. Ther. 112, 116-138.

Verri, W.A., Vicentini, F.T.M.C., Baracat, M.M., Georgetti, S.R., Cardoso, R.D.R., Cunha, T.M., Fonseca, M.J.V. , Casagrande R, 2012. Flavonoids as anti-inflammatory and analgesic drugs: Mechanisms of action and perspectives in the development of pharmaceutical forms, in: Atta-ur-Rahman. (Eds.), Studies in Natural Products Chemistry. Elsevier, Amsterdam, pp. 297-322.

Vicentini F.T., He, T., Shao, Y., Fonseca, M.J., Verri, W.A., Jr., Fisher, G.J., Xu, Y., 2011. Quercetin inhibits UV irradiation-induced inflammatory cytokine production in primary human keratinocytes by suppressing NF-kappaB pathway. J. Dermatol. Sci. 61, 162-168.

Yen F.L., Wu, T.H., Lin, L.T., Cham, T.M., Lin, C.C., 2009. Naringenin-loaded nanoparticles improve the physicochemical properties and the hepatoprotective effects of naringenin in orally-administered rats with CCl(4)-induced acute liver failure. Pharm. Res. 26, 893-902.

Yilma A.N., Singh, S.R., Morici, L., Dennis, V.A., 2013. Flavonoid naringenin: a potential immunomodulator for Chlamydia trachomatis inflammation. Mediators Inflamm. 2013, 102457.

Yu J., Wang, L., Walzem, R.L., Miller, E.G., Pike, L.M., Patil, B.S., 2005. Antioxidant activity of citrus limonoids, flavonoids, and coumarins. J. Agric. Food Chem. 53, 2009-2014.

Zhang S., Song, C., Zhou, J., Xie, L., Meng, X., Liu, P., Cao, J., Zhang, X., Ding, W.Q., Wu, J., 2012. Amelioration of radiation-induced skin injury by adenovirus-mediated heme oxygenase-1 (HO-1) overexpression in rats. Radiat. Oncol. 7, 4.

Figures

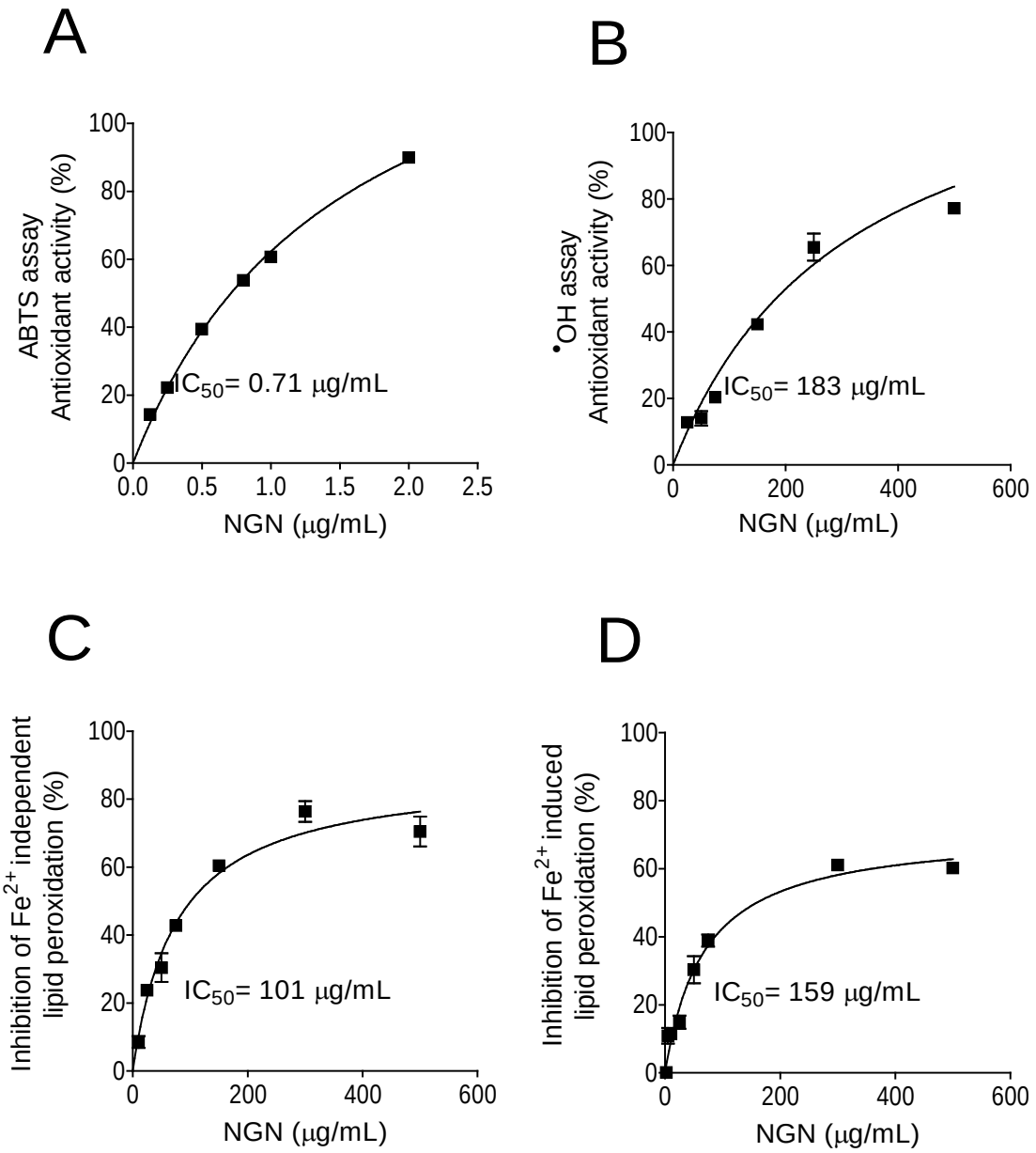

Fig. 1. *In vitro* antioxidant activity of NGN. NGN was added at indicated concentration and assayed for scavenging the radical ABTS (Panel A), HO• (Panel B), iron-independent lipid peroxidation (Panel C) and iron-induced lipid peroxidation (Panel D). Data are presented as percentage of inhibition relative to control. Results represent means ± SEM of triplicate values representative of two separate experiments.

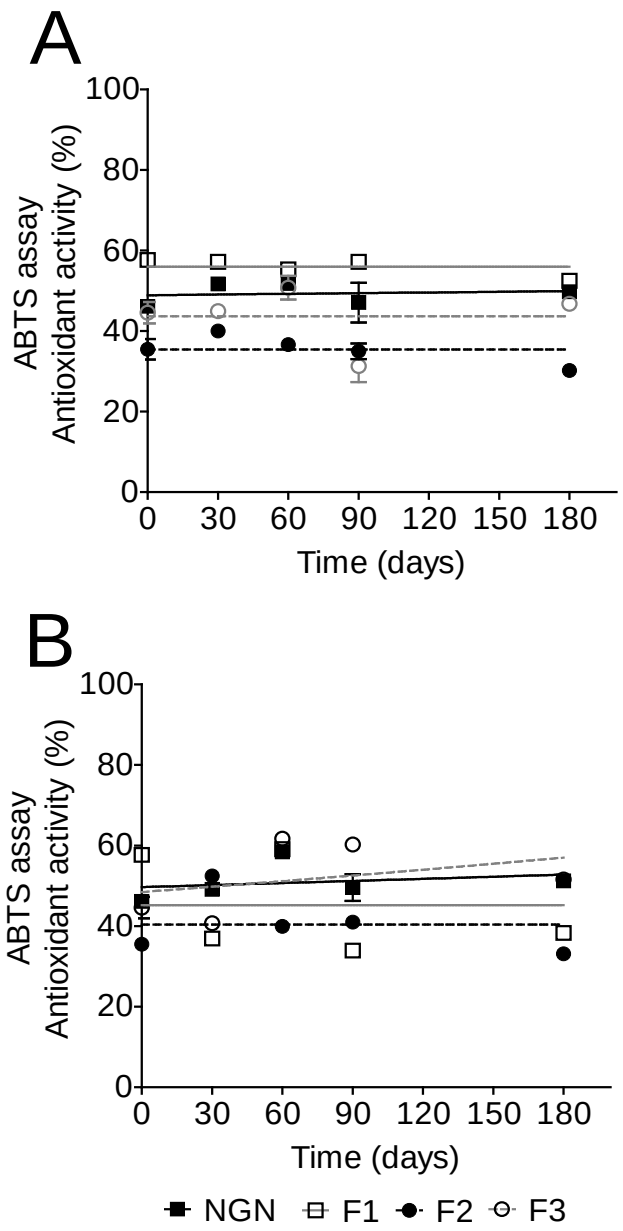

Fig. 2. Stability of ABTS radical scavenging ability of naringenin (NGN), F1, F2, and F3 containing NGN stored at 4°C (A) and 40°C (B) /75% RH for 6 months. Results are represented by mean ± SEM.

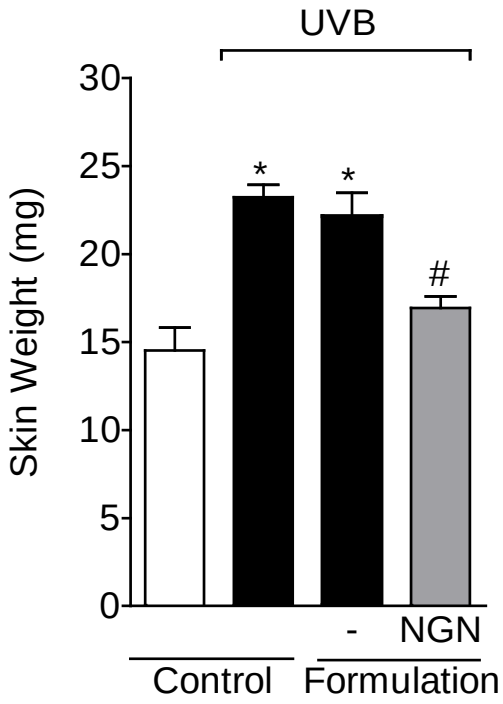

Fig. 3. Formulation containing naringenin (NGN) reduces skin edema induced by UVB irradiation. Samples of dorsal skin were collected 12 h after the end of irradiation and used to measure the edema. Bars represent means ± SEM of 5 mice per group per experiment and are representative of two separated experiments. *p<0.05 compared to the non-irradiated control group (white bar); #p<0.05 compared to the irradiated control groups (black bars).

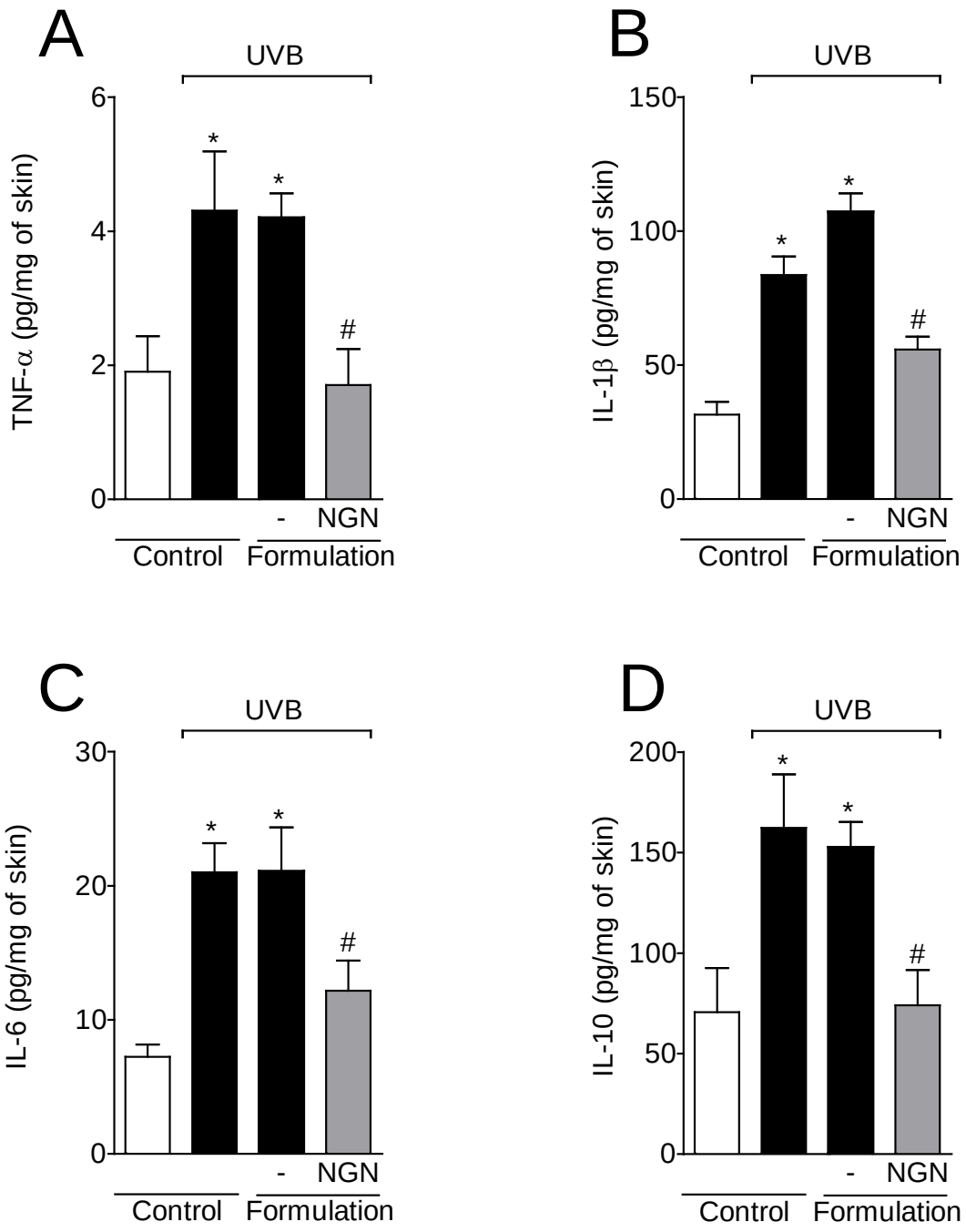

Fig. 4. Formulation containing naringenin (NGN) inhibits UVB irradiation-induced cytokine production. The levels of TNF-α (A), IL-1β (B), IL-6 (C) and IL-10 (D) were determined in samples collected 4 h after the end of irradiation. Bars represent means ± SEM of 5 mice per group per experiment and are representative of two separated experiments. *p<0.05 compared to the non-irradiated control group (white bar); #p<0.05 compared to the irradiated control groups (black bars).

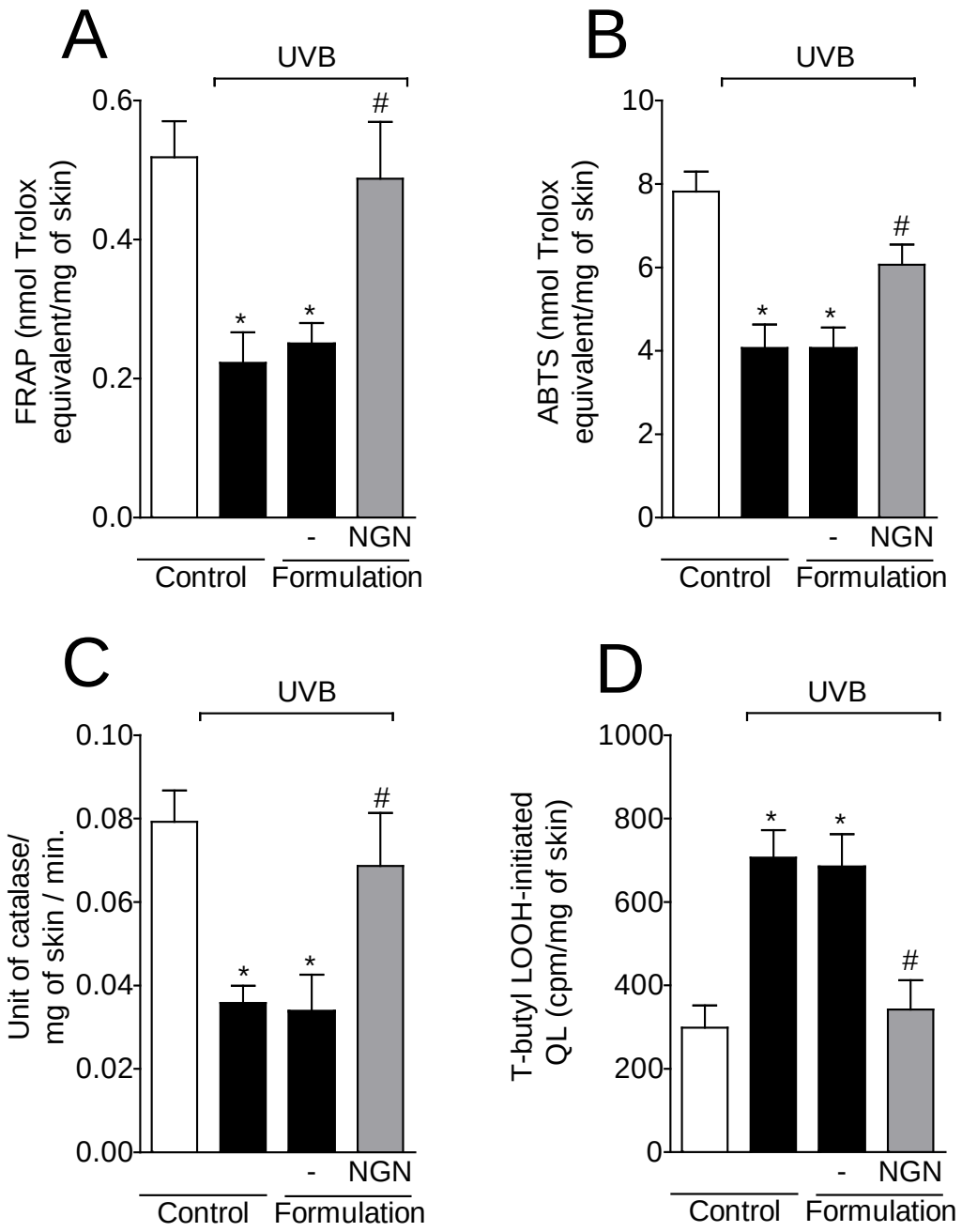

Fig. 5. Effect of formulation containing naringenin (NGN) on antioxidant capacity and lipid peroxidation of skin after UVB irradiation. The antioxidant capacity was measured using FRAP (A) and ABTS (B) assays in samples collected 12 h after the end of irradiation. (C) Catalase activity was determined in samples collected 2 h after the end of irradiation. (D) Lipid peroxidation was measured by tert-butyl hydroperoxide-initiated chemiluminescence assay in samples collected 4 h after the end of irradiation. Bars represent means ± SEM of 5 mice per group per experiment and are representative of two separated experiments. *p<0.05 compared to the non-irradiated control group (white bar); #p<0.05 compared to the irradiated control groups (black bars).

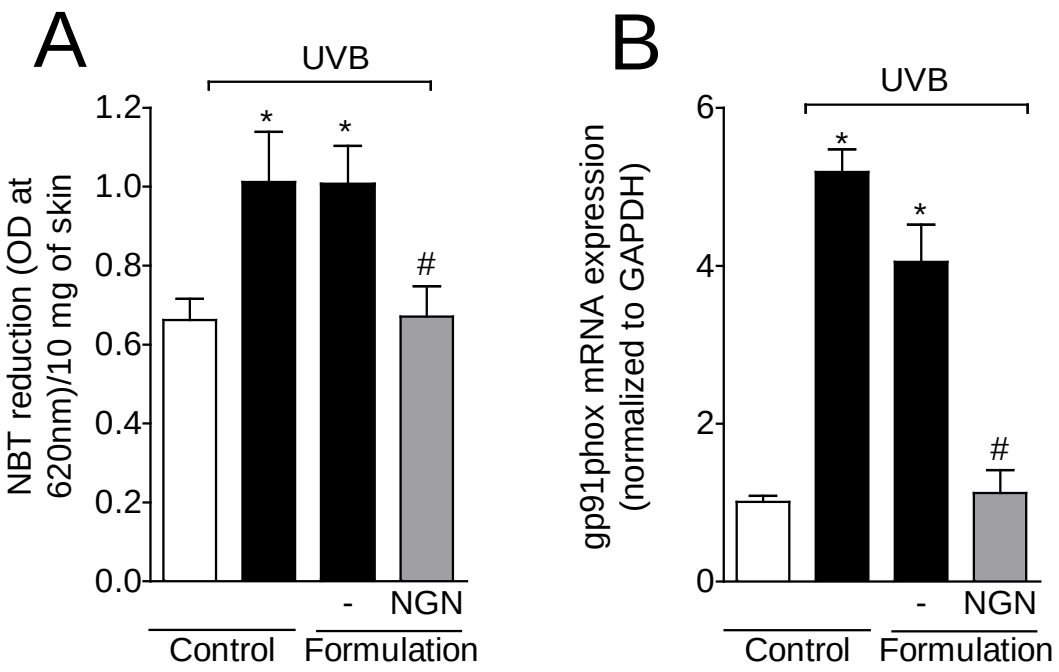

Fig. 6. Formulation containing naringenin (NGN) inhibits superoxide anion generation and gp91phox expression induced by UVB irradiation. (A) Superoxide anion production was measured by nitroblue tetrazolium (NBT) reduction assay in samples collected 2 h after the end of irradiation. (B) Expression of NADPH oxidase sub-unit Gp91phox in the skin was measured 4 h after the end of irradiation by quantitative PCR. Bars represent means ± SEM of 5 mice per group per experiment and are representative of two separated experiments. **p*<0.05 compared to the non-irradiated control group (white bar); #*p*<0.05 compared to the irradiated control groups (black bars).

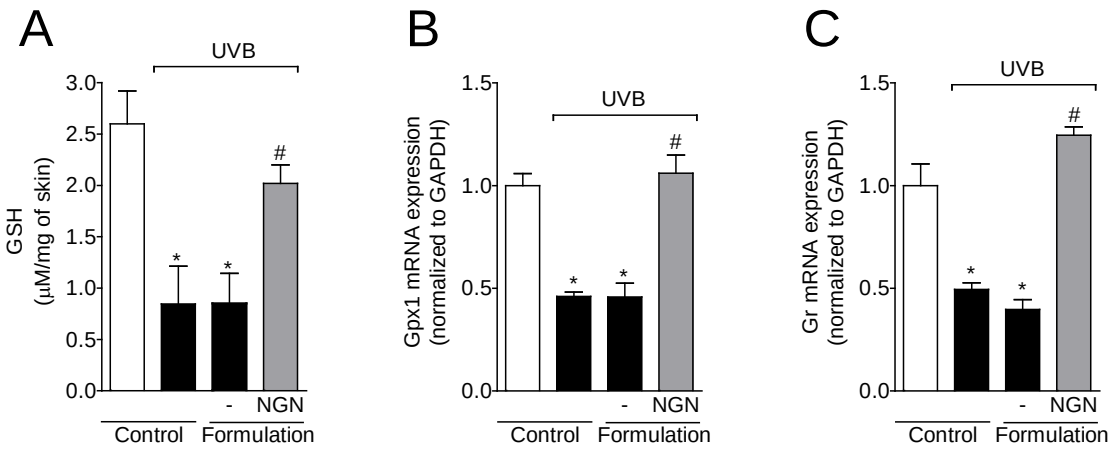

Fig. 7. Formulation containing naringenin (NGN) inhibits UVB irradiation-induced down-regulation of glutathione system components. (A) Reduced glutathione (GSH) levels were measured in samples collected 12 h after the end of irradiation. Expression of (B) glutathione peroxidase 1 (Gpx1) and (C) glutathione reductase (Gr) in the skin was measured 4 h after the end of irradiation by qPCR. Bars represent means ± SEM of 5 mice per group per experiment and are representative of two separated experiments. *p<0.05 compared to the non-irradiated control group (white bar); #p<0.05 compared to the irradiated control groups (black bars).

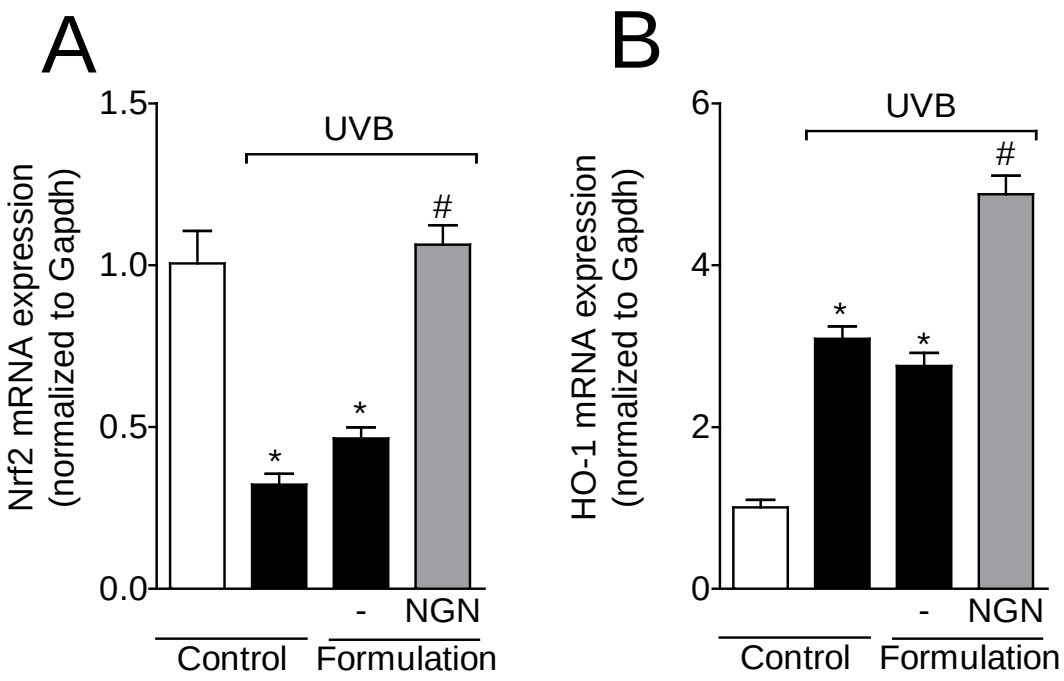

Fig. 8. Formulation containing naringenin (NGN) inhibits UVB irradiation-induced Nrf2 down-regulation and improves HO-1 expression in the skin. Expression of (A) Nrf2 and (B) heme oxygenase-1 (HO-1) in the skin was measured 4 h after the end of irradiation by qPCR. Bars represent means ± SEM of 5 mice per group per experiment and are representative of two separated experiments. *p<0.05 compared to the non-irradiated control group (white bar); #p<0.05 compared to the irradiated control groups (black bars).

Tables

Table 1. Percent composition (weight/weight) of formulation F1, F2 and F3

Components	F1	F2	F3
Polawax®[a]	10	_	_
Hostacerin SAF®[b]	_	5	_
Net FS®[c]	_	_	2
Caprylic/capric triglyceride	5	5	5
Carbopol® 940 (1%)[d] (qsp)*	_	_	100
Triethanolamine	_	_	0.5
Propylene glycol	6	6	6
Phenonip	0.4	0.4	0.4
Deionized water (qsp)*	100	100	_

*quantity sufficient for preparation
[a] Self-emulsifing wax (Cetostearyl alcohol and polyoxyethylene derived of a fatty acid ester of sorbitan 20 0E);
[b] Self-emulsifying was prepared without heating (Ammonium acryloyldimethyl-taurate/VP copolymer and rapeseed oil sorbitol esters and trilaureth-4 phosphate and mineral oil and isopropyl palmitate);
[c] Self-emulsifying was prepared without heating (Polyglyceryl-10 Myristate and Triethylhexanoin and Glycerin and Water);
[d] Carboxypolymethylene.

Table 2. Primer sequences.

Gene	Sense primer	Antisense primer
gp91phox	AGCTATGAGGTGGTGATGTTAGTGG	CACAATATTTGTACCAGACAGACTTGAG
Gpx1	CCAACACCCAGTGACGACC	CTCAAAGTTCCAGGCAATGTC
Gr	TGCGTGA ATGTTGGATGTGTACCC	CCGGCATTCTCCAGTTCCT CG
Nrf2	TCACACGAGATGAGCTTAGGGCAA	TACAGTTCTGGGCGGCGACTTTAT
HO-1	CCCAAAACTGGCCTGTAAAA	CGTGGTCAGTCAACATGGAT
Gapdh	CATACCAGGAAATGAGCTTG	ATGACATCAAGAAGGTGGTG

5. CONCLUSÕES

Os resultados dos ensaios *in vitro* demonstraram que a TC não atua como um antioxidante, o que pode ser atribuído a ausência na sua estrutura química de substituintes OH nos carbonos.

A HMC e a NGN *in vitro* demonstraram poder antioxidante em reduzir o ferro e o radical ABTS, capacidade de neutralizar o radical hidroxil e de inibir a LPO independente de ferro. A NGN apresentou maior atividade antioxidante em todas as metodologias utilizadas e inibiu também a LPO dependente de ferro, o que pode ser resultado do maior número de substituintes OH livres nos seus anéis aromáticos em comparação a HMC.

Nenhum dos flavonóides testados apresentou capacidade doadora de átomos de hidrogênio ao radical $DPPH^{\bullet}$ e atividade queladora do íon ferro, o que pode ser atribuído à ausência na estrutura química do grupo catecol no anel B e de substituinte OH no carbono 3'.

Os resultados *in vivo* demonstraram que os tratamentos sistêmicos com TC, HMC e NGN protegeram a pele dos danos oxidativos e inflamatórios induzidos pela radiação UVB. Os efeitos antioxidantes destes três flavonóides foram relacionados com a redução da expressão de RNAm para gp91 phox (subunidade da NADPH oxidase) e produção de ânion superóxido, o que resultou em uma melhora da capacidade antioxidante da pele pela manutenção dos níveis de GSH e atividade da catalase, e redução de processos deletérios como LPO e inflamação induzidos pela radiação UVB. Neste sentido, a TC, a HMC e a NGN também reduziram o edema cutâneo, o recrutamento de neutrófilos e a atividade da MMP-9 por reduzir a produção de diferentes citocinas induzidas pela radiação UVB.

Os efeitos anti-inflamatórios da TC podem ter resultado em menor estresse oxidativo *in vivo*, mas não necessariamente por um efeito antioxidante direto, uma vez que a TC não atuou como um antioxidante *in vitro*. Estes resultados sugerem que os flavonóides com atividade anti-inflamatória *in vivo*, não necessariamente apresentam atividade antioxidante *in vitro*, ou seja, qrupamentos antioxidantes nos flavonóides não são preditivos de efeito anti-inflamatório *in vivo*.

É importante mencionar que, as doses da NGN necessárias para controlar os danos cutâneos induzidos pela radiação UVB foram menores em comparação as doses da TC e da HMC, provavelmente este efeito está relacionado à sua estrutura química.

De três formulações tópicas preparadas contendo NGN, a mais estável no estudo de estabilidade físico-química e funcional foi a composta pela base auto-emulsionante Net FS®. A mesma protegeu a pele dos danos oxidativos e inflamatórios induzidos pela radiação UVB, por manter a expressão de RNAm de componentes antioxidantes celulares (glutationa peroxidase-1, glutationa redutase e Nrf2), por reduzir a expressão de RNAm da

hemeoxigenase-1 e por inibir a expressão de RNAm para gp91phox. Estes efeitos resultaram em uma melhora da capacidade antioxidante da pele, pela manutenção do poder redutor de ferro, da capacidade em reduzir o radical ABTS, dos níveis de GSH e atividade da catalase, e redução da produção de ânion superóxido. A formulação contendo NGN também reduziu o edema cutâneo, produção de hidroperóxidos lipídicos e citocinas (TNF-α, IL-1β, IL-6 e IL-10).

Em suma, mecanisticamente os efeitos da TC, da HMC e da NGN mostraram-se independentes da quelação de ferro e dependentes da inibição de oxidase (NADPH oxidase) e da redução da produção de diferentes citocinas, e consequentemente dependentes da redução do estresse oxidativo pela manutenção de componentes antioxidantes celulares. Os efeitos da HMC e da NGN mostraram-se também dependentes da neutralização direta de EROs, e ainda, os efeitos da NGN podem ser relacionados ao aumento da expressão do RNAm para Nrf2. Por sua vez o Nrf2 regula a expressão de várias moléculas antioxidantes e anti-inflamatórias.

Portanto, os resultados obtidos nesta pesquisa sugerem o uso da TC, da HMC e da NGN como abordagens terapêuticas promissoras para controlar os danos cutâneos inflamatórios e oxidativos causados pela exposição à radiação UVB, que merecem maiores investigações. Além disso, a formulação tópica contendo NGN pode ser utilizada como um produto potencial para controlar doenças cutâneas relacionadas com a exposição à radiação UVB.

6. REFERÊNCIAS

AEBI, H. Catalase in vitro. **Methods Enzymol**, v. 105, n. 121-126, 1984.

AFAQ, F. Natural agents: cellular and molecular mechanisms of photoprotection. **Arch Biochem Biophys**, v. 508, n. 2, p. 144-151, 2011.

AFAQ, F., & KATIYAR, S. K. Polyphenols: skin photoprotection and inhibition of photocarcinogenesis. **Mini Rev Med Chem**, v. 11, n. 14, p. 1200-1215, 2011.

AFAQ, F., ADHAMI, V. M., & MUKHTAR, H. Photochemoprevention of ultraviolet B signaling and photocarcinogenesis. **Mutat Res**, v. 571, n. 1-2, p. 153-173, 2005a.

AFAQ, F., SALEEM, M., KRUEGER, C. G., REED, J. D., & MUKHTAR, H. Anthocyanin- and hydrolyzable tannin-rich pomegranate fruit extract modulates MAPK and NF-kappaB pathways and inhibits skin tumorigenesis in CD-1 mice. **Int J Cancer**, v. 113, n. 3, p. 423-433, 2005b.

AGUILAR PERALTA, G. R., AREVALO GARDOQUI, J., LLAMAS MACIAS, F. J., NAVARRO CEJA, V. H., MENDOZA CISNEROS, S. A., & MARTINEZ MACIAS, C. G. Clinical and capillaroscopic evaluation in the treatment of chronic venous insufficiency with Ruscus aculeatus, hesperidin methylchalcone and ascorbic acid in venous insufficiency treatment of ambulatory patients. **Int Angiol**, v. 26, n. 4, p. 378-384, 2007.

AHSAN, H., AZIZ, M. H., & AHMAD, N. Ultraviolet B exposure activates Stat3 signaling via phosphorylation at tyrosine705 in skin of SKH1 hairless mouse: a target for the management of skin cancer? **Biochem Biophys Res Commun**, v. 333, n. 1, p. 241-246, 2005.

AL-REJAIE, S. S., ABUOHASHISH, H. M., AL-ENAZI, M. M., AL-ASSAF, A. H., PARMAR, M. Y., & AHMED, M. M. Protective effect of naringenin on acetic acid-induced ulcerative colitis in rats. **World J Gastroenterol**, v. 19, n. 34, p. 5633-5644, 2013.

ALLAERT, F. A., HUGUE, C., CAZAUBON, M., RENAUDIN, J. M., CLAVEL, T., & ESCOURROU, P. Correlation between improvement in functional signs and plethysmographic parameters during venoactive treatment (Cyclo 3 Fort). **Int Angiol**, v. 30, n. 3, p. 272-277, 2011.

ANRATHER, J., RACCHUMI, G., & IADECOLA, C. NF-kappaB regulates phagocytic NADPH oxidase by inducing the expression of gp91phox. **J Biol Chem**, v. 281, n. 9, p. 5657-5667, 2006.

ANTO, R. J., SUKUMARAN, K., KUTTAN, G., RAO, M. N., SUBBARAJU, V., & KUTTAN, R. Anticancer and antioxidant activity of synthetic chalcones and related compounds. **Cancer Lett**, v. 97, n. 1, p. 33-37, 1995.

AZUMA, T., SHIGESHIRO, M., KODAMA, M., TANABE, S., & SUZUKI, T. Supplemental naringenin prevents intestinal barrier defects and inflammation in colitic mice. **J Nutr**, v. 143, n. 6, p. 827-834, 2013.

BAI, X., ZHANG, X., CHEN, L., ZHANG, J., ZHANG, L., ZHAO, X., ZHAO, T., ZHAO, Y. Protective effect of naringenin in experimental ischemic stroke: down-regulated

NOD2, RIP2, NF-kappaB, MMP-9 and up-regulated claudin-5 expression. **Neurochem Res**, v. 39, n. 8, p. 1405-1415, 2014.

BALOGH, T. S., VELASCO, M. V., PEDRIALI, C. A., KANEKO, T. M., & BABY, A. R. Ultraviolet radiation protection: current available resources in photoprotection. **An Bras Dermatol**, v. 86, n. 4, p. 732-742, 2011.

BARCELOS, G. R., GROTTO, D., SERPELONI, J. M., ANGELI, J. P., ROCHA, B. A., DE OLIVEIRA SOUZA, V. C., VICENTINI, J. T., EMANUELLI, T., BASTOS, J. K., ANTUNES, L. M., KNASMULLER, S., BARBOSA, F., JR. Protective properties of quercetin against DNA damage and oxidative stress induced by methylmercury in rats. **Arch Toxicol**, v. 85, n. 9, p. 1151-1157, 2011.

BARRY, B., W. Dermatological Formulations: **Percutaneos absorption**. New York: Marcel Dekker, 1983.

BELTRAMINO, R., PENENORY, A., & BUCETA, A. M. An open-label, randomised multicentre study comparing the efficacy and safety of CYCLO 3 FORT versus hydroxyethyl rutoside in chronic venous lymphatic insufficiency. **Int Angiol**, v. 18, n. 4, p. 337-342, 1999.

BELTRAMINO, R., PENENORY, A., & BUCETA, A. M. An open-label, randomized multicenter study comparing the efficacy and safety of Cyclo 3 Fort versus hydroxyethyl rutoside in chronic venous lymphatic insufficiency. **Angiology**, v. 51, n. 7, p. 535-544, 2000.

BENZIE, I. F., & STRAIN, J. J. The ferric reducing ability of plasma (FRAP) as a measure of "antioxidant power": the FRAP assay. **Anal Biochem**, v. 239, n. 1, p. 70-76, 1996.

BHATIA, N., DEMMER, T. A., SHARMA, A. K., ELCHEVA, I., & SPIEGELMAN, V. S. Role of beta-TrCP ubiquitin ligase receptor in UVB mediated responses in skin. **Arch Biochem Biophys**, v. 508, n. 2, p. 178-184, 2011.

BOHM, H., BOEING, H., HEMPEL, J., RAAB, B., & KROKE, A. [Flavonols, flavone and anthocyanins as natural antioxidants of food and their possible role in the prevention of chronic diseases]. **Z Ernahrungswiss**, v. 37, n. 2, p. 147-163, 1998.

BOLANN, B. J., & ULVIK, R. J. Release of iron from ferritin by xanthine oxidase. Role of the superoxide radical. **Biochem J**, v. 243, n. 1, p. 55-59, 1987.

BORS, W., HELLER, W., MICHEL, C., & SARAN, M. Flavonoids as antioxidants: determination of radical-scavenging efficiencies. **Methods Enzymol**, v. 186, n. 343-355, 1990.

BOUAZIZ, N., MICHIELS, C., JANSSENS, D., BERNA, N., ELIAERS, F., PANCONI, E., & REMACLE, J. Effect of Ruscus extract and hesperidin methylchalcone on hypoxia-induced activation of endothelial cells. **Int Angiol**, v. 18, n. 4, p. 306-312, 1999.

BOUSKELA, E., CYRINO, F. Z., & MARCELON, G. Inhibitory effect of the Ruscus extract and of the flavonoid hesperidine methylchalcone on increased microvascular permeability induced by various agents in the hamster cheek pouch. **J Cardiovasc Pharmacol**, v. 22, n. 2, p. 225-230, 1993.

BOWIE, A., & O'NEILL, L. A. Oxidative stress and nuclear factor-kappaB activation: a reassessment of the evidence in the light of recent discoveries. **Biochem Pharmacol**, v. 59, n. 1, p. 13-23, 2000.

BOYLE, P., DIEHM, C., & ROBERTSON, C. Meta-analysis of clinical trials of Cyclo 3 Fort in the treatment of chronic venous insufficiency. **Int Angiol**, v. 22, n. 3, p. 250-262, 2003.

BRADLEY, P. P., PRIEBAT, D. A., CHRISTENSEN, R. D., & ROTHSTEIN, G. Measurement of cutaneous inflammation: estimation of neutrophil content with an enzyme marker. **J Invest Dermatol**, v. 78, n. 3, p. 206-209, 1982.

BRASIL. Resolução n° 1, de 29 de julho de 2005. Guia para a Realização de Estudos de Estabilidade. Diário Oficial, Brasília, DF, 01 maio 2005.

BUEGE, J. A., & AUST, S. D. Microsomal lipid peroxidation. **Methods Enzymol**, v. 52, n. 302-310, 1978.

BURDA, S., & OLESZEK, W. Antioxidant and antiradical activities of flavonoids. **J Agric Food Chem**, v. 49, n. 6, p. 2774-2779, 2001.

CAMPANINI, M. Z., CUSTODIO, D. L., IVAN, A. L., MARTINS, S. M., PARANZINI, M. J., MARTINEZ, R. M., VERRI, W. A., JR., VICENTINI, F. T., ARAKAWA, N. S., DE, J. F. T., BARACAT, M. M., CASAGRANDE, R., GEORGETTI, S. R. Topical formulations containing Pimenta pseudocaryophyllus extract: In vitro antioxidant activity and in vivo efficacy against UV-B-induced oxidative stress. **AAPS PharmSciTech**, v. 15, n. 1, p. 86-95, 2014.

CAIN, K., SKILLETER, D. N. in: K. SNELL, B. MULLOCKV (Eds.), Biochemical Toxicology, IRL Press, Oxford, 1987, pp. 217-254.

CAMPANINI, M. Z., PINHO-RIBEIRO, F. A., IVAN, A. L., FERREIRA, V. S., VILELA, F. M., VICENTINI, F. T., MARTINEZ, R. M., ZARPELON, A. C., FONSECA, M. J., FARIA, T. J., BARACAT, M. M., VERRI, W. A., JR., GEORGETTI, S. R., CASAGRANDE, R. Efficacy of topical formulations containing Pimenta pseudocaryophyllus extract against UVB-induced oxidative stress and inflammation in hairless mice. **J Photochem Photobiol B**, v. 127, n. 153-160, 2013.

CARINI, M., ALDINI, G., PICCONE, M., & FACINO, R. M. Fluorescent probes as markers of oxidative stress in keratinocyte cell lines following UVB exposure. **Farmaco**, v. 55, n. 8, p. 526-534, 2000.

CASAGRANDE, R., GEORGETTI, S. R., VERRI, W. A., JR., BORIN, M. F., LOPEZ, R. F., & FONSECA, M. J. In vitro evaluation of quercetin cutaneous absorption from topical formulations and its functional stability by antioxidant activity. **Int J Pharm**, v. 328, n. 2, p. 183-190, 2007.

CASAGRANDE, R., GEORGETTI, S. R., VERRI, W. A., JR., DORTA, D. J., DOS SANTOS, A. C., & FONSECA, M. J. Protective effect of topical formulations containing quercetin against UVB-induced oxidative stress in hairless mice. **J Photochem Photobiol B**, v. 84, n. 1, p. 21-27, 2006a.

CASAGRANDE, R., GEORGETTI, S. R., VERRI, W. A., JR., JABOR, J. R., SANTOS, A. C., & FONSECA, M. J. Evaluation of functional stability of quercetin as a raw material

and in different topical formulations by its antilipoperoxidative activity. **AAPS PharmSciTech**, v. 7, n. 1, p. E10, 2006b.

CAVIA-SAIZ, M., BUSTO, M. D., PILAR-IZQUIERDO, M. C., ORTEGA, N., PEREZ-MATEOS, M., & MUNIZ, P. Antioxidant properties, radical scavenging activity and biomolecule protection capacity of flavonoid naringenin and its glycoside naringin: a comparative study. **J Sci Food Agric**, v. 90, n. 7, p. 1238-1244, 2010.

CAZAROLLI, L. H., ZANATTA, L., ALBERTON, E. H., FIGUEIREDO, M. S., FOLADOR, P., DAMAZIO, R. G., PIZZOLATTI, M. G., SILVA, F. R. Flavonoids: prospective drug candidates. **Mini Rev Med Chem**, v. 8, n. 13, p. 1429-1440, 2008.

CHELIKANI, P., FITA, I., & LOEWEN, P. C. Diversity of structures and properties among catalases. **Cell Mol Life Sci**, v. 61, n. 2, p. 192-208, 2004.

CHOI, J. Y., CHOI, D. I., LEE, J. B., YUN, S. J., LEE, D. H., EUN, J. B., & LEE, S. C. Ethanol extract of peanut sprout induces Nrf2 activation and expression of antioxidant and detoxifying enzymes in human dermal fibroblasts: implication for its protection against UVB-irradiated oxidative stress. **Photochem Photobiol**, v. 89, n. 2, p. 453-460, 2013.

CHOI, K. S., KUNDU, J. K., CHUN, K. S., NA, H. K., & SURH, Y. J. Rutin inhibits UVB radiation-induced expression of COX-2 and iNOS in hairless mouse skin: p38 MAP kinase and JNK as potential targets. **Arch Biochem Biophys**, v. 559, n. 38-45, 2014.

CHOU, Y. C., SHEU, J. R., CHUNG, C. L., CHEN, C. Y., LIN, F. L., HSU, M. J., KUO, Y. H., HSIAO, G. Nuclear-targeted inhibition of NF-kappaB on MMP-9 production by N-2-(4-bromophenyl) ethyl caffeamide in human monocytic cells. **Chem Biol Interact**, v. 184, n. 3, p. 403-412, 2010.

CHUN, K. S., KUNDU, J., KUNDU, J. K., & SURH, Y. J. Targeting Nrf2-Keap1 signaling for chemoprevention of skin carcinogenesis with bioactive phytochemicals. **Toxicol Lett**, v. 229, n. 1, p. 73-84, 2014.

CIRCU, M. L., & AW, T. Y. Reactive oxygen species, cellular redox systems, and apoptosis. **Free Radic Biol Med**, v. 48, n. 6, p. 749-762, 2010.

CLUZAN, R. V., ALLIOT, F., GHABBOUN, S., & PASCOT, M. Treatment of secondary lymphedema of the upper limb with CYCLO 3 FORT. **Lymphology**, v. 29, n. 1, p. 29-35, 1996.

COOPER, S., RANGER-MOORE, J., & BOWDEN, T. G. Differential inhibition of UVB-induced AP-1 and NF-kappaB transactivation by components of the jun bZIP domain. **Mol Carcinog**, v. 43, n. 2, p. 108-116, 2005.

COSMI, L., MAGGI, L., SANTARLASCI, V., LIOTTA, F., & ANNUNZIATO, F. T helper cells plasticity in inflammation. **Cytometry A**, v. 85, n. 1, p. 36-42, 2014.

DEBENEDICTIS, C., JOUBEH, S., ZHANG, G., BARRIA, M., & GHOHESTANI, R. F. Immune functions of the skin. **Clin Dermatol**, v. 19, n. 5, p. 573-585, 2001.

DHANALAKSHMI, S., MALLIKARJUNA, G. U., SINGH, R. P., & AGARWAL, R. Silibinin prevents ultraviolet radiation-caused skin damages in SKH-1 hairless mice via a decrease in thymine dimer positive cells and an up-regulation of p53-p21/Cip1 in epidermis. **Carcinogenesis**, v. 25, n. 8, p. 1459-1465, 2004.

DOU, W., ZHANG, J., SUN, A., ZHANG, E., DING, L., MUKHERJEE, S., WEI, X., CHOU, G., WANG, Z. T., MANI, S. Protective effect of naringenin against experimental colitis via suppression of Toll-like receptor 4/NF-kappaB signalling. **Br J Nutr***,* v. 110, n. 4, p. 599-608, 2013.

DURÁN-ANIOTZ C., SEGAL, G., SALAZAR, L., PEREDA, C., FALCÓN, C., TEMPIO, F., AGUILERA, R., GONZÁLEZ, R., PÉREZ, C., TITTARELLI, A., CATALÁN, D., NERVI, B., LARRONDO, M., SALAZAR-ONFRAY, F., LÓPEZ, M.N. The immunological response and post-treatment survival of DC-vaccinated melanoma patients are associated with increased Th1/Th17 and reduced Th3 cytokine responses., **Cancer Immunol. Immunother**, v. 62 n.4, p. 761-772, 2013.

DUTHIE, G., & CROZIER, A. Plant-derived phenolic antioxidants. **Curr Opin Clin Nutr Metab Care***,* v. 3, n. 6, p. 447-451, 2000.

EL-MAHDY, M. A., ZHU, Q., WANG, Q. E., WANI, G., PATNAIK, S., ZHAO, Q., ARAFA EL, S., BARAKAT, B., MIR, S. N., WANI, A. A. Naringenin protects HaCaT human keratinocytes against UVB-induced apoptosis and enhances the removal of cyclobutane pyrimidine dimers from the genome. **Photochem Photobiol***,* v. 84, n. 2, p. 307-316, 2008.

EMRI, G., HORKAY, I., & REMENYIK, E. [The role of free radicals in the UV-induced skin damage. Photo-aging]. **Orv Hetil***,* v. 147, n. 16, p. 731-735, 2006.

ESMAEILI, M. A., & ALILOU, M. Naringenin attenuates CCl4 -induced hepatic inflammation by the activation of an Nrf2-mediated pathway in rats. **Clin Exp Pharmacol Physiol***,* v. 41, n. 6, p. 416-422, 2014.

FILIP, A., CLICHICI, S., DAICOVICIU, D., CATOI, C., BOLFA, P., POSTESCU, I. D., GAL, A., BALDEA, I., GHERMAN, C., MURESAN, A. Chemopreventive effects of Calluna vulgaris and Vitis vinifera extracts on UVB-induced skin damage in SKH-1 hairless mice. **J Physiol Pharmacol***,* v. 62, n. 3, p. 385-392, 2011.

FISHER, G. J., WANG, Z. Q., DATTA, S. C., VARANI, J., KANG, S., & VOORHEES, J. J. Pathophysiology of premature skin aging induced by ultraviolet light. **N Engl J Med***,* v. 337, n. 20, p. 1419-1428, 1997.

FONSECA, Y. M., CATINI, C. D., VICENTINI, F. T., CARDOSO, J. C., CAVALCANTI DE ALBUQUERQUE JUNIOR, R. L., & VIEIRA FONSECA, M. J. Efficacy of marigold extract-loaded formulations against UV-induced oxidative stress. **J Pharm Sci***,* v. 100, n. 6, p. 2182-2193, 2011.

FONSECA, Y. M., CATINI, C. D., VICENTINI, F. T., NOMIZO, A., GERLACH, R. F., & FONSECA, M. J. Protective effect of Calendula officinalis extract against UVB-induced oxidative stress in skin: evaluation of reduced glutathione levels and matrix metalloproteinase secretion. **J Ethnopharmacol***,* v. 127, n. 3, p. 596-601, 2010.

FORESTI, R., HOQUE, M., MONTI, D., GREEN, C. J., & MOTTERLINI, R. Differential activation of heme oxygenase-1 by chalcones and rosolic acid in endothelial cells. **J Pharmacol Exp Ther***,* v. 312, n. 2, p. 686-693, 2005.

FUCHS, J. Potentials and limitations of the natural antioxidants RRR-alpha-tocopherol, L-ascorbic acid and beta-carotene in cutaneous photoprotection. **Free Radic Biol Med***,* v. 25, n. 7, p. 848-873, 1998.

FUCHS, J., ZOLLNER, T. M., KAUFMANN, R., & PODDA, M. Redox-modulated pathways in inflammatory skin diseases. **Free Radic Biol Med**, v. 30, n. 4, p. 337-353, 2001.

FUNAKOSHI-TAGO, M., NAKAMURA, K., TSURUYA, R., HATANAKA, M., MASHINO, T., SONODA, Y., KASAHARA, T. The fixed structure of Licochalcone A by alpha, beta-unsaturated ketone is necessary for anti-inflammatory activity through the inhibition of NF-kappaB activation. **Int Immunopharmacol**, v. 10, n. 5, p. 562-571, 2010.

GABOR, M., & RAZGA, Z. Effect of benzopyrone derivatives on simultaneously induced croton oil ear oedema and carrageenin paw oedema in rats. **Acta Physiol Hung**, v. 77, n. 3-4, p. 197-207, 1991.

GALATI, E. M., MONFORTE, M. T., KIRJAVAINEN, S., FORESTIERI, A. M., TROVATO, A., & TRIPODO, M. M. Biological effects of hesperidin, a citrus flavonoid. (Note I): antiinflammatory and analgesic activity. **Farmaco**, v. 40, n. 11, p. 709-712, 1994.

GEORGETTI, S. R., CASAGRANDE, R., MOURA-DE-CARVALHO VICENTINI, F. T., VERRI, W. A., JR., & FONSECA, M. J. Evaluation of the antioxidant activity of soybean extract by different in vitro methods and investigation of this activity after its incorporation in topical formulations. **Eur J Pharm Biopharm**, v. 64, n. 1, p. 99-106, 2006.

GIL-IZQUIERDO, A., GIL, M. I., FERRERES, F., & TOMAS-BARBERAN, F. A. In vitro availability of flavonoids and other phenolics in orange juice. **J Agric Food Chem**, v. 49, n. 2, p. 1035-1041, 2001.

GIROTTI, A. W. Photosensitized oxidation of membrane lipids: reaction pathways, cytotoxic effects, and cytoprotective mechanisms. **J Photochem Photobiol B**, v. 63, n. 1-3, p. 103-113, 2001.

GOLDSTEIN, D. H., STOLMAN, A., & GOLDFARB, A. E. The Influence of Methyl Chalcone of Hesperidin on the Toxicity of Mapharsen in Rabbits. **Science**, v. 98, n. 2541, p. 245-246, 1943.

GUEX, J. J., AVRIL, L., ENRICI, E., ENRIQUEZ, E., LIS, C., & TAIEB, C. Quality of life improvement in Latin American patients suffering from chronic venous disorder using a combination of Ruscus aculeatus and hesperidin methyl-chalcone and ascorbic acid (quality study). **Int Angiol**, v. 29, n. 6, p. 525-532, 2010.

GUEX, J. J., ENRIQUEZ VEGA, D. M., AVRIL, L., BOUSSETTA, S., & TAIEB, C. Assessment of quality of life in Mexican patients suffering from chronic venous disorder - impact of oral Ruscus aculeatus-hesperidin-methyl-chalcone-ascorbic acid treatment - 'QUALITY Study'. **Phlebology**, v. 24, n. 4, p. 157-165, 2009.

HALLIDAY, G. M. Inflammation, gene mutation and photoimmunosuppression in response to UVR-induced oxidative damage contributes to photocarcinogenesis. **Mutat Res**, v. 571, n. 1-2, p. 107-120, 2005.

HALLIWELL, B. Oxygen and nitrogen are pro-carcinogens. Damage to DNA by reactive oxygen, chlorine and nitrogen species: measurement, mechanism and the effects of nutrition. **Mutat Res**, v. 443, n. 1-2, p. 37-52, 1999.

HALLIWELL, B. The wanderings of a free radical. **Free Radic Biol Med***,* v. 46, n. 5, p. 531-542, 2009.

HALLIWELL, B., GUTTERIDGE, J. M., & ARUOMA, O. I. The deoxyribose method: a simple "test-tube" assay for determination of rate constants for reactions of hydroxyl radicals. **Anal Biochem***,* v. 165, n. 1, p. 215-219, 1987.

HAN, S. C., KOO, D. H., KANG, N. J., YOON, W. J., KANG, G. J., KANG, H. K., & YOO, E. S. Docosahexaenoic Acid Alleviates Atopic Dermatitis by Generating Treg and IL-10/TGF-beta-Modified Macrophage via TGF-beta Dependent Mechanism. **J Invest Dermatol***,* v. n. 2014.

HASEGAWA, T., SHIMADA, S., ISHIDA, H., & NAKASHIMA, M. Chafuroside B, an Oolong tea polyphenol, ameliorates UVB-induced DNA damage and generation of photo-immunosuppression related mediators in human keratinocytes. **PLoS One***,* v. 8, n. 10, p. e77308, 2013.

HATTORI, H., SUBRAMANIAN, K. K., SAKAI, J., JIA, Y., LI, Y., PORTER, T. F., LOISON, F., SARRAJ, B., KASORN, A., JO, H., BLANCHARD, C., ZIRKLE, D., MCDONALD, D., PAI, S. Y., SERHAN, C. N., LUO, H. R. Small-molecule screen identifies reactive oxygen species as key regulators of neutrophil chemotaxis. **Proc Natl Acad Sci U S A***,* v. 107, n. 8, p. 3546-3551, 2010.

HEATH, W. R., & CARBONE, F. R. The skin-resident and migratory immune system in steady state and memory: innate lymphocytes, dendritic cells and T cells. **Nat Immunol***,* v. 14, n. 10, p. 978-985, 2013.

HEIM, K. E., TAGLIAFERRO, A. R., & BOBILYA, D. J. Flavonoid antioxidants: chemistry, metabolism and structure-activity relationships. **J Nutr Biochem***,* v. 13, n. 10, p. 572-584, 2002.

HERLAAR, E., & BROWN, Z. p38 MAPK signalling cascades in inflammatory disease. **Mol Med Today***,* v. 5, n. 10, p. 439-447, 1999.

HERMENEAN, A., ARDELEAN, A., STAN, M., HERMAN, H., MIHALI, C. V., COSTACHE, M., & DINISCHIOTU, A. Protective effects of naringenin on carbon tetrachloride-induced acute nephrotoxicity in mouse kidney. **Chem Biol Interact***,* v. 205, n. 2, p. 138-147, 2013.

HIJOVA, E. Bioavailability of chalcones. **Bratisl Lek Listy***,* v. 107, n. 3, p. 80-84, 2006.

HIRAMOTO, K., KOBAYASHI, H., YAMATE, Y., ISHII, M., & SATO, E. F. Intercellular pathway through hyaluronic acid in UVB-induced inflammation. **Exp Dermatol***,* v. 21, n. 12, p. 911-914, 2012.

HUSSEIN, M. R. Ultraviolet radiation and skin cancer: molecular mechanisms. **J Cutan Pathol***,* v. 32, n. 3, p. 191-205, 2005.

INCA. Instituto Nacional do Câncer. Incidência de câncer no Brasil. 2014. Disponível em: http://www.inca.gov.br/estimativa/2014/estimativa-24042014.pdf. Acesso em: 08 jan 2015.

IVAN, A. L., CAMPANINI, M. Z., MARTINEZ, R. M., FERREIRA, V. S., STEFFEN, V. S., VICENTINI, F. T., VILELA, F. M., MARTINS, F. S., ZARPELON, A. C., CUNHA, T.

M., FONSECA, M. J., BARACAT, M. M., GEORGETTI, S. R., VERRI, W. A., JR., CASAGRANDE, R. Pyrrolidine dithiocarbamate inhibits UVB-induced skin inflammation and oxidative stress in hairless mice and exhibits antioxidant activity in vitro. **J Photochem Photobiol B***,* v. 138, n. 124-133, 2014.

IWAMURA, C., SHINODA, K., YOSHIMURA, M., WATANABE, Y., OBATA, A., & NAKAYAMA, T. Naringenin chalcone suppresses allergic asthma by inhibiting the type-2 function of CD4 T cells. **Allergol Int***,* v. 59, n. 1, p. 67-73, 2010.

IWATA, S., NISHINO, T., NAGATA, N., SATOMI, Y., NISHINO, H., & SHIBATA, S. Antitumorigenic activities of chalcones. I. Inhibitory effects of chalcone derivatives on 32Pi-incorporation into phospholipids of HeLa cells promoted by 12-O-tetradecanoyl-phorbol 13-acetate (TPA). **Biol Pharm Bull***,* v. 18, n. 12, p. 1710-1713, 1995.

JAYARAMAN, J., VEERAPPAN, M., & NAMASIVAYAM, N. Potential beneficial effect of naringenin on lipid peroxidation and antioxidant status in rats with ethanol-induced hepatotoxicity. **J Pharm Pharmacol***,* v. 61, n. 10, p. 1383-1390, 2009.

JENKINS, G. Molecular mechanisms of skin ageing. **Mech Ageing Dev***,* v. 123, n. 7, p. 801-810, 2002.

JOHN, A., & TUSZYNSKI, G. The role of matrix metalloproteinases in tumor angiogenesis and tumor metastasis. **Pathol Oncol Res***,* v. 7, n. 1, p. 14-23, 2001.

KATALINIC, V., MODUN, D., MUSIC, I., & BOBAN, M. Gender differences in antioxidant capacity of rat tissues determined by 2,2'-azinobis (3-ethylbenzothiazoline 6-sulfonate; ABTS) and ferric reducing antioxidant power (FRAP) assays. **Comp Biochem Physiol C Toxicol Pharmacol***,* v. 140, n. 1, p. 47-52, 2005.

KHAN, M. B., KHAN, M. M., KHAN, A., AHMED, M. E., ISHRAT, T., TABASSUM, R., VAIBHAV, K., AHMAD, A., ISLAM, F. Naringenin ameliorates Alzheimer's disease (AD)-type neurodegeneration with cognitive impairment (AD-TNDCI) caused by the intracerebroventricular-streptozotocin in rat model. **Neurochem Int***,* v. 61, n. 7, p. 1081-1093, 2012.

KHAVKIN, J., & ELLIS, D. A. Aging skin: histology, physiology, and pathology. **Facial Plast Surg Clin North Am***,* v. 19, n. 2, p. 229-234, 2011.

KILPATRICK, L. E., SUN, S., LI, H., VARY, T. C., & KORCHAK, H. M. Regulation of TNF-induced oxygen radical production in human neutrophils: role of delta-PKC. **J Leukoc Biol***,* v. 87, n. 1, p. 153-164, 2010.

KIM, C. M., KANG, S. M., JEON, H. J., & SHIN, S. H. Production of Vibrio vulnificus metalloprotease VvpE begins during the early growth phase: usefulness of gelatin-zymography. **J Microbiol Methods***,* v. 70, n. 1, p. 96-102, 2007.

KIM, S. H., JUNG, E. Y., KANG, D. H., CHANG, U. J., HONG, Y. H., & SUH, H. J. Physical stability, antioxidative properties, and photoprotective effects of a functionalized formulation containing black garlic extract. **J Photochem Photobiol B***,* v. 117, n. 104-110, 2012.

KIM, S. Y., LEE, I. S., & MOON, A. 2-Hydroxychalcone and xanthohumol inhibit invasion of triple negative breast cancer cells. **Chem Biol Interact***,* v. 203, n. 3, p. 565-572, 2013.

KIM, T. H., KIM, G. D., AHN, H. J., CHO, J. J., PARK, Y. S., & PARK, C. S. The inhibitory effect of naringenin on atopic dermatitis induced by DNFB in NC/Nga mice. **Life Sci**, v. 93, n. 15, p. 516-524, 2013.

KIRTLEY, W. R., & PECK, F. B. Administration of massive doses of vitamin P hesperidin methyl chalcone. **Am J Med Sci**, v. 216, n. 1, p. 64-70, 1948.

KOBAYASHI, M., & YAMAMOTO, M. Molecular mechanisms activating the Nrf2-Keap1 pathway of antioxidant gene regulation. **Antioxid Redox Signal**, v. 7, n. 3-4, p. 385-394, 2005.

KOHEN, R. Skin antioxidants: their role in aging and in oxidative stress--new approaches for their evaluation. **Biomed Pharmacother**, v. 53, n. 4, p. 181-192, 1999.

KONDO, S. The roles of cytokines in photoaging. **J Dermatol Sci**, v. 23 Suppl 1, n. S30-36, 2000.

KUMAR, V., KUMAR, S., HASSAN, M., WU, H., THIMMULAPPA, R. K., KUMAR, A., SHARMA, S. K., PARMAR, V. S., BISWAL, S., MALHOTRA, S. V. Novel chalcone derivatives as potent Nrf2 activators in mice and human lung epithelial cells. **J Med Chem**, v. 54, n. 12, p. 4147-4159, 2011.

KVIETYS, P. R., & GRANGER, D. N. Role of reactive oxygen and nitrogen species in the vascular responses to inflammation. **Free Radic Biol Med**, v. 52, n. 3, p. 556-592, 2012.

LA, V. D., TANABE, S., & GRENIER, D. Naringenin inhibits human osteoclastogenesis and osteoclastic bone resorption. **J Periodontal Res**, v. 44, n. 2, p. 193-198, 2009.

LAMAR, J. M., IYER, V., & DIPERSIO, C. M. Integrin alpha3beta1 potentiates TGFbeta-mediated induction of MMP-9 in immortalized keratinocytes. **J Invest Dermatol**, v. 128, n. 3, p. 575-586, 2008.

LAMOKE, F., LABAZI, M., MONTEMARI, A., PARISI, G., VARANO, M., & BARTOLI, M. Trans-Chalcone prevents VEGF expression and retinal neovascularization in the ischemic retina. **Exp Eye Res**, v. 93, n. 4, p. 350-354, 2011.

LASCASAS-PORTO, C. L., MILHOMENS, A. L., VIRGINI-MAGALHAES, C. E., FERNANDES, F. F., SICURO, F. L., & BOUSKELA, E. Use of microcirculatory parameters to evaluate clinical treatments of chronic venous disorder (CVD). **Microvasc Res**, v. 76, n. 1, p. 66-72, 2008.

LEE, C. H., JEONG, T. S., CHOI, Y. K., HYUN, B. H., OH, G. T., KIM, E. H., HAN, J. I., BOK, S. H. Anti-atherogenic effect of citrus flavonoids, naringin and naringenin, associated with hepatic ACAT and aortic VCAM-1 and MCP-1 in high cholesterol-fed rabbits. **Biochem Biophys Res Commun**, v. 284, n. 3, p. 681-688, 2001.

LEMANSKA, K., SZYMUSIAK, H., TYRAKOWSKA, B., ZIELINSKI, R., SOFFERS, A. E., & RIETJENS, I. M. The influence of pH on antioxidant properties and the mechanism of antioxidant action of hydroxyflavones. **Free Radic Biol Med**, v. 31, n. 7, p. 869-881, 2001.

LIM, H., PARK, H., & KIM, H. P. Effects of flavonoids on matrix metalloproteinase-13 expression of interleukin-1beta-treated articular chondrocytes and their cellular

mechanisms: inhibition of c-Fos/AP-1 and JAK/STAT signaling pathways. **J Pharmacol Sci***,* v. 116, n. 2, p. 221-231, 2011.

LIN, S. H., & SHIH, Y. W. Antitumor effects of the flavone chalcone: inhibition of invasion and migration through the FAK/JNK signaling pathway in human gastric adenocarcinoma AGS cells. **Mol Cell Biochem***,* v. 391, n. 1-2, p. 47-58, 2014.

LINGNERT, H., VALENTIN, K., ERICKSON, C. E. Measurement of antioxidative effect in model system. **J Food Process**, v. 3, p. 87-104, 1979.

LOPEZ-TORRES, M., THIELE, J. J., SHINDO, Y., HAN, D., & PACKER, L. Topical application of alpha-tocopherol modulates the antioxidant network and diminishes ultraviolet-induced oxidative damage in murine skin. **Br J Dermatol***,* v. 138, n. 2, p. 207-215, 1998.

LOU, J. S., CHEN, X. E., ZHANG, Y., GAO, Z. W., CHEN, T. P., ZHANG, G. Q., & JI, C. Photoprotective and immunoregulatory capacity of ginsenoside Rg1 in chronic ultraviolet B-irradiated BALB/c mouse skin. **Exp Ther Med***,* v. 6, n. 4, p. 1022-1028, 2013.

LOWRY, O. H., ROSEBROUGH, N. J., FARR, A. L., & RANDALL, R. J. Protein measurement with the Folin phenol reagent. **J Biol Chem***,* v. 193, n. 1, p. 265-275, 1951.

MANACH, C., MORAND, C., GIL-IZQUIERDO, A., BOUTELOUP-DEMANGE, C., & REMESY, C. Bioavailability in humans of the flavanones hesperidin and narirutin after the ingestion of two doses of orange juice. **Eur J Clin Nutr***,* v. 57, n. 2, p. 235-242, 2003.

MANTENA, S. K., & KATIYAR, S. K. Grape seed proanthocyanidins inhibit UV-radiation-induced oxidative stress and activation of MAPK and NF-kappaB signaling in human epidermal keratinocytes. **Free Radic Biol Med***,* v. 40, n. 9, p. 1603-1614, 2006.

MARTINEZ, R. M., ZARPELON, A. C., ZIMERMANN, V. V. M., GEORGETTI, S. R., BARACAT, M.M., FONSECA, M. J. V., VICENTINI, F. T. M. C., MOREIRA, I. C., ANDREI, C.C., VERRI W. A. JR., CASAGRANDE, R. Tephrosia sinapou extract reduces inflammatory leukocyte recruitment in mice: effect on oxidative stress, nitric oxide and cytokine production. **Braz J Pharmacogn**, v. 22, n. 3, p. 587-597, 2012.

MERSHIBA, S. D., DASSPRAKASH, M. V., & SARASWATHY, S. D. Protective effect of naringenin on hepatic and renal dysfunction and oxidative stress in arsenic intoxicated rats. **Mol Biol Rep***,* v. 40, n. 5, p. 3681-3691, 2013.

MUKAI, R., SHIRAI, Y., SAITO, N., FUKUDA, I., NISHIUMI, S., YOSHIDA, K., & ASHIDA, H. Suppression mechanisms of flavonoids on aryl hydrocarbon receptor-mediated signal transduction. **Arch Biochem Biophys***,* v. 501, n. 1, p. 134-141, 2010.

MUTOU, Y., IBUKI, Y., & KOJIMA, S. Immunomodulatory effects of ultraviolet B irradiation on atopic dermatitis in NC/Nga mice. **Photodermatol Photoimmunol Photomed***,* v. 23, n. 4, p. 135-144, 2007.

NAM, T. W., YOO, C. I., KIM, H. T., KWON, C. H., PARK, J. Y., & KIM, Y. K. The flavonoid quercetin induces apoptosis and inhibits migration through a MAPK-dependent mechanism in osteoblasts. **J Bone Miner Metab***,* v. 26, n. 6, p. 551-560, 2008.

NATHAN, C., & SHILOH, M. U. Reactive oxygen and nitrogen intermediates in the relationship between mammalian hosts and microbial pathogens. **Proc Natl Acad Sci U S A**, v. 97, n. 16, p. 8841-8848, 2000.

NI, L., MENG, C. Q., SIKORSKI, J. A. Recent advances in therapeutic chalcones.Exper Opin Ther Patents, v. 14, n. 12, p. 1669-1691, 2004.

NICHOLS, J. A., & KATIYAR, S. K. Skin photoprotection by natural polyphenols: anti-inflammatory, antioxidant and DNA repair mechanisms. **Arch Dermatol Res**, v. 302, n. 2, p. 71-83, 2010.

NOWAKOWSKA, Z. A review of anti-infective and anti-inflammatory chalcones. **Eur J Med Chem**, v. 42, n. 2, p. 125-137, 2007.

ORSOLIC, N., GAJSKI, G., GARAJ-VRHOVAC, V., DIKIC, D., PRSKALO, Z. S., & SIROVINA, D. DNA-protective effects of quercetin or naringenin in alloxan-induced diabetic mice. **Eur J Pharmacol**, v. 656, n. 1-3, p. 110-118, 2011.

PARHIZ, H., ROOHBAKHSH, A., SOLTANI, F., REZAEE, R., & IRANSHAHI, M. Antioxidant and Anti-Inflammatory Properties of the Citrus Flavonoids Hesperidin and Hesperetin: An Updated Review of their Molecular Mechanisms and Experimental Models. **Phytother Res**, v. n. 2014.

PARI, L., & GNANASOUNDARI, M. Influence of naringenin on oxytetracycline mediated oxidative damage in rat liver. **Basic Clin Pharmacol Toxicol**, v. 98, n. 5, p. 456-461, 2006.

PARK, H. Y., KIM, G. Y., & CHOI, Y. H. Naringenin attenuates the release of pro-inflammatory mediators from lipopolysaccharide-stimulated BV2 microglia by inactivating nuclear factor-kappaB and inhibiting mitogen-activated protein kinases. **Int J Mol Med**, v. 30, n. 1, p. 204-210, 2012.

PARK, S. Y., KU, S. K., LEE, E. S., & KIM, J. A. 1,3-Diphenylpropenone ameliorates TNBS-induced rat colitis through suppression of NF-kappaB activation and IL-8 induction. **Chem Biol Interact**, v. 196, n. 1-2, p. 39-49, 2012.

PAZ, M. L., FERRARI, A., WEILL, F. S., LEONI, J., & MAGLIO, D. H. Time-course evaluation and treatment of skin inflammatory immune response after ultraviolet B irradiation. **Cytokine**, v. 44, n. 1, p. 70-77, 2008.

PEISER, M. Role of Th17 cells in skin inflammation of allergic contact dermatitis. **Clin Dev Immunol**, v. 2013, n. 261037, 2013.

PETROVA, A., DAVIDS, L. M., RAUTENBACH, F., & MARNEWICK, J. L. Photoprotection by honeybush extracts, hesperidin and mangiferin against UVB-induced skin damage in SKH-1 mice. **J Photochem Photobiol B**, v. 103, n. 2, p. 126-139, 2011.

PIETTA, P. G. Flavonoids as antioxidants. **J Nat Prod**, v. 63, n. 7, p. 1035-1042, 2000.

PINHO-RIBEIRO, F. A., HOHMANN, M. S., BORGHI, S. M., ZARPELON, A. C., GUAZELLI, C. F., MANCHOPE, M. F., CASAGRANDE R. VERRI, W. A., JR. Protective effects of the flavonoid hesperidin methyl chalcone in inflammation and pain in mice: Role of TRPV1, oxidative stress, cytokines and NF-kappaB. **Chem Biol Interact**, *v. 228*, n. 1, p. 88-99, 2015.

PISKIN, G., BOS, J. D., & TEUNISSEN, M. B. Neutrophils infiltrating ultraviolet B-irradiated normal human skin display high IL-10 expression. **Arch Dermatol Res**, v. 296, n. 7, p. 339-342, 2005.

PODDER, B., SONG, H. Y., & KIM, Y. S. Naringenin exerts cytoprotective effect against paraquat-induced toxicity in human bronchial epithelial BEAS-2B cells through NRF2 activation. **J Microbiol Biotechnol**, v. 24, n. 5, p. 605-613, 2014.

PORATH, D., RIEGGER, C., DREWE, J., & SCHWAGER, J. Epigallocatechin-3-gallate impairs chemokine production in human colon epithelial cell lines. **J Pharmacol Exp Ther**, v. 315, n. 3, p. 1172-1180, 2005.

PORTO, C. L., MILHOMENS, A. L., PIRES, C. E., XAVIER, S. S., SICURO, F., BOTTINO, D. A., & BOUSKELA, E. Changes on venous diameter and leg perimeter with different clinical treatments for moderate chronic venous disease: evaluation using Duplex scanning and perimeter measurements. **Int Angiol**, v. 28, n. 3, p. 222-231, 2009.

PRIOR, R. L., WU, X., & SCHAICH, K. Standardized methods for the determination of antioxidant capacity and phenolics in foods and dietary supplements. **J Agric Food Chem**, v. 53, n. 10, p. 4290-4302, 2005.

PROCHAZKOVA, D., BOUSOVA, I., & WILHELMOVA, N. Antioxidant and prooxidant properties of flavonoids. **Fitoterapia**, v. 82, n. 4, p. 513-523, 2011.

QUAN, T., QIN, Z., XIA, W., SHAO, Y., VOORHEES, J. J., & FISHER, G. J. Matrix-degrading metalloproteinases in photoaging. **J Investig Dermatol Symp Proc**, v. 14, n. 1, p. 20-24, 2009.

RAZA, S. S., KHAN, M. M., AHMAD, A., ASHAFAQ, M., ISLAM, F., WAGNER, A. P., SAFHI, M. M., ISLAM, F. Neuroprotective effect of naringenin is mediated through suppression of NF-kappaB signaling pathway in experimental stroke. **Neuroscience**, v. 230, n. 157-171, 2013.

RAZMI, A., ZARGHI, A., ARFAEE, S., NADERI, N., & FAIZI, M. Evaluation of Anti-nociceptive and Anti-inflammatory Activities of Novel Chalcone Derivatives. **Iran J Pharm Res**, v. 12, n. Suppl, p. 153-159, 2013.

RENUGADEVI, J., & PRABU, S. M. Naringenin protects against cadmium-induced oxidative renal dysfunction in rats. **Toxicology**, v. 256, n. 1-2, p. 128-134, 2009.

REUTER, S., GUPTA, S. C., CHATURVEDI, M. M., & AGGARWAL, B. B. Oxidative stress, inflammation, and cancer: how are they linked? **Free Radic Biol Med**, v. 49, n. 11, p. 1603-1616, 2010.

RITTIE, L., & FISHER, G. J. UV-light-induced signal cascades and skin aging. **Ageing Res Rev**, v. 1, n. 4, p. 705-720, 2002.

ROBBINS, D., & ZHAO, Y. The role of manganese superoxide dismutase in skin cancer. **Enzyme Res**, v. 2011, n. 409295, 2011.

RUDOFSKY, G. [Improving venous tone and capillary sealing. Effect of a combination of Ruscus extract and hesperidine methyl chalcone in healthy probands in heat stress]. **Fortschr Med**, v. 107, n. 19, p. 52, 55-58, 1989.

SAIJA, A., SCALESE, M., LANZA, M., MARZULLO, D., BONINA, F., & CASTELLI, F. Flavonoids as antioxidant agents: importance of their interaction with biomembranes. **Free Radic Biol Med**, v. 19, n. 4, p. 481-486, 1995.

SAW, C. L., HUANG, M. T., LIU, Y., KHOR, T. O., CONNEY, A. H., & KONG, A. N. Impact of Nrf2 on UVB-induced skin inflammation/photoprotection and photoprotective effect of sulforaphane. **Mol Carcinog**, v. 50, n. 6, p. 479-486, 2011.

SAW, C. L., YANG, A. Y., HUANG, M. T., LIU, Y., LEE, J. H., KHOR, T. O., SU, Z. Y., SHU, L., LU, Y., CONNEY, A. H., KONG, A. N. Nrf2 null enhances UVB-induced skin inflammation and extracellular matrix damages. **Cell Biosci**, v. 4, n. 39, 2014.

SHEN, K. H., CHANG, J. K., HSU, Y. L., & KUO, P. L. Chalcone arrests cell cycle progression and induces apoptosis through induction of mitochondrial pathway and inhibition of nuclear factor kappa B signalling in human bladder cancer cells. **Basic Clin Pharmacol Toxicol**, v. 101, n. 4, p. 254-261, 2007.

SHINDO, Y., WITT, E., HAN, D., & PACKER, L. Dose-response effects of acute ultraviolet irradiation on antioxidants and molecular markers of oxidation in murine epidermis and dermis. **J Invest Dermatol**, v. 102, n. 4, p. 470-475, 1994.

SIKANDER, M., MALIK, S., YADAV, D., BISWAS, S., KATARE, D. P., & JAIN, S. K. Cytoprotective activity of a trans-chalcone against hydrogen peroxide induced toxicity in hepatocellular carcinoma (HepG2) cells. **Asian Pac J Cancer Prev**, v. 12, n. 10, p. 2513-2516, 2011.

SINGH, P., ANAND, A., KUMAR, V. Recent developments in biological activities of chalcones: A mini Review. **European Journal of Medicinal Chemistry,** v. 85, n. 6, p. 758-777, 2014.

STANIFORTH, V., HUANG, W. C., ARAVINDARAM, K., & YANG, N. S. Ferulic acid, a phenolic phytochemical, inhibits UVB-induced matrix metalloproteinases in mouse skin via posttranslational mechanisms. **J Nutr Biochem**, v. 23, n. 5, p. 443-451, 2012.

STOIANOVA, V. [Cyclo 3 fort--alternative in chronic venous insufficiency]. **Akush Ginekol (Sofiia)**, v. 45 Suppl 3, n. 78-80, 2006.

STRIZ, I., BRABCOVA, E., KOLESAR, L., & SEKERKOVA, A. Cytokine networking of innate immunity cells: a potential target of therapy. **Clin Sci (Lond)**, v. 126, n. 9, p. 593-612, 2014.

SUBRAMANIAN, P., & ARUL, D. Attenuation of NDEA-induced hepatocarcinogenesis by naringenin in rats. **Cell Biochem Funct**, v. 31, n. 6, p. 511-517, 2013.

SUGIHARA, N., ARAKAWA, T., OHNISHI, M., & FURUNO, K. Anti- and pro-oxidative effects of flavonoids on metal-induced lipid hydroperoxide-dependent lipid peroxidation in cultured hepatocytes loaded with alpha-linolenic acid. **Free Radic Biol Med**, v. 27, n. 11-12, p. 1313-1323, 1999.

SULLIVAN, N. J., TOBER, K. L., BURNS, E. M., SCHICK, J. S., RIGGENBACH, J. A., MACE, T. A., BILL, M. A., YOUNG, G. S., OBERYSZYN, T. M., LESINSKI, G. B. UV light B-mediated inhibition of skin catalase activity promotes Gr-1+ CD11b+ myeloid cell expansion. **J Invest Dermatol**, v. 132, n. 3 Pt 1, p. 695-702, 2012.

SUN, Z. W., HWANG, E., LEE, H. J., LEE, T. Y., SONG, H. G., PARK, S. Y., SHIN, H. S., LEE, D. G., YI, T. H. Effects of Galla chinensis extracts on UVB-irradiated MMP-1 production in hairless mice. **J Nat Med***,* v. n. 2014.

TAKASE, S., DELANO, F. A., LEROND, L., BERGAN, J. J., & SCHMID-SCHONBEIN, G. W. Inflammation in chronic venous insufficiency. Is the problem insurmountable? **J Vasc Res***,* v. 36 Suppl 1, n. 3-10, 1999.

TAKEYA, R., & SUMIMOTO, H. Molecular mechanism for activation of superoxide-producing NADPH oxidases. **Mol Cells***,* v. 16, n. 3, p. 271-277, 2003.

TARAYRE, J. P., & LAURESSERGUES, H. [Some pharmacologic properties of a vasoactive combination]. **Ann Pharm Fr***,* v. 34, n. 9-10, p. 375-382, 1976.

TARAYRE, J. P., & LAURESSERGUES, H. Advantages of a combination of proteolytic enzymes, flavonoids and ascorbic acid in comparison with non-steroid anti-inflammatory agents. **Arzneimittelforschung***,* v. 27, n. 6, p. 1144-1149, 1977.

TOUITOU, E., & GODIN, B. Skin nonpenetrating sunscreens for cosmetic and pharmaceutical formulations. **Clin Dermatol***,* v. 26, n. 4, p. 375-379, 2008.

VAFEIADOU, K., VAUZOUR, D., LEE, H. Y., RODRIGUEZ-MATEOS, A., WILLIAMS, R. J., & SPENCER, J. P. The citrus flavanone naringenin inhibits inflammatory signalling in glial cells and protects against neuroinflammatory injury. **Arch Biochem Biophys***,* v. 484, n. 1, p. 100-109, 2009.

VAN ACKER, S. A., VAN DEN BERG, D. J., TROMP, M. N., GRIFFIOEN, D. H., VAN BENNEKOM, W. P., VAN DER VIJGH, W. J., & BAST, A. Structural aspects of antioxidant activity of flavonoids. **Free Radic Biol Med***,* v. 20, n. 3, p. 331-342, 1996.

VERRI, W. A., VICENTINI, F. T. M. C., BARACAT, M. M., GEORGETTI, S. R., CARDOSO, R. D. R., CUNHA, T. M., FONSECA, M. J. V. , CASAGRANDE R, 2012. Flavonoids as anti-inflammatory and analgesic drugs: Mechanisms of action and perspectives in the development of pharmaceutical forms, in: Atta-ur-Rahman. (Eds.), Studies in Natural Products Chemistry. Elsevier, Amsterdam, pp. 297-322.

VERRI, W. A., JR., GUERRERO, A. T., FUKADA, S. Y., VALERIO, D. A., CUNHA, T. M., XU, D., FERREIRA, S. H., LIEW, F. Y., CUNHA, F. Q. IL-33 mediates antigen-induced cutaneous and articular hypernociception in mice. **Proc Natl Acad Sci U S A***,* v. 105, n. 7, p. 2723-2728, 2008.

VICENTINI, F. T., HE, T., SHAO, Y., FONSECA, M. J., VERRI, W. A., JR., FISHER, G. J., & XU, Y. Quercetin inhibits UV irradiation-induced inflammatory cytokine production in primary human keratinocytes by suppressing NF-kappaB pathway. **J Dermatol Sci***,* v. 61, n. 3, p. 162-168, 2011.

VICENTINI, F. T., SIMI, T. R., DEL CIAMPO, J. O., WOLGA, N. O., PITOL, D. L., IYOMASA, M. M., BENTLEY, M. V., FONSECA, M. J. Quercetin in w/o microemulsion: in vitro and in vivo skin penetration and efficacy against UVB-induced skin damages evaluated in vivo. **Eur J Pharm Biopharm***,* v. 69, n. 3, p. 948-957, 2008.

WALLE, T. Methylation of dietary flavones greatly improves their hepatic metabolic stability and intestinal absorption. **Mol Pharm***,* v. 4, n. 6, p. 826-832, 2007.

WANG, H., & KOCHEVAR, I. E. Involvement of UVB-induced reactive oxygen species in TGF-beta biosynthesis and activation in keratinocytes. **Free Radic Biol Med**, v. 38, n. 7, p. 890-897, 2005.

DI WANG, H., PAGANO, P. J., DU, Y., CAYATTE, A. J., QUINN, M. T., BRECHER, P., & COHEN, R. A. Superoxide Anion From the Adventitia of the Rat Thoracic Aorta Inactivates Nitric Oxide. **Circulation Research**, v. 82 n. 7, p. 810-818, 1998.

WHITE, E. L., ROSS, L. J., SCHMID, S. M., KELLOFF, G. J., STEELE, V. E., & HILL, D. L. Screening of potential cancer preventing chemicals for induction of glutathione in rat liver cells. **Oncol Rep**, v. 5, n. 2, p. 507-512, 1998.

WITKO-SARSAT, V., RIEU, P., DESCAMPS-LATSCHA, B., LESAVRE, P., & HALBWACHS-MECARELLI, L. Neutrophils: molecules, functions and pathophysiological aspects. **Lab Invest**, v. 80, n. 5, p. 617-653, 2000.

XU, C., CHEN, J., ZHANG, J., HU, X., ZHOU, X., LU, Z., & JIANG, H. Naringenin inhibits angiotensin II-induced vascular smooth muscle cells proliferation and migration and decreases neointimal hyperplasia in balloon injured rat carotid arteries through suppressing oxidative stress. **Biol Pharm Bull**, v. 36, n. 10, p. 1549-1555, 2013.

XU, X. R., YU, H. T., HANG, L., SHAO, Y., DING, S. H., & YANG, X. W. Preparation of naringenin/ beta-cyclodextrin complex and its more potent alleviative effect on choroidal neovascularization in rats. **Biomed Res Int**, v. 2014, n. 623509, 2014.

XU, Y., FISHER, G. J. Ultraviolet (UV) light irradiation induced signal transduction in skin photoaging. **J Dermatol Sci Suppl**, v. 1, p. S1-S8, 2005.

YAAR, M., & GILCHREST, B. A. Photoageing: mechanism, prevention and therapy. **Br J Dermatol**, v. 157, n. 5, p. 874-887, 2007.

YADAV, V. R., PRASAD, S., SUNG, B., & AGGARWAL, B. B. The role of chalcones in suppression of NF-kappaB-mediated inflammation and cancer. **Int Immunopharmacol**, v. 11, n. 3, p. 295-309, 2011.

YAMAZAKI, Y., KAWANO, Y., NAGASHIMA, U. Structure-activity Relationship of α,β-Unsaturated Ketones for the Suppression of Tumor Necrosis Factor-α and Nitric Oxide Production in Lipopolysaccharide-stimulated Macrophages and Their Molecular Orbital Energies. **J Comput Chem Jpn**, v. 11, n. 3, p. 159-163, 2012.

YANG, J., LI, Q., ZHOU, X. D., KOLOSOV, V. P., & PERELMAN, J. M. Naringenin attenuates mucous hypersecretion by modulating reactive oxygen species production and inhibiting NF-kappaB activity via EGFR-PI3K-Akt/ERK MAPKinase signaling in human airway epithelial cells. **Mol Cell Biochem**, v. 351, n. 1-2, p. 29-40, 2011.

YEN, F. L., WU, T. H., LIN, L. T., CHAM, T. M., & LIN, C. C. Naringenin-loaded nanoparticles improve the physicochemical properties and the hepatoprotective effects of naringenin in orally-administered rats with CCl(4)-induced acute liver failure. **Pharm Res**, v. 26, n. 4, p. 893-902, 2009.

YILMA, A. N., SINGH, S. R., MORICI, L., & DENNIS, V. A. Flavonoid naringenin: a potential immunomodulator for Chlamydia trachomatis inflammation. **Mediators Inflamm**, v. 2013, n. 102457, 2013.

YOKOGAWA, M., TAKAISHI, M., NAKAJIMA, K., KAMIJIMA, R., DIGIOVANNI, J., & SANO, S. Imiquimod attenuates the growth of UVB-induced SCC in mice through Th1/Th17 cells. **Mol Carcinog***,* v. 52, n. 10, p. 760-769, 2013.

ZHANG, J., ZHANG, D. L., JIAO, X. L., & DONG, Q. S100A4 regulates migration and invasion in hepatocellular carcinoma HepG2 cells via NF-kappaB-dependent MMP-9 signal. **Eur Rev Med Pharmacol Sci***,* v. 17, n. 17, p. 2372-2382, 2013.

ZHANG, S., SONG, C., ZHOU, J., XIE, L., MENG, X., LIU, P., CAO, J., ZHANG, X., DING, W. Q., WU, J. Amelioration of radiation-induced skin injury by adenovirus-mediated heme oxygenase-1 (HO-1) overexpression in rats. **Radiat Oncol***,* v. 7, n. 4, 2012.

ZHAO, F., NOZAWA, H., DAIKONNYA, A., KONDO, K., KITANAKA, S. Inhibitors of nitric oxide production from hops (Humulus lupulus L.). Biol Pharma Bull, v. 26, n. 61, p. 61-65, 2003.

ZHOU, B. R., LIN, B. J., JIN, S. L., & LUO, D. Mitigation of acute ultraviolet B radiation-mediated damages by baicalin in mouse skin. **Photodermatol Photoimmunol Photomed***,* v. 25, n. 5, p. 250-258, 2009.

ANEXOS

ANEXO I - Resumo dos resultados *in vitro.*

ANEXO II - Documento de depósito de pedido de patente: "Formulação tópica contendo hesperidina metil chalcona para redução dos danos cutâneos induzidos pela radiação ultravioleta B".

ANEXO III - "Documento de depósito de pedido de patente: Formulação tópica contendo naringenina para redução dos danos cutâneos foto-oxidativos induzidos pela radiação ultravioleta B".

ANEXO I

Resumo dos resultados *in vitro.*

Tabela 1. Concentrações de trans-chalcona (TC), hesperidina metil chalcona (HMC) e naringenina (NGN) que inibem o processo oxidativo *in vitro* em 50% (IC_{50}) em diferentes metodologias antioxidantes.

Metodologias	IC_{50} (µg/mL)		
	TC	HMC	NGN
DPPH$^{\bullet}$	-	-	-
ABTS	-	19	0,71
Radical hidroxil	-	249	183
LPO independente de ferro	-	1120	101
LPO dependente de ferro	-	-	159
Quelação de ferro	-	-	-

Os resultados foram determinados por meio de uma curva hiperbólica de mensurações feitas em triplicata de cada concentração e são representativos de dois experimentos separados.

Tabela 2. Capacidade antioxidante dos flavonóides por meio do método de poder antioxidante redutor do ferro (FRAP) em µmol/L equivalente de trolox/ µg/mL de amostra.

Metodologia	µmol/L de Trolox/ µg/mL de flavonóide		
	TC	HMC	NGN
Poder antioxidante em reduzir o ferro (FRAP)	-	0,045	0,157

Os resultados foram apresentados pela média de mensurações feitas em triplicata de cada concentração e são representativos de dois experimentos separados.

Observação: os resultados *in vitro* da HMC serão utilizados na redação de outro artigo científico.

ANEXO II

< Uso exclusivo do INPI >

INPI INSTITUTO NACIONAL DA PROPRIEDADE INDUSTRIAL
cassandr
22/12/2014 015140002564
VP17/12/2014
RR 10 2014 032345 7

Espaço reservado para o protocolo | Espaço reservado para a etiqueta | Espaço reservado para o código QR

INSTITUTO NACIONAL DA PROPRIEDADE INDUSTRIAL
Sistema de Gestão da Qualidade
Diretoria de Patentes

DIRPA	Tipo de Documento: Formulário	DIRPA	Página: 1/3
Título do Documento: Depósito de Pedido de Patente		Código: FQ001	Versão: 2
		Procedimento: DIRPA-PQ006	

Ao Instituto Nacional da Propriedade Industrial:
O requerente solicita a concessão de um privilégio na natureza e nas condições abaixo indicadas:

1. Depositante (71):

1.1 Nome: Universidade Estadual de Londrina

1.2 Qualificação: Ensino Superior

1.3 CNPJ/CPF: 78.640.489/0001-53

1.4 Endereço Completo: Rod Celso Garcia Cid,PR 445 Km 380, Campus Universitário

1.5 CEP: 86057-970

1.6 Telefone: 43 33715812 1.7 Fax: 43 33715812

1.8 E-mail: aintecpi@uel.br

☐ continua em folha anexa

2. Natureza: ☒ Invenção ☐ Modelo de Utilidade ☐ Certificado de Adição

3. Título da Invenção ou Modelo de Utilidade (54):

Formulação tópica contendo hesperidina metil chalcona para redução dos danos cutâneos induzidos pela radiação ultravioleta B

☐ continua em folha anexa

4. Pedido de Divisão: do pedido Nº **Data de Depósito:**

5. Prioridade: ☐ Interna (66) ☐ Unionista (30)

O depositante reivindica a(s) seguinte(s):

País ou Organização do depósito	Número do depósito (se disponível)	Data de depósito

☐ continua em folha anexa

INSTITUTO NACIONAL DA PROPRIEDADE INDUSTRIAL
Sistema de Gestão da Qualidade
Diretoria de Patentes

DIRPA	Tipo de Documento: Formulário	DIRPA	Página: 2/3
Título do Documento: Depósito de Pedido de Patente		Código: FQ001	Versão: 2
		Procedimento: DIRPA-PQ006	

6. **Inventor (72):**

☐ Assinale aqui se o(s) mesmo(s) requer(em) a não divulgação de seus nome(s), neste caso não preencher os campos abaixo.

6.1 Nome: Rubia Casagrande

6.2 Qualificação: Docente

6.3 CPF: 276286868-85

6.4 Endereço Completo: Rua Paranagua, 1057, apto 403 Londrina/PR

6.5 CEP: 86020-030

6.6 Telefone: 43 9909-0705 6.7 FAX: 43 3371 5812

6.8 E-mail: rubiacasa@yahoo.com.br

☒ continua em folha anexa

7. **Declaração de divulgação anterior não prejudicial.** ☐
Artigo 12 da LPI – período de graça.
Informe no item 11.13 os documentos anexados, se houver.

8. **Declaração na forma do item 3.2 da Instrução Normativa PR nº 17/2013:**

☐ Declaro que os dados fornecidos no presente formulário são idênticos ao da certidão de depósito ou documento equivalente do pedido cuja prioridade está sendo reivindicada.

9. **Procurador (74):**

9.1 Nome: Marinete Violin

9.2 CNPJ/CPF: 533643179-68 9.3 API/OAB: 17033-PR

9.4 Endereço Completo: Rod Celso Garcia Cid, PR 445 Km 380, Campus Universitário

9.5 CEP: 86057-970

9.6 Telefone: 43 33715812 9.7 FAX: 43 33715812

9.8 E-mail: violin@uel.br

☐ continua em folha anexa

10. **Listagem de sequências biológicas.**
Informe nos itens 11.9 ao 11.12 os documentos anexados, se houver. ☐

INSTITUTO NACIONAL DA PROPRIEDADE INDUSTRIAL
Sistema de Gestão da Qualidade
Diretoria de Patentes

DIRPA	Tipo de Documento: Formulário	DIRPA	Página: 3/3
Título do Documento: Depósito de Pedido de Patente		Código: FQ001	Versão: 2
		Procedimento: DIRPA-PQ006	

11. Documentos Anexados:

(Assinale e indique também o número de folhas):
(Deverá ser indicado o número total de somente uma das vias de cada documento).

		Documentos Anexados	folhas
☒	11.1	Guia de Recolhimento da União (GRU).	1
☒	11.2	Procuração.	1
☐	11.3	Documentos de Prioridade.	
☐	11.4	Documento de contrato de trabalho.	
☒	11.5	Relatório descritivo.	19
☒	11.6	Reivindicações.	1
☒	11.7	Desenho(s) (se houver). Sugestão de figura a ser publicada com o resumo: nº, 1 por melhor representar a invenção (sujeito à avaliação do INPI).	5
☒	11.8	Resumo.	1
☐	11.9	Listagem de sequências em arquivo eletrônico: _____nº de CDs ou DVDs (original e cópia).	
☐	11.10	Código de controle alfanumérico no formato de código de barras referente às listagem de sequências.	
☐	11.11	Listagem de sequências em formato impresso.	
☐	11.12	Declaração relativa à Listagem de sequências.	
☒	11.13	Outros (especificar) RG, CPF, Declaração de cessão, Comp de vinculo, Ato de nomeação do Reitor, anexo formulário, LIQUIDAÇÃO DE EMPENHO	24

12. Total de folhas anexadas: 52 **fls.**

13. Declaro, sob as penas da Lei que todas as informações acima prestadas são completas e verdadeiras.

Londrina, 02 de dezembro de 2014
Local e Data

Assinatura e Carimbo
Marinete Violin
Advogada - OAB/PR 17.03

ANEXO

6. INVENTOR (72)

6.1. Nome: Marcela Maria Baracat

6.2. Qualificação: Docente

6.3 CPF: 11824691831

6.4. Endereço: Rua Antônio Pisicchio, 100, apto 401– Londrina/PR

6.5. CEP: 86050-482

6.6. Telefone: (043) 33340799 6.7 Fax: (043) 3371-5812

6.8. e-mail: baracat@uel.br

6.1. Nome: Sandra Regina Georgetti

6.2. Qualificação: Docente

6.3 CPF: 28597768851

6.4. Endereço: Rua Fernando de Noronha, 775, apto 701 – Londrina/PR

6.5. CEP: 86020-300

6.6. Telefone: (43) 33231890 6.7 Fax: (043) 3371-5812

6.8. e-mail: sangeorgetti@gmail.com

6.1 Nome: Renata Michele Martinez

6.2 Qualificação: Doutoranda

6.3 CPF: 354.788.728-30

6.4 Endereço: Rua José Ribeiro Fernandes, 212 – Londrina/PR

6.5 CEP: 86020-030

6.6 Telefone: (43) 9987-4052 6.7 FAX: (43) 3371-5812

6.8 E-mail: renatamimartinez@gmail.com

6.1. Nome: Waldiceu Aparecido Verri Junior

6.2. Qualificação: Docente

6.3 CPF: 02565289936

6.4. Endereço: Rua Paranagua, 1057, apto 403 – Londrina/PR

6.5. CEP: 86020-030

6.6. Telefone: (43) 3323-4798 6.7Fax: (043) 3371-5812

6.8. e-mail: waldiceujr@yahoo.com.br

6.1. Nome: Felipe Almeida Pinho-Ribeiro
6.2. Qualificação: Doutorando
6.3 CPF: 05925180941
6.4. Endereço: Rua Izabel Gomes Colli 147, Jardim Pequena Londres – Londrina/PR
6.5. CEP: 86040-026
6.6. Telefone: (43) 88012420 6.7Fax: (043) 3371-5812
6.8. e-mail: pinho.fe@gmail.com

Universidade Estadual de Londrina

PARANÁ
GOVERNO DO ESTADO

PROCURAÇÃO

Pelo presente instrumento particular de procuração a **UNIVERSIDADE ESTADUAL DE LONDRINA**, pessoa jurídica de direito público interno, constituída sob a forma de autarquia, nos termos da Lei nº 9.663, de 16 de julho de 1991, com sede na cidade de Londrina, Estado do Paraná, no campus universitário, Rodovia Celso Garcia Cid (PR 445), Km. 380, inscrita no CNPJ/MF sob o nº 78.640.489/0001-53, neste ato representada, na forma de seus estatutos, por sua Reitora, Profa. Dra. **Berenice Quinzani Jordão**, brasileira, professora universitária, portadora do RG 6.070.116/SSP/SP inscrita no CPF nº364.796.169-87, residente e domiciliado nesta cidade de Londrina, Estado do Paraná, constitui sua bastante procuradora a advogada **Marinete Violin**, brasileira, advogada, inscrita na OAB, Seção do Paraná, sob o nº 17033/PR, com endereço à Rodovia Celso Garcia Cid (PR 445), s/nº, Campus Universitário, CP. 6001, em Londrina, Estado do Paraná, à qual confere os poderes da cláusula ***ad judicia eet extra*, especialmente para atuar perante o INPI - Instituto Nacional de Propriedade Industrial,** no pedido de patente cujo título é **"Formulação tópica contendo hesperidina metil chalcona para redução dos danos cutâneos induzidos pela radiação ultravioleta B"**, podendo, para tanto, firmar todos os requerimentos, petições e documentos necessários, apresentar defesa, requerer providências, ter vista de processos e retirá-los em carga, enfim, propor todas as medidas necessárias para a defesa de quaisquer interesses e direitos relacionados com a referida invenção, inclusive substabelecer.

Londrina, 02 de dezembro de 2014.

Berenice Quinzani Jordão

UNIVERSIDADE ESTADUAL DE LONDRINA
Profa. Dra. Berenice Quinzani Jordão
Reitora

1

ANEXO III

< Uso exclusivo do INPI >

INPI INSTITUTO NACIONAL DA PROPRIEDADE INDUSTRIAL
PROTOCOLO GERAL
cassandr
22/12/2014 015140002561
VP17/12/2014
BR 10 2014 032344 9

Espaço reservado para o protocolo | Espaço reservado para a etiqueta | Espaço reservado para o código QR

INPI INSTITUTO NACIONAL DA PROPRIEDADE INDUSTRIAL
Sistema de Gestão da Qualidade
Diretoria de Patentes

DIRPA	Tipo de Documento: Formulário	DIRPA	Página: 1/3
Título do Documento: Depósito de Pedido de Patente		Código: FQ001	Versão: 2
		Procedimento: DIRPA-PQ006	

Ao Instituto Nacional da Propriedade Industrial:
O requerente solicita a concessão de um privilégio na natureza e nas condições abaixo indicadas:

1. Depositante (71):

1.1 Nome: Universidade Estadual de Londrina

1.2 Qualificação: Ensino Superior

1.3 CNPJ/CPF: 78.640.489/0001-53

1.4 Endereço Completo: Rod Celso Garcia Cid,PR 445 Km 380, Campus Universitário

1.5 CEP: 86057-970

1.6 Telefone: 43 33715812 1.7 Fax: 43 33715812

1.8 E-mail: aintecpi@uel.br

☐ continua em folha anexa

2. Natureza: ☒ Invenção ☐ Modelo de Utilidade ☐ Certificado de Adição

3. Título da Invenção ou Modelo de Utilidade (54):

Formulação tópica contendo naringenina para redução dos danos cutâneos foto-oxidativos induzidos pela radiação ultravioleta B.

☐ continua em folha anexa

4. Pedido de Divisão: do pedido Nº **Data de Depósito:**

5. Prioridade: ☐ Interna (66) ☐ Unionista (30)

O depositante reivindica a(s) seguinte(s):

País ou Organização do depósito	Número do depósito (se disponível)	Data de depósito

☐ continua em folha anexa

INSTITUTO NACIONAL DA PROPRIEDADE INDUSTRIAL
Sistema de Gestão da Qualidade
Diretoria de Patentes

DIRPA	Tipo de Documento: Formulário	DIRPA	Página: 2/3
Título do Documento: Depósito de Pedido de Patente		Código: FQ001	Versão: 2
		Procedimento: DIRPA-PQ006	

6. **Inventor (72):**

☐ Assinale aqui se o(s) mesmo(s) requer(em) a não divulgação de seus nome(s), neste caso não preencher os campos abaixo.

6.1 Nome: Rubia Casagrande

6.2 Qualificação: Docente

6.3 CPF: 276286868-85

6.4 Endereço Completo: Rua Paranagua, 1057, apto 403 Londrina/PR

6.5 CEP: 86020-030

6.6 Telefone: 43 9909-0705 6.7 FAX: 43 3371 5812

6.8 E-mail: rubiacasa@yahoo.com.br

☒ continua em folha anexa

7. **Declaração de divulgação anterior não prejudicial.** ☐
Artigo 12 da LPI – período de graça.
Informe no item 11.13 os documentos anexados, se houver.

8. **Declaração na forma do item 3.2 da Instrução Normativa PR nº 17/2013:**

☐ Declaro que os dados fornecidos no presente formulário são idênticos ao da certidão de depósito ou documento equivalente do pedido cuja prioridade está sendo reivindicada.

9. **Procurador (74):**

9.1 Nome: Marinete Violin

9.2 CNPJ/CPF: 533643179-68 9.3 API/OAB: 17033-PR

9.4 Endereço Completo: Rod Celso Garcia Cid,PR 445 Km 380, Campus Universitário

9.5 CEP: 86057-970

9.6 Telefone: 43 33715812 9.7 FAX: 43 33715812

9.8 E-mail: violin@uel.br

☐ continua em folha anexa

10. **Listagem de sequências biológicas.**
Informe nos itens 11.9 ao 11.12 os documentos anexados, se houver. ☐

INSTITUTO NACIONAL DA PROPRIEDADE INDUSTRIAL
Sistema de Gestão da Qualidade
Diretoria de Patentes

DIRPA	Tipo de Documento: Formulário	DIRPA	Página: 3/3
Título do Documento: Depósito de Pedido de Patente		Código: FQ001	Versão: 2
		Procedimento: DIRPA-PQ006	

11. Documentos Anexados:

(Assinale e indique também o número de folhas):
(Deverá ser indicado o número total de somente uma das vias de cada documento).

		Documentos Anexados	folhas
☒	11.1	Guia de Recolhimento da União (GRU).	1
☒	11.2	Procuração.	1
☐	11.3	Documentos de Prioridade.	
☐	11.4	Documento de contrato de trabalho.	
☒	11.5	Relatório descritivo.	8
☒	11.6	Reivindicações.	3
☒	11.7	Desenho(s) (se houver). Sugestão de figura a ser publicada com o resumo: nº, 1 por melhor representar a invenção (sujeito à avaliação do INPI).	4
☒	11.8	Resumo.	1
☐	11.9	Listagem de sequências em arquivo eletrônico: ____nº de CDs ou DVDs (original e cópia).	
☐	11.10	Código de controle alfanumérico no formato de código de barras referente às listagem de sequências.	
☐	11.11	Listagem de sequências em formato impresso.	
☐	11.12	Declaração relativa à Listagem de sequências.	
☒	11.13	Outros (especificar) RG, CPF, Declaração de cessão, Comp de vinculo, Ato de nomeação do Reitor, anexo formulário.	30

12. Total de folhas anexadas: 56 **fls.**

13. Declaro, sob as penas da Lei que todas as informações acima prestadas são completas e verdadeiras.

Londrina, 02 de dezembro de 2014
Local e Data

Assinatura e Carimbo
Marinete Violin
Advogada - OAB/PR 17.033

ANEXO

6. INVENTOR (72)

6.1. Nome: Marcela Maria Baracat

6.2. Qualificação: Docente

6.3 CPF: 11824691831

6.4. Endereço: Rua Antônio Pisicchio, 100, apto 401– Londrina/PR

6.5. CEP: 86050-482

6.6. Telefone: (043) 33340799 6.7 Fax: (043) 3371-5812

6.8. e-mail: baracat@uel.br

6.1. Nome: Sandra Regina Georgetti

6.2. Qualificação: Docente

6.3 CPF: 28597768851

6.4. Endereço: Rua Fernando de Noronha, 775, apto 701 – Londrina/PR

6.5. CEP: 86020-300

6.6. Telefone: (43) 33231890 6.7 Fax: (043) 3371-5812

6.8. e-mail: sangeorgetti@gmail.com

6.1 Nome: Renata Michele Martinez

6.2 Qualificação: Doutoranda

6.3 CPF: 354.788.728-30

6.4 Endereço: Rua José Ribeiro Fernandes, 212 – Londrina/PR

6.5 CEP: 86020-030

6.6 Telefone: (43) 9987-4052 6.7 FAX: (43) 3371-5812

6.8 E-mail: renatamimartinez@gmail.com

6.1. Nome: Waldiceu Aparecido Verri Junior

6.2. Qualificação: Docente

6.3 CPF: 02565289936

6.4. Endereço: Rua Paranagua, 1057, apto 403 – Londrina/PR

6.5. CEP: 86020-030

6.6. Telefone: (43) 3323-4798 6.7Fax: (043) 3371-5812

6.8. e-mail: waldiceujr@yahoo.com.br

6.1. Nome: Felipe Almeida Pinho-Ribeiro
6.2. Qualificação: Doutorando
6.3 CPF: 05925180941
6.4. Endereço: Rua Izabel Gomes Colli 147, Jardim Pequena Londres – Londrina/PR
6.5. CEP: 86040-026
6.6. Telefone: (43) 88012420 6.7Fax: (043) 3371-5812
6.8. e-mail: pinho.fe@gmail.com

6.1. Nome: Carla Venturelli Caviglione
6.2. Qualificação: Aluna de Iniciação científica
6.3 CPF: 06677662942
6.4. Endereço: Rua Caracas, 377 apto 202 – Londrina/PR
6.5. CEP: 86050-070
6.6. Telefone: (43) 99233217 6.7Fax: (043) 3371-5812
6.8. e-mail: venturelli.carla@gmail.com

6.1. Nome: Vinicius Steffen
6.2. Qualificação: Aluno de Iniciação científica
6.3 CPF: 09434102901
6.4. Endereço: Rua Rubens Carlos de Jesus, 111, casa 57 – Londrina/PR
6.5. CEP: 86.055-240
6.6. Telefone: (43) 9943-9304 6.7Fax: (043) 3371-5812
6.8. e-mail: vssteffen@gmail.com

Universidade Estadual de Londrina

PARANÁ
Governo do Estado

PROCURAÇÃO

Pelo presente instrumento particular de procuração a **UNIVERSIDADE ESTADUAL DE LONDRINA**, pessoa jurídica de direito público interno, constituída sob a forma de autarquia, nos termos da Lei nº 9.663, de 16 de julho de 1991, com sede na cidade de Londrina, Estado do Paraná, no campus universitário, Rodovia Celso Garcia Cid (PR 445), Km. 380, inscrita no CNPJ/MF sob o nº 78.640.489/0001-53, neste ato representada, na forma de seus estatutos, por sua Reitora, Profa. Dra. **Berenice Quinzani Jordão**, brasileira, professora universitária, portadora do RG 6.070.116/SSP/SP inscrita no CPF nº364.796.169-87, residente e domiciliado nesta cidade de Londrina, Estado do Paraná, constitui sua bastante procuradora a advogada **Marinete Violin**, brasileira, advogada, inscrita na OAB, Seção do Paraná, sob o nº 17033/PR, com endereço à Rodovia Celso Garcia Cid (PR 445), s/nº, Campus Universitário, CP. 6001, em Londrina, Estado do Paraná, à qual confere os poderes da cláusula ***ad judicia* eet *extra*, especialmente para atuar perante o INPI - Instituto Nacional de Propriedade Industrial,** no pedido de patente cujo título é **"Formulação tópica contendo naringenina para redução dos danos cutâneos foto-oxidativos induzidos pela radiação ultravioleta B"**, podendo, para tanto, firmar todos os requerimentos, petições e documentos necessários, apresentar defesa, requerer providências, ter vista de processos e retirá-los em carga, enfim, propor todas as medidas necessárias para a defesa de quaisquer interesses e direitos relacionados com a referida invenção, inclusive substabelecer.

Londrina, 02 de dezembro de 2014.

Berenice Quinzani Jordão

UNIVERSIDADE ESTADUAL DE LONDRINA
Profa. Dra. Berenice Quinzani Jordão
Reitora

1